



Fundamentals of **Nuclear Physics**

Davis Grayson

Fundamentals of Nuclear Physics

Fundamentals of Nuclear Physics

Davis Grayson

Published by The English Press,
5 Penn Plaza,
19th Floor,
New York, NY 10001, USA

Copyright © 2021 The English Press

This book contains information obtained from authentic and highly regarded sources. All chapters are published with permission under the Creative Commons Attribution Share Alike License or equivalent. A wide variety of references are listed. Permissions and sources are indicated; for detailed attributions, please refer to the permissions page. Reasonable efforts have been made to publish reliable data and information, but the authors, editors and publisher cannot assume any responsibility for the validity of all materials or the consequences of their use.

Copyright of this ebook is with The English Press, rights acquired from the original print publisher, Willford Press.

Trademark Notice: Registered trademark of products or corporate names are used only for explanation and identification without intent to infringe.

ISBN: 978-1-64728-079-6

Cataloging-in-Publication Data

Fundamentals of nuclear physics / Davis Grayson.

p. cm.

Includes bibliographical references and index.

ISBN 978-1-64728-079-6

1. Nuclear physics. 2. Physics. I. Grayson, Davis.

QC776 .F86 2021

539.7--dc23

TABLE OF CONTENTS

Preface	VII
Chapter 1 Introduction	1
▪ Nucleus	1
▪ Nuclear Physics	10
▪ Nuclear Force	14
▪ Nuclear Structure	15
▪ Nuclear Reaction	17
Chapter 2 Models of a Nucleus	19
▪ Liquid Drop	19
▪ Interacting Boson Model	20
▪ Nuclear Shell Model	29
Chapter 3 Nuclear Fission and Fusion	32
▪ Nuclear Fission	32
▪ Nuclear Fission Products	49
▪ Spontaneous Fission	59
▪ Photofission	62
▪ Nuclear Fusion	62
▪ Cold Fusion	74
▪ Thermonuclear Fusion	75
▪ Controlled Fusion	78
Chapter 4 Radioactive Decay	86
▪ Radioactivity	86
▪ Radioactive Decay	102
▪ Alpha Decay	103
▪ Beta Decay	104
▪ Double Beta Decay	116

▪ Beta Plus Decay	121
▪ Gamma Decay	123
▪ Cluster Decay	125
▪ Decay Chain	130
▪ Decay Energy	135
▪ Proton Decay	136
Chapter 5 Applications of Nuclear Technology	138
▪ Medical Applications	138
▪ Military Applications	189
▪ Fusion Reactor	228
▪ Fusion Power	235
▪ Neutron Generator	260

Permissions

Index

PREFACE

The purpose of this book is to help students understand the fundamental concepts of this discipline. It is designed to motivate students to learn and prosper. I am grateful for the support of my colleagues. I would also like to acknowledge the encouragement of my family.

Nuclear physics deals with the study of atomic nuclei and their constituents. It is a sub-field of physics and is also concerned with the study of many other forms of nuclear matter. It focuses on studying the nuclei under extreme conditions like excitation energy and high spin along with studying the extreme shapes and extreme neutron-to-proton ratios. It primarily aims to study two processes: nuclear fusion and nuclear fission. The process in which two low weighted nuclei come in close contact with each other and merge due to strong forces around them is known as nuclear fusion. Nuclear fission is the process by which a heavy nucleus is broken down into two subsequent nuclei. The field finds its application in areas such as nuclear medicine, radiocarbon dating, magnetic resonance imaging, ion implantation, nuclear power, etc. This discipline is an upcoming field of science that has undergone rapid development over the past few decades. The topics covered in this extensive book deal with the core aspects of nuclear physics. It will serve as a valuable source of reference for those interested in this field.

A foreword for all the chapters is provided below:

Chapter - Introduction

The atomic nucleus is the small, dense region consisting of protons and neutrons at the center of an atom. Nuclear physics deals with the study of protons and neutrons and their interactions at the center of the atom. This chapter has been carefully written to provide an easy understanding of nuclear physics.

Chapter - Models of a Nucleus

Different models of nucleus have been developed depending on the nuclear behavior of atoms. It includes interacting Boson model, nuclear shell model, liquid drop model, etc. This is an introductory chapter which will briefly introduce about the different models of a nucleus.

Chapter - Nuclear Fission and Fusion

Nuclear fission is a radioactive decay process in nuclear physics in which an atomic nuclei breaks down into two or more atomic nuclei. Nuclear fusion is a nuclear reaction in which two or more atomic nuclei combine to form a greater nucleus. The topics elaborated in this chapter will help in gaining a better perspective of nuclear fission and fusion.

Chapter - Radioactive Decay

The process in which an unstable atomic nucleus loses its energy due to radiation is termed as radioactive decay. Alpha decay, beta decay and gamma decay, etc. are studied under its domain. This chapter closely examines the aspects associated with radioactive decay to provide an extensive understanding of the subject.

Chapter - Applications of Nuclear Technology

There are a wide range of applications of nuclear technology in the fields of medicine and defense. It is used in gamma camera, fast neutron therapy, radiation therapy, nuclear weapon design and delivery, underground nuclear weapon testing, etc. This chapter discusses the applications of nuclear technology in detail.

Davis Grayson

Introduction

1

CHAPTER

The atomic nucleus is the small, dense region consisting of protons and neutrons at the center of an atom. Nuclear physics deals with the study of protons and neutrons and their interactions at the center of the atom. This chapter has been carefully written to provide an easy understanding of nuclear physics.

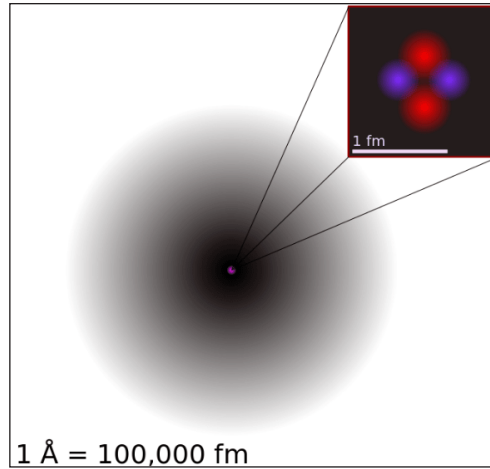
NUCLEUS

In physics, the atomic nucleus is the central part of an atom. In comparison to an atom, it is much smaller and contains most of the mass of the atom. The atomic nucleus also contains all of its positive electric charge (in protons), while all of its negative charge is distributed in the electron cloud.

The atomic nucleus was discovered by Ernest Rutherford, who proposed a new model of the atom based on Geiger-Marsden experiments. These experiments were performed between 1908 and 1913 by Hans Geiger and Ernest Marsden under the direction of Ernest Rutherford. These experiments were a landmark series of experiments by which scientists discovered that every atom contains a nucleus (whose diameter is of the order 10^{-14}m) where all of its positive charge and most of its mass are concentrated in a small region called an atomic nucleus. In Rutherford's atom, the diameter of its sphere (about 10^{-10} m) of influence is determined by its electrons. In other words, the nucleus occupies only about 10^{-12} of the total volume of the atom or less (the nuclear atom is largely empty space), but it contains all the positive charge and at least 99.95% of the total mass of the atom.

After discovery of the neutron in 1932 by the English physicist James Chadwick, models for a nucleus composed of protons and neutrons were quickly developed by Dmitri Ivanenko and Werner Heisenberg.

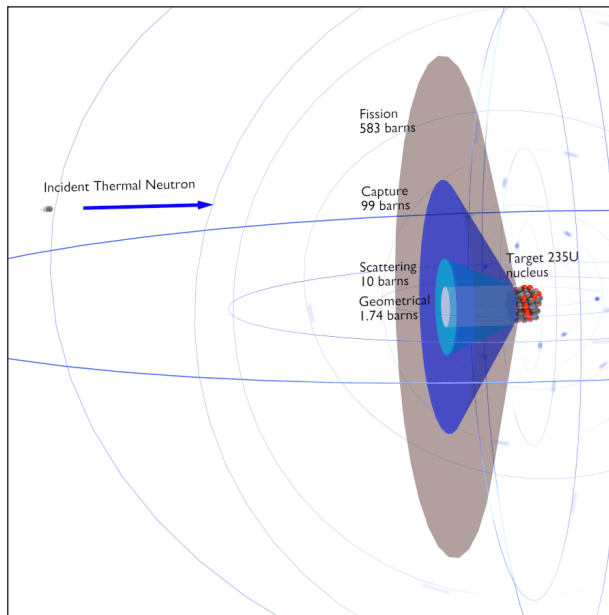
All matter except dark matter is made of molecules, which are themselves made of atoms. The atoms consist of two parts. An atomic nucleus and an electron cloud, which are bound together by electrostatic force. The nucleus itself is generally made of protons and neutrons but even these are composite objects. Inside the protons and neutrons, we find the quarks.



A figurative depiction of the helium-4 atom with the electron cloud in shades of gray. Protons and neutrons are most likely found in exactly the same space, at the central point.

Inside the atomic nucleus, the residual strong force, also known as the nuclear force, acts to hold neutrons and protons together in nuclei. In nuclei, this force acts against the enormous repulsive electromagnetic force of the protons. The term residual is associated with the fact; it is the residuum of the fundamental strong interaction between the quarks that make up the protons and neutrons. The residual strong force acts indirectly through the virtual π and ρ mesons, which transmit the force between nucleons that holds the nucleus together.

Properties of Nucleus

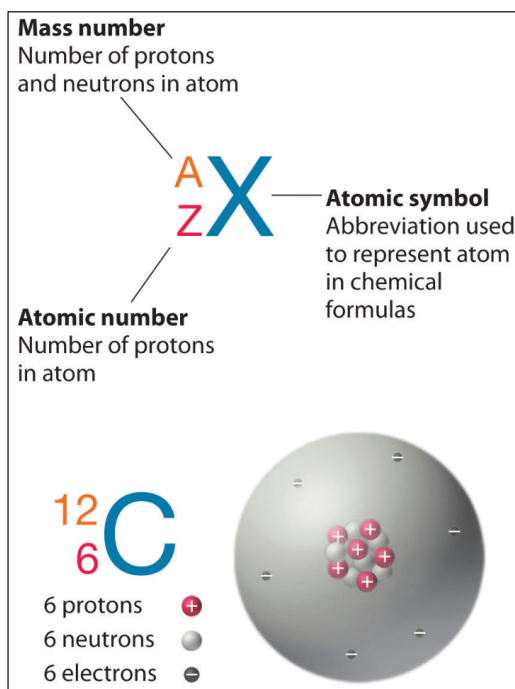


The nuclear properties (atomic mass, nuclear cross-sections) of the element are

determined by the number of protons (atomic number) and number of neutrons (neutron number). For example, actinides with odd neutron number are usually fissile (fissionable with slow neutrons) while actinides with even neutron number are usually not fissile (but are fissionable with fast neutrons). Heavy nuclei with an even number of protons and an even number of neutrons are (due to Pauli exclusion principle) very stable thanks to the occurrence of 'paired spin'. On the other hand, nuclei with an odd number of protons and neutrons are mostly unstable.

Mass of Nucleus

As was written, almost all of the mass of an atom is located in the nucleus, with a very small contribution from the electron cloud. The mass of the nucleus is associated with the atomic mass number, which is the total number of protons and neutrons in the nucleus of an atom. The mass number is different for each different isotope of a chemical element. The mass number is written either after the element name or as a superscript to the left of an element's symbol. For example, the most common isotope of carbon is carbon-12, or ^{12}C .



The size and mass of atoms are so small that the use of normal measuring units, while possible, is often inconvenient. Units of measure have been defined for mass and energy on the atomic scale to make measurements more convenient to express. The unit of measure for mass is the atomic mass unit (amu). One atomic mass unit is equal to 1.66×10^{-24} grams.

Besides the standard kilogram, it is a second mass standard. It is the carbon-12 atom,

which, by international agreement, has been assigned a mass of 12 atomic mass units (u). The relation between the two units is one atomic mass unit is equal:

$$1\text{u} = 1.66 \times 10^{-24} \text{ grams.}$$

One unified atomic mass unit is approximately the mass of one nucleon (either a single proton or neutron) and is numerically equivalent to 1 g/mol.

For ^{12}C the atomic mass is exactly 12u, since the atomic mass unit is defined from it. For other isotopes, the isotopic mass usually differs and is usually within 0.1 u of the mass number. For example, ^{63}Cu (29 protons and 34 neutrons) has a mass number of 63 and an isotopic mass in its nuclear ground state is 62.91367 u.

There are two reasons for the difference between mass number and isotopic mass, known as the mass defect:

- The neutron is slightly heavier than the proton. This increases the mass of nuclei with more neutrons than protons relative to the atomic mass unit scale based on ^{12}C with equal numbers of protons and neutrons.
- The nuclear binding energy varies between nuclei. A nucleus with greater binding energy has a lower total energy, and therefore a lower mass according to Einstein's mass-energy equivalence relation $E = mc^2$. For ^{63}Cu the atomic mass is less than 63 so this must be the dominant factor.

Note that, it was found the rest mass of an atomic nucleus is measurably smaller than the sum of the rest masses of its constituent protons, neutrons and electrons. Mass was no longer considered unchangeable in the closed system. The difference is a measure of the nuclear binding energy which holds the nucleus together. According to the Einstein relationship ($E=mc^2$), this binding energy is proportional to this mass difference and it is known as the mass defect.

Radius and Density of Atomic Nucleus

Typical nuclear radii are of the order 10^{-14} m. Assuming spherical shape; nuclear radii can be calculated according to following formula:

$$r = r_0 \cdot A^{1/3}$$

Where, $r_0 = 1.2 \times 10^{-15} \text{ m} = 1.2 \text{ fm}$.

If we use this approximation, we therefore expect the geometrical cross-sections of nuclei to be of the order of πr^2 or $4.5 \times 10^{-30} \text{ m}^2$ for hydrogen nuclei or $1.74 \times 10^{-28} \text{ m}^2$ for ^{238}U nuclei.

Nuclear density is the density of the nucleus of an atom. It is the ratio of mass per unit volume inside the nucleus. Since atomic nucleus carries most of atom's mass and atomic nucleus is very small in comparison to entire atom, the nuclear density is very high.

The nuclear density for a typical nucleus can be approximately calculated from the size of the nucleus and from its mass. For example, natural uranium consists primarily of isotope ^{238}U (99.28%), therefore the atomic mass of uranium element is close to the atomic mass of ^{238}U isotope (238.03u). Its radius of this nucleus will be:

$$r = r_0 \cdot A^{1/3} = 7.44 \text{ fm.}$$

Assuming it is spherical, its volume will be:

$$V = 4\pi r^3/3 = 1.73 \times 10^{-42} \text{ m}^3.$$

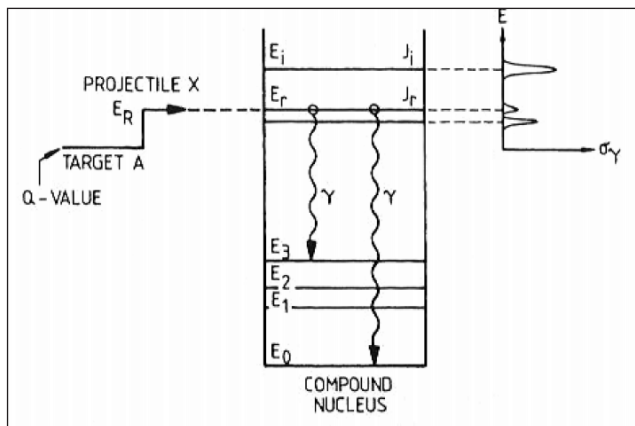
The usual definition of nuclear density gives for its density:

$$\rho_{\text{nucleus}} = m/V = 238 \times 1.66 \times 10^{-27}/(1.73 \times 10^{-42}) = 2.3 \times 10^{17} \text{ kg/m}^3.$$

Thus, the density of nuclear material is more than 2.10^{14} times greater than that of water. It is an immense density. The descriptive term nuclear density is also applied to situations where similarly high densities occur, such as within neutron stars. Such immense densities are also found in neutron stars.

Excited Nucleus – Nuclear Resonance

Highly excited nuclei formed by the combination of the incident particle and target nucleus are known as nuclear resonances. If a target nucleus X is bombarded with particles a, it is sometimes observed that the ensuing nuclear reaction takes place with appreciable probability only if the energy of the particle a is in the neighborhood of certain definite energy values. These energy values are referred to as resonance energies. The compound nuclei of these certain energies are referred to as nuclear resonances. Resonances are usually found only at relatively low energies of the projectile. The widths of the resonances increase in general with increasing energies. At higher energies the widths may reach the order of the distances between resonances and then no resonances can be observed.



Energy levels of compound state. For neutron absorption reaction on ^{238}U the first resonance E_1 corresponds to the excitation energy of 6.67eV. E_0 is a base state of ^{239}U .

Nuclear Stability

Nuclear size is defined by nuclear radius; nuclear density can be calculated from nuclear size.

Nuclear size is defined by nuclear radius, also called rms charge radius. It can be measured by the scattering of electrons by the nucleus and also inferred from the effects of finite nuclear size on electron energy levels as measured in atomic spectra.

The problem of defining a radius for the atomic nucleus is similar to the problem of atomic radius, in that neither atoms nor their nuclei have definite boundaries. However, the nucleus can be modelled as a sphere of positive charge for the interpretation of electron scattering experiments: because there is no definite boundary to the nucleus, the electrons “see” a range of cross-sections, for which a mean can be taken. The qualification of “rms” (for “root mean square”) arises because it is the nuclear cross-section, proportional to the square of the radius, which is determining for electron scattering.

The first estimate of a nuclear charge radius was made by Hans Geiger and Ernest Marsden in 1909, under the direction of Ernest Rutherford at the Physical Laboratories of the University of Manchester, UK. The famous Rutherford gold foil experiment involved the scattering of α -particles by gold foil, with some of the particles being scattered through angles of more than 90° , that is coming back to the same side of the foil as the α -source, as shown in figure. Rutherford was able to put an upper limit on the radius of the gold nucleus of 34 femtometers (fm).

Later studies found an empirical relation between the charge radius and the mass number, A , for heavier nuclei ($A > 20$): $R \approx r \cdot A^{1/3}$ where r is an empirical constant of $1.2 - 1.5$ fm. This gives a charge radius for the gold nucleus ($A=197$) of about 7.5 fm.

Nuclear density is the density of the nucleus of an atom, averaging about $4 \cdot 10^{17} \text{kg/m}^3$. The nuclear density for a typical nucleus can be approximately calculated from the size of the nucleus:

$$n = \frac{A}{\frac{4}{3}\pi R^3}$$

The stability of an atom depends on the ratio and number of protons and neutrons, which may represent closed and filled quantum shells.

The stability of an atom depends on the ratio of its protons to its neutrons, as well as on whether it contains a “magic number” of neutrons or protons that would represent closed and filled quantum shells. These quantum shells correspond to energy levels

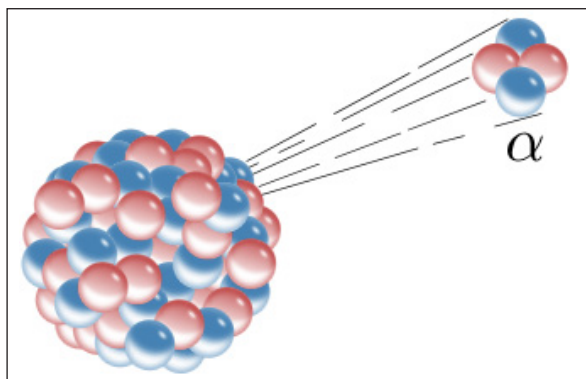
within the shell model of the nucleus. Filled shells, such as the filled shell of 50 protons in the element tin, confers unusual stability on the nuclide. Of the 254 known stable nuclides, only four have both an odd number of protons and an odd number of neutrons:

- Hydrogen-2 (deuterium)
- Lithium-6
- Boron-10
- Nitrogen-14

Also, only four naturally occurring, radioactive odd-odd nuclides have a half-life greater than a billion years:

- Potassium-40
- Vanadium-50
- Lanthanum-138
- Tantalum-180m

Most odd-odd nuclei are highly unstable with respect to beta decay because the decay products are even-even and therefore more strongly bound, due to nuclear pairing effects.



Alpha Decay: Alpha decay is one type of radioactive decay. An atomic nucleus emits an alpha particle and thereby transforms (“decays”) into an atom with a mass number smaller by four and an atomic number smaller by two. Many other types of decay are possible.

An atom with an unstable nucleus, called a radionuclide, is characterized by excess energy available either for a newly created radiation particle within the nucleus or via internal conversion. During this process, the radionuclide is said to undergo radioactive decay. Radioactive decay results in the emission of gamma rays and subatomic

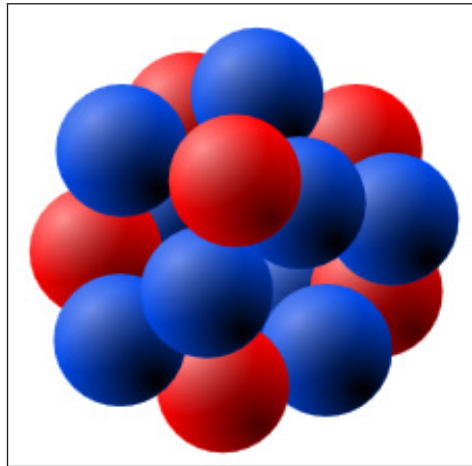
particles such as alpha or beta particles. These emissions constitute ionizing radiation. Radionuclides occur naturally but can also be produced artificially.

All elements form a number of radionuclides, although the half-lives of many are so short that they are not observed in nature. Even the lightest element, hydrogen, has a well-known radioisotope: Tritium. The heaviest elements (heavier than bismuth) exist only as radionuclides. For every chemical element, many radioisotopes that do not occur in nature (due to short half-lives or the lack of a natural production source) have been produced artificially.

Binding Energy and Nuclear Forces

Nuclear force is the force that is responsible for binding of protons and neutrons into atomic nuclei.

The nuclear force is the force between two or more component parts of atomic nuclei. The component parts are neutrons and protons, which collectively are called nucleons. Nuclear force is responsible for the binding of protons and neutrons into atomic nuclei.



Drawing of Atomic Nucleus: A model of the atomic nucleus showing it as a compact bundle of the two types of nucleons: protons (red) and neutrons (blue).

To disassemble a nucleus into unbound protons and neutrons would require working against the nuclear force. Conversely, energy is released when a nucleus is created from free nucleons or other nuclei—known as the nuclear binding energy. The binding energy of nuclei is always a positive number, since all nuclei require net energy to separate into individual protons and neutrons. Because of mass-energy equivalence (i.e., Einstein’s famous formula $E = mc^2$), releasing this energy causes the mass of the nucleus to be lower than the total mass of the individual nucleons (leading to “mass deficit”). Binding energy is the energy used in nuclear power plants and nuclear weapons.

The nuclear force is powerfully attractive between nucleons at distances of about 1

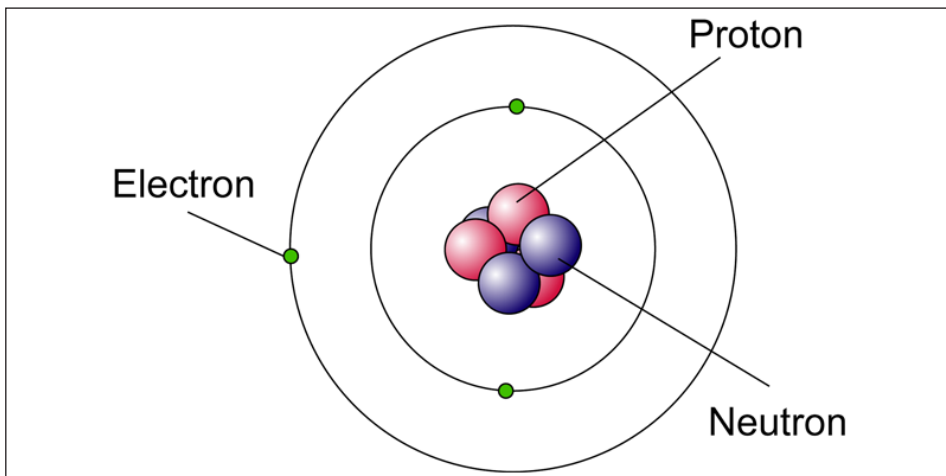
femtometer (fm) between their centers, but rapidly decreases to relative insignificance at distances beyond about 2.5 fm. At very short distances (less than 0.7 fm) it becomes repulsive; it is responsible for the physical size of nuclei since the nucleons can come no closer than the force allows.

The nuclear force is now understood as a residual effect of an even more powerful “strong force” or strong interaction. It is the attractive force that binds together particles known as quarks (to form the nucleons themselves). This more powerful force is mediated by particles called gluons. Gluons hold quarks together with a force like that of an electric charge (but of far greater power).

The nuclear forces arising between nucleons are now seen as analogous to the forces in chemistry between neutral atoms or molecules (called London forces). Such forces between atoms are much weaker than the attractive electrical forces that hold together the atoms themselves (i.e., that bind electrons to the nucleus), and their range between atoms is shorter because they arise from a small separation of charges inside the neutral atom.

Similarly, even though nucleons are made of quarks in combinations which cancel most gluon forces (they are “color neutral”), some combinations of quarks and gluons leak away from nucleons in the form of short-range nuclear force fields that extend from one nucleon to another nucleon in close proximity. These nuclear forces are very weak compared to direct gluon forces (“color forces” or “strong forces”) inside nucleons and the nuclear forces extend over only a few nuclear diameters, falling exponentially with distance. Nevertheless, they are strong enough to bind neutrons and protons over short distances, as well as overcome the electrical repulsion between protons in the nucleus. Like London forces, nuclear forces also stop being attractive, and become repulsive when nucleons are brought too close together.

Nucleons



A nucleon is one of the particles of the atomic nucleus. Each atomic nucleus includes

one or more Nucleons. These are surrounded by one or more electrons. They occupy small space within the nucleus. Every atom is made up of nucleons which are further divided into electrons, protons, and neutrons that orbit the nucleus. An atom is just like a mini-solar system, with electrons orbiting a central star which is the nucleus, composed of nucleons.

Protons and neutrons are the best-known components of atomic nuclei. They can be found on their own not being part of the larger nucleus. A proton is the nucleus of the hydrogen-1 atom on its own which is the most abundant isotope of hydrogen.

Binding Energy Per Nucleon

Nuclei consist of neutron and protons, but the mass of the nucleus is less than the sum of individual masses of the protons and neutrons. The difference is the measure of binding energy per nucleon that holds the nucleons together. The binding energy can be determined from the Einstein relationship:

$$\text{Nuclear binding energy} = \Delta mc^2$$

$\Delta m = 0.0304$ u for alpha particles and gives a binding energy of 28.3 MeV.

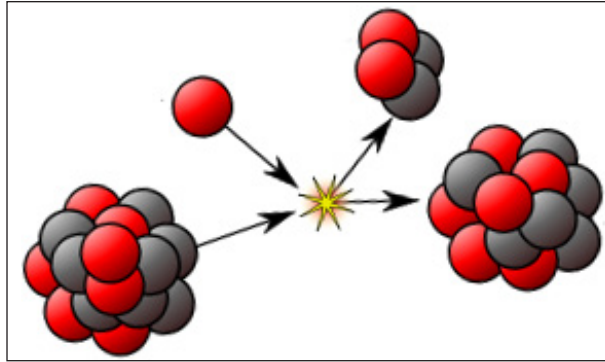
Properties of Nucleons

A neutron is not stable on its own, but it can be found in nuclear reactions and used in scientific analysis. Both proton and neutron consist of three quarks. The proton has two up quarks (the lightest of all quarks and a major constituent of matter and a type of elementary particle) and one down quark (the second lightest), while a neutron is made up of one up quark and two down quarks.

These are an integral part of the atomic nucleus since they cannot exist as independent nucleons. The atomic nucleus holds the nucleons with a strong force. However when the force is broken, it can produce a lot of power, and that power is termed as the nuclear energy which is similar to what is used in nuclear bombs. Nucleons present in radioactive decay substances such as uranium can be harmful since it can spread alpha radiation in a few seconds.

NUCLEAR PHYSICS

Nuclear physics is the field of Physics that studies atomic nuclei. In other words, nuclear physics deals with the components and structure of the nucleus. Nuclear reaction comprises the merging of nuclei, radioactive decay, fusion, fission and break-up of a nucleus.



Nuclear Physics and Atomic Physics

- The simple difference between nuclear physics and atomic physics is that nuclear physics deals with the nucleus while atomic physics deals with an entire atom.
- Atomic physics deals with the properties of an atom as a whole, mainly due to its electronic configuration. Of course, the nucleus is a part of this but only in terms of its overall contribution.
- Nuclear physics, on the other hand, deals exclusively with nuclei, their structures, properties, reactions and interactions. Nuclear physics Atoms make up all the matter in the universe.
- By understanding the concepts of quarks and gluons, the forces related to nuclear physics are understandable.
- The application of nuclear physics is largely in the field of power generation using nuclear energy. Once the force holding the nucleus was understood, we started splitting and fusing neutrons.
- The energy evolved in this process can be used in the splitting of the nucleus to generate energy in Nuclear Fission and fusing two neutrons to generate energy is Nuclear Fusion.

Radius of Nucleus

'R' represents the radius of nucleus.

$$R = R_0 A^{\frac{1}{3}}$$

Where,

- R_0 is the proportionality constant.

- A is the mass number of the element.

Total Number of Protons and Neutrons in a Nucleus

The mass number (A), also known as the nucleon number, is the total number of neutrons and protons in a nucleus.

$$A = Z + N$$

Where,

- N is the neutron number.
- A is the mass number.
- Z is the proton number.

Mass Defect

Mass defect takes place when some of the mass is lost during the nuclei generation:

$$\Delta m = Zm_p + (A - Z)m_n - M$$

Where,

- M is the mass of the nucleus.
- Δm is the difference between mass of the nucleons and mass of the nucleus.
- m_p is the Mass of the Proton.
- m_n is the mass of the Neutron.

Packing Fraction

Packing fraction is defined as Mass defect per nucleon. Packing fraction (f) = Mass defect per nucleons:

$$\text{Packing Fraction}(f) = \frac{[Zm_p + (A - Z)m_n - A]}{A}$$

Use of Nuclear Physics

- The continuous research in the field of nuclear physics has helped us find various other uses. For example, we now have nuclear medicine, nuclear weapons and have even found its uses in geology and archaeology in terms of carbon dating.
- Atomic Physics: An atom is made of a dense nucleus having neutrons and protons at the core surrounded by orbiting electrons as per the configuration. The

centre is positively charged and the surrounding cloud of electrons carries a negative charge. As a whole the atoms in consideration can either be neutral or carry a charge (in this case we call them ions).

- In many places, you may have seen that atomic energy is the source of energy production in terms of nuclear fission and fusion. Let this not confuse you as they both are often used and associated together.
- Atomic physics concerns itself with the entire atom and how electronic configuration of electrons can change. When an atom loses an electron, it becomes positively charged (cations) and when it gains an electron it becomes negatively charged (anions).

Law of Radioactivity

- Radioactivity occurs due to decay of the nucleus.
- External parameters such as temperature and pressure do not affect the rate of decay.
- Radioactivity is based on the law of conservation of charge.
- The daughter nuclei will have unique physical and chemical properties (that is different from parent nuclei).
- Decay rate of any radioactive material is directly proportional to the number of atoms present at that instant.
- α , β , and γ rays are followed during the radioactivity.

Units of Radioactivity

There are two units of radioactivity and they are:

- Curie (Ci): If the radioactive substance decay at the rate of 3.7×10^{10} decays per second, then the unit used is Curie.
- Rutherford (rd): If the radioactive substance decay at the rate of 10^6 decays per second, then the unit is Rutherford.

Nature of Nuclear Force

Nuclear physics is based on the forces known as nuclear force. The nature of nuclear force is given as:

- Nuclear forces are attractive in nature.
- These forces are independent of charges.

- The ranges of nuclear forces are short.
- As the distance between two nucleons reduces, the nuclear force becomes weak between them.
- Nuclear force is dependent on the spin.

NUCLEAR FORCE

Nuclear force is one of the four fundamental forces of nature, the others being gravitational and electromagnetic forces. In fact, being 10 million times stronger than the chemical binding forces, they are also known as the strong forces. We can define nuclear force as:

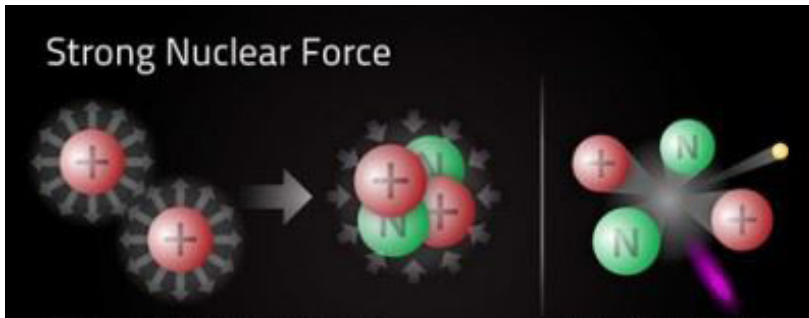
“The nuclear force is a force that acts between the protons and neutrons of atoms.”

The nuclear force is the force that binds the protons and neutrons in a nucleus together. This force can exist between protons and protons, neutrons and protons or neutrons and neutrons. This force is what holds the nucleus together.

The charge of protons, which is $+1e$, tends to push them away from each other with a strong electric field repulsive force, following Coulomb’s law. But nuclear force is strong enough to keep them together and to overcome that resistance at short range.

Properties of Nuclear Force

- It is attractive in nature but with a repulsive core. That is the reason that the nucleus is held together without collapsing in itself.
- The range of a nuclear force is very short. At 1 Fermi, the distance between particles in a nucleus is extremely small. At this range, the nuclear force is much stronger than the repulsive Coulomb’s force that pushes the particles away. However, if the distance is anything more than 2.5 Fermi, nuclear force is practically non-existent.
- The nuclear force is identical for all nucleons. It does not matter if it is a neutron or proton, once the Coulomb resistance is taken into consideration, nuclear force affects everything in the same way.
- At a distance of less than 0.7 Fermi, this force becomes repulsive. It is one of the most interesting properties of nuclear force, as this repulsive component of the force is what decides the size of the nucleus. The nucleons come closer to each other till the point that the force allows, after which they cannot come any closer because of the repulsive property of the force.



Strong Nuclear force.

Nuclear Force Examples

The most obvious example of Nuclear Force is the binding of protons, which are repulsive in nature because of their positive charge:

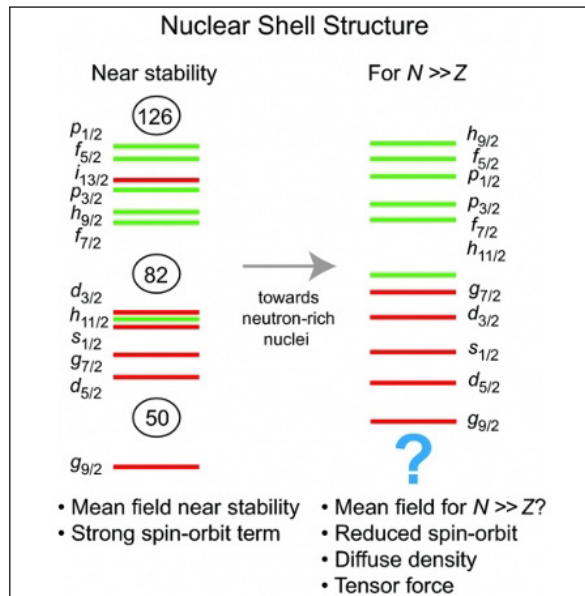
- On a larger scale, this force is responsible for the immense destructive power of nuclear weapons. The release of energy when a nuclear weapon detonated is due to strong nuclear forces. It is also used in Nuclear power plants to generate heat for the purpose of generating energy, such as electricity.
- A weaker nuclear force can transform a neutron to proton and proton into a neutron. These forces occur in many reactions such as radioactive decay, burning of the sun, radiocarbon dating etc.

NUCLEAR STRUCTURE

The atomic nucleus is a strongly-interacting, many-body quantum mechanical system that exhibits a fascinating variety of shapes and excitation modes, from spherical to super deformed (axis ratio 2:1), and from excitations of single protons and neutrons to collective vibrations and rotations of the nucleus as a whole. The study of nuclear structure attempts to elucidate the unifying mechanisms by which these rich patterns of behaviour emerge from the common underlying strong nuclear interaction between the nucleons (protons and neutrons) that form the nucleus.

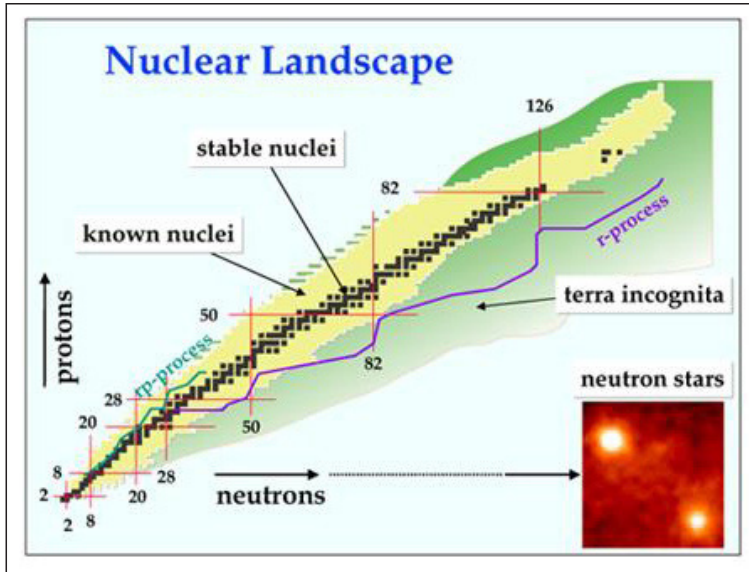
Central to these studies is the concept of nuclear shell structure, in which protons and neutrons occupy quantized energy levels within a potential generated by their interactions with all of the other nucleons. As shown on the left side of figure, these quantized energy levels cluster into groups, or shells, and the filling of major energy shells leads to particularly stable configurations associated with the proton and neutron “magic numbers”: 2, 8, 20, 28, 50, 82, and 126. Nuclei near closed shells tend to have spherical ground states, while those far from shell closures are deformed and exhibit low-energy collective rotational excitations.

While the nuclear shell structure and magic numbers have been well studied close to the “valley of stability” defined by the ~ 300 stable isotopes found in nature (black pixels in figure.) investigations of exotic nuclei with unusual proton-to-neutron ratios are revealing an evolution of this shell structure as one moves away from the stable isotopes. Understanding of this complex evolution of nuclear shell structure is of fundamental interest both as an emergent property of the nuclear quantum many-body system and as an important input to understanding the nuclear reaction processes by which the heavy chemical elements have been, and continue to be, synthesized in explosive astrophysical environments. As shown schematically in figure, nuclear shell structure in extremely neutron-rich nuclei plays a major role in the pathway for the rapid neutron capture (r) process, thought to be responsible for producing approximately half of the elements heavier than iron. Neither the exact locations of the shell gaps in these neutron-rich isotopes, nor the exact astrophysical events in which the r -process takes place, are, however, definitively established at present.



Nuclear shell structure with large gaps in the single particle energy levels (left) is well established in nuclei near stability. This shell structure is expected to evolve in more neutron-rich isotopes, with important implications for both nuclear structure and the synthesis of the heavy chemical elements in explosive astrophysical events.

Figure shows schematic of the nuclear landscape in which each pixel represents a particular number of protons and neutrons in the atomic nucleus. Slightly less than 300 stable isotopes (black pixels) occur in nature, while there are believed to be some 6000 bound isotopes (green region), the majority of which have never been produced or studied in terrestrial laboratories. These radioactive isotopes play crucial roles in the synthesis of the heavy chemical elements in explosive astrophysical events such as supernovae and neutron star mergers.



Gamma-ray spectroscopy provides powerful techniques to study nuclear shell structure through measurements of gamma-ray energies and angular correlations in low-energy decay experiments and through measurements of electromagnetic transition matrix elements between nuclear states in Coulomb excitation experiments with accelerated radioactive ion beams.

NUCLEAR REACTION

Nuclear reaction is the change in the identity or characteristics of an atomic nucleus, induced by bombarding it with an energetic particle. The bombarding particle may be an alpha particle, a gamma-ray photon, a neutron, a proton, or a heavy ion. In any case, the bombarding particle must have enough energy to approach the positively charged nucleus to within range of the strong nuclear force.

A typical nuclear reaction involves two reacting particles—a heavy target nucleus and a light bombarding particle—and produces two new particles—a heavier product nucleus and a lighter ejected particle. In the first observed nuclear reaction, Ernest Rutherford bombarded nitrogen with alpha particles and identified the ejected lighter particles as hydrogen nuclei or protons (${}^1_1\text{H}$ or p) and the product nuclei as a rare oxygen isotope. In the first nuclear reaction produced by artificially accelerated particles, the English physicists J.D. Cockcroft and E.T.S. Walton bombarded lithium with accelerated protons and thereby produced two helium nuclei, or alpha particles. As it has become possible to accelerate charged particles to increasingly greater energy, many high-energy nuclear reactions have been observed that produce a variety of subatomic particles called mesons, baryons, and resonance particles.

References

- What-is-atomic-nucleus-definition: periodic-table.org, Retrieved 02 June, 2020
- The-nucleus, boundless-physics: courses.lumenlearning.com, Retrieved 23 January, 2020
- Nucleon, physics: byjus.com, Retrieved 16 June, 2020
- Nuclear-structure: physics.uoguelph.ca, Retrieved 13 April, 2020
- Nuclear-reaction, science: britannica.com, Retrieved 04 May, 2020

Models of a Nucleus

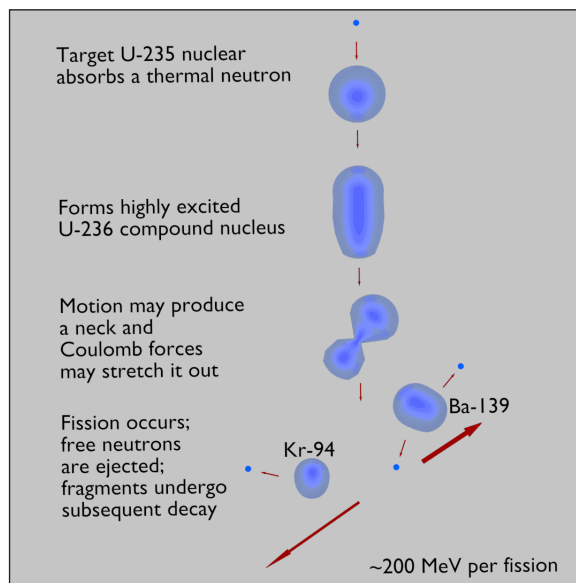
2

CHAPTER

Different models of nucleus have been developed depending on the nuclear behavior of atoms. It includes interacting Boson model, nuclear shell model, liquid drop model, etc. This is an introductory chapter which will briefly introduce about the different models of a nucleus.

LIQUID DROP

One of the first models which could describe very well the behavior of the nuclear binding energies and therefore of nuclear masses was the mass formula of von Weizsaecker (also called the semi-empirical mass formula – SEMF), that was published in 1935 by German physicist Carl Friedrich von Weizsäcker. This theory is based on the liquid drop model proposed by George Gamow.



According to this model, the atomic nucleus behaves like the molecules in a drop of liquid. But in this nuclear scale, the fluid is made of nucleons (protons and neutrons), which are held together by the strong nuclear force. The liquid drop model of the nucleus takes into account the fact that the nuclear forces on the nucleons on the surface are

different from those on nucleons in the interior of the nucleus. The interior nucleons are completely surrounded by other attracting nucleons. Here is the analogy with the forces that form a drop of liquid.

In the ground state the nucleus is spherical. If the sufficient kinetic or binding energy is added, this spherical nucleus may be distorted into a dumbbell shape and then may be splitted into two fragments. Since these fragments are a more stable configuration, the splitting of such heavy nuclei must be accompanied by energy release. This model does not explain all the properties of the atomic nucleus, but does explain the predicted nuclear binding energies.

The nuclear binding energy as a function of the mass number A and the number of protons Z based on the liquid drop model can be written as:

$$E_b \text{ (MeV)} = a_v A - a_s A^{\frac{2}{3}} - a_c \frac{Z^2}{A^{\frac{1}{3}}} - a_A \frac{(A-2Z)^2}{A} \pm \delta(A, Z)$$

$$+ \delta_o f \text{ or } Z, N \text{ even}$$

$$\delta(A, Z) =$$

$$- \delta_o f \text{ or } Z, N \text{ odd}$$

This formula is called the Weizsaecker Formula (or the semi-empirical mass formula).

INTERACTING BOSON MODEL

In nuclear physics and nuclear chemistry, the nuclear shell model is a model of the atomic nucleus which uses the Pauli exclusion principle to describe the structure of the nucleus in terms of energy levels. The first shell model was proposed by Dmitry Ivanenko (together with E. Gapon) in 1932. The model was developed in 1949 following independent work by several physicists, most notably Eugene Paul Wigner, Maria Goeppert Mayer and J. Hans D. Jensen, who shared the 1963 Nobel Prize in Physics for their contributions.

The shell model is partly analogous to the atomic shell model which describes the arrangement of electrons in an atom, in that a filled shell results in greater stability. When adding nucleons (protons or neutrons) to a nucleus, there are certain points where the binding energy of the next nucleon is significantly less than the last one. This observation, that there are certain magic numbers of nucleons (2, 8, 20, 28, 50, 82, 126) which are more tightly bound than the next higher number, is the origin of the shell model.

The shells for protons and for neutrons are independent of each other. Therefore, “magic nuclei” exist in which one nucleon type or the other is at a magic number, and

“doubly magic nuclei”, where both are. Due to some variations in orbital filling, the upper magic numbers are 126 and, speculatively, 184 for neutrons but only 114 for protons, playing a role in the search for the so-called island of stability. Some semi-magic numbers have been found, notably $Z = 40$ giving nuclear shell filling for the various elements; 16 may also be a magic number.

In order to get these numbers, the nuclear shell model starts from an average potential with a shape something between the square well and the harmonic oscillator. To this potential, a spin orbit term is added. Even so, the total perturbation does not coincide with experiment, and an empirical spin orbit coupling must be added with at least two or three different values of its coupling constant, depending on the nuclei being studied.

Nevertheless, the magic numbers of nucleons, as well as other properties, can be arrived at by approximating the model with a three-dimensional harmonic oscillator plus a spin-orbit interaction. A more realistic but also complicated potential is known as Woods-Saxon potential.

Modified Harmonic Oscillator Model

Consider a three-dimensional harmonic oscillator. This would give, for example, in the first three levels (“ ℓ ” is the angular momentum quantum number).

level n	ℓ	m_ℓ	m_s
0	0	0	$+\frac{1}{2}$
			$-\frac{1}{2}$
1	1	+1	$+\frac{1}{2}$
			$-\frac{1}{2}$
		0	$+\frac{1}{2}$
		$-\frac{1}{2}$	
	-1	$+\frac{1}{2}$	
		$-\frac{1}{2}$	
2	0	0	$+\frac{1}{2}$
			$-\frac{1}{2}$
	2	+2	$+\frac{1}{2}$
			$-\frac{1}{2}$
		+1	$+\frac{1}{2}$
			$-\frac{1}{2}$
		0	$+\frac{1}{2}$
			$-\frac{1}{2}$
		-1	$+\frac{1}{2}$
			$-\frac{1}{2}$
-2			$+\frac{1}{2}$
			$-\frac{1}{2}$

We can imagine ourselves building a nucleus by adding protons and neutrons. These will always fill the lowest available level. Thus the first two protons fill level zero, the next six protons fill level one, and so on. As with electrons in the periodic table, protons in the outermost shell will be relatively loosely bound to the nucleus if there are only few protons in that shell, because they are farthest from the center of the nucleus. Therefore, nuclei which have a full outer proton shell will have a higher binding energy than other nuclei with a similar total number of protons. All this is true for neutrons as well.

This means that the magic numbers are expected to be those in which all occupied shells are full. We see that for the first two numbers we get 2 (level 0 full) and 8 (levels 0 and 1 full), in accord with experiment. However the full set of magic numbers does not turn out correctly. These can be computed as follows:

In a three-dimensional harmonic oscillator the total degeneracy at level n is:

$$\frac{(n+1)(n+2)}{2}$$

Due to the spin, the degeneracy is doubled and is $(n+1)(n+2)$. Thus, the magic numbers would be:

$$\sum_{n=0}^k (n+1)(n+2) = \frac{(k+1)(k+2)(k+3)}{3}$$

For all integer k . This gives the following magic numbers: 2, 8, 20, 40, 70, 112, ..., etc. which agree with experiment only in the first three entries. These numbers are twice the tetrahedral numbers (1, 4, 10, 20, 35, 56, ..., etc.) from the Pascal Triangle.

In particular, the first six shells are:

- Level 0: 2 states ($\ell = 0$) = 2.
- Level 1: 6 states ($\ell = 1$) = 6.
- Level 2: 2 states ($\ell = 0$) + 10 states ($\ell = 2$) = 12.
- Level 3: 6 states ($\ell = 1$) + 14 states ($\ell = 3$) = 20.
- Level 4: 2 states ($\ell = 0$) + 10 states ($\ell = 2$) + 18 states ($\ell = 4$) = 30.
- Level 5: 6 states ($\ell = 1$) + 14 states ($\ell = 3$) + 22 states ($\ell = 5$) = 42.

Where for every ℓ there are $2\ell+1$ different values of m_l and 2 values of m_s , giving a total of $4\ell+2$ states for every specific level.

These numbers are twice the values of triangular numbers from the Pascal Triangle: 1, 3, 6, 10, 15, 21, ..., etc.

Including a Spin-orbit Interaction

We next include a spin-orbit interaction. First we have to describe the system by the quantum numbers j , m_j and parity instead of ℓ , m_ℓ and m_s , as in the hydrogen-like atom. Since every even level includes only even values of ℓ , it includes only states of even (positive) parity. Similarly, every odd level includes only states of odd (negative) parity. Thus we can ignore parity in counting states. The first six shells, described by the new quantum numbers, are:

- Level 0 ($n = 0$): 2 states ($j = \frac{1}{2}$). Even parity.
- Level 1 ($n = 1$): 2 states ($j = \frac{1}{2}$) + 4 states ($j = \frac{3}{2}$) = 6. Odd parity.
- Level 2 ($n = 2$): 2 states ($j = \frac{1}{2}$) + 4 states ($j = \frac{3}{2}$) + 6 states ($j = \frac{5}{2}$) = 12. Even parity.
- Level 3 ($n = 3$): 2 states ($j = \frac{1}{2}$) + 4 states ($j = \frac{3}{2}$) + 6 states ($j = \frac{5}{2}$) + 8 states ($j = \frac{7}{2}$) = 20. Odd parity.
- Level 4 ($n = 4$): 2 states ($j = \frac{1}{2}$) + 4 states ($j = \frac{3}{2}$) + 6 states ($j = \frac{5}{2}$) + 8 states ($j = \frac{7}{2}$) + 10 states ($j = \frac{9}{2}$) = 30. Even parity.
- Level 5 ($n = 5$): 2 states ($j = \frac{1}{2}$) + 4 states ($j = \frac{3}{2}$) + 6 states ($j = \frac{5}{2}$) + 8 states ($j = \frac{7}{2}$) + 10 states ($j = \frac{9}{2}$) + 12 states ($j = \frac{11}{2}$) = 42. Odd parity.

Where for every j there are $2j+1$ different state from different values of m_j .

Due to the spin-orbit interaction the energies of states of the same level but with different j will no longer be identical. This is because in the original quantum numbers, when \vec{s} is parallel to \vec{l} , the interaction energy is positive; and in this case $j = \ell + s = \ell + \frac{1}{2}$. When \vec{s} is anti-parallel to \vec{l} (i.e. aligned oppositely), the interaction energy is negative, and in this case $j = \ell - s = \ell - \frac{1}{2}$. Furthermore, the strength of the interaction is roughly proportional to ℓ .

For example, consider the states at level 4:

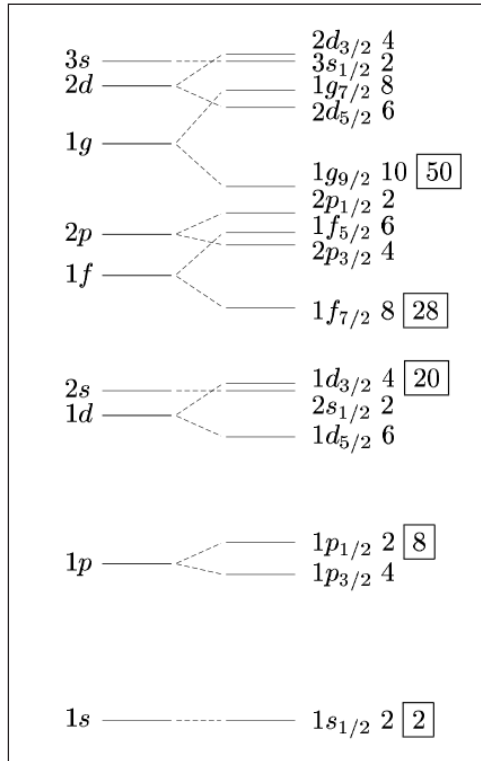
- The 10 states with $j = \frac{9}{2}$ come from $\ell = 4$ and s parallel to ℓ . Thus they have a positive spin-orbit interaction energy.
- The 8 states with $j = \frac{7}{2}$ came from $\ell = 4$ and s anti-parallel to ℓ . Thus they have a negative spin-orbit interaction energy.
- The 6 states with $j = \frac{5}{2}$ came from $\ell = 2$ and s parallel to ℓ . Thus they have a positive spin-orbit interaction energy. However its magnitude is half compared to the states with $j = \frac{9}{2}$.
- The 4 states with $j = \frac{3}{2}$ came from $\ell = 2$ and s anti-parallel to ℓ . Thus they have a negative spin-orbit interaction energy. However its magnitude is half compared to the states with $j = \frac{7}{2}$.

- The 2 states with $j = \frac{1}{2}$ came from $\ell = 0$ and thus have zero spin-orbit interaction energy.

Changing the Profile of the Potential

The harmonic oscillator potential $V(r) = \mu\omega^2 r^2 / 2$ grows infinitely as the distance from the center r goes to infinity. A more realistic potential, such as Woods–Saxon potential, would approach a constant at this limit. One main consequence is that the average radius of nucleons’ orbits would be larger in a realistic potential; this leads to a reduced term $\hbar^2 l(l+1) / 2mr^2$ in the Laplace operator of the Hamiltonian. Another main difference is that orbits with high average radii, such as those with high n or high ℓ , will have a lower energy than in a harmonic oscillator potential. Both effects lead to a reduction in the energy levels of high ℓ orbits.

Predicted Magic Numbers



Low-lying energy levels in a single-particle shell model with an oscillator potential (with a small negative l^2 term) without spin-orbit (left) and with spin-orbit (right) interaction. The number to the right of a level indicates its degeneracy, $(2j+1)$. The boxed integers indicate the magic numbers.

Together with the spin-orbit interaction, and for appropriate magnitudes of both effects, one is led to the following qualitative picture: At all levels, the highest j states have their energies shifted downwards, especially for high n (where the highest j is high). This is both due to the negative spin-orbit interaction energy and to the reduction in energy

resulting from deforming the potential to a more realistic one. The second-to-highest j states, on the contrary, have their energy shifted up by the first effect and down by the second effect, leading to a small overall shift. The shifts in the energy of the highest j states can thus bring the energy of states of one level to be closer to the energy of states of a lower level. The “shells” of the shell model are then no longer identical to the levels denoted by n , and the magic numbers are changed.

We may then suppose that the highest j states for $n = 3$ have an intermediate energy between the average energies of $n = 2$ and $n = 3$, and suppose that the highest j states for larger n (at least up to $n = 7$) have an energy closer to the average energy of $n-1$. Then we get the following shells.

- 1st shell: 2 states ($n = 0, j = 1/2$).
- 2nd shell: 6 states ($n = 1, j = 1/2$ or $3/2$).
- 3rd shell: 12 states ($n = 2, j = 1/2, 3/2$ or $5/2$).
- 4th shell: 8 states ($n = 3, j = 7/2$).
- 5th shell: 22 states ($n = 3, j = 1/2, 3/2$ or $5/2$; $n = 4, j = 9/2$).
- 6th shell: 32 states ($n = 4, j = 1/2, 3/2, 5/2$ or $7/2$; $n = 5, j = 11/2$).
- 7th shell: 44 states ($n = 5, j = 1/2, 3/2, 5/2, 7/2$ or $9/2$; $n = 6, j = 13/2$).
- 8th shell: 58 states ($n = 6, j = 1/2, 3/2, 5/2, 7/2, 9/2$ or $11/2$; $n = 7, j = 15/2$) and so on.

Note that the numbers of states after the 4th shell are doubled triangular numbers plus two. Spin-orbit coupling causes so-called ‘intruder levels’ to drop down from the next higher shell into the structure of the previous shell. The sizes of the intruders are such that the resulting shell sizes are themselves increased to the very next higher doubled triangular numbers from those of the harmonic oscillator. For example, $1f2p$ has 20 nucleons, and spin-orbit coupling adds $1g^{9/2}$ (10 nucleons) leading to a new shell with 30 nucleons. $1g2d3s$ has 30 nucleons, and addition of intruder $1h11/2$ (12 nucleons) yields a new shell size of 42, and so on.

The magic numbers are then:

- 2
- $8=2+6$
- $20=2+6+12$
- $28=2+6+12+8$
- $50=2+6+12+8+22$

- $82=2+6+12+8+22+32$
- $126=2+6+12+8+22+32+44$
- $184=2+6+12+8+22+32+44+58$ and so on.

This gives all the observed magic numbers, and also predicts a new one (the so-called island of stability) at the value of 184 (for protons, the magic number 126 has not been observed yet, and more complicated theoretical considerations predict the magic number to be 114 instead).

Another way to predict magic (and semi-magic) numbers is by laying out the idealized filling order (with spin-orbit splitting but energy levels not overlapping). For consistency s is split into $j = 1/2$ and $j = -1/2$ components with 2 and 0 members respectively. Taking leftmost and rightmost total counts within sequences marked bounded by/here gives the magic and semi-magic numbers.

- $s(2, 0)/p(4, 2) > 2, 2/6, 8$, so (semi)magic numbers 2, 2/6, 8.
- $d(6, 4):s(2, 0)/f(8, 6):p(4, 2) > 14, 18:20, 20/28, 34:38, 40$, so 14, 20/28, 40.
- $g(10, 8):d(6, 4):s(2, 0)/h(12, 10):f(8, 6):p(4, 2) > 50, 58, 64, 68, 70, 70/82, 92, 100, 106, 110, 112$, so 50, 70/82, 112.
- $i(14, 12):g(10, 8):d(6, 4):s(2, 0)/j(16, 14):h(12, 10):f(8, 6):p(4, 2) > 126, 138, 148, 156, 162, 166, 168, 168/184, 198, 210, 220, 228, 234, 238, 240$, so 126, 168/184, 240.

The rightmost predicted magic numbers of each pair within the quartets bisected by/are double tetrahedral numbers from the Pascal Triangle: 2, 8, 20, 40, 70, 112, 168, 240 are $2 \times 1, 4, 10, 20, 35, 56, 84, 120, \dots$ and the leftmost members of the pairs differ from the rightmost by double triangular numbers: $2 - 2 = 0, 8 - 6 = 2, 20 - 14 = 6, 40 - 28 = 12, 70 - 50 = 20, 112 - 82 = 30, 168 - 126 = 42, 240 - 184 = 56$, where 0, 2, 6, 12, 20, 30, 42, 56, ... are $2 \times 0, 1, 3, 6, 10, 15, 21, 28, \dots$

Other Properties of Nuclei

This model also predicts or explains with some success other properties of nuclei, in particular spin and parity of nuclei ground states, and to some extent their excited states as well. Take $^{17}_8\text{O}$ (oxygen-17) as an example: Its nucleus has eight protons filling the three first proton “shells”, eight neutrons filling the three first neutron “shells”, and one extra neutron. All protons in a complete proton shell have total angular momentum zero, since their angular momenta cancel each other. The same is true for neutrons. All protons in the same level (n) have the same parity (either +1 or -1), and since the parity of a pair of particles is the product of their parities, an even number of protons from the same level (n) will have +1 parity. Thus the total angular momentum

of the eight protons and the first eight neutrons is zero, and their total parity is $+1$. This means that the spin (i.e. angular momentum) of the nucleus, as well as its parity, are fully determined by that of the ninth neutron. This one is in the first (i.e. lowest energy) state of the 4th shell, which is a d-shell ($\ell = 2$), and since $p = (-1)^\ell$, this gives the nucleus an overall parity of $+1$. This 4th d-shell has a $j = 5/2$, thus the nucleus of $^{17}_8\text{O}$ is expected to have positive parity and total angular momentum $5/2$, which indeed it has.

The rules for the ordering of the nucleus shells are similar to Hund's Rules of the atomic shells, however, unlike its use in atomic physics the completion of a shell is not signified by reaching the next n , as such the shell model cannot accurately predict the order of excited nuclei states, though it is very successful in predicting the ground states. The order of the first few terms are listed as follows: $1s$, $1p^{3/2}$, $1p^{1/2}$, $1d^{5/2}$, $2s$, $1d^{3/2}$, ..., etc.

For nuclei farther from the magic numbers one must add the assumption that due to the relation between the strong nuclear force and angular momentum, protons or neutrons with the same n tend to form pairs of opposite angular momenta. Therefore, a nucleus with an even number of protons and an even number of neutrons has 0 spin and positive parity. A nucleus with an even number of protons and an odd number of neutrons (or vice versa) has the parity of the last neutron (or proton), and the spin equal to the total angular momentum of this neutron (or proton). By "last" we mean the properties coming from the highest energy level.

In the case of a nucleus with an odd number of protons and an odd number of neutrons, one must consider the total angular momentum and parity of both the last neutron and the last proton. The nucleus parity will be a product of theirs, while the nucleus spin will be one of the possible results of the sum of their angular momenta (with other possible results being excited states of the nucleus).

The ordering of angular momentum levels within each shell is according to the principles - due to spin-orbit interaction, with high angular momentum states having their energies shifted downwards due to the deformation of the potential (i.e. moving from a harmonic oscillator potential to a more realistic one). For nucleon pairs, however, it is often energetically favorable to be at high angular momentum, even if its energy level for a single nucleon would be higher. This is due to the relation between angular momentum and the strong nuclear force.

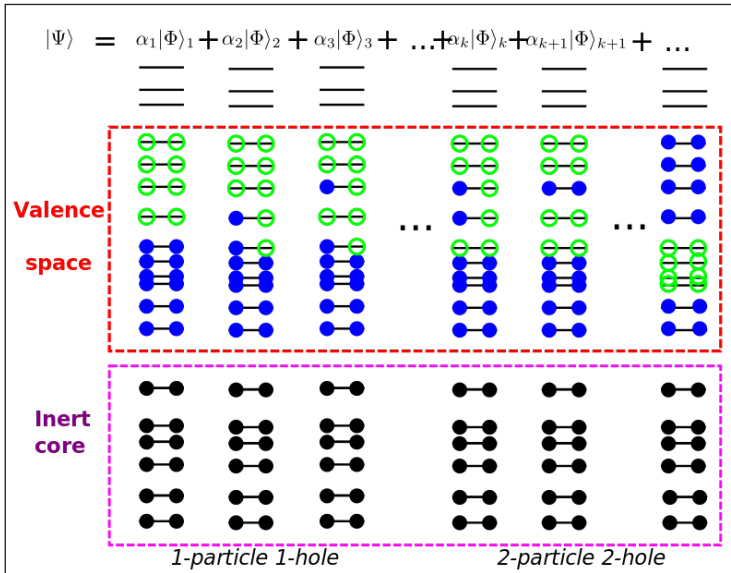
Nuclear magnetic moment is partly predicted by this simple version of the shell model. The magnetic moment is calculated through j , ℓ and s of the "last" nucleon, but nuclei are not in states of well-defined ℓ and s . Furthermore, for odd-odd nuclei, one has to consider the two "last" nucleons, as in deuterium. Therefore, one gets several possible answers for the nuclear magnetic moment, one for each possible combined ℓ and s state, and the real state of the nucleus is a superposition of them. Thus the real (measured) nuclear magnetic moment is somewhere in between the possible answers.

The electric dipole of a nucleus is always zero, because its ground state has a definite

parity, so its matter density (ψ^2 , where ψ is the wavefunction) is always invariant under parity. This is usually the situations with the atomic electric dipole as well.

Higher electric and magnetic multipole moments cannot be predicted by this simple version of the shell model, for the reasons similar to those in the case of deuterium.

Including Residual Interactions



Residual interactions among valence nucleons are included by diagonalising an effective Hamiltonian in a valence space outside an inert core. As indicated, only single-particle states lying in the valence space are active in the basis used.

For nuclei having two or more valence nucleons (i.e. nucleons outside a closed shell) a residual two-body interaction must be added. This residual term comes from the part of the inter-nucleon interaction not included in the approximative average potential. Through this inclusion different shell configurations are mixed and the energy degeneracy of states corresponding to the same configuration is broken.

These residual interactions are incorporated through shell model calculations in a truncated model space (or valence space). This space is spanned by a basis of many-particle states where only single-particle states in the model space are active. The Schrödinger equation is solved in this basis, using an effective Hamiltonian specifically suited for the model space. This Hamiltonian is different from the one of free nucleons as it among other things has to compensate for excluded configurations.

One can do away with the average potential approximation entirely by extending the model space to the previously inert core and treat all single-particle states up to the model space truncation as active. This forms the basis of the no-core shell model, which is an ab initio method. It is necessary to include a three-body interaction in such calculations to achieve agreement with experiments.

Collective Rotation and the Deformed Potential

In 1953, the first experimental examples were found of rotational bands in nuclei, with their energy levels following the same $J(J+1)$ pattern of energies as in rotating molecules. Quantum mechanically, it is impossible to have a collective rotation of a sphere, so this implied that the shape of these nuclei was nonspherical. In principle, these rotational states could have been described as coherent superpositions of particle-hole excitations in the basis consisting of single-particle states of the spherical potential. But in reality, the description of these states in this manner is intractable, due to the large number of valence particles and this intractability was even greater in the 1950s, when computing power was extremely rudimentary. For these reasons, Aage Bohr, Ben Mottelson, and Sven Gösta Nilsson constructed models in which the potential was deformed into an ellipsoidal shape. The first successful model of this type is the one now known as the Nilsson model. It is essentially the harmonic oscillator model, but with anisotropy added, so that the oscillator frequencies along the three Cartesian axes are not all the same. Typically the shape is a prolate ellipsoid, with the axis of symmetry taken to be z . Because the potential is not spherically symmetric, the single-particle states are not states of good angular momentum J . However, a Lagrange multiplier $-\omega \cdot J$, known as a “cranking” term, can be added to the Hamiltonian. Usually the angular frequency vector ω is taken to be perpendicular to the symmetry axis, although tilted-axis cranking can also be considered. Filling the single-particle states up to the Fermi level then produces states whose expected angular momentum along the cranking axis J_x is the desired value.

Related Models

Igal Talmi developed a method to obtain the information from experimental data and use it to calculate and predict energies which have not been measured. This method has been successfully used by many nuclear physicists and has led to deeper understanding of nuclear structure. The theory which gives a good description of these properties was developed. This description turned out to furnish the shell model basis of the elegant and successful interacting boson model.

A model derived from the nuclear shell model is the alpha particle model developed by Henry Margenau, Edward Teller, J. K. Perin, T. H. Skyrme, also sometimes called the Skyrme model. Note, however, that the Skyrme model is usually taken to be a model of the nucleon itself, as a “cloud” of mesons (pions), rather than as a model of the nucleus as a “cloud” of alpha particles.

NUCLEAR SHELL MODEL

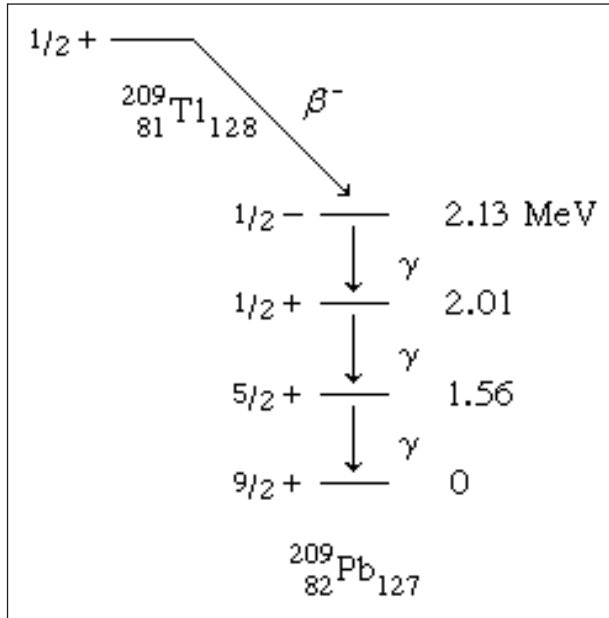
The overall trends of nuclear binding energies were described in terms of a charged-liquid-drop model. Yet there were noted periodic binding-energy irregularities at the

magic numbers. The periodic occurrence of magic numbers of extra stability is strongly analogous to the extra electronic stabilities occurring at the atomic numbers of the noble-gas atoms. The explanations of these stabilities are quite analogous in atomic and nuclear cases as arising from filling of particles into quantized orbitals of motion. The completion of filling of a shell of orbitals is accompanied by an extra stability. The nuclear model accounting for the magic numbers is the shell model. In its simplest form, this model can account for the occurrence of spin zero for all even–even nuclear ground states; the nucleons fill pairwise into orbitals with angular momenta canceling. The shell model also readily accounts for the observed nuclear spins of the odd-mass nuclei adjacent to doubly magic nuclei, such as $^{208}_{82}\text{Pb}$. Here, the spins of $1/2$ for neighbouring $^{207}_{81}\text{Tl}$ and $^{207}_{82}\text{Pb}$ are accounted for by having all nucleons fill pairwise into the lowest energy orbits and putting the odd nucleon into the last available orbital before reaching the doubly magic configuration (the Pauli exclusion principle dictates that no more than two nucleons may occupy a given orbital, and their spins must be oppositely directed); calculations show the last available orbitals below lead-208 to have angular momentum $1/2$. Likewise, the spins of $9/2$ for $^{209}_{82}\text{Pb}$ and $^{209}_{83}\text{Bi}$ are understandable because spin- $9/2$ orbitals are the next available orbitals beyond doubly magic lead-208. Even the associated magnetization, as expressed by the magnetic dipole moment, is rather well explained by the simple spherical-shell model.

The orbitals of the spherical-shell model are labeled in a notation close to that for electronic orbitals in atoms. The orbital configuration of calcium-40 has protons and neutrons filling the following orbitals: $1s_{1/2}$, $1p_{3/2}$, $1p_{1/2}$, $1d_{5/2}$, and $1d_{3/2}$. The letter denotes the orbital angular momentum in usual spectroscopic notation, in which the letters s , p , d , f , g , h , i , etc., represent integer values of l running from zero for s through six for i . The fractional subscript gives the total angular momentum j with values of $l + 1/2$ and $l - 1/2$ allowed, as the intrinsic spin of a nucleon is $1/2$. The first integer is a radial quantum number taking successive values 1, 2, 3, etc., for successively higher energy values of an orbital of given l and j . Each orbital can accommodate a maximum of $2j + 1$ nucleons. The exact order of various orbitals within a shell differs somewhat for neutrons and protons. The parity associated with an orbital is even (+) if l is even (s , d , g , i) and odd (–) if l is odd (p , f , h).

Spherical-shell-model orbitals	
Shell closure number	
2	$1s_{1/2}$
8	$1p_{3/2}$, $1p_{1/2}$
20	$1d_{5/2}$, $2s_{1/2}$, $1d_{3/2}$
28	$1f_{7/2}$
50	$2p_{3/2}$, $1f_{5/2}$, $2p_{1/2}$, $1g_{9/2}$
82	$1g_{7/2}$, $2d_{5/2}$, $1h_{11/2}$, $2d_{3/2}$, $3s_{1/2}$
126	$2f_{7/2}$, $1h_{9/2}$, $1i_{13/2}$, $3p_{3/2}$, $2f_{5/2}$, $3p_{1/2}$
184 (?)	$2g_{9/2}$, $1i_{11/2}$, $1j_{15/2}$, $3d_{5/2}$, $2g_{7/2}$, $4s_{1/2}$, $3d_{3/2}$

An example of a spherical-shell-model interpretation is provided by the beta-decay scheme of 2.2-minute thallium-209 shown below, in which spin and parity are given for each state. The ground and lowest excited states of lead-209 are to be associated with occupation by the 127th neutron of the lowest available orbitals above the closed shell of 126. From the last line of the table, it is to be noted that there are available $g_{9/2}$, $d_{5/2}$, and $s_{1/2}$ orbitals with which to explain the ground and first two excited states. Low-lying states associated with the $i_{11/2}$ and $j_{15/2}$ orbitals are known from nuclear-reaction studies, but they are not populated in the beta decay.



The 2.13-MeV state that receives the primary beta decay is not so simply interpreted as the other states. It is to be associated with the promotion of a neutron from the $3p_{1/2}$ orbital below the 126 shell closure. The density (number per MeV) of states increases rapidly above this excitation, and the interpretations become more complex and less certain.

By suitable refinements, the spherical-shell model can be extended further from the doubly magic region. Primarily, it is necessary to drop the approximation that nucleons move independently in orbitals and to invoke a residual force, mainly short-range and attractive, between the nucleons. The spherical-shell model augmented by residual interactions can explain and correlate around the magic regions a large amount of data on binding energies, spins, magnetic moments, and the spectra of excited states.

Nuclear Fission and Fusion

3

CHAPTER

Nuclear fission is a radioactive decay process in nuclear physics in which an atomic nuclei breaks down into two or more atomic nuclei. Nuclear fusion is a nuclear reaction in which two or more atomic nuclei combine to form a greater nucleus. The topics elaborated in this chapter will help in gaining a better perspective of nuclear fission and fusion.

NUCLEAR FISSION

Nuclear fission is the subdivision of a heavy atomic nucleus that of uranium or plutonium, into two fragments of roughly equal mass. The process is accompanied by the release of a large amount of energy.

In nuclear fission the nucleus of an atom breaks up into two lighter nuclei. The process may take place spontaneously in some cases or may be induced by the excitation of the nucleus with a variety of particles (e.g., neutrons, protons, deuterons, or alpha particles) or with electromagnetic radiation in the form of gamma rays. In the fission process, a large quantity of energy is released, radioactive products are formed, and several neutrons are emitted. These neutrons can induce fission in a nearby nucleus of fissionable material and release more neutrons that can repeat the sequence, causing a chain reaction in which a large number of nuclei undergo fission and an enormous amount of energy is released. If controlled in a nuclear reactor, such a chain reaction can provide power for society's benefit. If uncontrolled, as in the case of the so-called atomic bomb, it can lead to an explosion of awesome destructive force.

The discovery of nuclear fission has opened a new era—the “Atomic Age.” The potential of nuclear fission for good or evil and the risk/benefit ratio of its applications have not only provided the basis of many sociological, political, economic, and scientific advances but grave concerns as well. Even from a purely scientific perspective, the process of nuclear fission has given rise to many puzzles and complexities, and a complete theoretical explanation is still not at hand.

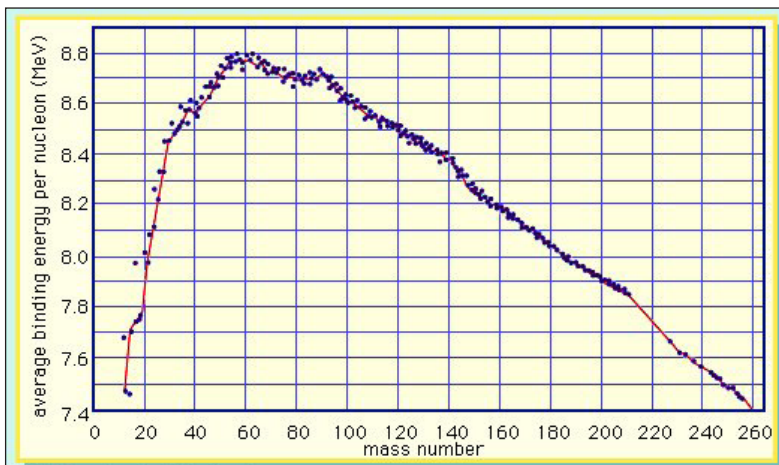
Fundamentals of the Fission Process

Structure and Stability of Nuclear Matter

The fission process may be best understood through a consideration of the structure and stability of nuclear matter. Nuclei consist of nucleons (neutrons and protons), the

total number of which is equal to the mass number of the nucleus. The actual mass of a nucleus is always less than the sum of the masses of the free neutrons and protons that constitute it, the difference being the mass equivalent of the energy of formation of the nucleus from its constituents. The conversion of mass to energy follows Einstein's equation, $E = mc^2$, where E is the energy equivalent of a mass, m , and c is the velocity of light. This difference is known as the mass defect and is a measure of the total binding energy (and, hence, the stability) of the nucleus. This binding energy is released during the formation of a nucleus from its constituent nucleons and would have to be supplied to the nucleus to decompose it into its individual nucleon components.

A curve illustrating the average binding energy per nucleon as a function of the nuclear mass number is shown in figure. The largest binding energy (highest stability) occurs near mass number 56—the mass region of the element iron. Figure indicates that any nucleus heavier than mass number 56 would become a more stable system by breaking into lighter nuclei of higher binding energy, the difference in binding energy being released in the process. (It should be noted that nuclei lighter than mass number 56 can gain in stability by fusing to produce a heavier nucleus of greater mass defect—again, with the release of the energy equivalent of the mass difference. It is the fusion of the lightest nuclei that provides the energy released by the Sun and constitutes the basis of the hydrogen, or fusion, bomb. Efforts to harness fusion reaction for power production have been actively pursued).

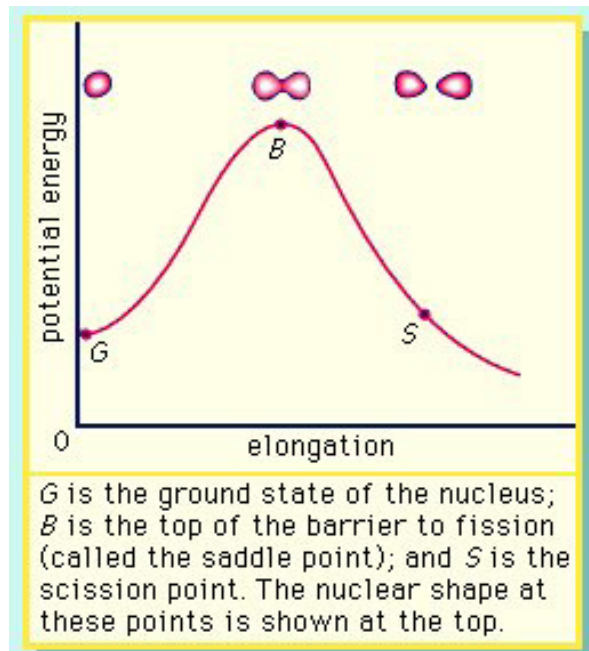


The average binding energy per nucleon as a function of the mass number, A . The line connects the odd- A points.

On the basis of energy considerations alone, figure would indicate that all matter should seek its most stable configuration, becoming nuclei of mass number near 56. However, this does not happen, because barriers to such a spontaneous conversion are provided by other factors. A good qualitative understanding of the nucleus is achieved by treating it as analogous to a uniformly charged liquid drop. The strong attractive nuclear force between pairs of nucleons is of short range and acts only between the closest neighbours. Since nucleons near the surface of the drop have fewer close neighbours

than those in the interior, a surface tension is developed, and the nuclear drop assumes a spherical shape in order to minimize this surface energy. (The smallest surface area enclosing a given volume is provided by a sphere). The protons in the nucleus exert a long-range repulsive (Coulomb) force on each other because of their positive charge. As the number of nucleons in a nucleus increases beyond about 40, the number of protons must be diluted with an excess of neutrons to maintain relative stability.

If the nucleus is excited by some stimulus and begins to oscillate (i.e., deform from its spherical shape), the surface forces will increase and tend to restore it to a sphere, where the surface tension is at a minimum. On the other hand, the Coulomb repulsion decreases as the drop deforms and the protons are positioned farther apart. These opposing tendencies set up a barrier in the potential energy of the system, as indicated in figure.



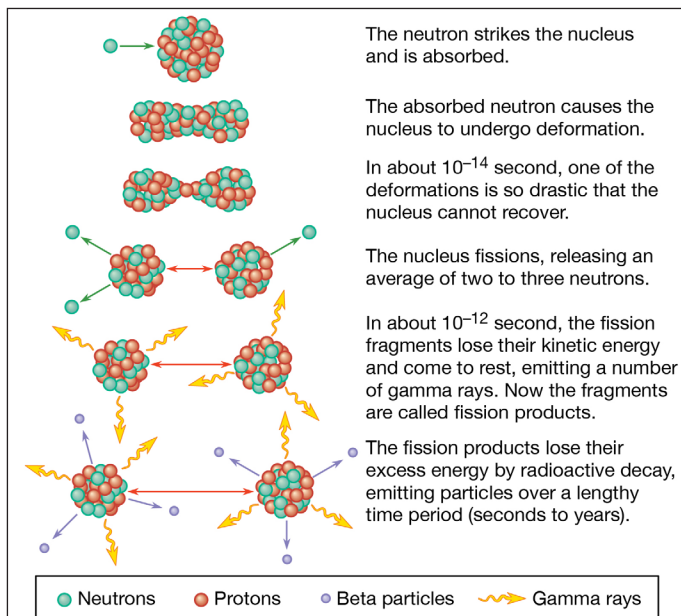
The potential energy as a function of elongation of a fissioning nucleus. G is the ground state of the nucleus; B is the top of the barrier to fission (called the saddle point); and S is the scission point. The nuclear shape at these points is shown at the top.

The curve in figure rises initially with elongation, since the strong, short-range nuclear force that gives rise to the surface tension increases. The Coulomb repulsion between protons decreases faster with elongation than the surface tension increases, and the two are in balance at point B, which represents the height of the barrier to fission. (This point is called the “saddle point” because, in a three-dimensional view of the potential energy surface, the shape of the pass over the barrier resembles a saddle.) Beyond point B, the Coulomb repulsion between the protons drives the nucleus into further elongation until at some point, S (the scission point), the nucleus breaks in two. Qualitatively, at least, the fission process is thus seen to be a consequence of the Coulomb repulsion between protons.

Induced Fission

The height and shape of the fission barrier are dependent on the particular nucleus being considered. Fission can be induced by exciting the nucleus to energy equal to or greater than that of the barrier. This can be done by gamma-ray excitation (photofission) or through excitation of the nucleus by the capture of a neutron, proton, or other particle (particle-induced fission). The binding energy of a particular nucleon to a nucleus will depend on—in addition to the factors considered above—the odd–even character of the nucleus. Thus, if a neutron is added to a nucleus having an odd number of neutrons, an even number of neutrons will result, and the binding energy will be greater than for the addition of a neutron that makes the total number of neutrons odd. This “pairing energy” accounts in part for the difference in behaviour of nuclides in which fission can be induced with slow (low-energy) neutrons and those that require fast (higher-energy) neutrons. Although the heavy elements are unstable with respect to fission, the reaction takes place to an appreciable extent only if sufficient energy of activation is available to surmount the fission barrier. Most nuclei that are fissionable with slow neutrons contain an odd number of neutrons (e.g., uranium-233, uranium-235, or plutonium-239), whereas most of those requiring fast neutrons (e.g., thorium-232 or uranium-238) have an even number. The addition of a neutron in the former case liberates sufficient binding energy to induce fission. In the latter case, the binding energy is less and may be insufficient to surmount the barrier and induce fission. Additional energy must then be supplied in the form of the kinetic energy of the incident neutron. (In the case of thorium-232 or uranium-238, a neutron having about 1 MeV of kinetic energy is required).

The Stages of Fission



Sequence of events in the fission of a uranium nucleus by a neutron.

A pictorial representation of the sequence of events in the fission of a heavy nucleus is given in figure. The approximate time elapse between stages of the process is indicated at the bottom of the figure.

Phenomenology of Fission

When a heavy nucleus undergoes fission, a variety of fragment pairs may be formed, depending on the distribution of neutrons and protons between the fragments. This leads to probability distribution of both mass and nuclear charge for the fragments. The probability of formation of a particular fragment is called its fission yield and is expressed as the percentage of fissions leading to it.

The separated fragments experience a large Coulomb repulsion due to their nuclear charges, and they recoil from each other with kinetic energies determined by the fragment charges and the distance between the charge centres at the time of scission. Variations in these parameters lead to a distribution of kinetic energies, even for the same mass split.

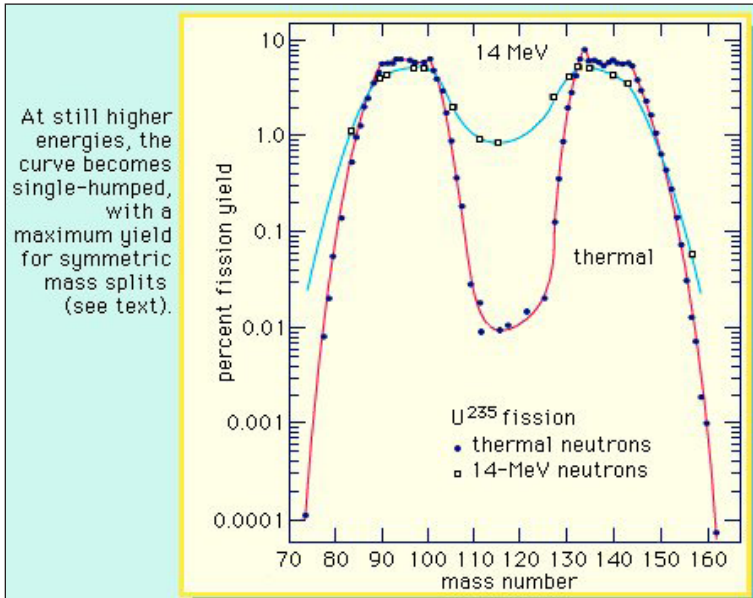
The initial velocities of the recoiling fragments are too fast for the outer (atomic) electrons of the fissioning atom to keep pace, and many of them are stripped away. Thus, the nuclear charge of the fragment is not fully neutralized by the atomic electrons, and the fission fragments fly apart as highly charged atoms. As the nucleus of the fragment adjusts from its deformed shape to a more stable configuration, the deformation energy (i.e., the energy required to deform it) is recovered and converted into internal excitation energy, and neutrons and prompt gamma rays (an energetic form of electromagnetic radiation given off nearly coincident with the fission event) may be evaporated from the moving fragment. The fast-moving, highly charged atom collides with the atoms of the medium through which it is moving, and its kinetic energy is transferred to ionization and heating of the medium as it slows down and comes to rest. The range of fission fragments in air is only a few centimetres.

During the slowing-down process, the charged atom picks up electrons from the medium and becomes neutral by the time it stops. At this stage in the sequence of events, the atom produced is called a fission product to distinguish it from the initial fission fragment formed at scission. Since a few neutrons may have been lost in the transition from fission fragment to fission product, the two may not have the same mass number. The fission product is still not a stable species but is radioactive, and it finally reaches stability by undergoing a series of beta decays, which may vary over a time scale of fractions of a second to many years. The beta emission consists of electrons and anti-neutrinos, often accompanied by gamma rays and X-rays.

The distributions in mass, charge, and kinetic energy of the fragments have been found to be dependent on the fissioning species as well as on the excitation energy at which the fission act occurs. Many other aspects of fission have been observed, adding to the

extensive phenomenology of the process and providing an intriguing set of problems for interpretation. These include the systematics of fission cross sections (a measure of the probability for fission to occur); the variation of the number of prompt neutrons emitted as a function of the fissioning species and the particular fragment mass split; the angular distribution of the fragments with respect to the direction of the beam of particles inducing fission; the systematics of spontaneous fission half-lives; the occurrence of spontaneous fission isomers (excited states of the nucleus); the emission of light particles (hydrogen-3, helium-3, helium-4, etc.) in small but significant numbers in some fission events; the presence of delayed neutron emitters among the fission products; the time scale on which the various stages of the process take place; and the distribution of the energy release in fission among the particles and radiations produced.

Fission Fragment Mass Distributions



Mass distribution dependence on the energy excitation in the fission of uranium-235. At still higher energies, the curve becomes single-humped, with a maximum yield for symmetric mass split.

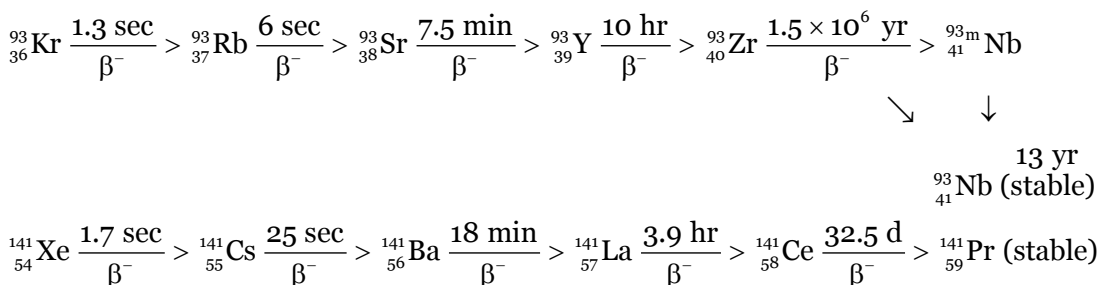
The distribution of the fragment masses formed in fission is one of the most striking features of the process. It is dependent on the mass of the fissioning nucleus and the excitation energy at which the fission occurs. At low excitation energy, the fission of such nuclides as uranium-235 or plutonium-239 is asymmetric; i.e., the fragments are formed in a two-humped probability (or yield) distribution favouring an unequal division in mass. The light group of fragment masses shifts to higher mass numbers as the mass of the fissioning nucleus increases, whereas the position of the heavy group remains nearly stationary. As the excitation energy of the fission increases, the probability for a symmetric mass split increases, while that for asymmetric division decreases. Thus, the valley between the two peaks increases in probability (yield of formation),

and at high excitations the mass distribution becomes single-humped, with the maximum yield at symmetry. Radium isotopes show interesting triple-humped mass distributions, and nuclides lighter than radium show a single-humped, symmetric mass distribution. (These nuclides, however, require a relatively high activation energy to undergo fission.) For very heavy nuclei in the region of fermium-260, the mass-yield curve becomes symmetric (single-humped) even for spontaneous fission, and the kinetic energies of the fragments are unusually high. An understanding of these mass distributions has been one of the major puzzles of fission, and a complete theoretical interpretation is still lacking, albeit much progress has been made.

Fission Decay Chains and Charge Distribution

In order to maintain stability, the neutron-to-proton (n/p) ratio in nuclei must increase with increasing proton number. The ratio remains at unity up to the element calcium, with 20 protons. It then gradually increases until it reaches a value of about 1.5 for the heaviest elements. When a heavy nucleus fissions, a few neutrons are emitted; however, this still leaves too high an n/p ratio in the fission fragments to be consistent with stability for them. They undergo radioactive decay and reach stability by successive conversions of neutrons to protons with the emission of a negative electron (called a beta particle, β^-) and an antineutrino. The mass number of the nucleus remains the same, but the nuclear charge (atomic number) increases by one, and a new element is formed for each such conversion. The successive beta decays constitute an isobaric, fission-product decay chain for each mass number. The half-lives for the decay of the radioactive species generally increase as they approach the stable isobar of the chain. (Species of the same element characterized by the same nuclear charge, Z [number of protons], but differing in their number of neutrons [and therefore in mass number A] are called isotopes. Species that have the same mass number, A , but differ in Z are known as isobars.)

For a typical mass split in the neutron-induced fission of uranium-235, the complementary fission-product masses of 93 and 141 may be formed following the emission of two neutrons from the initial fragments. The division of charge (i.e., protons) between the fragments represents an important parameter in the fission process. Thus, for the mass numbers 93 and 141, the following isobaric fission-product decay chains would be formed (the half-lives for the beta-decay processes are indicated above the arrows):



(The left subscript on the element symbol denotes Z , while the superscript denotes A .) The 92 protons of the uranium nucleus must be conserved and complementary fission-product pairs—such as krypton-36 with barium-56, rubidium-37 with cesium-55, or strontium-38 with xenon-54—would be possible.

The percentage of fissions in which a particular nuclide is formed as a primary fission product (i.e., as the direct descendant of an initial fragment following its de-excitation) is called the independent yield of that product. The total yield for any nuclide in the isobaric decay chain is the sum of its independent yield and the independent yields of all of its precursors in the chain. The total yield for the entire chain is called the cumulative yield for that mass number.

Extensive radiochemical investigations have suggested that the most probable charge division is one that is displaced from stability about the same distance in both chains. This empirical observation is called the equal charge displacement (ECD) hypothesis, and it has been confirmed by several physical measurements. In the above example the ECD would predict the most probable charges at about rubidium-37 and cesium-55. A strong shell effect modifies the ECD expectations for fragments having 50 protons. The dispersion of the charge formation probability about the most probable charge (Z_p) is rather narrow and approximately Gaussian in shape and is nearly independent of the mass split as well as of the fissioning species. The most probable charge for an isobaric chain is a useful concept in the description of the charge dispersion, and it need not have an integral value. As the energy of fission increases, the charge division tends toward maintaining the n/p ratio in the fragments the same as that in the fissioning nucleus. This is referred to as an unchanged charge distribution.

Prompt Neutrons in Fission

The average number of neutrons emitted per fission (represented by the symbol $\bar{\nu}$) varies with the fissioning nucleus. It is about 2.0 for the spontaneous fission of uranium-238 and 4.0 for that of fermium-257. In the thermal-neutron induced fission of uranium-235, $\bar{\nu} = 2.4$. The actual number of neutrons emitted, however, varies with each fission event, depending on the mass split. Although there is still controversy regarding the number of neutrons emitted at the instant of scission, it is generally agreed that most of the neutrons are given off by the recoiling fission fragments soon after scission occurs. The number of neutrons emitted from each fragment depends on the amount of energy the fragment possesses. The energy can be in the form of internal excitation (heat) energy or stored as energy of deformation of the fragment to be released when the fragment returns to its stable equilibrium shape.

Delayed Neutrons in Fission

A few of the fission products have beta-decay energies that exceed the binding energy of a neutron in the daughter nucleus. This is likely to happen when the daughter nucleus

contains one or two neutrons more than a closed shell of 50 or 82 neutrons, since these “extra” neutrons are more loosely bound. The beta decay of the precursor may take place to an excited state of the daughter from which a neutron is emitted. The neutron emission is “delayed” by the beta-decay half-life of the precursor. Six such delayed neutron emitters have been identified, with half-lives varying from about 0.5 to 56 seconds. The yield of the delayed neutrons is only about 1 percent of that of the prompt neutrons, but they are very important for the control of the chain reaction in a nuclear reactor.

Energy Release in Fission

The total energy release in a fission event may be calculated from the difference in the rest masses of the reactants (e.g., $^{235}\text{U} + \text{n}$) and the final stable products (e.g., $^{93}\text{Nb} + ^{141}\text{Pr} + 2\text{n}$). The energy equivalent of this mass difference is given by the Einstein relation, $E = mc^2$. The total energy release depends on the mass split, but a typical fission event would have the total energy release distributed approximately as follows for the major components in the thermal neutron-induced fission of uranium-235:

Energy Components	Number per Fission	Total Energy
Kinetic Energy of Fission Fragments	2	170 MeV
Kinetic Energy of Prompt Neutrons	2.5	5
Binding Energy from Capture of Prompt Neutrons	2.5	~12
Prompt Gamma Rays	8	8
Total = 195 MeV		

(The energy release from the capture of the prompt neutrons depends on how they are finally stopped, and some will escape the core of a nuclear reactor).

This energy is released on a time scale of about 10-12 second and is called the prompt energy release. It is largely converted to heat within an operating reactor and is used for power generation. Also, there is a delayed release of energy from the radioactive decay of the fission products varying in half-life from fractions of a second to many years. The shorter-lived species decay in the reactor, and their energy adds to the heat generated; however, the longer-lived species remain radioactive and pose a problem in the handling and disposition of the reactor fuel elements when they need to be replaced. The antineutrinos that accompany the beta decay of the fission products are unreactive, and their kinetic energy (about 10 MeV per fission) is not recovered. Overall, about 200 MeV of energy per fission may be recovered for power applications.

Fission Theory

Nuclear fission is a complex process that involves the rearrangement of hundreds of nucleons in a single nucleus to produce two separate nuclei. A complete theoretical understanding of this reaction would require a detailed knowledge of the forces involved

in the motion of each of the nucleons through the process. Since such knowledge is still not available, it is necessary to construct simplified models of the actual system to simulate its behaviour and gain as accurate a description as possible of the steps in the process. The successes and failures of the models in accounting for the various observations of the fission process can provide new insights into the fundamental physics governing the behaviour of real nuclei, particularly at the large nuclear deformations encountered in a nucleus undergoing fission.

The framework for understanding nuclear reactions is analogous to that for chemical reactions and involves the concept of a potential-energy surface on which the reaction occurs. The driving force for physical or chemical reactions is the tendency to lower the potential energy and increase the stability of the system. Thus, for example, a stone at the top of a hill will roll down the hill, converting its potential energy at the top to kinetic energy of motion, and will come to rest at the bottom in a more stable state of lower potential energy. The potential energy is calculated as a function of various parameters of the system being studied. In the case of fission, the potential energy may be calculated as a function of the shape of the system as it proceeds over the barrier to the scission point, and the path of lowest potential energy may be determined.

As has been pointed out, an exact calculation of the nuclear potential energy is not yet possible, and it is to approximate this calculation that various models have been constructed to simulate the real system. Some of the models were developed to address aspects of nuclear structure and spectroscopy as well as features of nuclear reactions, and they also have been employed in attempts to understand the complexity of nuclear fission. The models are based on different assumptions and approximations of the nature of the nuclear forces and the dynamics of the path to scission. No one model can account for all of the extensive phenomenology of fission, but each addresses different aspects of the process and provides a foundation for further development toward a complete theory.

Nuclear Models and Nuclear Fission

The nucleus exhibits some properties that reflect the collective motion of all its constituent nucleons as a unit, as well as other properties that are dependent on the motion and state of the individual nucleons.

The analogy of the nucleus to a drop of an incompressible liquid was first suggested by George Gamow in 1935 and later adapted to a description of nuclear reactions and to fission. Bohr proposed the so-called compound nucleus description of nuclear reactions, in which the excitation energy of the system formed by the absorption of a neutron or photon, for example, is distributed among a large number of degrees of freedom of the system. This excited state persists for a long time relative to the periods of motion of nucleons across the nucleus and then decays by emission of radiation, the evaporation of neutrons or other particles, or by fission. The liquid-drop model of the

nucleus accounts quite well for the general collective behaviour of nuclei and provides an understanding of the fission process on the basis of the competition between the cohesive nuclear force and the disruptive Coulomb repulsion between protons. It predicts, however, a symmetric division of mass in fission, whereas an asymmetric mass division is observed. Moreover, it does not provide an accurate description of fission barrier systematics or of the ground-state masses of nuclei. The liquid-drop model is particularly useful in describing the behaviour of highly excited nuclei, but it does not provide an accurate description for nuclei in their ground or low-lying excited states. Many versions of the liquid-drop model employing improved sets of parameters have been developed. However, investigators have found that mass asymmetry and certain other features in fission cannot be adequately described on the basis of the collective behaviour posited by such models alone.

A preference for the formation of unequal masses (i.e., an asymmetric division) was observed early in fission research, and it has remained the most puzzling feature of the process to account for. Investigators have invoked various models other than that of the liquid drop in an attempt to address this question. Dealing with the mutual interaction of all the nucleons in a nucleus has been simplified by treating it as if it were equivalent to the interaction of one particle with an average spherical static potential field that is generated by all the other nucleons. The methods of quantum mechanics provide the solution for the motion of a nucleon in such a potential. A characteristic set of energy levels for neutrons and protons is obtained, and, analogous to the set of levels of the electrons in an atom, the levels group themselves into shells at certain so-called magic numbers of nucleons. (For both neutrons and protons, these numbers are 2, 8, 20, 28, 50, 82, and 126.) Shell closures at these nuclear numbers are marked by especially strong binding, or extra stability. This constitutes the essence of the spherical-shell model (sometimes called the independent-particle, or single-particle, model), as developed by Maria Goeppert Mayer and J. Hans D. Jensen and their colleagues. It accounts well for ground-state masses and spins and for the existence of isomeric nuclear states (excited states having measurable half-lives) that occur when nuclear levels of widely differing spins lie relatively close to each other. The agreement with observations is excellent for spherical nuclei with nucleon numbers near the magic shell numbers. The spherical-shell model, however, does not agree well with the properties of nuclei that have other nucleon numbers—e.g., the nuclei of the lanthanide and actinide elements, with nucleon numbers between the magic numbers.

In the lanthanide and actinide nuclei, the ground state is not spherical but rather deformed into a prolate spheroidal shape—that of a football or watermelon. For such nuclei, the allowed states of motion of a nucleon must be calculated in a potential having a symmetry corresponding to a spheroid rather than a sphere. This was first done by Aage Bohr, Ben R. Mottelson, and Sven G. Nilsson in 1955, and the level structure was calculated as a function of the deformation of the nucleus. A spheroid has three axes of symmetry, and it can rotate in space as a unit about any one of them. The rotation can

occur independent of the internal state of excitation of the individual nucleons. Various modes of vibration of the spheroid also may take place. Since this deformed shell model has components of both the independent-particle motion and the collective motion of the nucleus as a whole (i.e., rotations and vibrations), it is sometimes referred to as the unified model.

In Aage Bohr's application of the unified model to the fission process, the sequence of potential-energy surfaces for the excited states of the system are considered to be functions of a deformation parameter (i.e., elongation) characterizing the motion toward fission and evaluated at the saddle point. As the system passes over the saddle point, most of its excitation energy is used up in deforming the nucleus, and the system remains "cold"; i.e., it manifests little excitation, or heat, energy. Thus, only the low-lying excited states are available to the system. The spin and parity of the particular state (or channel) in which the system exists as it passes over the saddle point are then expected to determine the fission properties. In this channel (or transition-state) analysis of fission, a number of characteristics of the process are qualitatively accounted for. Hence, fission thresholds would depend on the spin and parity of the compound nuclear state, the fission fragment angular distribution would be governed by the collective rotational angular momentum of the state, and asymmetry in the mass distribution would result from passage over the barrier in a state of negative parity (which does not possess reflection symmetry). This model gives a good qualitative interpretation of many fission phenomena, but it must assume that at least some of the properties of the transition state at the saddle point are not altered by dynamical considerations in the descent of the system to the scission point. It is the only model that provides a satisfactory interpretation of the angular distributions of fission fragments, and it has attractive features that must be included in any complete theory of fission.

The first application of the spherical-shell model to fission was the recognition that the positions of the peaks in the fission mass distribution correlated fairly well with the magic numbers and suggested a qualitative interpretation of the asymmetric mass division. Thus, a preference for the formation of nuclei with neutron numbers close to 82 would favour the formation of nuclides near the peak in the heavy group and would thus determine the mass split for the fissioning system. Some extra stability for nuclear configurations of 50 protons would also be expected, but this is not particularly evident. In fact, the so-called doubly magic nucleus tin-132, with 50 protons and 82 neutrons, has a rather low yield in low-energy fission.

A more quantitative application of the spherical-shell model to fission was undertaken by Peter Fong in the United States in 1956. He related the probability of formation of a given pair of fragments to the available density of states for that pair of fragments at the scission point in a statistical-model approach. A model of this sort predicts that the system, in its random motions, will experience all possible configurations and so will have a greater probability of being in the region where the greatest number of such configurations (or states) is concentrated. The model assumes that the potential energy

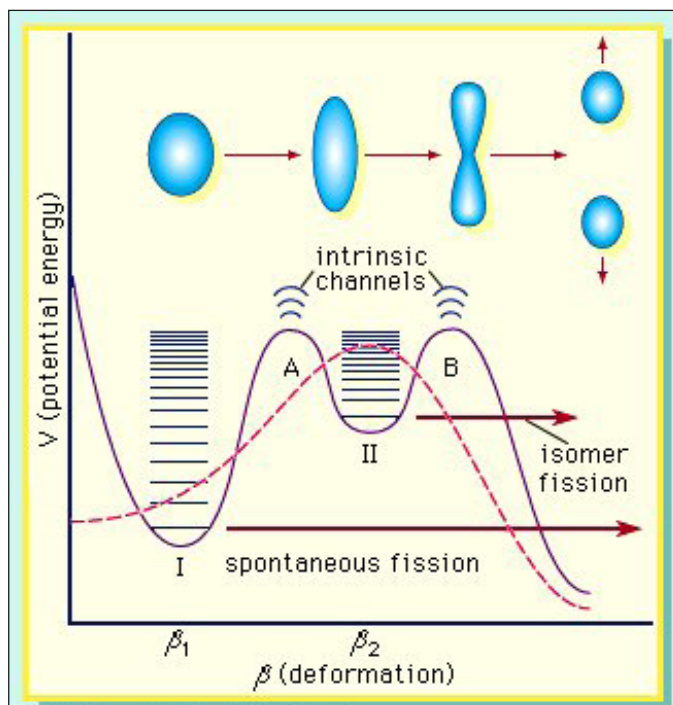
at the saddle point is essentially all converted to excitation energy and that a statistical equilibrium among all possible states is established at the scission point. The extra binding energy for closed-shell nuclei leads to a higher density of states at a given excitation energy than is present for other nuclei and, hence, leads to a higher probability of formation. An asymmetric mass distribution in good agreement with that observed for the neutron-induced fission of uranium-235 is obtained. Moreover, the changes in the mass distribution with increased excitation energy of fission (e.g., an increase in the probability of symmetric fission relative to asymmetric fission) are accounted for by the decrease in importance of the shell effects as the excitation energy increases. Other features of the fission process also are qualitatively explained; however, extensive changes in the parameters of the model are required to obtain agreement with experiments for other fissionable nuclides. Then, too, there are fundamental problems concerning the validity of some of the basic assumptions of the model.

The fundamental question as to the validity of models that evaluate the properties of the system at the scission point (the so-called scission-point models of fission) is whether the system remains long enough at this point on the steep decline of the potential-energy surface for a quasi-equilibrium condition to be established. There is some evidence that such a condition may indeed prevail, but it is not clearly established. Nonetheless, such models have proved quite useful in interpreting observations of mass, charge, and kinetic energy distributions, as well as of neutron emission dependence on fragment mass. It seems very likely that the fragment shell structure plays a significant role in determining the course of the fission process.

Although the single-particle models provide a good description of various aspects of nuclear structure, they are not successful in accounting for the energy of deformation of nuclei (i.e., surface energy), particularly at the large deformations encountered in the fission process. A major breakthrough occurred when a hybrid model incorporating shell effects as a correction to the potential energy of the liquid-drop model was proposed by the Russian physicist V.M. Strutinskii in 1967. This approach retains the dominant collective surface and Coulomb effects while adding shell and pairing corrections that depend on deformation. Shell corrections of several million electron volts are calculated, and these can have a significant effect on a liquid-drop barrier of about 5 MeV. The nucleon numbers at which the shells appear depend on the deformation and may differ from the spherical model magic numbers. In the vicinity of the fission barrier, the shells introduce structure in the liquid-drop potential-energy curve, as illustrated in figure. The relative heights and widths of the two peaks vary with the mass and charge of the fissioning system.

Figure shows schematic illustrations of single-humped and double-humped fission barriers. The former are represented by the dashed line and the latter by the continuous line. Intrinsic excitations in the first and second wells at deformations β_1 and β_2 are designated class I and class II states, respectively. Intrinsic channels at the two barriers also are illustrated. The transition in the shape of the nucleus as a function of

deformation is schematically represented in the upper part of the figure. Spontaneous fission of the ground state and isomeric state occurs from the lowest energy class I and class II states, respectively.



The double-humped barrier provides a satisfactory explanation for a number of puzzling observations in fission. The existence of short-lived, spontaneous fission isomers, for example, is understood as the consequence of the population of states in the second well (class II). These isomers have a much smaller barrier to penetrate and so exhibit a much shorter spontaneous fission half-life. The change in shape associated with these states, as compared to class I states, also hinders a rapid return to the ground state by gamma emission. (Class II states are also called shape isomers.) The systematics of neutron-induced fission cross sections and structure in some fission-fragment angular distributions also find an interpretation in the implications of the double-humped barrier.

The Strutinskii procedure provided a strong stimulus for calculations of the potential-energy surfaces appropriate to fissioning systems, since it provided a consistent and useful prescription for treating both the macroscopic (liquid-drop) and microscopic (single-particle) effects in deformed nuclei. Many calculations of the potential-energy surface employing different model potentials and parameters have been carried out as functions of the shapes of the system. The work of the American nuclear physicists W.J. Swiatecki, James R. Nix, and their collaborators has been particularly noteworthy in such studies, which also include some attempts to treat the dynamical evolution of the fission process.

Calculations for the actinide elements indicate that, at deformations corresponding to the second barrier, the potential energy for asymmetric mass splits is lower than that for symmetric ones; hence, the former are favoured at that stage of the process. For larger deformations, however, a single potential does not represent the incipient formation of two fragments very well. In fact, a discontinuity occurs at the scission point, and the results of the calculation depend on whether the scission configuration is treated as one nucleus or as two separate nuclei.

A two-centre potential may also be used to represent the nature of the forces at work in a fissioning nucleus. In such a model, the potential energy surfaces are represented by two overlapping spheres or spheroids. It is equivalent to a one-centre potential when there is a complete overlap at small deformations, and it has the correct asymptotic behaviour as the nascent fragments separate. This approach indicates a preformation of the final shell structure of the fragments early in the process.

Although the validity of the assumptions inherent in scission-point models may be in question, the results obtained with them are in excellent agreement with observation. Representative of such a model is the Argonne Scission-Point model, which uses a macroscopic-microscopic calculation with deformed fragment shell and pairing corrections to determine the potential energy of a system of two nearly touching spheroids and which includes their interaction in terms of a neck connecting them. Models of this kind provide a simple approach to a highly quantitative and detailed study of the dependence of the probability of formation of a given fragment pair on the neutron and proton number and on the deformation in each fragment. They account very well for the mass, charge, and kinetic-energy distributions and the neutron-emission dependence on mass number for a broad range of fissioning nuclei. The scission-point models, however, do not address questions of fission probability or the angular distributions of the fragments. As the fission-excitation energy increases, the shell correction diminishes and the macroscopic (liquid-drop) behaviour dominates.

Nuclides in the region of fermium-264 have been observed to undergo symmetric fission with unusually high fragment kinetic energies. This appears to be the consequence of the stability for the magic number configurations of 50 protons and 82 neutrons. The formation of two doubly magic fragments of tin-132 is strongly favoured energetically, whereas the formation of only one such fragment in the low-energy fission of uranium or plutonium isotopes is not. The fragments of tin-132 are spherical rather than deformed, and a more compact configuration at the scission point (with the charge centres closer together) leads to higher fragment kinetic energies.

It is evident that shell effects, both in the fissioning system at the saddle point and in the deformed fragments near the scission point, are important in interpreting many of the features of the fission process. The stage of the process at which the various fragment distributions are determined is, however, not clearly established. All the components

of a reasonable understanding of fission seem to be at hand, but they have yet to be synthesized into a complete, dynamic theory.

Considerations of the dynamics of the descent of the system on the potential-energy surface from the saddle point to the scission point involve two extreme points of view. An “adiabatic” approximation may be valid if the collective motion of the system is considered to be so slow—or the coupling between the collective and internal single-particle degrees of freedom (i.e., between macroscopic and microscopic behaviour) so weak—that the fast single-particle motions can readily adjust to the changes in shape of the fissioning nucleus as it progresses toward scission. In this case, the changes in the system take place without the gain or loss of heat energy. The decrease in potential energy between the saddle and scission points will then appear primarily in the collective degrees of freedom at scission and be associated with the kinetic energy of the relative motion of the nascent fragments (referred to as pre-scission kinetic energy). On the other hand, if the collective motion toward scission is relatively fast or the coupling-to-particle motion stronger, collective energy can be transformed into internal excitation (heat) energy of the nucleons. (This is analogous to heating in the motion of a viscous fluid.) In such a “non-adiabatic” process the mixing among the single-particle degrees of freedom may be sufficiently complete that a statistical model may be applicable at the scission point. Both extreme represents an approximation of complex behaviour, and some experimental evidence in support of either interpretation may be advanced. As in most such instances in nature, the truth probably lies somewhere between the extremes, with both playing some role in the fission process.

Fission Chain Reactions and their Control

The emission of several neutrons in the fission process leads to the possibility of a chain reaction if at least one of the fission neutrons induces fission in another fissile nucleus, which in turn fissions and emits neutrons to continue the chain. If more than one neutron is effective in inducing fission in other nuclei, the chain multiplies more rapidly. The condition for a chain reaction is usually expressed in terms of a multiplication factor, k , which is defined as the ratio of the number of fissions produced in one step (or neutron generation) in the chain to the number of fissions in the preceding generation. If k is less than unity, a chain reaction cannot be sustained. If $k = 1$, a steady-state chain reaction can be maintained; and if k is greater than 1, the number of fissions increases at each step, resulting in a divergent chain reaction. The term critical assembly is applied to a configuration of fissionable material for which $k = 1$; if $k > 1$, the assembly is said to be supercritical. A critical assembly might consist of the fissile material in the form of a metal or oxide, a moderator to slow the fission neutrons, and a reflector to scatter neutrons that would otherwise be lost back into the assembly core.

In a fission bomb it is desirable to have k as large as possible and the time between steps in the chain as short as possible so that many fissions occur and a large amount

of energy is generated within a brief period ($\sim 10^{-7}$ second) to produce a devastating explosion. If one kilogram of uranium-235 were to fission, the energy released would be equivalent to the explosion of 20,000 tons of the chemical explosive trinitrotoluene (TNT). In a controlled nuclear reactor, k is kept equal to unity for steady-state operation. A practical reactor, however, must be designed with k somewhat greater than unity. This permits power levels to be increased if desired, as well as allowing for the following: the gradual loss of fuel by the fission process; the buildup of “poisons” among the fission products being formed that absorb neutrons and lower the k value; and the use of some of the neutrons produced for research studies or the preparation of radioactive species for various applications. The value of k is controlled during the operation of a reactor by the positioning of movable rods made of a material that readily absorbs neutrons (i.e., one with a high neutron-capture cross section), such as boron, cadmium, or hafnium. The delayed-neutron emitters among the fission products increase the time between successive neutron generations in the chain reaction and make the control of the reaction easier to accomplish by the mechanical movement of the control rods.

Fission reactors can be classified by the energy of the neutrons that propagate the chain reaction. The most common type, called a thermal reactor, operates with thermal neutrons (those having the same energy distribution as gas molecules at ordinary room temperatures). In such a reactor, the fission neutrons produced (with an average kinetic energy of more than 1 MeV) must be slowed down to thermal energy by scattering from a moderator, usually consisting of ordinary water, heavy water (D_2O), or graphite. In another type, termed an intermediate reactor, the chain reaction is maintained by neutrons of intermediate energy, and a beryllium moderator may be used. In a fast reactor, fast fission neutrons maintain the chain reaction, and no moderator is needed. All of the reactor types require a coolant to remove the heat generated; water, a gas, or a liquid metal may be used for this purpose, depending on the design needs.

Uses of Fission Reactors and Fission Products

A nuclear reactor is essentially a furnace used to produce steam or hot gases that can provide heat directly or drive turbines to generate electricity. Nuclear reactors are employed for commercial electric-power generation throughout much of the world and as a power source for propelling submarines and certain kinds of surface vessels. Another important use for reactors is the utilization of their high neutron fluxes for studying the structure and properties of materials and for producing a broad range of radionuclides, which, along with a number of fission products, have found many different applications. Heat generated by radioactive decay can be converted into electricity through the thermoelectric effect in semiconductor materials and thereby produce what is termed an atomic battery. When powered by either a long-lived beta-emitting fission product (e.g., strontium-90 or promethium-147) or one that emits alpha particles (plutonium-238 or curium-244), these batteries are a particularly useful source of energy for

cardiac pacemakers and for instruments employed in remote unmanned facilities, such as those in outer space, the polar regions of the Earth, or the open seas.

NUCLEAR FISSION PRODUCTS

Nuclear fission products are the atomic fragments left after a large atomic nucleus undergoes nuclear fission. Typically, a large nucleus like that of uranium fissions by splitting into two smaller nuclei, along with a few neutrons, the release of heat energy (kinetic energy of the nuclei), and gamma rays. The two smaller nuclei are the fission products.

About 0.2% to 0.4% of fissions are ternary fissions, producing a third light nucleus such as helium-4 (90%) or tritium (7%).

The fission products themselves are usually unstable and therefore radioactive; due to being relatively neutron-rich for their atomic number, many of them quickly undergo beta decay. This releases additional energy in the form of beta particles, anti-neutrinos, and gamma rays. Thus, fission events normally result in beta and gamma radiation, even though this radiation is not produced directly by the fission event itself.

The produced radionuclides have varying half-lives, and therefore vary in radioactivity. For instance, strontium-89 and strontium-90 are produced in similar quantities in fission, and each nucleus decays by beta emission. But ^{90}Sr has a 30-year half-life and ^{89}Sr a 50.5-day half-life. Thus in the 50.5 days it takes half the ^{89}Sr atoms to decay, emitting the same number of beta particles as there were decays, less than 0.4% of the ^{90}Sr atoms have decayed, emitting only 0.4% of the betas. The radioactive emission rate is highest for the shortest lived radionuclides, although they also decay the fastest. Additionally, less stable fission products are less likely to decay to stable nuclides, instead decaying to other radionuclides, which undergo further decay and radiation emission, adding to the radiation output. It is these short lived fission products that are the immediate hazard of spent fuel, and the energy output of the radiation also generates significant heat which must be considered when storing spent fuel. As there are hundreds of different radionuclides created, the initial radioactivity level fades quickly as short lived radionuclides decay, but never ceases completely as longer lived radionuclides make up more and more of the remaining unstable atoms.

Formation and Decay

The sum of the atomic mass of the two atoms produced by the fission of one fissile atom is always less than the atomic mass of the original atom. This is because some of

the mass is lost as free neutrons, and once kinetic energy of the fission products has been removed (i.e., the products have been cooled to extract the heat provided by the reaction), then the mass associated with this energy is lost to the system also, and thus appears to be “missing” from the cooled fission products.

Since the nuclei that can readily undergo fission are particularly neutron-rich (e.g. 61% of the nucleons in uranium-235 are neutrons), the initial fission products are often more neutron-rich than stable nuclei of the same mass as the fission product (e.g. stable zirconium-90 is 56% neutrons compared to unstable strontium-90 at 58%). The initial fission products therefore may be unstable and typically undergo beta decay to move towards a stable configuration, converting a neutron to a proton with each beta emission. (Fission products do not decay via alpha decay.)

A few neutron-rich and short-lived initial fission products decay by ordinary beta decay (this is the source of perceptible half-life, typically a few tenths of a second to a few seconds), followed by immediate emission of a neutron by the excited daughter-product. This process is the source of so-called delayed neutrons, which play an important role in control of a nuclear reactor.

The first beta decays are rapid and may release high energy beta particles or gamma radiation. However, as the fission products approach stable nuclear conditions, the last one or two decays may have a long half-life and release less energy.

Radioactivity over Time

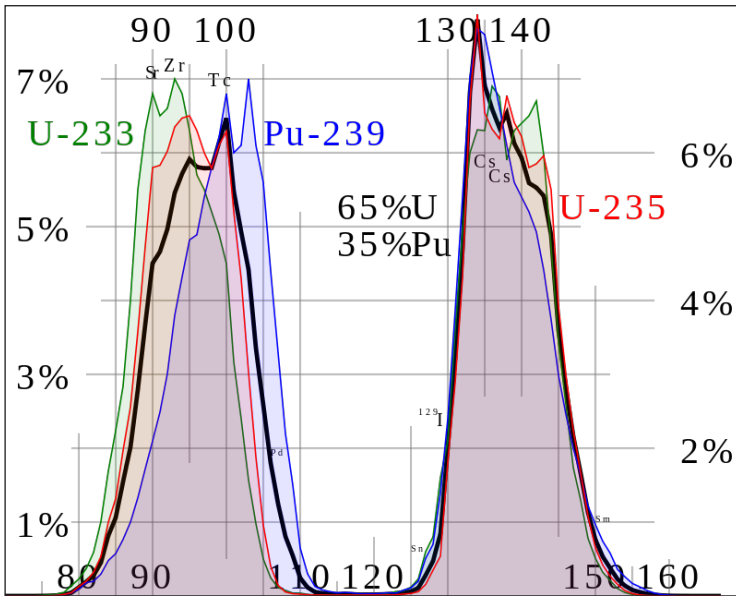
Fission products have half-lives of 90 years (samarium-151) or less, except for seven long-lived fission products that have half-lives of 211,100 years (technetium-99) and more. Therefore, the total radioactivity of a mixture of pure fission products decreases rapidly for the first several hundred years (controlled by the short-lived products) before stabilizing at a low level that changes little for hundreds of thousands of years (controlled by the seven long-lived products).

This behavior of pure fission products with actinides removed, contrasts with the decay of fuel that still contains actinides. This fuel is produced in the so-called “open” (i.e., no nuclear reprocessing) nuclear fuel cycle. A number of these actinides have half lives in the missing range of about 100 to 200,000 years, causing some difficulty with storage plans in this time-range for open cycle non-reprocessed fuels.

Proponents of nuclear fuel cycles which aim to consume all their actinides by fission, such as the Integral Fast Reactor and molten salt reactor, use this fact to claim that within 200 years, their fuel wastes are no more radioactive than the original uranium ore.

Fission products emit beta radiation, while actinides primarily emit alpha radiation. Many of each also emit gamma radiation.

Yield



Fission product yields by mass for thermal neutron fission of U-235, Pu-239, a combination of the two typical of current nuclear power reactors, and U-233 used in the thorium cycle.

Each fission of a parent atom produces a different set of fission product atoms. However, while an individual fission is not predictable, the fission products are statistically predictable. The amount of any particular isotope produced per fission is called its yield, typically expressed as percent per parent fission; therefore, yields total to 200%, not 100%. (The true total is in fact slightly greater than 200%, owing to rare cases of ternary fission).

While fission products include every element from zinc through the lanthanides, the majority of the fission products occur in two peaks. One peak occurs at about (expressed by atomic number) strontium to ruthenium while the other peak is at about tellurium to neodymium. The yield is somewhat dependent on the parent atom and also on the energy of the initiating neutron.

In general the higher the energy of the state that undergoes nuclear fission, the more likely that the two fission products have similar mass. Hence, as the neutron energy increases and/or the energy of the fissile atom increases, the valley between the two peaks becomes shallower. For instance, the curve of yield against mass for ²³⁹Pu has a more shallow valley than that observed for ²³⁵U when the neutrons are thermal neutrons. The curves for the fission of the later actinides tend to make even more shallow valleys. In extreme cases such as ²⁵⁹Fm, only one peak is seen; this is a consequence of symmetric fission becoming dominant due to shell effects.

The adjacent figure shows a typical fission product distribution from the fission of uranium. Note that in the calculations used to make this graph, the activation of fission

products was ignored and the fission was assumed to occur in a single moment rather than a length of time. In this bar chart results are shown for different cooling times — time after fission. Because of the stability of nuclei with even numbers of protons and/or neutrons, the curve of yield against element is not a smooth curve but tends to alternate. Note that the curve against mass number is smooth.

Production

Small amounts of fission products are naturally formed as the result of either spontaneous fission of natural uranium, which occurs at a low rate or as a result of neutrons from radioactive decay or reactions with cosmic ray particles. The microscopic tracks left by these fission products in some natural minerals (mainly apatite and zircon) are used in fission track dating to provide the cooling (crystallization) ages of natural rocks. The technique has an effective dating range of 0.1 Ma to >1.0 Ga depending on the mineral used and the concentration of uranium in that mineral.

About 1.5 billion years ago in a uranium ore body in Africa, a natural nuclear fission reactor operated for a few hundred thousand years and produced approximately 5 tonnes of fission products. These fission products were important in providing proof that the natural reactor had occurred. Fission products are produced in nuclear weapon explosions, with the amount depending on the type of weapon. The largest source of fission products is from nuclear reactors. In current nuclear power reactors, about 3% of the uranium in the fuel is converted into fission products as a by-product of energy generation. Most of these fission products remain in the fuel unless there is fuel element failure or a nuclear accident, or the fuel is reprocessed.

Power Reactors

In commercial nuclear fission reactors, the system is operated in the otherwise self-extinguishing prompt subcritical state. The reactor specific physical phenomenon that nonetheless maintains the temperature above the decay heat level, are the predictably delayed, and therefore easily controlled, transformations or movements of a vital class of fission product as they decay. Delayed neutrons are emitted by neutron rich fission fragments that are called the “delayed neutron precursors.” Bromine-87 is one such long-lived “ember”, with a half-life of about a minute and thus it emits a delayed neutron upon decay. Operating in this delayed critical state, which depends on the inherently delayed transformation or movement of fission products to maintain the temperature, temperatures change slowly enough to permit human feedback. In an analogous manner to fire dampers varying the opening to control the movement of wood embers towards new fuel, control rods are comparatively varied up or down, as the nuclear fuel burns up over time.

In a nuclear power reactor, the main sources of radioactivity are fission products, alongside actinides and activation products. Fission products are the largest source of

radioactivity for the first several hundred years, while actinides are dominant roughly 103 to 105 years after fuel use.

Fission occurs in the nuclear fuel, and the fission products are primarily retained within the fuel close to where they are produced. These fission products are important to the operation of the reactor because some fission products contribute delayed neutrons that are useful for reactor control while others are neutron poisons that tend to inhibit the nuclear reaction. The buildup of the fission product poisons is a key factor in determining the maximum duration a given fuel element can be kept within the reactor. The decay of short-lived fission products also provide a source of heat within the fuel that continues even after the reactor has been shut down and the fission reactions stopped. It is this decay heat that sets the requirements for cooling of a reactor after shutdown.

If the fuel cladding around the fuel develops holes, then fission products can leak into the primary coolant. Depending on the fission product chemistry, it may settle within the reactor core or travel through the coolant system. Coolant systems include chemistry control systems that tend to remove such fission products. In a well-designed power reactor running under normal conditions, the radioactivity of the coolant is very low.

It is known that the isotope responsible for the majority of the gamma exposure in fuel reprocessing plants (and the Chernobyl site in 2005) is Cs-137. Iodine-129 is one of the major radioactive elements released from reprocessing plants. In nuclear reactors both Cs-137 and strontium-90 are found in locations remote from the fuel. This is because these isotopes are formed by the beta decay of noble gases (xenon-137 {half-life of 3.8 minutes} and krypton-90 {half-life 32 seconds}) which enable these isotopes to be deposited in locations remote from the fuel (e.g. on control rods).

Nuclear Reactor Poisons

Some fission products decay with the release of a neutron. Since there may be a short delay in time between the original fission event (which releases its own prompt neutrons immediately) and the release of these neutrons, the latter are termed “delayed neutrons”. These delayed neutrons are important to nuclear reactor control.

Some of the fission products, such as xenon-135 and samarium-149, have a high neutron absorption cross section. Since a nuclear reactor depends on a balance in the neutron production and absorption rates, those fission products that remove neutrons from the reaction will tend to shut the reactor down or “poison” the reactor. Nuclear fuels and reactors are designed to address this phenomenon through such features as burnable poisons and control rods. Build-up of xenon-135 during shutdown or low-power operation may poison the reactor enough to impede restart or to interfere with normal control of the reaction during restart or restoration of full power, possibly causing or contributing to an accident scenario.

Nuclear Weapons

Nuclear weapons use fission as either the partial or the main energy source. Depending on the weapon design and where it is exploded, the relative importance of the fission product radioactivity will vary compared to the activation product radioactivity in the total fallout radioactivity.

The immediate fission products from nuclear weapon fission are essentially the same as those from any other fission source, depending slightly on the particular nuclide that is fissioning. However, the very short time scale for the reaction makes a difference in the particular mix of isotopes produced from an atomic bomb.

For example, the $^{134}\text{Cs}/^{137}\text{Cs}$ ratio provides an easy method of distinguishing between fallout from a bomb and the fission products from a power reactor. Almost no Cs-134 is formed by nuclear fission (because xenon-134 is stable). The ^{134}Cs is formed by the neutron activation of the stable ^{133}Cs which is formed by the decay of isotopes in the isobar ($A = 133$). So in a momentary criticality by the time that the neutron flux becomes zero too little time will have passed for any ^{133}Cs to be present. While in a power reactor plenty of time exists for the decay of the isotopes in the isobar to form ^{133}Cs , the ^{133}Cs thus formed can then be activated to form ^{134}Cs only if the time between the start and the end of the criticality is long.

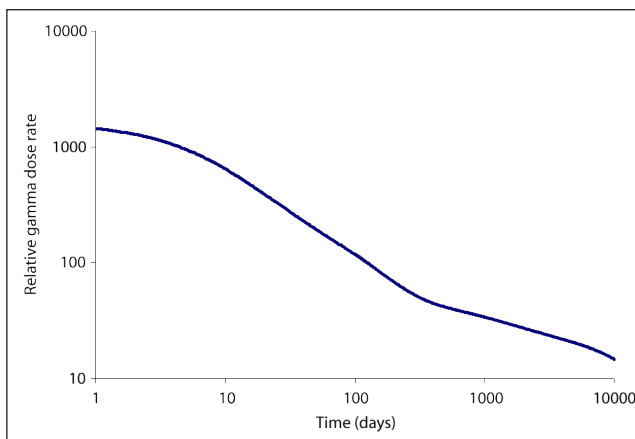
According to Jiri Hala's textbook, the radioactivity in the fission product mixture in an atom bomb is mostly caused by short-lived isotopes such as I-131 and Ba-140. After about four months Ce-141, Zr-95/Nb-95, and Sr-89 represent the largest share of radioactive material. After two to three years, Ce-144/Pr-144, Ru-106/Rh-106, and Promethium-147 are the bulk of the radioactivity. After a few years, the radiation is dominated by strontium-90 and caesium-137, whereas in the period between 10,000 and a million years it is technetium-99 that dominates.

Application

Some fission products (such as Cs-137) are used in medical and industrial radioactive sources. $^{99}\text{TcO}_4^-$ ion can react with steel surfaces to form a corrosion resistant layer. In this way these metaloxo anions act as anodic corrosion inhibitors - it renders the steel surface passive. The formation of $^{99}\text{TcO}_2$ on steel surfaces is one effect which will retard the release of ^{99}Tc from nuclear waste drums and nuclear equipment which has become lost prior to decontamination (e.g. nuclear submarine reactors which have been lost at sea).

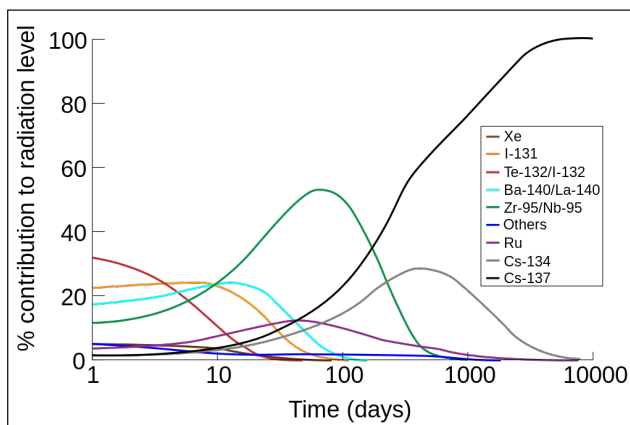
In a similar way the release of radio-iodine in a serious power reactor accident could be retarded by adsorption on metal surfaces within the nuclear plant. Much of the other work on the iodine chemistry which would occur during a bad accident has been done.

Decay



The external gamma dose for a person in the open near the Chernobyl disaster site.

For fission of uranium-235, the predominant radioactive fission products include isotopes of iodine, caesium, strontium, xenon and barium. The threat becomes smaller with the passage of time. Locations where radiation fields once posed immediate mortal threats, such as much of the Chernobyl Nuclear Power Plant on day one of the accident and the ground zero sites of U.S. atomic bombings in Japan (6 hours after detonation) are now relatively safe because the radioactivity has decayed to a low level. Many of the fission products decay through very short-lived isotopes to form stable isotopes, but a considerable number of the radioisotopes have half-lives longer than a day.



The portion of the total radiation dose (in air) contributed by each isotope versus time after the Chernobyl disaster, at the site thereof. Note that this image was drawn using data from the OECD report, and the second edition of 'The radiochemical manual'.

The radioactivity in the fission product mixture is initially mostly caused by short lived isotopes such as Iodine-131 and ^{140}Ba ; after about four months ^{141}Ce , $^{95}\text{Zr}/^{95}\text{Nb}$ and ^{89}Sr take the largest share, while after about two or three years the largest share is taken by $^{144}\text{Ce}/^{144}\text{Pr}$, $^{106}\text{Ru}/^{106}\text{Rh}$ and ^{147}Pm . Later ^{90}Sr and ^{137}Cs are the main radioisotopes, being succeeded by ^{99}Tc . In the case of a release of radioactivity from a power reactor or used fuel, only some

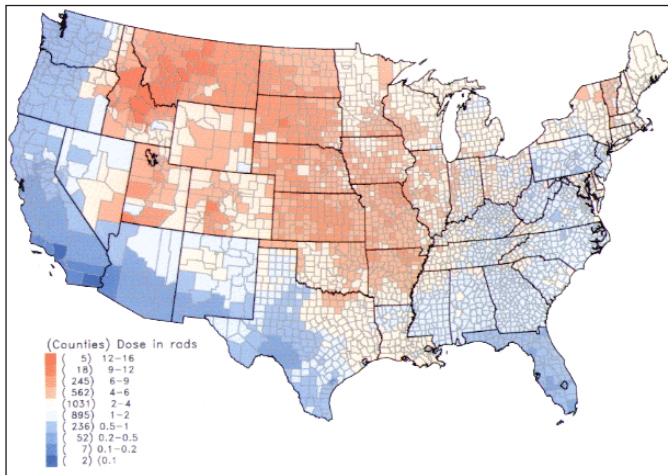
elements are released; as a result, the isotopic signature of the radioactivity is very different from an open air nuclear detonation, where all the fission products are dispersed.

Fallout Countermeasures

The purpose of radiological emergency preparedness is to protect people from the effects of radiation exposure after a nuclear accident or bomb. Evacuation is the most effective protective measure. However, if evacuation is impossible or even uncertain, then local fallout shelters and other measures provide the best protection.

Iodine

At least three isotopes of iodine are important. ^{129}I , ^{131}I (radioiodine) and ^{132}I . Open air nuclear testing and the Chernobyl disaster both released iodine-131.



Per capita thyroid doses in the continental United States of iodine-131 resulting from all exposure routes from all atmospheric nuclear tests conducted at the Nevada Test Site.

The short-lived isotopes of iodine are particularly harmful because the thyroid collects and concentrates iodide – radioactive as well as stable. Absorption of radioiodine can lead to acute, chronic, and delayed effects. Acute effects from high doses include thyroiditis, while chronic and delayed effects include hypothyroidism, thyroid nodules, and thyroid cancer. It has been shown that the active iodine released from Chernobyl and Mayak has resulted in an increase in the incidence of thyroid cancer in the former Soviet Union.

One measure which protects against the risk from radio-iodine is taking a dose of potassium iodide (KI) before exposure to radioiodine. The non-radioactive iodide ‘saturates’ the thyroid, causing less of the radioiodine to be stored in the body. Administering potassium iodide reduces the effects of radio-iodine by 99% and is a prudent, inexpensive supplement to fallout shelters. A low-cost alternative to commercially available iodine pills is a saturated solution of potassium iodide. Long-term storage of KI is normally in the form of reagent grade crystals.

The administration of known goitrogen substances can also be used as a prophylaxis in reducing the bio-uptake of iodine, (whether it be the nutritional non-radioactive iodine-127 or radioactive iodine, radioiodine - most commonly iodine-131, as the body cannot discern between different iodine isotopes). A perchlorate ion, a common water contaminant in the USA due to the aerospace industry, has been shown to reduce iodine uptake and thus is classified as a goitrogen. Perchlorate ions are a competitive inhibitor of the process by which iodide is actively deposited into thyroid follicular cells. Studies involving healthy adult volunteers determined that at levels above 0.007 milligrams per kilogram per day (mg/(kg·d)), perchlorate begins to temporarily inhibit the thyroid gland's ability to absorb iodine from the bloodstream ("iodide uptake inhibition", thus perchlorate is a known goitrogen). The reduction of the iodide pool by perchlorate has dual effects – reduction of excess hormone synthesis and hyperthyroidism, on the one hand, and reduction of thyroid inhibitor synthesis and hypothyroidism on the other. Perchlorate remains very useful as a single dose application in tests measuring the discharge of radioiodide accumulated in the thyroid as a result of many different disruptions in the further metabolism of iodide in the thyroid gland.

Treatment of thyrotoxicosis (including Graves' disease) with 600-2,000 mg potassium perchlorate (430-1,400 mg perchlorate) daily for periods of several months or longer was once common practice, particularly in Europe, and perchlorate use at lower doses to treat thyroid problems continues to this day. Although 400 mg of potassium perchlorate divided into four or five daily doses was used initially and found effective, higher doses were introduced when 400 mg/day was discovered not to control thyrotoxicosis in all subjects.

Current regimens for treatment of thyrotoxicosis (including Graves' disease), when a patient is exposed to additional sources of iodine, commonly include 500 mg potassium perchlorate twice per day for 18–40 days.

Prophylaxis with perchlorate-containing water at concentrations of 17 ppm, which corresponds to 0.5 mg/kg-day personal intake, if one is 70 kg and consumes 2 litres of water per day, was found to reduce baseline radioiodine uptake by 67%. This is equivalent to ingesting a total of just 35 mg of perchlorate ions per day. In another related study where subjects drank just 1 litre of perchlorate-containing water per day at a concentration of 10 ppm, i.e. daily 10 mg of perchlorate ions were ingested, an average 38% reduction in the uptake of iodine was observed.

However, when the average perchlorate absorption in perchlorate plant workers subjected to the highest exposure has been estimated as approximately 0.5 mg/kg-day, as in the above paragraph, a 67% reduction of iodine uptake would be expected. Studies of chronically exposed workers though have thus far failed to detect any abnormalities of thyroid function, including the uptake of iodine. This may well be attributable to sufficient daily exposure or intake of healthy iodine-127 among the workers and the short 8 hr biological half-life of perchlorate in the body.

To completely block the uptake of iodine-131 by the purposeful addition of perchlorate ions to a populace's water supply, aiming at dosages of 0.5 mg/kg-day, or a water concentration of 17 ppm, would therefore be grossly inadequate at truly reducing radioiodine uptake. Perchlorate ion concentrations in a region's water supply would need to be much higher, at least 7.15 mg/kg of body weight per day, or a water concentration of 250 ppm, assuming people drink 2 liters of water per day, to be truly beneficial to the population at preventing bioaccumulation when exposed to a radioiodine environment, independent of the availability of iodate or iodide drugs.

The continual distribution of perchlorate tablets or the addition of perchlorate to the water supply would need to continue for no less than 80–90 days, beginning immediately after the initial release of radioiodine was detected. After 80–90 days passed, released radioactive iodine-131 would have decayed to less than 0.1% of its initial quantity, at which time the danger from bioaccumulation of iodine-131 is essentially over.

In the event of a radioiodine release, the ingestion of prophylaxis potassium iodide, if available, or even iodate, would rightly take precedence over perchlorate administration, and would be the first line of defense in protecting the population from a radioiodine release. However, in the event of a radioiodine release too massive and widespread to be controlled by the limited stock of iodide and iodate prophylaxis drugs, then the addition of perchlorate ions to the water supply, or distribution of perchlorate tablets would serve as a cheap, efficacious, second line of defense against carcinogenic radioiodine bioaccumulation.

The ingestion of goitrogen drugs is, much like potassium iodide also not without its dangers, such as hypothyroidism. In all these cases however, despite the risks, the prophylaxis benefits of intervention with iodide, iodate, or perchlorate outweigh the serious cancer risk from radioiodine bioaccumulation in regions where radioiodine has sufficiently contaminated the environment.

Caesium

The Chernobyl accident released a large amount of caesium isotopes which were dispersed over a wide area. ^{137}Cs is an isotope which is of long-term concern as it remains in the top layers of soil. Plants with shallow root systems tend to absorb it for many years. Hence grass and mushrooms can carry a considerable amount of ^{137}Cs , which can be transferred to humans through the food chain.

One of the best countermeasures in dairy farming against ^{137}Cs is to mix up the soil by deeply ploughing the soil. This has the effect of putting the ^{137}Cs out of reach of the shallow roots of the grass; hence the level of radioactivity in the grass will be lowered. Also the removal of top few centimeters of soil and its burial in a shallow trench will reduce the dose to humans and animals as the gamma photons from ^{137}Cs will be attenuated by their passage through the soil. The deeper and more remote the trench is, the better the degree of protection. Fertilizers containing potassium can be used to dilute cesium and limit its uptake by plants.

In livestock farming, another countermeasure against ^{137}Cs is to feed to animal's prussian blue. This compound acts as an ion-exchanger. The cyanide is so tightly bonded to the iron that it is safe for a human to consume several grams of prussian blue per day. The prussian blue reduces the biological half-life (different from the nuclear half-life) of the caesium. The physical or nuclear half-life of ^{137}Cs is about 30 years. Caesium in humans normally has a biological half-life of between one and four months. An added advantage of the prussian blue is that the caesium which is stripped from the animal in the droppings is in a form which is not available to plants. Hence it prevents the caesium from being recycled. The form of prussian blue required for the treatment of animals, including humans is a special grade. Attempts to use the pigment grade used in paints have not been successful.

Strontium

The addition of lime to soils which are poor in calcium can reduce the uptake of strontium by plants. Likewise in areas where the soil is low in potassium, the addition of a potassium fertilizer can discourage the uptake of cesium into plants. However such treatments with either lime or potash should not be undertaken lightly as they can alter the soil chemistry greatly, so resulting in a change in the plant ecology of the land.

SPONTANEOUS FISSION

Spontaneous fission (SF) is a form of radioactive decay that is found only in very heavy chemical elements. The nuclear binding energy of the elements reaches its maximum at an atomic mass number of about 56; spontaneous breakdown into smaller nuclei and a few isolated nuclear particles becomes possible at greater atomic mass numbers.

The first nuclear fission process discovered was fission induced by neutrons. Because cosmic rays produce some neutrons, it was difficult to distinguish between induced and spontaneous events. Cosmic rays can be reliably shielded by a thick layer of rock or water. Spontaneous fission was identified in 1940 by Soviet physicists Georgy Flyorov and Konstantin Petrzhak by their observations of uranium in the Moscow Metro Dinamo station, 60 metres (200 ft) underground.

Cluster decay was shown to be a superasymmetric spontaneous fission process.

Feasibility

Elemental

Spontaneous fission is feasible over practical observation times only for atomic masses of 232 amu or more. These are elements at least as heavy as thorium-232 – which has a half-life somewhat longer than the age of the universe. ^{232}Th , ^{235}U , and ^{238}U are

primordial nuclides and have left evidence of undergoing spontaneous fission in their minerals.

The known elements most susceptible to spontaneous fission are the synthetic high-atomic-number actinides and transactinides with atomic numbers from 100 onwards.

For naturally occurring thorium-232, uranium-235, and uranium-238, spontaneous fission does occur rarely, but in the vast majority of the radioactive decay of these atoms, alpha decay or beta decay occurs instead. Hence, the spontaneous fission of these isotopes is usually negligible, except in using the exact branching ratios when finding the radioactivity of a sample of these elements.

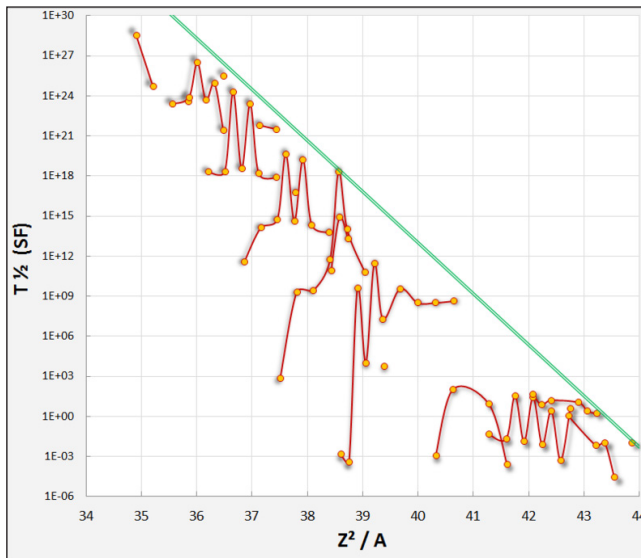
Mathematical

The liquid drop model predicts approximately that spontaneous fission can occur in a time short enough to be observed by present methods when:

$$\frac{Z^2}{A} \geq 47$$

Where, Z is the atomic number and A is the mass number (e.g., $Z^2/A = 36$ for uranium-235). However, all known nuclides which undergo spontaneous fission as their main decay mode do not reach this value of 47, as the liquid drop model is not very accurate for the heaviest known nuclei due to strong shell effects.

Spontaneous Fission Rates



Spontaneous fission half-life of various nuclides depending on their Z^2/A ratio. Nuclides of the same element are linked with a red line. The green line shows the upper limit of half-life.

Nu-clide	Half-life (yrs)	Fission prob. per decay (%)	Neutrons per		Spontaneous half-life (yrs)	Z ² /A
			Fission	Gram-sec		
²³⁵ U	7.04·10 ⁸	2.0·10 ⁻⁷	1.86	0.0003	3.5·10 ¹⁷	36.0
²³⁸ U	4.47·10 ⁹	5.4·10 ⁻⁵	2.07	0.0136	8.4·10 ¹⁵	35.6
²³⁹ Pu	24100	4.4·10 ⁻¹⁰	2.16	0.022	5.5·10 ¹⁵	37.0
²⁴⁰ Pu	6569	5.0·10 ⁻⁶	2.21	920	1.16·10 ¹¹	36.8
²⁵⁰ Cm	8300	~74	3.31	1.6·10 ¹⁰	1.12·10 ⁴	36.9
²⁵² Cf	2.6468	3.09	3.73	2.3·10 ¹²	85.7	38.1

In practice, ²³⁹Pu will invariably contain a certain amount of ²⁴⁰Pu due to the tendency of ²³⁹Pu to absorb an additional neutron during production. ²⁴⁰Pu's high rate of spontaneous fission events makes it an undesirable contaminant. Weapons-grade plutonium contains no more than 7.0% ²⁴⁰Pu.

The rarely used gun-type atomic bomb has a critical insertion time of about one millisecond, and the probability of a fission during this time interval should be small. Therefore, only ²³⁵U is suitable. Almost all nuclear bombs use some kind of implosion method.

Spontaneous fission can occur much more rapidly when the nucleus of an atom undergoes superdeformation.

Poisson Process

Spontaneous fission gives much the same result as induced nuclear fission. However, like other forms of radioactive decay, it occurs due to quantum tunneling, without the atom having been struck by a neutron or other particle as in induced nuclear fission. Spontaneous fissions release neutrons as all fissions do, so if a critical mass is present, a spontaneous fission can initiate a self-sustaining chain reaction. Radioisotopes for which spontaneous fission is not negligible can be used as neutron sources. For example, californium-252 (half-life 2.645 years, SF branch ratio about 3.1 percent) can be used for this purpose. The neutrons released can be used to inspect airline luggage for hidden explosives, to gauge the moisture content of soil in highway and building construction, or to measure the moisture of materials stored in silos, for example.

As long as the spontaneous fission gives a negligible reduction of the number of nuclei that can undergo such fission, this process can be approximated closely as a Poisson process. In this situation, for short time intervals the probability of a spontaneous fission is directly proportional to the length of time.

The spontaneous fission of uranium-238 and uranium-235 does leave trails of damage in the crystal structure of uranium-containing minerals when the fission fragments recoil through them. These trails, or fission tracks, are the foundation of the radiometric dating method called fission track dating.

PHOTOFISSION

Photofission is a process in which a nucleus, after absorbing a gamma ray, undergoes nuclear fission and splits into two or more fragments.

The reaction was discovered in 1940 by a small team of engineers and scientists operating the Westinghouse Atom Smasher at the company's Research Laboratories in Forest Hills, Pennsylvania. They used a 5 MeV proton beam to bombard fluorine and generate high-energy photons, which then irradiated samples of uranium and thorium.

Gamma radiation of modest energies, in the low tens of MeV, can induce fission in traditionally fissile elements such as the actinides thorium, uranium, plutonium, and neptunium. Experiments have been conducted with much higher energy gamma rays, finding that the photofission cross section varies little within ranges in the low GeV range.

Baldwin et al made measurements of the yields of photo-fission in uranium and thorium together with a search for photo-fission in other heavy elements, using continuous x-rays from a 100-Mev betatron. Fission was detected in the presence of an intense background of x-rays by a differential ionization chamber and linear amplifier; the substance investigated being coated on an electrode of one chamber. They deduced the maximum cross section being of the order of $5 \times 10^{-26} \text{ cm}^2$ for uranium and half that for thorium. In the other elements studied, the cross section must be below 10^{-29} cm^2 .

Photodisintegration

Photodisintegration (also called phototransmutation) is a similar but different physical process, in which an extremely high energy gamma ray interacts with an atomic nucleus and causes it to enter an excited state, which immediately decays by emitting a subatomic particle.

NUCLEAR FUSION

Nuclear fusion is the process by which nuclear reactions between light elements form heavier elements (up to iron). In cases where the interacting nuclei belong to elements with low atomic numbers (e.g., hydrogen [atomic number 1] or its isotopes deuterium and tritium), substantial amounts of energy are released. The vast energy potential of nuclear fusion was first exploited in thermonuclear weapons, or hydrogen bombs, which were developed in the decade immediately following World War II. Meanwhile, the potential peaceful applications of nuclear fusion, especially in view of the essentially limitless supply of fusion fuel on Earth, have encouraged an immense effort to harness this process for the production of power.

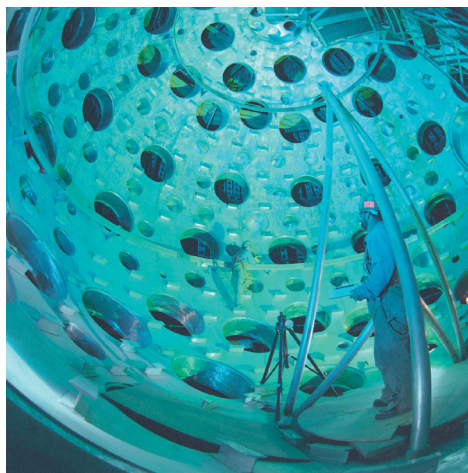


Figure shows laser-activated fusionInterior of the U.S. Department of Energy’s National Ignition Facility (NIF), located at Lawrence Livermore National Laboratory, Livermore, California. The NIF target chamber uses a high-energy laser to heat fusion fuel to temperatures sufficient for thermonuclear ignition. The facility is used for basic science, fusion energy research, and nuclear weapons testing.

Fusion Reaction

Fusion reactions constitute the fundamental energy source of stars, including the Sun. The evolution of stars can be viewed as a passage through various stages as thermonuclear reactions and nucleosynthesis cause compositional changes over long time spans. Hydrogen (H) “burning” initiates the fusion energy source of stars and leads to the formation of helium (He). Generation of fusion energy for practical use also relies on fusion reactions between the lightest elements that burn to form helium. In fact, the heavy isotopes of hydrogen—deuterium (D) and tritium (T)—react more efficiently with each other, and, when they do undergo fusion, they yield more energy per reaction than do two hydrogen nuclei. (The hydrogen nucleus consists of a single proton. The deuterium nucleus has one proton and one neutron, while tritium has one proton and two neutrons).

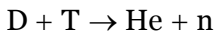
Fusion reactions between light elements, like fission reactions that split heavy elements, release energy because of a key feature of nuclear matter called the binding energy, which can be released through fusion or fission. The binding energy of the nucleus is a measure of the efficiency with which its constituent nucleons are bound together. Take, for example, an element with Z protons and N neutrons in its nucleus. The element’s atomic weight A is $Z + N$, and its atomic number is Z . The binding energy B is the energy associated with the mass difference between the Z protons and N neutrons considered separately and the nucleons bound together ($Z + N$) in a nucleus of mass M . The formula is:

$$B = (Zm_p + Nm_n - M) c^2$$

Where, m_p and m_n are the proton and neutron masses and c is the speed of light. It has been determined experimentally that the binding energy per nucleon is a maximum of about 1.4×10^{-12} joule at an atomic mass number of approximately 60—that is, approximately the atomic mass number of iron. Accordingly, the fusion of elements lighter than iron or the splitting of heavier ones generally leads to a net release of energy.

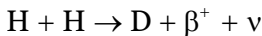
Two Types of Fusion Reactions

Fusion reactions are of two basic types: (1) those that preserve the number of protons and neutrons and (2) those that involve a conversion between protons and neutrons. Reactions of the first type are most important for practical fusion energy production, whereas those of the second type are crucial to the initiation of star burning. An arbitrary element is indicated by the notation ${}^A_Z\text{X}$, where Z is the charge of the nucleus and A is the atomic weight. An important fusion reaction for practical energy generation is that between deuterium and tritium (the D-T fusion reaction). It produces helium (He) and a neutron (n) and is written:



To the left of the arrow (before the reaction) there are two protons and three neutrons. The same is true on the right.

The other reaction, that which initiates star burning, involves the fusion of two hydrogen nuclei to form deuterium (the H-H fusion reaction):



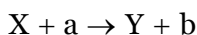
Where, β^+ represents a positron and ν stands for a neutrino. Before the reaction there are two hydrogen nuclei (that is, two protons). Afterward there are one proton and one neutron (bound together as the nucleus of deuterium) plus a positron and a neutrino (produced as a consequence of the conversion of one proton to a neutron).

Both of these fusion reactions are exoergic and so yield energy. The German-born physicist Hans Bethe proposed in the 1930s that the H-H fusion reaction could occur with a net release of energy and provide, along with subsequent reactions, the fundamental energy source sustaining the stars. However, practical energy generation requires the D-T reaction for two reasons: first, the rate of reactions between deuterium and tritium is much higher than that between protons; second, the net energy release from the D-T reaction is 40 times greater than that from the H-H reaction.

Energy Released in Fusion Reactions

Energy is released in a nuclear reaction if the total mass of the resultant particles is less

than the mass of the initial reactants. To illustrate, suppose two nuclei, labeled X and a, react to form two other nuclei, Y and b, denoted:



The particles a and b are often nucleons, either protons or neutrons, but in general can be any nuclei. Assuming that none of the particles is internally excited (i.e., each is in its ground state), the energy quantity called the Q-value for this reaction is defined as:

$$Q = (m_x + m_a - m_b - m_y) c^2$$

Where, the m-letters refer to the mass of each particle and c is the speed of light. When the energy value Q is positive, the reaction is exoergic; when Q is negative, the reaction is endoergic (i.e., absorbs energy). When both the total proton number and the total neutron number are preserved before and after the reaction (as in D-T reactions), then the Q-value can be expressed in terms of the binding energy B of each particle as:

$$Q = B_y + B_b - B_x - B_a$$

The D-T fusion reaction has a positive Q-value of 2.8×10^{-12} joule. The H-H fusion reaction is also exoergic, with a Q-value of 6.7×10^{-14} joule. To develop a sense for these figures, one might consider that one metric ton (1,000 kg, or almost 2,205 pounds) of deuterium would contain roughly 3×10^{32} atoms. If one ton of deuterium were to be consumed through the fusion reaction with tritium, the energy released would be 8.4×10^{20} joules. This can be compared with the energy content of one ton of coal—namely, 2.9×10^{10} joules. In other words, one ton of deuterium has the energy equivalent of approximately 29 billion tons of coal.

Rate and Yield of Fusion Reactions

The energy yield of a reaction between nuclei and the rate of such reactions are both important. These quantities have a profound influence in scientific areas such as nuclear astrophysics and the potential for nuclear production of electrical energy.

When a particle of one type passes through a collection of particles of the same or different type, there is a measurable chance that the particles will interact. The particles may interact in many ways, such as simply scattering, which means that they change direction and exchange energy, or they may undergo a nuclear fusion reaction. The measure of the likelihood that particles will interact is called the cross section, and the magnitude of the cross section depends on the type of interaction and the state and energy of the particles. The product of the cross section and the atomic density of the target particle is called the macroscopic cross section. The inverse of the macroscopic cross section is particularly noteworthy as it gives the mean distance an incident particle will travel before interacting with a target particle; this inverse measure is called

the mean free path. Cross sections are measured by producing a beam of one particle at a given energy, allowing the beam to interact with a (usually thin) target made of the same or a different material, and measuring deflections or reaction products. In this way it is possible to determine the relative likelihood of one type of fusion reaction versus another, as well as the optimal conditions for a particular reaction.

The cross sections of fusion reactions can be measured experimentally or calculated theoretically, and they have been determined for many reactions over a wide range of particle energies. They are well known for practical fusion energy applications and are reasonably well known, though with gaps, for stellar evolution. Fusion reactions between nuclei, each with a positive charge of one or more, are the most important for both practical applications and the nucleosynthesis of the light elements in the burning stages of stars. Yet, it is well known that two positively charged nuclei repel each other electrostatically—i.e., they experience a repulsive force inversely proportional to the square of the distance separating them. This repulsion is called the Coulomb barrier. It is highly unlikely that two positive nuclei will approach each other closely enough to undergo a fusion reaction unless they have sufficient energy to overcome the Coulomb barrier. As a result, the cross section for fusion reactions between charged particles is very small unless the energy of the particles is high, at least 10^4 electron volts ($1 \text{ eV} \cong 1.602 \times 10^{-19}$ joules) and often more than 10^5 or 10^6 eV. This explains why the centre of a star must be hot for the fuel to burn and why fuel for practical fusion energy systems must be heated to at least 50,000,000 kelvins (K; 90,000,000 °F). Only then will a reasonable fusion reaction rate and power output be achieved.

The phenomenon of the Coulomb barrier also explains a fundamental difference between energy generation by nuclear fusion and nuclear fission. While fission of heavy elements can be induced by either protons or neutrons, generation of fission energy for practical applications is dependent on neutrons to induce fission reactions in uranium or plutonium. Having no electric charge, the neutron is free to enter the nucleus even if its energy corresponds to room temperature. Fusion energy, relying as it does on the fusion reaction between light nuclei, occurs only when the particles are sufficiently energetic to overcome the Coulomb repulsive force. This requires the production and heating of the gaseous reactants to the high temperature state known as the plasma state.

The Plasma State

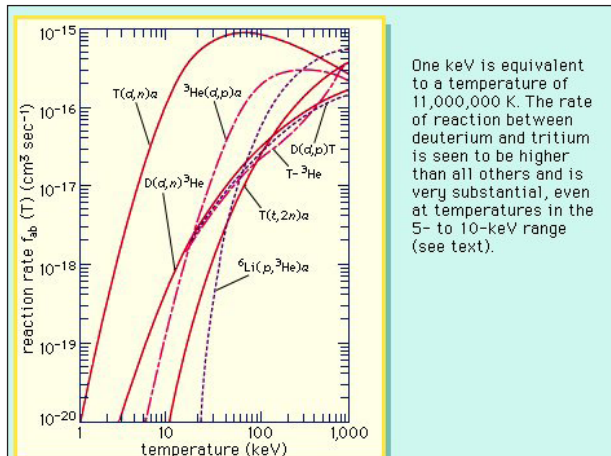
Typically, plasma is a gas that has had some substantial portion of its constituent atoms or molecules ionized by the dissociation of one or more of their electrons. These free electrons enable plasmas to conduct electric charges, and plasma is the only state of matter in which thermonuclear reactions can occur in a self-sustaining manner. Astrophysics and magnetic fusion research, among other fields, require extensive knowledge of how gases behave in the plasma state. The stars, the solar wind, and much of

interstellar space are examples where the matter present is in the plasma state. Very high-temperature plasmas are fully ionized gases, which means that the ratio of neutral gas atoms to charged particles is small. For example, the ionization energy of hydrogen is 13.6 eV, while the average energy of a hydrogen ion in plasma at 50,000,000 K is 6,462 eV. Thus, essentially all of the hydrogen in this plasma would be ionized.

A reaction-rate parameter more appropriate to the plasma state is obtained by accounting for the fact that the particles in plasma, as in any gas, have a distribution of energies. That is to say, not all particles have the same energy. In simple plasmas this energy distribution is given by the Maxwell-Boltzmann distribution law, and the temperature of the gas or plasma is, within a proportionality constant, two-thirds of the average particle energy; i.e., the relationship between the average energy E and temperature T is $E = 3kT/2$, where k is the Boltzmann constant, 8.62×10^{-5} eV per kelvin. The intensity of nuclear fusion reactions in plasma is derived by averaging the product of the particles' speed and their cross sections over a distribution of speeds corresponding to a Maxwell-Boltzmann distribution. The cross section for the reaction depends on the energy or speed of the particles. The averaging process yields a function for a given reaction that depends only on the temperature and can be denoted $f(T)$. The rate of energy released (i.e., the power released) in a reaction between two species, a and b , is:

$$P_{ab} = n_a n_b f_{ab}(T) U_{ab}$$

Where, n_a and n_b are the density of species a and b in the plasma, respectively, and U_{ab} is the energy released each time a and b undergo a fusion reaction. The parameter P_{ab} properly takes into account both the rate of a given reaction and the energy yield per reaction.

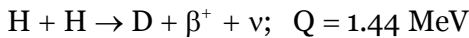


The reaction rate as a function of plasma temperature, expressed in kiloelectron volts (keV; 1 keV is equivalent to a temperature of 11,000,000 K). The rate of reaction between deuterium and tritium is seen to be higher than all others and is very substantial, even at temperatures in the 5-to-10-keV range.

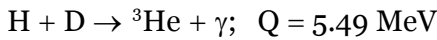
Fusion Reactions in Stars

Fusion reactions are the primary energy source of stars and the mechanism for the nucleosynthesis of the light elements. In the late 1930s Hans Bethe first recognized that the fusion of hydrogen nuclei to form deuterium is exoergic (i.e., there is a net release of energy) and, together with subsequent nuclear reactions, leads to the synthesis of helium. The formation of helium is the main source of energy emitted by normal stars, such as the Sun, where the burning-core plasma has a temperature of less than 15,000,000 K. However, because the gas from which a star is formed often contains some heavier elements, notably carbon (C) and nitrogen (N), it is important to include nuclear reactions between protons and these nuclei. The reaction chain between protons that ultimately leads to helium is the proton-proton cycle. When protons also induce the burning of carbon and nitrogen, the CN cycle must be considered; and, when oxygen (O) is included, still another alternative scheme, the CNO bi-cycle, must be accounted for.

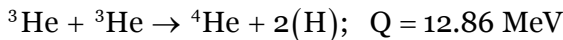
The proton-proton nuclear fusion cycle in a star containing only hydrogen begins with the reaction:



Where, the Q-value assumes annihilation of the positron by an electron. The deuterium could react with other deuterium nuclei, but, because there is so much hydrogen, the D/H ratio is held to very low values, typically 10^{-18} . Thus, the next step is:



Where, γ indicates that gamma rays carry off some of the energy yield. The burning of the helium-3 isotope then gives rise to ordinary helium and hydrogen via the last step in the chain:



At equilibrium, helium-3 burns predominantly by reactions with itself because its reaction rate with hydrogen is small, while burning with deuterium is negligible due to the very low deuterium concentration. Once helium-4 builds up, reactions with helium-3 can lead to the production of still-heavier elements, including beryllium-7, beryllium-8, lithium-7, and boron-8, if the temperature is greater than about 10,000,000 K.

The stages of stellar evolution are the result of compositional changes over very long periods. The size of a star, on the other hand, is determined by a balance between the pressure exerted by the hot plasma and the gravitational force of the star's mass. The energy of the burning core is transported toward the surface of the star, where it is radiated at an effective temperature. The effective temperature of the Sun's surface is about 6,000 K, and significant amounts of radiation in the visible and infrared wavelength ranges are emitted.

Fusion Reactions for Controlled Power Generation

Reactions between deuterium and tritium are the most important fusion reactions for controlled power generation because the cross sections for their occurrence are high, the practical plasma temperatures required for net energy release are moderate, and the energy yield of the reactions are high—17.58 MeV for the basic D-T fusion reaction.

It should be noted that any plasma containing deuterium automatically produces some tritium and helium-3 from reactions of deuterium with other deuterium ions. Other fusion reactions involving elements with an atomic number above 2 can be used, but only with much greater difficulty. This is because the Coulomb barrier increases with increasing charge of the nuclei, leading to the requirement that the plasma temperature exceed 1,000,000,000 K if a significant rate is to be achieved. Some of the more interesting reactions are:

1. $\text{H} + {}^{11}\text{B} \rightarrow 3({}^4\text{He})$; $Q = 8.68 \text{ MeV}$;
2. $\text{H} + {}^6\text{Li} \rightarrow {}^3\text{He} + {}^4\text{He}$; $Q = 4.023 \text{ MeV}$;
3. ${}^3\text{He} + {}^6\text{Li} \rightarrow \text{H} + 2({}^4\text{He})$; $Q = 16.88 \text{ MeV}$;
4. ${}^3\text{He} + {}^6\text{Li} \rightarrow \text{D} + {}^7\text{Be}$; $Q = 0.113 \text{ MeV}$.

Reaction (2nd) converts lithium-6 to helium-3 and ordinary helium. Interestingly, if reaction (2nd) is followed by reaction (3rd), then a proton will again be produced and be available to induce reaction (2nd), thereby propagating the process. Unfortunately, it appears that reaction (4th) is 10 times more likely to occur than reaction (3rd).

Methods of Achieving Fusion Energy

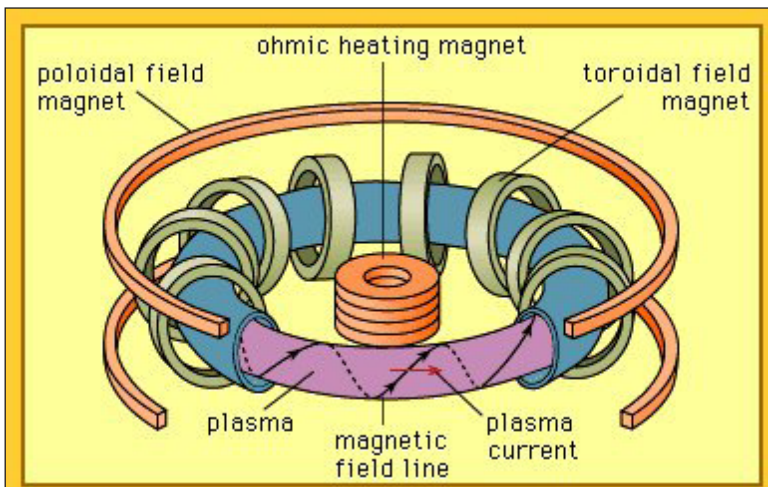
Practical efforts to harness fusion energy involve two basic approaches to containing a high-temperature plasma of elements that undergo nuclear fusion reactions: magnetic confinement and inertial confinement. A much less likely but nevertheless interesting approach is based on fusion catalyzed by muons; research on this topic is of intrinsic interest in nuclear physics.

Magnetic Confinement

In magnetic confinement the particles and energy of a hot plasma are held in place using magnetic fields. A charged particle in a magnetic field experiences a Lorentz force that is proportional to the product of the particle's velocity and the magnetic field. This force causes electrons and ions to spiral about the direction of the magnetic line of force, thereby confining the particles. When the topology of the magnetic field yields an effective magnetic well and the pressure balance between the plasma and the field is stable, the plasma can be confined away from material boundaries. Heat and particles are transported both along and across the field, but energy losses can be prevented

in two ways. The first is to increase the strength of the magnetic field at two locations along the field line. Charged particles contained between these points can be made to reflect back and forth, an effect called magnetic mirroring. In a basically straight system with a region of intensified magnetic field at each end, particles can still escape through the ends due to scattering between particles as they approach the mirroring points. Such end losses can be avoided altogether by creating a magnetic field in the topology of a torus (i.e., configuration of a doughnut or inner tube).

External magnets can be arranged to create a magnetic field topology for stable plasma confinement, or they can be used in conjunction with magnetic fields generated by currents induced to flow in the plasma itself. The late 1960s witnessed a major advance by the Soviet Union in harnessing fusion reactions for practical energy production. Soviet scientists achieved a high plasma temperature (about 3,000,000 K), along with other physical parameters, in a machine referred to as a tokamak. A tokamak is a toroidal magnetic confinement system in which the plasma is kept stable both by an externally generated, doughnut-shaped magnetic field and by electric currents flowing within the plasma. Since the late 1960s the tokamak has been the major focus of magnetic fusion research worldwide, though other approaches such as the stellarator, the compact torus, and the reversed field pinch (RFP) have also been pursued. In these approaches, the magnetic field lines follow a helical, or screwlike, path as the lines of magnetic force proceed around the torus. In the tokamak the pitch of the helix is weak, so the field lines wind loosely around the poloidal direction (through the central hole) of the torus. In contrast, RFP field lines wind much tighter, wrapping many times in the poloidal direction before completing one loop in the toroidal direction (around the central hole).



Tokamak magnetic confinement.

Magnetically confined plasma must be heated to temperatures at which nuclear fusion is vigorous, typically greater than 75,000,000 K (equivalent to energy of 4,400 eV). This can be achieved by coupling radio-frequency waves or microwaves to the plasma particles, by injecting energetic beams of neutral atoms that become ionized and heat

the plasma, by magnetically compressing the plasma, or by the ohmic heating (also known as Joule heating) that occurs when an electric current passes through the plasma.

Employing the tokamak concept, scientists and engineers in the United States, Europe, and Japan began in the mid-1980s to use large experimental tokamak devices to attain conditions of temperature, density, and energy confinement that now match those necessary for practical fusion power generation. The machines employed to achieve these results include the Joint European Torus (JET) of the European Union, the Japanese Tokamak-60 (JT-60), and, until 1997, the Tokamak Fusion Test Reactor (TFTR) in the United States. Indeed, in both the TFTR and the JET devices, experiments using deuterium and tritium produced more than 10 megawatts of fusion power and essentially energy breakeven conditions in the plasma itself. Plasma conditions approaching those achieved in tokamaks were also achieved in large stellarator machines in Germany and Japan during the 1990s.

Inertial Confinement Fusion (ICF)

In this approach, a fuel mass is compressed rapidly to densities 1,000 to 10,000 times greater than normal by generating a pressure as high as 10^{17} pascals (10^{12} atmospheres) for periods as short as a nanosecond (10^{-9} second). Near the end of this time period, the implosion speed exceeds about 3×10^5 metres per second. At maximum compression of the fuel, which is now in a cool plasma state, the energy in converging shock waves is sufficient to heat the very centre of the fuel to temperatures high enough to induce fusion reactions (greater than an equivalent energy of about 4,400 eV). If the mass of this highly compressed fuel material is large enough, energy will be generated through fusion reactions before this hot plasma ball disassembles. Under proper conditions, much more energy can be released than is required to compress and shock heat the fuel to thermonuclear burning conditions.

The physical processes in ICF bear a relationship to those in thermonuclear weapons and in star formation—namely, collapse, compression heating, and the onset of nuclear fusion. The situation in star formation differs in one respect: gravity is the cause of the collapse, and a collapsed star begins to expand again due to heat from exoergic nuclear fusion reactions. The expansion is ultimately arrested by the gravitational force associated with the enormous mass of the star, at which point a state of equilibrium in both size and temperature is achieved. In contrast, the fuel in a thermonuclear weapon or ICF completely disassembles. In the ideal ICF case, however, this does not occur until about 30 percent of the fusion fuel has burned.

Over the decades, very significant progress has been made in developing the technology and systems for high-energy, short-time-pulse drivers that are necessary to implode the fusion fuel. The most common driver is a high-power laser, though particle accelerators capable of producing beams of high-energy ions are also used. Lasers that

produce more than 100,000 joules in pulses of about one nanosecond are now used in experiments, and the power available in short bursts exceeds 10^{14} watts.

Two lasers capable of delivering up to 5,000,000 joules in equally short bursts, generating a power level on the fusion targets in excess of 5×10^{14} watts, are operational. One facility is the Laser MegaJoule in Bordeaux, France. The other is the National Ignition Facility at the Lawrence Livermore National Laboratory in Livermore, Calif., U.S.

Muon-catalyzed Fusion

The need in traditional schemes of nuclear fusion to confine very high-temperature plasmas has led some researchers to explore alternatives that would permit fusion reactants to approach each other more closely at much lower temperatures. One method involves substituting muons (μ) for the electrons that ordinarily surround the nucleus of a fuel atom. Muons are negatively charged subatomic particles similar to electrons, except that their mass is a little more than 200 times the electron mass and they are unstable, having a half-life of about 2.2×10^{-6} second. In fact, fusion has been observed in liquid and gas mixtures of deuterium and tritium at cryogenic temperatures when muons were injected into the mixture.

Muon-catalyzed fusion is the name given to the process of achieving fusion reactions by causing a deuteron (deuterium nucleus, D^+), a triton (tritium nucleus, T^+), and a muon to form what is called a muonic molecule. Once a muonic molecule is formed, the rate of fusion reactions is approximately 3×10^{-8} second. However, the formation of a muonic molecule is complex, involving a series of atomic, molecular, and nuclear processes.

In schematic terms, when a muon enters a mixture of deuterium and tritium, the muon is first captured by one of the two hydrogen isotopes in the mixture, forming either atomic $D^+-\mu$ or $T^+-\mu$, with the atom now in an excited state. The excited atom relaxes to the ground state through a cascade collision process, in which the muon may be transferred from a deuteron to a triton or vice versa. More important, it is also possible that a muonic molecule ($D^+-\mu-T^+$) will be formed. Although a much rarer reaction, once a muonic molecule does form, fusion takes place almost immediately, releasing the muon in the mixture to be captured again by a deuterium or tritium nucleus and allowing the process to continue. In this sense the muon acts as a catalyst for fusion reactions within the mixture. The key to practical energy production is to generate enough fusion reactions before the muon decays.

The complexities of muon-catalyzed fusion are many and include generating the muons (at an energy expenditure of about five billion electron volts per muon) and immediately injecting them into the deuterium-tritium mixture. In order to produce more energy than what is required to initiate the process, about 300 D-T fusion reactions must take place within the half-life of a muon.

Cold Fusion and Bubble Fusion

Two disputed fusion experiments merit mention. In 1989 two chemists, Martin Fleischmann of the University of Utah and Stanley Pons of the University of Southampton in England, announced that they had produced fusion reactions at essentially room temperature. Their system consisted of electrolytic cells containing heavy water (deuterium oxide, D_2O) and palladium rods that absorbed the deuterium from the heavy water. Efforts to give a theoretical explanation of the results failed, as did worldwide efforts to reproduce the claimed cold fusion.

In 2002 Rusi Taleyarkhan and colleagues at Purdue University in Lafayette, Ind., claimed to have observed a statistically significant increase in nuclear emissions of products of fusion reactions (neutrons and tritium) during acoustic cavitation experiments with chilled deuterated (bombarded with deuterium) acetone. Their experimental setup was based on the known phenomenon of sonoluminescence. In sonoluminescence a gas bubble is imploded with high-pressure sound waves. At the end of the implosion process, and for a short time afterward, conditions of high density and temperature are achieved that lead to light emission. By starting with larger, millimetre-sized cavitations (bubbles) that had been deuterated in the acetone liquid, the researchers claimed to have produced densities and temperatures sufficient to induce fusion reactions just before the bubbles broke up. As with cold fusion, most attempts to replicate their results have failed.

Conditions for Practical Fusion Yield

Two conditions must be met to achieve practical energy yields from fusion. First, the plasma temperature must be high enough that fusion reactions occur at a sufficient rate. Second, the plasma must be confined so that the energy released by fusion reactions, when deposited in the plasma, maintains its temperature against loss of energy by such phenomena as conduction, convection, and radiation. When these conditions are achieved, the plasma is said to be ignited. In the case of stars, or some approaches to fusion by magnetic confinement, a steady state can be achieved, and no energy beyond what is supplied from fusion reactions is needed to sustain the system. In other cases, such as the ICF approach, there is a large temperature excursion once fuel ignition is achieved. The energy yield can far exceed the energy required to attain plasma ignition conditions, but this energy is released in a burst, and the process has to be repeated roughly once every second for practical power to be produced.

The conditions for plasma ignition are readily derived. When fusion reactions occur in plasma, the power released is proportional to the square of plasma ion density, n^2 . The plasma loses energy when electrons scatter from positively charged ions, accelerating and radiating in the process. Such radiation is called bremsstrahlung and is proportional to $n^2T^{1/2}$, where T is the plasma temperature. Other mechanisms by which heat can escape

the plasma lead to a characteristic energy-loss time denoted by τ . The energy content of the plasma at temperature T is $3nkT$, where k is the Boltzmann constant. The rate of energy loss by mechanisms other than bremsstrahlung is thus simply $3nkT/\tau$. The energy balance of the plasma is the balance between the fusion energy heating the plasma and the energy-loss rate, which is the sum of $3nkT/\tau$ and the bremsstrahlung. The condition satisfying this balance is called the ignition condition. An equation relates the product of density and energy confinement time, denoted $n\tau$, to a function that depends only on the plasma temperature and the type of fusion reaction. For example, when the plasma is composed of deuterium and tritium, the smallest value of $n\tau$ required to achieve ignition is about 2×10^{20} particles per cubic metre times seconds, and the required temperature corresponds to an energy of about 25,000 eV. If the only energy losses are due to bremsstrahlung escaping from the plasma (meaning τ is infinite), the ignition temperature decreases to an energy level of 4,400 eV. Hence, the keys to generating usable amounts of fusion energy are to attain a sufficient plasma temperature and a sufficient confinement quality, as measured by the product $n\tau$. At a temperature equivalent to 10,000 eV, the $n\tau$ product must be about 3×10^{20} particles per cubic metre times seconds.

Magnetic fusion energy generally creates plasmas with a density of about 3×10^{20} particles per cubic metre, which is about 10^{-8} of normal density. Hence, the characteristic time for heat to escape must be greater than about one second. This is a measure of the required degree of magnetic insulation for the heat content. Under these conditions the plasma remains in energy balance and can operate continuously if the ash of the nuclear fusion, namely helium, is removed (otherwise it will quench the plasma) and fuel is replenished.

ICF creates plasmas of much higher density, generally between 10^{31} and 10^{32} particles per cubic metre, or 1,000 to 10,000 times the normal density. As such, the confinement time, or minimum burn time, can be as short as 20×10^{-12} second. The objective in ICF is to achieve a temperature equivalent of 4,400 eV at the centre of the highly compressed fuel mass, while still having sufficient mass left around the centre so that the disassembly time will exceed the minimum burn time.

COLD FUSION

Cold fusion is a hypothesized type of nuclear reaction that would occur at, or near, room temperature. It would contrast starkly with the “hot” fusion that is known to take place naturally within stars and artificially in hydrogen bombs and prototype fusion reactors under immense pressure and at temperatures of millions of degrees, and be distinguished from muon-catalyzed fusion. There is currently no accepted theoretical model that would allow cold fusion to occur.

In 1989, two electrochemists, Martin Fleischmann and Stanley Pons reported that their apparatus had produced anomalous heat (“excess heat”) of a magnitude they asserted

would defy explanation except in terms of nuclear processes. They further reported measuring small amounts of nuclear reaction byproducts, including neutrons and tritium. The small tabletop experiment involved electrolysis of heavy water on the surface of a palladium (Pd) electrode. The reported results received wide media attention and raised hopes of a cheap and abundant source of energy.

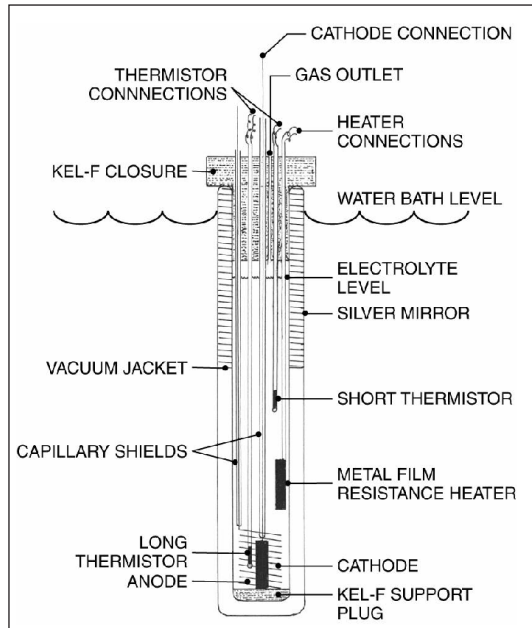


Diagram of an open-type calorimeter used at the New Hydrogen Energy Institute in Japan.

Many scientists tried to replicate the experiment with the few details available. Hopes faded due to the large number of negative replications, the withdrawal of many reported positive replications, the discovery of flaws and sources of experimental error in the original experiment, and finally the discovery that Fleischmann and Pons had not actually detected nuclear reaction byproducts. By late 1989, most scientists considered cold fusion claims dead, and cold fusion subsequently gained a reputation as pathological science. In 1989 the United States Department of Energy (DOE) concluded that the reported results of excess heat did not present convincing evidence of a useful source of energy and decided against allocating funding specifically for cold fusion. A second DOE review in 2004, which looked at new research, reached similar conclusions and did not result in DOE funding of cold fusion.

THERMONUCLEAR FUSION

Thermonuclear fusion is a way to achieve nuclear fusion by using extremely high temperatures. There are two forms of thermonuclear fusion: uncontrolled, in which the resulting energy is released in an uncontrolled manner, as it is in thermonuclear weapons

(“hydrogen bombs”) and in most stars; and controlled, where the fusion reactions take place in an environment allowing some or all of the energy released to be harnessed for constructive purposes.

Temperature Requirements

Temperature is a measure of the average kinetic energy of particles, so by heating the material it will gain energy. After reaching sufficient temperature, given by the Lawson criterion, the energy of accidental collisions within the plasma is high enough to overcome the Coulomb barrier and the particles may fuse together.

In a deuterium–tritium fusion reaction, for example, the energy necessary to overcome the Coulomb barrier is 0.1 MeV. Converting between energy and temperature shows that the 0.1 MeV barriers would be overcome at a temperature in excess of 1.2 billion kelvins.

There are two effects that lower the actual temperature needed. One is the fact that temperature is the average kinetic energy, implying that some nuclei at this temperature would actually have much higher energy than 0.1 MeV, while others would be much lower. It is the nuclei in the high-energy tail of the velocity distribution that account for most of the fusion reactions. The other effect is quantum tunnelling. The nuclei do not actually have to have enough energy to overcome the Coulomb barrier completely. If they have nearly enough energy, they can tunnel through the remaining barrier. For these reasons fuel at lower temperatures will still undergo fusion events, at a lower rate.

Thermonuclear fusion is one of the methods being researched in the attempts to produce fusion power. If thermonuclear fusion becomes favorable to use, it would significantly reduce the world’s carbon footprint.

Confinement

The key problem in achieving thermonuclear fusion is how to confine the hot plasma. Due to the high temperature, the plasma can not be in direct contact with any solid material, so it has to be located in a vacuum. Also, high temperatures imply high pressures. The plasma tends to expand immediately and some force is necessary to act against it. This force can take one of three forms: gravitation in stars, magnetic forces in magnetic confinement fusion reactors, or inertial as the fusion reaction may occur before the plasma starts to expand, so the plasma’s inertia is keeping the material together.

Gravitational Confinement

One force capable of confining the fuel well enough to satisfy the Lawson criterion is gravity. The mass needed, however, is so great that gravitational confinement is only

found in stars—the least massive stars capable of sustained fusion are red dwarfs, while brown dwarfs are able to fuse deuterium and lithium if they are of sufficient mass. In stars heavy enough, after the supply of hydrogen is exhausted in their cores, their cores (or a shell around the core) start fusing helium to carbon. In the most massive stars (at least 8–11 solar masses), the process is continued until some of their energy is produced by fusing lighter elements to iron. As iron has one of the highest binding energies, reactions producing heavier elements are generally endothermic. Therefore significant amounts of heavier elements are not formed during stable periods of massive star evolution, but are formed in supernova explosions. Some lighter stars also form these elements in the outer parts of the stars over long periods of time, by absorbing energy from fusion in the inside of the star, by absorbing neutrons that are emitted from the fusion process.

All of the elements heavier than iron have some potential energy to release, in theory. At the extremely heavy end of element production, these heavier elements can produce energy in the process of being split again back toward the size of iron, in the process of nuclear fission. Nuclear fission thus releases energy which has been stored, sometimes billions of years before, during stellar nucleosynthesis.

Magnetic Confinement

Electrically charged particles (such as fuel ions) will follow magnetic field lines. The fusion fuel can therefore be trapped using a strong magnetic field. A variety of magnetic configurations exist, including the toroidal geometries of tokamaks and stellarators and open-ended mirror confinement systems.

Inertial Confinement

A third confinement principle is to apply a rapid pulse of energy to a large part of the surface of a pellet of fusion fuel, causing it to simultaneously “implode” and heat to very high pressure and temperature. If the fuel is dense enough and hot enough, the fusion reaction rate will be high enough to burn a significant fraction of the fuel before it has dissipated. To achieve these extreme conditions, the initially cold fuel must be explosively compressed. Inertial confinement is used in the hydrogen bomb, where the driver is x-rays created by a fission bomb. Inertial confinement is also attempted in “controlled” nuclear fusion, where the driver is a laser, ion, or electron beam, or a Z-pinch. Another method is to use conventional high explosive material to compress a fuel to fusion conditions. The UTIAS explosive-driven-implosion facility was used to produce stable, centred and focused hemispherical implosions to generate neutrons from D-D reactions. The simplest and most direct method proved to be in a predetonated stoichiometric mixture of deuterium-oxygen. The other successful method was using a miniature Voitenko compressor, where a plane diaphragm was driven by the implosion wave into a secondary small spherical cavity that contained pure deuterium gas at one atmosphere.

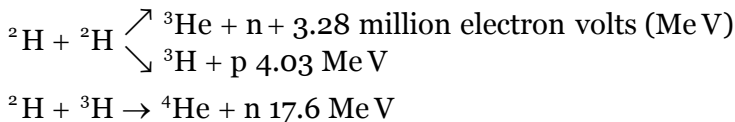
Electrostatic Confinement

There are also electrostatic confinement fusion devices. These devices confine ions using electrostatic fields. The best known is the Fusor. This device has a cathode inside an anode wire cage. Positive ions fly towards the negative inner cage, and are heated by the electric field in the process. If they miss the inner cage they can collide and fuse. Ions typically hit the cathode, however, creating prohibitory high conduction losses. Also, fusion rates in fusors are very low due to competing physical effects, such as energy loss in the form of light radiation. Designs have been proposed to avoid the problems associated with the cage, by generating the field using a non-neutral cloud. These include a plasma oscillating device, a penning trap and the polywell. The technology is relatively immature, however, and many scientific and engineering questions remain.

CONTROLLED FUSION

Controlled fusion is the fusion of light atomic nuclei that occurs at high temperatures under controlled conditions and is accompanied by an energy release. Thermonuclear reactions proceed slowly because of the Coulomb repulsion of positively charged nuclei. Therefore, fusion occurs with an appreciable intensity only between light nuclei that have a small positive charge and only at high temperatures, where the kinetic energy of colliding nuclei is sufficient to overcome the Coulomb potential barrier.

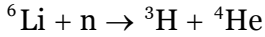
Under natural conditions, thermonuclear reactions between hydrogen nuclei, or protons, occur deep inside stars, particularly in the interior regions of the sun, and thus serve as a constant energy source that governs the radiation of stars. The burning of hydrogen in stars occurs at a low rate, but the huge dimensions and densities of the stars ensure the continuous emission of tremendous energy fluxes for billions of years. Reactions between the heavy isotopes of hydrogen, deuterium ^2H and tritium ^3H , occur at an incomparably higher rate and result in the formation of strongly bound helium nuclei:



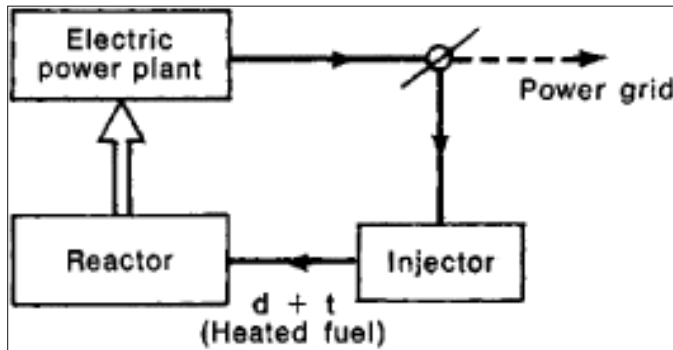
These reactions are of the greatest interest in controlled fusion. The second reaction, which is accompanied by a large energy release and occurs at a significant rate, is particularly interesting. Tritium is radioactive, with a half-life of 12.5 years, and is not found in nature.

Consequently, to ensure the operation of a proposed fusion reactor that uses tritium as the fuel, the tritium must be bred. For this purpose, the reaction zone of the proposed

system may be surrounded by a blanket of a light isotope of lithium, and the following breeding process would occur in that blanket:



The probability or effective cross section of thermonuclear reactions increases rapidly with temperature but, even under optimum conditions remains incomparably smaller than the probability or effective cross section of atomic collisions. For this reason, fusion reactions must occur in completely ionized plasma heated to a high temperature. In such plasma, the ionization and excitation of atoms do not occur and, sooner or later, deuteron-deuteron or deuteron-triton collisions culminate in nuclear fusion.



The specific power output of a fusion reactor is obtained by multiplying the number of nuclear reactions that occur each second per unit volume of the reaction zone of the reactor by the energy released in each reaction event.

The Lawson Criterion

The use of the laws of conservation of energy and particle number makes it possible to elucidate some general requirements imposed on a fusion reactor, requirements that are independent of any particular engineering or design characteristics of the system in question. A schematic diagram of the operation of a reactor is provided. A device of arbitrary design contains pure hydrogen plasma with a density n and a temperature T . Fuel, such as a mixture of equal parts of deuterium and tritium already heated to the required temperature is injected into the reactor. Inside the reactor the injected particles collide with one another from time to time, and nuclear interactions occur. This is a useful process. At the same time, however, energy escapes from the reactor as a result of the electromagnetic radiation of the plasma, and some “hot,” that is, high-energy; particles that have not undergone nuclear interactions escape from the reaction zone.

Let τ be the mean particle confinement time in the reactor; the meaning of the quantity τ is that, on the average, n/τ particles of each sign escape from 1 cm^3 of the plasma in

1 sec. In steady-state operation the same number of particles (calculated per unit volume) must be injected into the reactor each second. To cover the energy losses, the fuel supplied must be fed into the reaction zone with an energy exceeding the energy of the flux of escaping particles. This additional energy must be compensated for by the fusion energy released in the reaction zone and by the partial recovery of electromagnetic radiation and corpuscular fluxes in the reactor walls and blanket.

Let us assume, for simplicity's sake, that the ratio of conversion into electrical energy is identical for the nuclear reaction products, electromagnetic radiation, and thermal particles and is equal to η . The quantity η is often called the efficiency. When the system operates in the steady state and the effective power output is zero, the energy balance equation for the reactor has the form:

$$\eta(P_o + P_r + P_t) = P_r + P_t$$

Where, P_o is the energy released as nuclear power, P_r is the power of the radiation flux, and P_t is the power of the escaping particle flux. When the left-hand side of the equation is made greater than the right-hand side, the reactor stops expending energy and begins operating as a thermonuclear electric power plant. In writing previous equation, it is assumed that all the recovered energy is returned without losses to the reactor through the injector, together with the flow of the heated fuel that is supplied. Since the quantities P_o , P_r , and P_t depend in a known way on the plasma temperature, we can easily calculate from the balance equation the product:

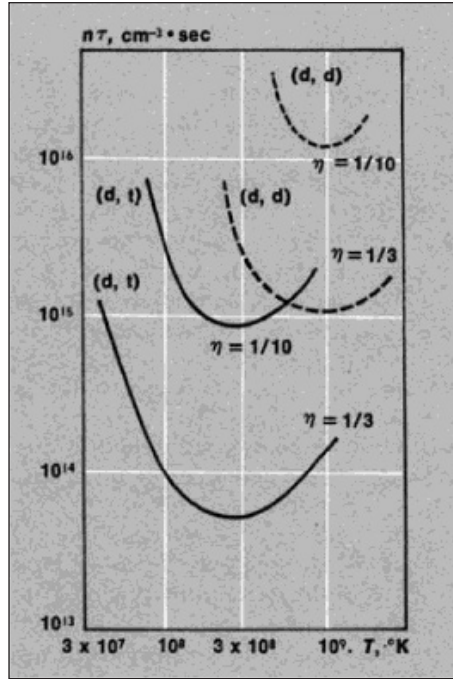
$$n\tau = f(T)$$

Here, $f(T)$ for a given value of the efficiency η and the type of fuel selected is a well-defined function of temperature. Plots of $f(T)$ are given in figure for two values of η and for both deuterium-deuterium (d, d) and deuterium-tritium (d, t) reactions. If the values of $n\tau$ attained in a given device lie above the curve of $f(T)$, the system will operate as an energy generator. When $\eta = \frac{1}{2}$, the operation of the reactor in producing useful power corresponds under optimum conditions (the minimum of the curves in figure) to the following condition, which is called the Lawson criterion: for (d, d) reactions, $n\tau \geq 10^{15} \text{ cm}^{-3} \cdot \text{sec}$, and $T \sim 10^{90} \text{ K}$; for (d, t) reactions, $n\tau \geq 0.5 \times 10^{14} \text{ cm}^{-3} \cdot \text{sec}$, and $T \sim 2 \times 10^{80} \text{ K}$.

Thus, even under optimum conditions and with very optimistic assumptions concerning the value of η temperatures of about $2 \times 10^{80} \text{ K}$ must be attained for the case of greatest interest, namely, a reactor fueled by a mixture of equal parts of deuterium and tritium. In this case, confinement times of the order of seconds must be achieved for plasma with a density of about 10^{14} cm^{-3} . The reactor, of course, may produce useful energy at lower temperatures, but the energy must be "paid for" by higher values of $n\tau$.

In short, the construction of a fusion reactor presupposes (1) the creation of plasma heated to temperatures of hundreds of millions of degrees and (2) the maintenance of

a plasma configuration for the time required for nuclear reactions to occur. Research in controlled fusion is following two paths—the development of quasi-steady-state systems, on the one hand, and the development of extremely high-speed devices, on the other.



Controlled Fusion with Magnetic Confinement

Let us first consider quasi-steady-state systems. An energy yield at the level of 10^5 kilowatts per cubic meter (kW/m^3) is achieved for (d, t) reactions when the plasma density is about 10^{15} cm^{-3} and the temperature is about 10^{80} K . This means that the size of a reactor with an output of 10^6 – 10^7 kW —the typical output of large present-day electric power plants—should be in the range 10 – 100 m^3 , which is entirely acceptable. The main problem is how to confine the hot plasma in the reaction zone. The diffusive particle and heat fluxes at the cited values of n and T are huge, and no material walls are suitable. A ground-breaking idea advanced in 1950 in the Soviet Union and the USA consists in the use of the principle of magnetic confinement of the plasma. When the charged particles that form the plasma are located in a magnetic field, they cannot move freely perpendicular to the field’s lines of force. As a result, the coefficients of diffusion and thermal conductivity across the magnetic field decrease very rapidly with increasing field strength in the case of a stable plasma; for example, with fields of $\sim 10^5$ gauss the coefficients are reduced by 14–15 orders of magnitude as opposed to their “unmagnetized” value for a plasma with the density and temperature indicated above. Thus, in principle, the use of a sufficiently strong magnetic field opens the way to the design of a fusion reactor.

There are three areas of research in the field of controlled fusion with magnetic confinement: (1) open, or mirror-type, magnetic traps, (2) closed magnetic systems, and (3) pulsed machines.

In open traps, particles cannot easily escape, across the lines of force, from the reaction zone to the walls of the device. The particles escape either during “magnetized” diffusion—that is, very slowly—or by means of charge exchange with the molecules of the residual, that is, un-ionized gas. The escape of the plasma along the lines of force is likewise inhibited by regions of intensified magnetic field located at the open ends of the trap; such regions are called magnetic mirrors, or end plugs. The traps are usually filled with plasma by injecting plasmoids or individual high-energy particles. Additional plasma heating can be accomplished with the aid of adiabatic compression in a rising magnetic field.

In closed systems, such as Tokamaks and stellarators, the escape of particles to the walls of a toroidal device across a longitudinal magnetic field is also difficult and occurs as a result of magnetized diffusion and charge exchange. The plasma column in a Tokamak is heated in the initial stages by a ring current that flows through the column. As the temperature rises, however, Joule heating becomes increasingly less effective, since the resistance of the plasma decreases rapidly with increasing temperature. Methods of heating by a high-frequency electromagnetic field and by the injection of energy with the aid of fluxes of fast neutral particles are used to heat the plasma above 10^{70} K.

In pulsed machines, such as the Z pinch and 8 pinches, plasma heating and plasma confinement are accomplished by strong short-period currents that flow through the plasma. As the current and magnetic pressure increase simultaneously, the plasma is squeezed away from the walls of the containment vessel. This effect ensures that the plasma is confined. The temperature increases as a result of Joule heating, adiabatic compression of the plasma column, and, apparently, turbulent processes associated with the development of plasma instability.

The study of hot plasmas in high-frequency (HF) fields is an independent area of research. As the experiments of P. L. Kapitsa have shown, in hydrogen and helium a freely hovering plasma column with an electron temperature of about 10^{60} K can be produced in HF fields at sufficiently high pressure. Such a system allows for the closing of the column into a ring and the superposition of an additional longitudinal magnetic field.

The successful operation of any of the devices listed above is possible only if the initial plasma structure is macroscopically stable and maintains a specified shape for the entire period of time necessary for the reaction to occur. Furthermore, microscopic instabilities must be suppressed in the plasma. When such instabilities arise and develop, the energy distribution of the particles ceases to be an equilibrium distribution, and the particle and heat fluxes across the lines of force increase sharply in comparison with their theoretical values. Since 1950 most research in magnetic systems has been

directed at the stabilization of plasma configurations; this work still cannot be regarded as completed.

Ultrahigh-speed controlled fusion systems with inertia! Confinement. The difficulties associated with the magnetic confinement of plasma can be obviated in principle if the nuclear fuel is burned for extremely short periods of time, during which the heated matter cannot disperse from the reaction zone. In accordance with the Lawson criterion, useful energy can be obtained with this method of burning only if the fuel has a very high density. To avoid a high-power thermonuclear explosion, very small amounts of fuel must be used. The initial thermonuclear fuel must be in the form of small pellets, 1–2 mm in diameter, prepared from a mixture of deuterium and tritium and injected into the reactor before each reaction cycle. The main problem consists in supplying the necessary energy to heat the fuel pellets. As of 1976, the solution of this problem lies in the use of laser beams or high-power electron beams. Research in controlled fusion with the use of laser heating was begun in 1964; the use of electron beams is in an early stage of study—thus far, relatively few electron-beam fusion experiments have been performed.

Estimates show that the energy W that must be supplied to sustain the operation of a reactor is expressed as:

$$W \geq \frac{10^8}{\eta^3 \alpha^2} \text{Joules (J)}$$

Here, η is a general expression for the efficiency of the device and α is the coefficient of target compression. As this equation shows, even with very optimistic assumptions regarding the possible value of η the value of W when $\alpha = 1$ is disproportionately large. Admissible values of W can therefore be approached only in conjunction with a sharp increase in the density of the target (by a factor of approximately 10^4) in comparison with the initial density of a solid (d, t) target. Rapid heating of the target is accompanied by the vaporization of its surface layers and the reaction compression of its interior regions. If the power supplied is time-programmed in a specific manner, then, as calculations show, the coefficients of compression indicated can be attained. Another possibility is to program the radial distribution of the target density. In both cases, the energy required is reduced to 106J, which is technically feasible considering the rapid development of laser devices.

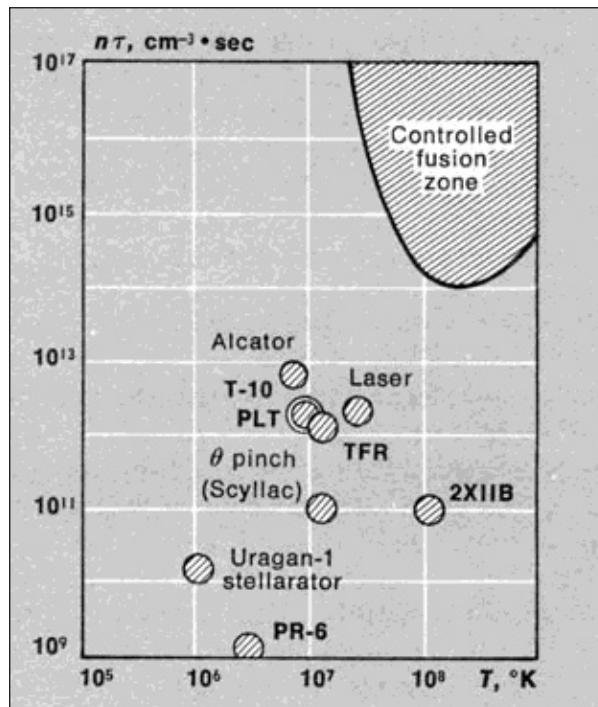
Difficulties and Prospects

Research in controlled fusion encounters major difficulties that are both purely physical and technical in nature. The physical difficulties include the cited problem of the stability of hot plasma placed in a magnetic trap. It is true that the use of strong magnetic fields with a special configuration suppresses the particle fluxes escaping from the reaction zone and, in a number of cases, makes it possible to obtain sufficiently stable

plasma formations. With n of about 10^{15} cm^{-3} , T of about 10^8 K , and a possible reactor size of $10\text{--}100 \text{ m}^3$, electromagnetic radiation freely escapes from the plasma. However, for a purely hydrogen plasma, the energy losses are determined solely by electron bremsstrahlung and, in the case of (d, t) reactions, are compensated for by the energy released as nuclear power at temperatures above $4 \times 10^7 \text{ K}$.

The second fundamental difficulty is connected with the problem of impurities. Even a small impurity of foreign atoms with a high atomic weight, which are in a highly ionized state at the temperatures considered, leads to a sharp increase in the intensity of the continuous spectrum, to the appearance of a line spectrum, and to an increase in energy losses to a level above the acceptable level. Extraordinary efforts, such as the continuous improvement of evacuation equipment, the use of refractory and nonsputtering metals as the orifice material, and the use of special devices to trap foreign atoms, are required to minimize the amount of impurities in the plasma. More accurately, the "lethal" concentration that makes it impossible for thermonuclear reactions to occur is, for example, a few tenths of 1 percent for a tungsten or molybdenum impurity.

The parameters achieved in various machines as of mid-1976 are shown in figure in a plot of $n\tau$ against T . Tokamaks and laser systems come the closest to the region where the Lawson criterion is met, and a self-sustaining thermonuclear reaction can occur. It would be erroneous, however, to make categorical conclusions, on the basis of the available data, as to the type of device that will be used as a future thermonuclear reactor. The development of this field of technical physics is proceeding too rapidly, and many estimates will change over the next decade.



The tremendous importance attached to research in controlled fusion is explained by a number of factors. The growing pollution of the environment urgently requires the conversion of the planet's industrial production to a closed cycle with a minimum of waste. However, such a reorganization of industry inevitably entails a sharp increase in energy consumption. Meanwhile, the resources of fossil fuels are limited and, at the current rate of development of power engineering, will be exhausted in the next few decades—as in the case of petroleum and gaseous fuels—or centuries—as in the case of coal. The best alternative, of course, would be the use of solar energy, but the lower power density of incident solar radiation greatly complicates the efficient solution of this problem. The conversion to the use of nuclear fission reactors on a global scale raises complex problems of the burial of tremendous amounts of radioactive wastes; the alternative is to eject the radioactive wastes into space. According to available estimates, the radiation danger of controlled fusion installations should be three orders of magnitude less than that of fission reactors. In the future, the best solution would be a combination of solar energy and controlled fusion.

Figure shows parameters attained by mid-1976 in various machines for studying the problem of controlled fusion: (T-10) a Tokamak machine at the I. V. Kurchatov Institute of Atomic Energy, USSR; (PLT) a Tokamak machine at the Princeton Plasma Physics Laboratory, USA; (Alcator) a Tokamak machine at the Massachusetts Institute of Technology, USA; (TFR) a Tokamak machine at Fontanay-aux-Roses, France; (PR-6) an open trap at the I. V. Kurchatov Institute of Atomic Energy, USSR; (2XIIB) an open trap at the Lawrence Livermore Laboratory, USA; (O pinch [Scyllac]) a machine at the Los Alamos Scientific Laboratory, USA; (Uragan-1 stellarator) a machine at the Ukrainian Physicotechnical Institute, USSR; (Laser) pulsed laser-heated systems, USSR and USA.

References

- Nuclear-fission, science: britannica.com, Retrieved 08 April, 2020
- Controlled-Fusion: encyclopedia2.thefreedictionary.com, Retrieved 19 May, 2020
- Paşca, H.; Andreev, A.V.; Adamian, G.G.; Antonenko, N.V. (2018). “Charge distributions of fission fragments of low- and high-energy fission of Fm, No, and Rf isotopes”. *Physical Review C*. 97 (3): 034621–1–034621–12. doi:10.1103/PhysRevC.97.034621
- Shultis, J. Kenneth; Richard E. Faw (2008). *Fundamentals of Nuclear Science and Engineering*. CRC Press. pp. 141 (table 6.2). ISBN 978-1-4200-5135-3
- Silano, J.A.; Karwowski, H.J. (2018-11-19). “Near-barrier Photofission in ^{232}Th and ^{238}U ”. *Physical Review C*. 98: 054609. doi:10.1103/PhysRevC.98.054609. Retrieved 2019-12-09
- Nuclear-fusion, science: britannica.com, Retrieved 17 August, 2020
- Biberian, Jean-Paul (2007), “Condensed Matter Nuclear Science (Cold Fusion): An Update” (PDF), *International Journal of Nuclear Energy Science and Technology*, 3 (1): 31–42, CiteSeerX 10.1.1.618.6441, doi:10.1504/IJNEST.2007.012439, archived (PDF) from the original on 30 May 2008

Radioactive Decay

4

CHAPTER

The process in which an unstable atomic nucleus loses its energy due to radiation is termed as radioactive decay. Alpha decay, beta decay and gamma decay, etc. are studied under its domain. This chapter closely examines the aspects associated with radioactive decay to provide an extensive understanding of the subject.

RADIOACTIVITY

Radioactivity is the property exhibited by certain types of matter of emitting energy and subatomic particles spontaneously. It is, in essence, an attribute of individual atomic nuclei.

An unstable nucleus will decompose spontaneously, or decay, into a more stable configuration but will do so only in a few specific ways by emitting certain particles or certain forms of electromagnetic energy. Radioactive decay is a property of several naturally occurring elements as well as of artificially produced isotopes of the elements. The rate at which a radioactive element decays is expressed in terms of its half-life; i.e., the time required for one-half of any given quantity of the isotope to decay. Half-lives range from more than 1,000,000,000 years for some nuclei to less than 10^{-9} second. The product of a radioactive decay process—called the daughter of the parent isotope—may it be unstable, in which case it, too, will decay. The process continues until a stable nuclide has been formed.

The Nature of Radioactive Emissions

The emissions of the most common forms of spontaneous radioactive decay are the alpha (α) particle, the beta (β) particle, the gamma (γ) ray, and the neutrino. The alpha particle is actually the nucleus of a helium-4 atom, with two positive charges ${}^4_2\text{He}$. Such charged atoms are called ions. The neutral helium atom has two electrons outside its nucleus balancing these two charges. Beta particles may be negatively charged (beta minus, symbol e^-), or positively charged (beta plus, symbol e^+). The beta minus [β^-] particle is actually an electron created in the nucleus during beta decay without any relationship to the orbital electron cloud of the atom. The beta plus particle, also called the positron, is the antiparticle of the electron; when brought together, two such particles will mutually annihilate each other. Gamma rays are electromagnetic radiations

such as radio waves, light, and X-rays. Beta radioactivity also produces the neutrino and antineutrino, particles that have no charge and very little mass, symbolized by ν and $\bar{\nu}$, respectively.

In the less common forms of radioactivity, fission fragments, neutrons, or protons may be emitted. Fission fragments are themselves complex nuclei with usually between one-third and two-thirds the charge Z and mass A of the parent nucleus. Neutrons and protons are, of course, the basic building blocks of complex nuclei, having approximately unit mass on the atomic scale and having zero charge or unit positive charge, respectively. The neutron cannot long exist in the Free State. It is rapidly captured by nuclei in matter; otherwise, in free space it will undergo beta-minus decay to a proton, an electron, and an antineutrino with a half-life of 12.8 minutes. The proton is the nucleus of ordinary hydrogen and is stable.

Occurrence of Radioactivity

Some species of radioactivity occur naturally on Earth. A few species have half-lives comparable to the age of the elements (about 6×10^9 years), so that they have not decayed away after their formation in stars. Notable among these are uranium-238, uranium-235, and thorium-232. Also, there is potassium-40, the chief source of irradiation of the body through its presence in potassium of tissue. Of lesser significance are the beta emitters vanadium-50, rubidium-87, indium-115, tellurium-123, lanthanum-138, lutetium-176, and rhenium-187, and the alpha emitters cerium-142, neodymium-144, samarium-147, gadolinium-152, dysprosium-156, hafnium-174, platinum-190, and lead-204. Besides these approximately 10^9 -year species, there are the shorter-lived daughter activities fed by one or another of the above species; e.g., by various nuclei of the elements between lead ($Z = 82$) and thorium ($Z = 90$).

Another category of natural radioactivity includes species produced in the upper atmosphere by cosmic ray bombardment. Notable are 5,720-year carbon-14 and 12.3-year tritium (hydrogen-3), 53-day beryllium-7, and 2,700,000-year beryllium-10. Meteorites are found to contain additional small amounts of radioactivity, the result of cosmic ray bombardments during their history outside the Earth's atmospheric shield. Activities as short-lived as 35-day argon-37 have been measured in fresh falls of meteorites. Nuclear explosions since 1945 have injected additional radioactivities into the environment, consisting of both nuclear fission products and secondary products formed by the action of neutrons from nuclear weapons on surrounding matter.

The fission products encompass most of the known beta emitters in the mass region 75–160. They are formed in varying yields, rising to maxima of about 7 percent per fission in the mass region 92–102 (light peak of the fission yield versus atomic mass curve) and 134–144 (heavy peak). Two kinds of delayed hazards caused by radioactivity are recognized. First, the general radiation level is raised by fallout settling to Earth. Protection can be provided by concrete or earth shielding until the activity has decayed

to a sufficiently low level. Second, ingestion or inhalation of even low levels of certain radioactive species can pose a special hazard, depending on the half-life, nature of radiations, and chemical behaviour within the body.

Nuclear reactors also produce fission products but under conditions in which the activities may be contained. Containment and waste-disposal practices should keep the activities confined and eliminate the possibility of leaching into groundwaters for times that are long compared to the half-lives. A great advantage of thermonuclear fusion power over fission power, if it can be practically realized, is not only that its fuel reserves, heavy hydrogen and lithium, are vastly greater than uranium, but also that the generation of radioactive fission product wastes can be largely avoided. In this connection, it may be noted that a major source of heat in the interior of both the Earth and the Moon is provided by radioactive decay. Theories about the formation and evolution of the Earth, Moon, and other planets must take into account these large heat production sources.

Desired radioactivities other than natural activities and fission products may be produced either by irradiation of certain selected target materials by reactor neutrons or by charged particle beams or gamma ray beams of accelerators.

Energetics and Kinetics of Radioactivity

Energy Release in Radioactive Transitions

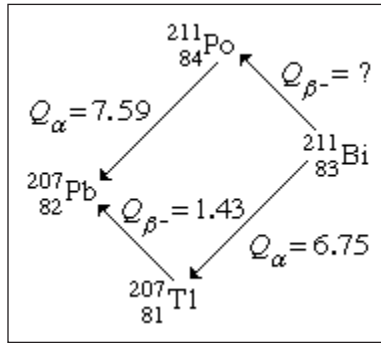
Consideration of the energy release of various radioactive transitions leads to the fundamental question of nuclear binding energies and stabilities. A much-used method of displaying nuclear-stability relationships is an isotope chart, those positions on the same horizontal row corresponding to a given proton number (Z) and those on the same vertical column to a given neutron number (N). The irregular bold line surrounds the region of presently known nuclei. The area encompassed by this is often referred to as the valley of stability because the chart may be considered a map of a binding energy surface, the lowest areas of which are the most stable. The most tightly bound nuclei of all are the abundant iron and nickel isotopes. Near the region of the valley containing the heaviest nuclei (largest mass number A ; i.e., largest number of nucleons, $N + Z$), the processes of alpha decay and spontaneous fission are most prevalent; both these processes relieve the energetically unfavourable concentration of positive charge in the heavy nuclei.

Along the region that borders on the valley of stability on the upper left-hand side are the positron-emitting and electron-capturing radioactive nuclei, with the energy release and decay rates increasing the farther away the nucleus is from the stability line. Along the lower right-hand border region, beta-minus decay is the predominant process, with energy release and decay rates increasing the farther the nucleus is from the stability line.

The grid lines of the graph are at the nucleon numbers corresponding to extra stability, the “magic numbers”. The circles labeled “deformed regions” enclose regions in which nuclei should exhibit cigar shapes; elsewhere the nuclei are spherical. Outside the dashed lines nuclei would be unbound with respect to neutron or proton loss and would be exceedingly short-lived (less than 10–19 second).

Calculation and Measurement of Energy

By the method of closed energy cycles, it is possible to use measured radioactive-energy-release (Q) values for alpha and beta decay to calculate the energy release for unmeasured transitions. An illustration is provided by the cycle of four nuclei below:



In this cycle, energies from two of the alpha decays and one beta decay are measurable. The unmeasured beta-decay energy for bismuth-211, $Q_{\beta^-}(\text{Bi})$, is readily calculated because conservation of energy requires the sum of Q values around the cycle to be zero. Thus, $Q_{\beta^-}(\text{Bi}) + 7.59 - 1.43 - 6.75 = 0$. Solving this equation gives $Q_{\beta^-}(\text{Bi}) = 0.59$ MeV. This calculation by closed energy cycles can be extended from stable lead-207 back up the chain of alpha and beta decays to its natural precursor uranium-235 and beyond. In this manner the nuclear binding energies of a series of nuclei can be linked together. Because alpha decay decreases the mass number A by 4, and beta decay does not change A , closed α - β -cycle calculations based on lead-207 can link up only those nuclei with mass numbers of the general type $A = 4n + 3$, in which n is an integer. Another, the $4n$ series, has as its natural precursor thorium-232 and its stable end product lead-208. Another, the $4n + 2$ series, has uranium-238 as its natural precursor and lead-206 as its end product.

In early research on natural radioactivity, the classification of isotopes into the series cited above was of great significance because they were identified and studied as families. Newly discovered radioactivities were given symbols relating them to the family and order of occurrence therein. Thus, thorium-234 was known as UX_1 , the isomers of protactinium-234 as UX_2 and UZ , uranium-234 as U_{II} , and so forth. These original symbols and names are occasionally encountered in more recent literature but are mainly of historical interest. The remaining $4n + 1$ series is not naturally occurring but comprises well-known artificial activities decaying down to stable thallium-205.

To extend the knowledge of nuclear binding energies, it is clearly necessary to make measurements to supplement the radioactive-decay energy cycles. In part, this extension can be made by measurement of Q values of artificial nuclear reactions. For example, the neutron-binding energies of the lead isotopes needed to link the energies of the four radioactive families together can be measured by determining the threshold gamma-ray energy to remove a neutron (photonuclear reaction); or the energies of incoming deuteron and outgoing proton in the reaction can be measured to provide this information.

Further extensions of nuclear-binding-energy measurements rely on precision mass spectroscopy. By ionizing, accelerating, and magnetically deflecting various nuclides, their masses can be measured with great precision. A precise measurement of the masses of atoms involved in radioactive decay is equivalent to direct measurement of the energy release in the decay process. The atomic mass of naturally occurring but radioactive potassium-40 is measured to be 39.964008 amu. Potassium-40 decays predominantly by β -emission to calcium-40, having a measured mass 39.962589. Through Einstein's equation, energy is equal to mass (m) times velocity of light (c) squared, or $E = mc^2$, the energy release (Q) and the mass difference, Δm , are related, the conversion factor being one amu, equal to 931.478 MeV. Thus, the excess mass of potassium-40 over calcium-40 appears as the total energy release Q_{β^-} in the radioactive decay $Q_{\beta^-} = (39.964008 - 39.962589) \times 931.478 \text{ MeV} = 1.31 \text{ MeV}$. The other neighbouring isobar (same mass number, different atomic number) to argon-40 is also of lower mass, 39.962384, than potassium-40. This mass difference converted to energy units gives an energy release of 1.5 MeV, this being the energy release for EC decay to argon-40. The maximum energy release for positron emission is always less than that for electron capture by twice the rest mass energy of an electron ($2m_0c^2 = 1.022 \text{ MeV}$); thus, the maximum positron energy for this reaction is $1.5 - 1.02$, or 0.48 MeV.

To connect alpha-decay energies and nuclear mass differences requires a precise knowledge of the alpha-particle (helium-4) atomic mass. The mass of the parent minus the sum of the masses of the decay products gives the energy release. Thus, for alpha decay of plutonium-239 to uranium-235 and helium-4 the calculation goes as follows:

$$\begin{array}{r}
 M(^{239}\text{Pu}) \quad 239.05216 \\
 -M(^{235}\text{U}) \quad -235.04393 \\
 -M(^4\text{He}) \quad - \quad \underline{4.00260} \\
 \hline
 \qquad \qquad \qquad 0.00563 \times 931.478 \\
 Q_{\alpha} = 5.24 \text{ MeV}
 \end{array}$$

By combining radioactive-decay-energy information with nuclear-reaction Q values and precision mass spectroscopy, extensive tables of nuclear masses have been prepared. From them the Q values of unmeasured reactions or decay may be calculated.

Alternative to the full mass, the atomic masses may be expressed as mass defect, symbolized by the Greek letter delta, Δ (the difference between the exact mass M and the integer A , the mass number), either in energy units or atomic mass units.

Absolute Nuclear Binding Energy

The absolute nuclear binding energy is the hypothetical energy release if a given nuclide were synthesized from Z separate hydrogen atoms and N (equal to $A - Z$) separate neutrons. An example is the calculation giving the absolute binding energy of the stablest of all nuclei, iron-56:

$$\begin{array}{rcl}
 26 \times M(^1\text{H}) & 26 \times 1.007825 & = 26.20345 \\
 30 \times M(\text{n}) & 30 \times 1.008665 & = 30.25995 \\
 M(^{56}\text{Fe}) & & - 55.93493 \\
 \text{Binding Energy} & = & 0.52847 \times 931.478 \\
 & & = 492.58 \text{ MeV}
 \end{array}$$

$$\begin{array}{rcl}
 \text{Average Binding Energy} & & \\
 \text{per Nucleon of } ^{56}\text{Fe} & = & 492.58 / 56 = 8.796 \text{ MeV}
 \end{array}$$

A general survey of the average binding energy per nucleon (for nuclei of all elements grouped according to ascending mass) shows a maximum at iron-56 falling off gradually on both sides to about 7 MeV at helium-4 and to about 7.4 MeV for the most massive nuclei known. Most of the naturally occurring nuclei are thus not stable in an absolute nuclear sense. Nuclei heavier than iron would gain energy by degrading into nuclear products closer to iron, but it is only for the elements of greatest mass that the rates of degradation processes such as alpha decay and spontaneous fission attain observable rates. In a similar manner, nuclear energy is to be gained by fusion of most elements lighter than iron. The coulombic repulsion between nuclei, however, keeps the rates of fusion reactions unobservably low unless the nuclei are subjected to temperatures of greater than 10^7 K. Only in the hot cores of the Sun and other stars or in thermonuclear bombs or controlled fusion plasmas are these temperatures attained and nuclear-fusion energy released.

Rates of Radioactive Transitions

There is a vast range of the rates of radioactive decay, from undetectably slow to unmeasurably short. Before considering the factors governing particular decay rates in detail, it seems appropriate to review the mathematical equations governing radioactive decay and the general methods of rate measurement in different ranges of half-life.

Exponential-decay Law

Radioactive decay occurs as a statistical exponential rate process. That is to say, the

number of atoms likely to decay in a given infinitesimal time interval (dN/dt) is proportional to the number (N) of atoms present. The proportionality constant, symbolized by the Greek letter lambda, λ , is called the decay constant. Mathematically, this statement is expressed by the first-order differential equation,

$$-\frac{dN}{dt} = \lambda N$$

This equation is readily integrated to give:

$$N(t) = N_0 e^{-\lambda t}$$

In which N_0 is the number of atoms present when time equals zero. From the above two equations it may be seen that a disintegration rate, as well as the number of parent nuclei, falls exponentially with time. An equivalent expression in terms of half-life $t_{1/2}$ is:

$$N(t) = N_0 (1/2)^{t/t_{1/2}}; \quad r = t/t_{1/2}$$

It can readily be shown that the decay constant λ and half-life ($t_{1/2}$) are related as follows: $\lambda = \log_e 2/t_{1/2} = 0.693/t_{1/2}$. The reciprocal of the decay constant λ is the mean life, symbolized by the Greek letter tau, τ .

For a radioactive nucleus such as potassium-40 that decays by more than one process (89 percent β^- , 11 percent electron capture), the total decay constant is the sum of partial decay constants for each decay mode. (The partial half-life for a particular mode is the reciprocal of the partial decay constant times 0.693.) It is helpful to consider a radioactive chain in which the parent (generation 1) of decay constant λ_1 decays into a radioactive daughter (generation 2) of decay constant λ_2 . The case in which none of the daughter isotope is originally present yields an initial growth of daughter nuclei followed by its decay. The equation giving the number (N_2) of daughter nuclei existing at time t in terms of the number $N_1(0)$ of parent nuclei present when time equals zero is:

$$N_2(t) = \lambda_1 N_1(0) \frac{e^{-\lambda_1 t} - e^{-\lambda_2 t}}{\lambda_2 - \lambda_1}$$

In which e represents the logarithmic constant 2.71828.

The general equation for a chain of n generations with only the parent initially present (when time equals zero) is as follows:

$$N_n(t) = N_1(0)(C_1 e^{-\lambda_1 t} + C_2 e^{-\lambda_2 t} + \dots + C_n e^{-\lambda_n t}) \lambda_1 \lambda_2 \dots \lambda_{n-1}$$

In which e represents the logarithmic constant 2.71828.

$$C_1 = \frac{1}{(\lambda_2 - \lambda_1)(\lambda_3 - \lambda_1) \dots (\lambda_n - \lambda_1)}$$

$$C_2 = \frac{1}{(\lambda_1 - \lambda_2)(\lambda_3 - \lambda_2) \cdots (\lambda_n - \lambda_2)}$$

$$C_n = \frac{1}{(\lambda_1 - \lambda_n)(\lambda_2 - \lambda_n) \cdots (\lambda_{n-1} - \lambda_n)}$$

These equations can readily be modified to the case of production of isotopes in the steady neutron flux of a reactor or in a star. In such cases, the chain of transformations might be mixed with some steps occurring by neutron capture and some by radioactive decay. The neutron-capture probability for a nucleus is expressed in terms of an effective cross-sectional area. If one imagines the nuclei replaced by spheres of the same cross-sectional area, the rate of reaction in a neutron flux would be given by the rate at which neutrons strike the spheres. The cross section is usually symbolized by the Greek letter sigma, σ , with the units of barns (10^{-24} cm^2) or millibarns (10^{-3} b) or microbarns (10^{-6} b). Neutron flux is often symbolized by the letters $n\nu$ (neutron density, n , or number per cubic centimetre, times average speed, ν) and given in neutrons per square centimetre per second.

The modification of the transformation equations merely involves substituting the product $n\nu\sigma_i$ in place of λ_i for any step involving neutron capture rather than radioactive decay. Reactor fluxes $n\nu$ even higher than 10^{15} neutrons per square centimetre per second are available in several research reactors, but usual fluxes are somewhat lower by a factor of 1,000 or so. Tables of neutron-capture cross sections of the naturally occurring nuclei and some radioactive nuclei can be used for calculation of isotope production rates in reactors.

Measurement of Half-life

The measurement of half-lives of radioactivity in the range of seconds to a few years commonly involves measuring the intensity of radiation at successive times over a time range comparable to the half-life. The logarithm of the decay rate is plotted against time, and a straight line is fitted to the points. The time interval for this straight-line decay curve to fall by a factor of 2 is read from the graph as the half-life, by virtue of equations ($-\frac{dN}{dt} = \lambda N$) and ($N(t) = N_0 e^{-\lambda t}$). If there is more than one activity present in the sample, the decay curve will not be a straight line over its entire length, but it should be resolvable graphically (or by more sophisticated statistical analysis) into sums and differences of straight-line exponential terms. The general equations ($N_n(t) = N_1(0)(C_1 e^{-\lambda_1 t} + C_2 e^{-\lambda_2 t} + \cdots C_n e^{-\lambda_n t}) \lambda_1 \lambda_2 \cdots \lambda_{n-1}$) for chain decays show a time dependence given by sums and differences of exponential terms, though special modified equations are required in the unlikely case that two or more decay constants are identically equal.

For half-lives longer than several years it is often not feasible to measure accurately

the decrease in counting rate over a reasonable length of time. In such cases, a measurement of specific activity may be resorted to; i.e., a carefully weighed amount of the radioactive isotope is taken for counting measurements to determine the disintegration rate, D . Then by equation $(-\frac{dN}{dt} = \lambda N)$ the decay constant λ may be calculated. Alternatively, it may be possible to produce the activity of interest in such a way that the number of nuclei, N , is known, and again with a measurement of D equation $(-\frac{dN}{dt} = \lambda N)$ may be used. The number of nuclei, N , might be known from counting the decay of a parent activity or from knowledge of the production rate by a nuclear reaction in a reactor or accelerator beam.

Half-lives from 100 microseconds to one nanosecond are measured electronically in coincidence experiments. The radiation yielding the species of interest is detected to provide a start pulse for an electronic clock, and the radiation by which the species decays is detected in another device to provide a stop pulse. The distribution of these time intervals is plotted semi-logarithmically and the half-life is determined from the slope of the straight line.

Half-lives in the range of 100 microseconds to one second must often be determined by special techniques. For example, the activities produced may be deposited on rapidly rotating drums or moving tapes, with detectors positioned along the travel path. The activity may be produced so as to travel through a vacuum at a known velocity and the disintegration rate measured as a function of distance; however, this method usually applies to shorter half-lives in or beyond the range of the electronic circuit.

Species with half-lives shorter than the electronic measurement limit are not considered as separate radioactivities, and the various techniques of determining their half-lives will hence not be cited here.

Alpha Decay

Alpha decay, the emission of helium ions, exhibits sharp line spectra when spectroscopic measurements of the alpha-particle energies are made. For even-even alpha emitters the most intense alpha group or line is always that leading to the ground state of the daughter. Weaker lines of lower energy go to excited states, and there are frequently numerous lines observable.

The main decay group of even-even alpha emitters exhibits a highly regular dependence on the atomic number, Z , and the energy release, Q_α . (Total alpha energy release, Q_α , is equal to alpha-particle energy, E_α , plus daughter recoil energy needed for conservation of momentum; $E_{\text{recoil}} = (m_\alpha/[m_\alpha + M_d])E_\alpha$, with m_α equal to the mass of the alpha particle and M_d the mass of the daughter product.) As early as 1911 the German physicist Johannes Wilhelm Geiger, together with the British physicist John Mitchell Nuttall, noted the regularities of rates for even-even nuclei and proposed a remarkably

successful equation for the decay constant, $\log \lambda = a + b \log r$, in which r is the range in air, b is a constant, and a is given different values for the different radioactive series. The decay constants of odd alpha emitters (odd A or odd Z or both) are not quite so regular and may be much smaller. The values of the constant b that were used by Geiger and Nuttall implied a roughly 90th-power dependence of λ on Q_α . There is a tremendous range of known half-lives from the 2×10^{15} years of ${}^{144}_{60}\text{Nd}$ (neodymium) with its 1.83-MeV alpha-particle energy (E_α) to the 0.3 microsecond of ${}^{212}_{84}\text{Po}$ (polonium) with $E_\alpha = 8.78$ MeV.

The theoretical basis for the Geiger–Nuttall empirical rate law remained unknown until the formulation of wave mechanics. A dramatic early success of wave mechanics was the quantitative theory of alpha-decay rates. One curious feature of wave mechanics is that particles may have a nonvanishing probability of being in regions of negative kinetic energy. In classical mechanics a ball that is tossed to roll up a hill will slow down until its gravitational potential energy equals its total energy, and then it will roll back toward its starting point. In quantum mechanics the ball has a certain probability of tunneling through the hill and popping out on the other side. For objects large enough to be visible to the eye, the probability of tunneling through energetically forbidden regions is unobservably small. For submicroscopic objects such as alpha particles, nucleons, or electrons, however, quantum mechanical tunneling can be an important process—as in alpha decay.

The logarithm of tunneling probability on a single collision with an energy barrier of height B and thickness D is a negative number proportional to thickness D , to the square root of the product of B and particle mass m . The size of the proportionality constant will depend on the shape of the barrier and will depend inversely on Planck's constant h .

In the case of alpha decay, the electrostatic repulsive potential between alpha particle and nucleus generates an energetically forbidden region, or potential barrier, from the nuclear radius out to several times this distance. The maximum height (B) of this alpha barrier is given approximately by the expression $B = 2Ze^2/R$, in which Z is the charge of the daughter nucleus, e is the elementary charge in electrostatic units, and R is the nuclear radius. Numerically, B is roughly equal to $2Z/A^{1/3}$, with A the mass number and B in energy units of MeV. Thus, although the height of the potential barrier for ${}^{212}_{84}\text{Po}$ decay is nearly 28 MeV, the total energy released is $Q_\alpha = 8.95$ MeV. The thickness of the barrier (i.e., distance of the alpha particle from the centre of the nucleus at the moment of recoil) is about twice the nuclear radius of 8.8×10^{-13} centimetre. The tunneling calculation for the transition probability (P) through the barrier gives approximately,

$$P = \exp \left[\left(-\frac{\sqrt{2MBR}}{\hbar} \right) \left(\frac{\pi B^{1/2}}{Q^{1/2}} - 4 \right) \right]$$

In which M is the mass of the alpha particle and \hbar is Planck's constant h divided by 2π . By making simple assumptions about the frequency of the alpha particle striking the barrier, the penetration formula can be used to calculate an effective nuclear radius for alpha decay. This method was one of the early ways of estimating nuclear sizes. In more sophisticated modern techniques the radius value is taken from other experiments, and alpha-decay data and penetrabilities are used to calculate the frequency factor.

The form of equation $P = \exp\left[\left(-\frac{\sqrt{2MBR}}{\hbar}\right)\left(\frac{\pi B^{1/2}}{Q^{1/2}} - 4\right)\right]$ suggests the correlation of decay rates by an empirical expression relating the half-life ($t_{1/2}$) of decay in seconds to the release energy (Q_α) in MeV:

$$\log t_{1/2} = \frac{a}{\sqrt{Q_\alpha}} + b$$

Values of the constants a and b that give best fits to experimental rates of even-even nuclei with neutron number greater than 126 are given in the table. The nuclei with 126 or fewer neutrons decay more slowly than the heavier nuclei, and constants a and b must be readjusted to fit their decay rates.

Semiempirical constants		
	a	b
98 californium (Cf)	152.86	-52.9506
96 curium (Cm)	152.44	-53.6825
94 plutonium (Pu)	146.23	-52.0899
92 uranium (U)	147.49	-53.6565
90 thorium (Th)	144.19	-53.2644
88 radium (Ra)	139.17	-52.1476
86 radon (Rn)	137.46	-52.4597
84 polonium (Po)	129.35	-49.9229

The alpha-decay rates to excited states of even-even nuclei and to ground and excited states of nuclei with odd numbers of neutrons, protons, or both may exhibit retardations from equation ($\log t_{1/2} = \frac{a}{\sqrt{Q_\alpha}} + b$) rates ranging to factors of thousands or more.

The factor by which the rate is slower than the rate formula ($\log t_{1/2} = \frac{a}{\sqrt{Q_\alpha}} + b$) is the

hindrance factor. The existence of uranium-235 in nature rests on the fact that alpha decay to the ground and low excited states exhibits hindrance factors of over 1,000. Thus the uranium-235 half-life is lengthened to 7×10^8 years, a time barely long enough compared to the age of the elements in the solar system for uranium-235 to exist in nature today.

The alpha hindrance factors are fairly well understood in terms of the orbital motion of the individual protons and neutrons that make up the emitted alpha particle. The alpha-emitting nuclei heavier than radium are considered to be cigar-shaped, and alpha hindrance factor data have been used to infer the most probable zones of emission on the nuclear surface—whether polar, equatorial, or intermediate latitudes.

Beta Decay

The processes separately introduced at the beginning of this topic as beta-minus decay, beta-plus decay, and orbital electron capture can be appropriately treated together. They all are processes whereby neutrons and protons may transform to one another by weak interaction. In striking contrast to alpha decay, the electrons (minus or plus charged) emitted in beta-minus and beta-plus decay do not exhibit sharp, discrete energy spectra but have distributions of electron energies ranging from zero up to the maximum energy release, Q_β . Furthermore, measurements of heat released by beta emitters (most radiation stopped in surrounding material is converted into heat energy) show a substantial fraction of the energy, Q_β , is missing. These observations, along with other considerations involving the spins or angular momenta of nuclei and electrons, led Wolfgang Pauli to postulate the simultaneous emission of the neutrino. The neutrino, as a light and uncharged particle with nearly no interaction with matter, was supposed to carry off the missing heat energy. Today, neutrino theory is well accepted with the elaboration that there are six kinds of neutrinos, the electron neutrino, mu neutrino, and tau neutrino and corresponding antineutrinos of each. The electron neutrinos are involved in nuclear beta-decay transformations, the mu neutrinos are encountered in decay of muons to electrons and the tau neutrinos are produced when a massive lepton called a tau breaks down.

Although in general the more energetic the beta decay the shorter is its half-life, the rate relationships do not show the clear regularities of the alpha-decay dependence on energy and atomic number.

The first quantitative rate theory of beta decay was given by Enrico Fermi in 1934, and the essentials of this theory form the basis of modern theory. As an example, in the simplest beta-decay process, a free neutron decays into a proton, a negative electron, and an antineutrino: $n \rightarrow p + e^- + \bar{\nu}$. The weak interaction responsible for this process, in which there is a change of species (n to p) by a nucleon with creation of electron and antineutrino, is characterized in Fermi theory by a universal constant, g . The sharing of energy between electron and antineutrino is governed by statistical probability laws giving a probability factor for each particle proportional to the square of its linear momentum (defined by mass times velocity for speeds much less than the speed of light and by a more complicated, relativistic relation for faster speeds). The overall probability law from Fermi theory gives the probability per unit time per unit electron energy interval, $P(W)$, as follows:

$$P(W) = \frac{64 \pi^4 m_0^5 c^4 g^2}{h^7} W(W^2 - 1)^{1/2} (W_0 - W)^2$$

In which W is the electron energy in relativistic units ($W = 1 + E/m_0c^2$) and W_0 is the maximum ($W_0 = 1 + Q_\beta/m_0c^2$), m_0 the rest mass of the electron, c the speed of light, and h Planck's constant. This rate law expresses the neutron beta-decay spectrum in good agreement with experiment, the spectrum falling to zero at lowest energies by the factor W and falling to zero at the maximum energy by virtue of the factor $(W_0 - W)^2$.

In Fermi's original formulation, the spins of an emitted beta and neutrino are opposing and so cancel to zero. Later work showed that neutron beta decay partly proceeds with the $1/2 \hbar$ spins of beta and neutrino adding to one unit of \hbar . The former process is known as Fermi decay (F) and the latter Gamow-Teller (GT) decay, after George Gamow and Edward Teller, the physicists who first proposed it. The interaction constants are determined to be in the ratio $g_{GT}^2/g_F^2 = 1.4$. Thus, g^2 in equation ($P(W) = \frac{64\pi^4 m_0^5 c^4 g^2}{h^7} W(W^2 - 1)^{1/2} (W_0 - W)^2$) should be replaced by $(g_F^2 + g_{GT}^2)$.

The scientific world was shaken in 1957 by the measurement in beta decay of maximum violation of the law of conservation of parity. The meaning of this non-conservation in the case of neutron beta decay considered above is that the preferred direction of electron emission is opposite to the direction of the neutron spin. By means of a magnetic field and low temperature it is possible to cause neutrons in cobalt-60 and other nuclei, or free neutrons, to have their spins set preferentially in the up direction perpendicular to the plane of the coil generating the magnetic field. The fact that beta decay prefers the down direction for spin means that the reflection of the experiment as seen in a mirror parallel to the coil represents an unphysical situation: conservation of parity, obeyed by most physical processes, demands that experiments with positions reversed by mirror reflection should also occur. Further consequences of parity violation in beta decay are that spins of emitted neutrinos and electrons are directed along the direction of flight, totally so for neutrinos and partially so by the ratio of electron speed to the speed of light for electrons.

The overall half-life for beta decay of the free neutron, measured as 12 minutes, may be related to the interaction constants g^2 (equal to $g_F^2 + g_{GT}^2$) by integrating (summing) probability expression ($P(W) = \frac{64\pi^4 m_0^5 c^4 g^2}{h^7} W(W^2 - 1)^{1/2} (W_0 - W)^2$) over all possible electron energies from zero to the maximum. The result for the decay constant is:

$$\lambda = \frac{64\pi^4 m_0^5 c^4 g^2}{h^7} \left\{ (W_0^2 - 1)^{1/2} \left(\frac{W_0^4}{30} - \frac{W_0^2}{20} - \frac{2}{15} \right) + \frac{W_0}{4} \ln [W_0 + (W_0^2 - 1)^{1/2}] \right\}$$

In which W_0 is the maximum beta-particle energy in relativistic units ($W_0 = 1 + Q_\beta/m_0c^2$), with m_0 the rest mass of the electron, c the speed of light, and h Planck's constant. The best g value from decay rates is approximately 10^{-49} erg per cubic centimetre. As may be noted from previous equation, there is limiting fifth-power energy dependence for highest decay energies.

In the case of a decaying neutron not free but bound within a nucleus, the above formulas must be modified. First, as the nuclear charge Z increases, the relative probability of low-energy electron emission increases by virtue of the coulombic attraction. For positron emission, which is energetically impossible for free protons but can occur for bound protons in proton-rich nuclei, the nuclear coulomb charge suppresses lower energy positrons from the shape given by equation $P(W) = \frac{64\pi^4 m_0^5 c^4 g^2}{h^7} W(W^2 - 1)^{1/2} (W_0 - W)^2$.

This equation can be corrected by a factor $F(Z,W)$ depending on the daughter atomic number Z and electron energy W . The factor can be calculated quantum mechanically. The coulomb charge also affects the overall rate expression $\lambda = \frac{64\pi^4 m_0^5 c^4 g^2}{h^7} \left\{ (W_0^2 - 1)^{1/2} \left(\frac{W_0^4}{30} - \frac{W_0^2}{20} - \frac{2}{15} \right) + \frac{W_0}{4} \ln [W_0 + (W_0^2 - 1)^{1/2}] \right\}$ such that

it can no longer be expressed as an algebraic function, but tables are available for analysis of beta decay rates. The rates are analyzed in terms of a function $f(Z, Q_\beta)$ calculated by integration of equation $P(W) = \frac{64\pi^4 m_0^5 c^4 g^2}{h^7} W(W^2 - 1)^{1/2} (W_0 - W)^2$ with correction factor $F(Z,W)$.

Approximate expressions for the f functions usable for decay energies Q between 0.1 MeV and 10 MeV, in which Q is measured in MeV, and Z is the atomic number of the daughter nucleus, are as follows (the symbol \approx means approximately equal to):

$$f_{\beta^-} \approx 6.0 Q^{4-0.005(Z-1)} \cdot 10^{Z/50},$$

$$f_{\beta^+} \approx 6.2 Q^4 / 10^{0.007Z} \cdot 10^{0.009Z(\log_{10} 1/3Q)^2}$$

For electron capture, a much weaker dependence on energy is found:

$$f_{EC} \approx (Z+1)^{3.5} Q / 4 \times 10^5$$

The basic beta decay rate expression obeyed by the class of so-called super allowed transitions, including decay of the neutron and several light nuclei is:

$$\lambda_\beta \approx \frac{64\pi^4 m_0^5 c^4 g^2}{h^7} f_\beta$$

Like the ground-to-ground alpha transitions of even-even nuclei, the superallowed beta transitions obey the basic rate law, but most beta transitions go much more slowly. The extra retardation is explained in terms of mismatched orbitals of neutrons and protons involved in the transition. For the superallowed transitions the orbitals in initial and final states are almost the same. Most of them occur between mirror nuclei, with one more or less neutron than protons; i.e., beta-minus decay of hydrogen-3, electron capture of beryllium-7 and positron emission of carbon-11, oxygen-15, neon-19, ..., titanium-43.

The nuclear retardation of beta decay rates below those of the superallowed class may be expressed in a fundamental way by multiplying the right side of equation $\lambda_\beta \approx \frac{64\pi^4 m_0^5 c^4 g^2}{h^7} f_\beta$ by the square of a nuclear matrix element (a quantity of quantum mechanics), which may range from unity down to zero depending on the degree of mismatch of initial and final nuclear states of internal motion. A more usual way of expressing the nuclear factor of the beta rate is the $\log ft$ value, in which f refers to the function $f(Z, Q_\beta)$. Because the half-life is inversely proportional to the decay constant λ , the product $f_\beta t_{1/2}$ will be a measure of (inversely proportional to) the square of the nuclear matrix element. For the $\log ft$ value, the beta half-life is taken in seconds, and the ordinary logarithm to the base 10 is used. The superallowed transitions have $\log ft$ values in the range of 3 to 3.5. Beta $\log ft$ values are known up to as large as ~ 23 in the case of indium-115. There is some correlation of $\log ft$ values with spin changes between parent and daughter nucleons, the indium-115 decay involving a spin change of four, whereas the superallowed transitions all have spin changes of zero or one.

Gamma Transition

The nuclear gamma transitions belong to the large class of electromagnetic transitions encompassing radio-frequency emission by antennas or rotating molecules, infrared emission by vibrating molecules or hot filaments, visible light, ultraviolet light, and X-ray emission by electronic jumps in atoms or molecules. The usual relations apply for connecting frequency ν , wavelength λ , and photon quantum energy E with speed of light c and Planck's constant h ; namely, $\lambda = c/\nu$ and $E = h\nu$. It is sometimes necessary to consider the momentum (p) of the photon given by $p = E/c$.

Classically, radiation accompanies any acceleration of electric charge. Quantum mechanically there is a probability of photon emission from higher to lower energy nuclear states, in which the internal state of motion involves acceleration of charge in the transition. Therefore, purely neutron orbital acceleration would carry no radiative contribution.

A great simplification in nuclear gamma transition rate theory is brought about by the circumstance that the nuclear diameters are always much smaller than the shortest wavelengths of gamma radiation in radioactivity—i.e., the nucleus is too small to be a good antenna for the radiation. The simplification is that nuclear gamma transitions can be classified according to multipolarity, or amount of spin angular momentum carried off by the radiation. One unit of angular momentum in the radiation is associated with dipole transitions (a dipole consists of two separated equal charges, plus and minus). If there is a change of nuclear parity, the transition is designated electric dipole (E1) and is analogous to the radiation of a linear half-wave dipole radio antenna. If there is no parity change, the transition is magnetic dipole (M1) and is analogous to the radiation of a full-wave loop antenna. With two units of angular momentum change, the transition is electric quadrupole (E2), analogous to a full-wave linear antenna of

two dipoles out-of-phase, and magnetic quadrupole (M2), analogous to coaxial loop antennas driven out-of-phase. Higher multipolarity radiation also frequently occurs with radioactivity.

Transition rates are usually compared to the single-proton theoretical rate, or Weisskopf formula, named after the American physicist Victor Frederick Weisskopf, who developed it. The table gives the theoretical reference rate formulas in their dependence on nuclear mass number A and gamma-ray energy E_γ (in MeV).

Gamma transition rates		
transition type	partial half-life t_γ (seconds)	illustrative t_γ values for $A = 125$, $E = 0.1$ MeV (seconds)
E1	$5.7 \times 10^{-15} E^{-3} A^{-2/3}$	2×10^{-13}
E2	$6.7 \times 10^{-9} E^{-5} A^{-4/3}$	1×10^{-6}
E3	$1.2 \times 10^{-2} E^{-7} A^{-2}$	8
E4	$3.4 \times 10^4 E^{-9} A^{-8/3}$	9×10^7
E5	$1.3 \times 10^{11} E^{-11} A^{-10/3}$	1×10^{15}
M1	$2.2 \times 10^{-14} E^{-3}$	2×10^{-11}
M2	$2.6 \times 10^{-8} E^{-5} A^{-2/3}$	1×10^{-4}
M3	$4.9 \times 10^{-2} E^{-7} A^{-4/3}$	8×10^2
M4	$1.3 \times 10^5 E^{-9} A^{-2}$	8×10^9
M5	$5.0 \times 10^{11} E^{-11} A^{-8/3}$	1×10^{17}

The energies E are expressed in MeV. The nuclear radius parameter r_0 has been taken as 1.3 fermis. It is to be noted that t_γ is the partial half-life for γ emission only; the occurrence of internal conversion will always shorten the measured half-life.

It is seen for the illustrative case of gamma energy 0.1 MeV and mass number 125 that there occurs an additional factor of 107 retardation with each higher multipole order. For a given multipole, magnetic radiation should be a factor of 100 or so slower than electric. These rate factors ensure that nuclear gamma transitions are nearly purely one multipole, the lowest permitted by the nuclear spin change. There are many exceptions, however; mixed M1–E2 transitions are common, because E2 transitions are often much faster than the Weisskopf formula gives and M1 transitions are generally slower. All E1 transitions encountered in radioactivity are much slower than the Weisskopf formula. The other higher multipolarities show some scatter in rates, ranging from agreement to considerable retardation. In most cases the retardations are well understood in terms of nuclear model calculations.

Though not literally a gamma transition, electric monopole (E0) transitions may appropriately be mentioned here. These may occur when there is no angular momentum change between initial and final nuclear states and no parity change. For spin-zero to spin-zero transitions, single gamma emission is strictly forbidden. The electric monopole transition occurs largely by the ejection of electrons from the orbital cloud in heavier elements and by positron–electron pair creation in the lighter elements.

RADIOACTIVE DECAY

Radioactive decay is the emission of energy in the form of ionizing radiation. The ionizing radiation that is emitted can include alpha particles, beta particles and/or gamma rays. Radioactive decay occurs in unbalanced atoms called radionuclides.

Elements in the periodic table can take on several forms. Some of these forms are stable; other forms are unstable. Typically, the most stable form of an element is the most common in nature. However, all elements have an unstable form. Unstable forms emit ionizing radiation and are radioactive. There are some elements with no stable form that are always radioactive, such as uranium. Elements that emit ionizing radiation are called radionuclides.

Periodic Table: Radioactive Elements

1 H 1.008 Hydrogen												2 He 4.003 Helium																							
3 Li 6.94 Lithium		4 Be 9.012 Beryllium												5 B 10.81 Boron		6 C 12.011 Carbon		7 N 14.007 Nitrogen		8 O 15.999 Oxygen		9 F 18.998 Fluorine		10 Ne 20.180 Neon											
11 Na 22.990 Sodium		12 Mg 24.305 Magnesium												13 Al 26.982 Aluminum		14 Si 28.085 Silicon		15 P 30.974 Phosphorus		16 S 32.06 Sulfur		17 Cl 35.45 Chlorine		18 Ar 39.948 Argon											
19 K 39.098 Potassium		20 Ca 40.078 Calcium		21 Sc 44.956 Scandium		22 Ti 47.867 Titanium		23 V 50.942 Vanadium		24 Cr 51.996 Chromium		25 Mn 54.938 Manganese		26 Fe 55.845 Iron		27 Co 58.933 Cobalt		28 Ni 58.693 Nickel		29 Cu 63.546 Copper		30 Zn 65.38 Zinc		31 Ga 69.723 Gallium		32 Ge 72.630 Germanium		33 As 74.922 Arsenic		34 Se 78.971 Selenium		35 Br 79.904 Bromine		36 Kr 83.798 Krypton	
37 Rb 85.468 Rubidium		38 Sr 87.62 Strontium		39 Y 88.906 Yttrium		40 Zr 91.224 Zirconium		41 Nb 92.906 Niobium		42 Mo 95.95 Molybdenum		43 Tc (98) Technetium		44 Ru 101.07 Ruthenium		45 Rh 102.906 Rhodium		46 Pd 106.42 Palladium		47 Ag 107.868 Silver		48 Cd 112.414 Cadmium		49 In 114.818 Indium		50 Sn 118.710 Tin		51 Sb 121.760 Antimony		52 Te 127.60 Tellurium		53 I 126.904 Iodine		54 Xe 131.293 Xenon	
55 Cs 132.905 Cesium		56 Ba 137.327 Barium		57 La 138.905 Lanthanum		71 Hf 178.49 Hafnium		72 Ta 180.948 Tantalum		73 W 183.84 Tungsten		74 Re 186.207 Rhenium		75 Os 190.23 Osmium		76 Ir 192.217 Iridium		77 Pt 195.084 Platinum		78 Au 196.967 Gold		79 Hg 200.592 Mercury		80 Tl 204.38 Thallium		81 Pb 207.2 Lead		82 Bi 208.980 Bismuth		83 Po (209) Polonium		84 At (210) Astatine		85 Rn (222) Radon	
87 Fr (223) Francium		88 Ra (226) Radium		89 Ac (227) Actinium		104 Rf (261) Rutherfordium		105 Db (262) Dubnium		106 Sg (263) Seaborgium		107 Bh (264) Bohrium		108 Hs (265) Hassium		109 Mt (266) Meitnerium		110 Ds (271) Darmstadtium		111 Rg (272) Roentgenium		112 Cn (285) Copernicium		113 Nh (286) Nihonium		114 Fl (289) Flerovium		115 Mc (290) Moscovium		116 Lv (293) Livermorium		117 Ts (294) Tennessine		118 Og (294) Oganesson	
Lanthanide Series		57 La Lanthanum		58 Ce Cerium		59 Pr Praseodymium		60 Nd Neodymium		61 Pm (145) Promethium		62 Sm Samarium		63 Eu Europium		64 Gd Gadolinium		65 Tb Terbium		66 Dy Dysprosium		67 Ho Holmium		68 Er Erbium		69 Tm Thulium		70 Yb Ytterbium		71 Lu Lutetium					
Actinide Series		89 Ac Actinium		90 Th Thorium		91 Pa Protactinium		92 U Uranium		93 Np Neptunium		94 Pu Plutonium		95 Am Americium		96 Cm Curium		97 Bk Berkelium		98 Cf Californium		99 Es Einsteinium		100 Fm Fermium		101 Md Mendelevium		102 No Nobelium		103 Lr Lawrencium					

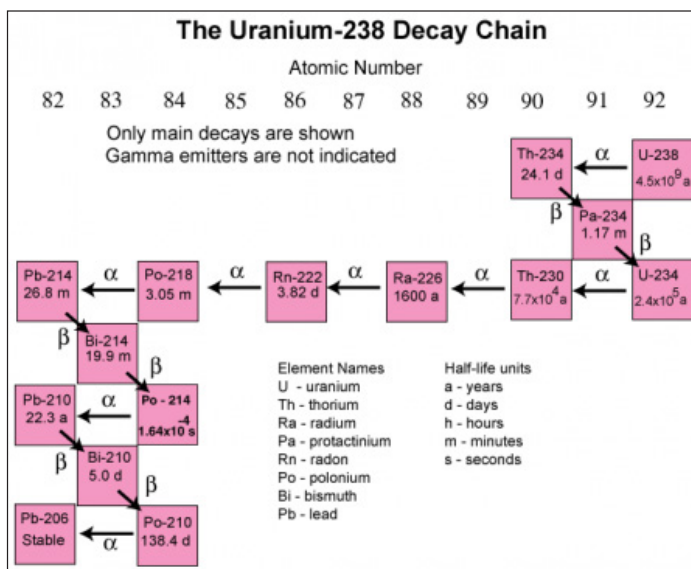
When it decays, a radionuclide transforms into a different atom - a decay product. The atoms keep transforming to new decay products until they reach a stable state and are no longer radioactive. The majority of radionuclides only decay once before becoming stable. Those that decay in more than one step are called series radionuclides. The series of decay products created to reach this balance is called the decay chain.

Each series has its own unique decay chain. The decay products within the chain are always radioactive. Only the final, stable atom in the chain is not radioactive. Some decay products are a different chemical element.

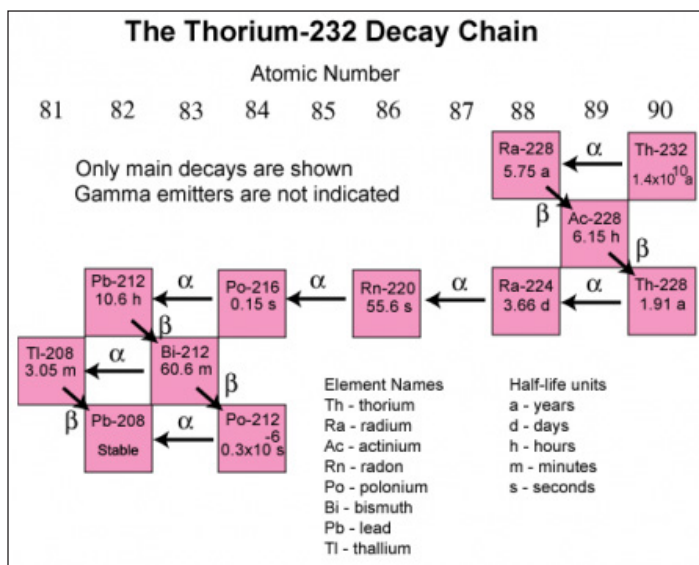
Every radionuclide has a specific decay rate, which is measured in terms of “half-life”. Radioactive half-life is the time required for half of the radioactive atoms present to decay. Some radionuclides have half-lives of mere seconds, but others have half-lives of hundreds or millions or billions of years.

Two decay chains are shown below:

1. Uranium-238:



2. Thorium-232



ALPHA DECAY

Alpha (α) decay is a type of radioactive disintegration in which some unstable atomic nuclei dissipate excess energy by spontaneously ejecting an alpha particle. Because

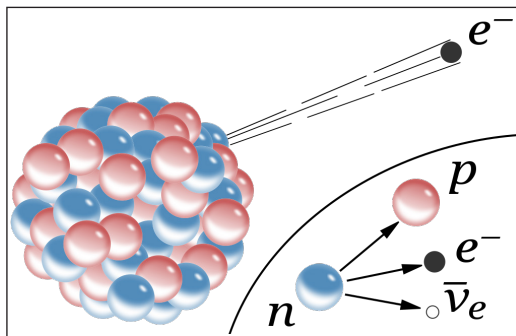
alpha particles have two positive charges and a mass of four units, their emission from nuclei produces daughter nuclei having a positive nuclear charge or atomic number two units less than their parents and a mass of four units less. Thus polonium-210 (mass number 210 and atomic number 84, i.e., a nucleus with 84 protons) decays by alpha emission to lead-206 (atomic number 82).

The speed and hence the energy of an alpha particle ejected from a given nucleus is a specific property of the parent nucleus and determines the characteristic range or distance the alpha particle travels. Though ejected at speeds of about one-tenth that of light, alpha particles are not very penetrating. They have ranges in air of only about one to four inches (corresponding to an energy range of about 4 million to 10 million electron volts).

The principal alpha emitters are found among the elements heavier than bismuth (atomic number 83) and also among the rare-earth elements from neodymium (atomic number 60) to lutetium (atomic number 71). Half-lives for alpha decay range from about a microsecond (10^{-6} second) to about 10^{17} seconds.

BETA DECAY

In nuclear physics, beta decay (β -decay) is a type of radioactive decay in which a beta particle (fast energetic electron or positron) is emitted from an atomic nucleus, transforming the original nuclide to an isobar. For example, beta decay of a neutron transforms it into a proton by the emission of an electron accompanied by an antineutrino; or, conversely a proton is converted into a neutron by the emission of a positron with a neutrino in so-called positron emission. Neither the beta particle nor its associated (anti-)neutrino exist within the nucleus prior to beta decay, but are created in the decay process. By this process, unstable atoms obtain a more stable ratio of protons to neutrons. The probability of a nuclide decaying due to beta and other forms of decay is determined by its nuclear binding energy. The binding energies of all existing nuclides form what is called the nuclear band or valley of stability. For either electron or positron emission to be energetically possible, the energy release or Q value must be positive.



β^- decay in an atomic nucleus (the accompanying antineutrino is omitted). The inset shows beta decay of a free neutron. In both processes, an intermediate virtual W^- boson is not shown.

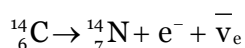
Beta decay is a consequence of the weak force, which is characterized by relatively lengthy decay times. Nucleons are composed of up quarks and down quarks, and the weak force allows a quark to change its flavour by emission of a W boson leading to creation of an electron/antineutrino or positron/neutrino pair. For example, a neutron, composed of two down quarks and an up quark, decays to a proton composed of a down quark and two up quarks.

Electron capture is sometimes included as a type of beta decay, because the basic nuclear process, mediated by the weak force, is the same. In electron capture, an inner atomic electron is captured by a proton in the nucleus, transforming it into a neutron, and an electron neutrino is released.

The two types of beta decay are known as beta minus and beta plus. In beta minus (β^-) decay, a neutron is converted to a proton, and the process creates an electron and an electron antineutrino; while in beta plus (β^+) decay, a proton is converted to a neutron and the process creates a positron and an electron neutrino. β^+ decay is also known as positron emission.

Beta decay conserves a quantum number known as the lepton number, or the number of electrons and their associated neutrinos (other leptons are the muon and tau particles). These particles have lepton number $+1$, while their antiparticles have lepton number -1 . Since a proton or neutron has lepton number zero, β^+ decay (a positron, or antielectron) must be accompanied with an electron neutrino, while β^- decay (an electron) must be accompanied by an electron antineutrino.

An example of electron emission (β^- decay) is the decay of carbon-14 into nitrogen-14 with a half-life of about 5,730 years:

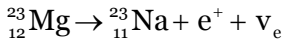


In this form of decay, the original element becomes a new chemical element in a process known as nuclear transmutation. This new element has an unchanged mass number A , but an atomic number Z that is increased by one. As in all nuclear decays, the decaying element (in this case ${}^{14}_6\text{C}$) is known as the parent nuclide while the resulting element (in this case ${}^{14}_7\text{N}$) is known as the daughter nuclide.

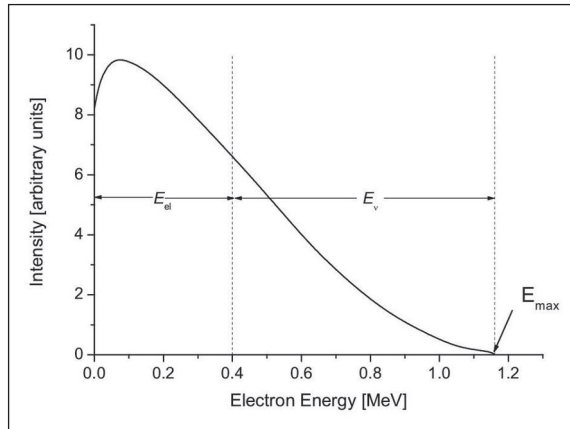
Another example is the decay of hydrogen-3 (tritium) into helium-3 with a half-life of about 12.3 years:



An example of positron emission (β^+ decay) is the decay of magnesium-23 into sodium-23 with a half-life of about 11.3 s:

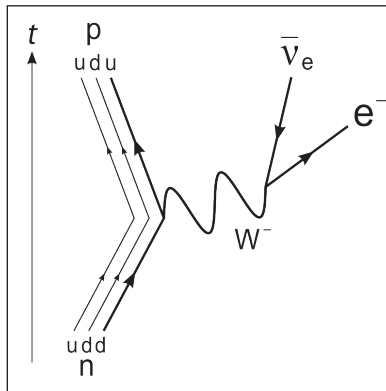


β^+ decay also results in nuclear transmutation, with the resulting element having an atomic number that is decreased by one.



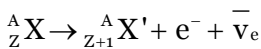
A beta spectrum, showing a typical division of energy between electron and antineutrino.

β^- decay



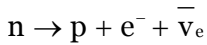
The leading-order Feynman diagram for β^- decay of a neutron into a proton, electron, and electron antineutrino via an intermediate W^- boson.

In β^- decay, the weak interaction converts an atomic nucleus into a nucleus with atomic number increased by one, while emitting an electron (e^-) and an electron antineutrino ($\bar{\nu}_e$). β^- decay generally occurs in neutron-rich nuclei. The generic equation is:

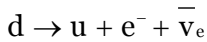


Where, A and Z are the mass number and atomic number of the decaying nucleus, and X and X' are the initial and final elements, respectively.

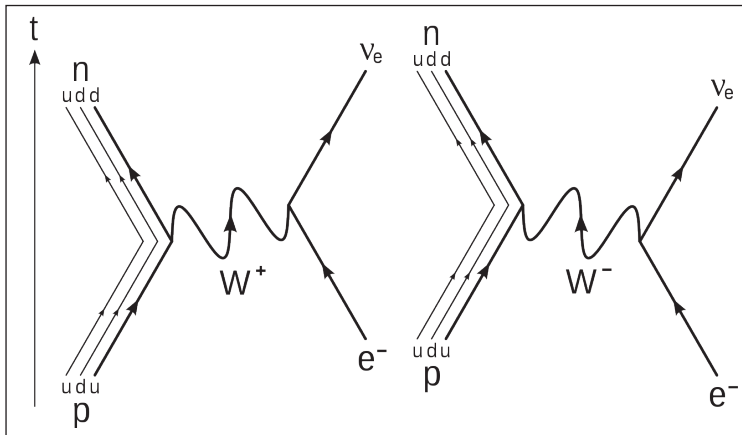
Another example is when the free neutron (${}^1_0\text{n}$) decays by β^- decay into a proton (p):



At the fundamental level (as depicted in the Feynman diagram on the right), this is caused by the conversion of the negatively charged ($-1/3 e$) down quark to the positively charged ($+2/3 e$) up quark by emission of a W^- boson; the W^- boson subsequently decays into an electron and an electron antineutrino:

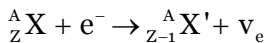


Electron Capture (K-capture)

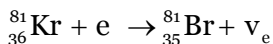


The leading-order Feynman diagrams for electron capture decay. An electron interacts with an up quark in the nucleus via a W boson to create a down quark and electron neutrino. Two diagrams comprise the leading (second) order, though as a virtual particle, the type (and charge) of the W -boson is indistinguishable.

In all cases where β^+ decay (positron emission) of a nucleus is allowed energetically, so too is electron capture allowed. This is a process during which a nucleus captures one of its atomic electrons, resulting in the emission of a neutrino:



An example of electron capture is one of the decay modes of krypton-81 into bromine-81:

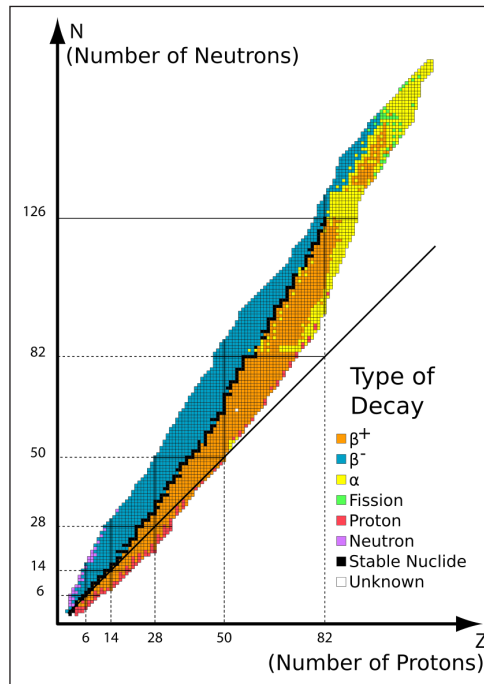


All emitted neutrinos are of the same energy. In proton-rich nuclei where the energy difference between the initial and final states is less than $2m_e c^2$, β^+ decay is not energetically possible, and electron capture is the sole decay mode.

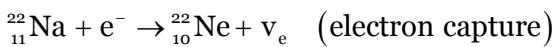
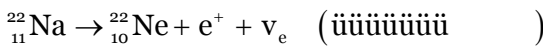
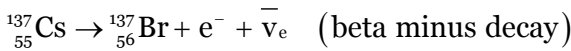
If the captured electron comes from the innermost shell of the atom, the K-shell, which has the highest probability to interact with the nucleus, the process is called K-capture. If it comes from the L-shell, the process is called L-capture, etc.

Electron capture is a competing (simultaneous) decay process for all nuclei that can undergo β^+ decay. The converse, however, is not true: electron capture is the only type of decay that is allowed in proton-rich nuclides that do not have sufficient energy to emit a positron and neutrino.

Nuclear Transmutation



If the proton and neutron are part of an atomic nucleus, the decay processes transmute one chemical element into another. For example:



Beta decay does not change the number (A) of nucleons in the nucleus, but changes only its charge Z. Thus the set of all nuclides with the same A can be introduced; these isobaric nuclides may turn into each other via beta decay. For a given A there is one that is most stable. It is said to be beta stable, because it presents a local minima of the mass excess: if such a nucleus has (A, Z) numbers, the neighbour nuclei (A, Z-1) and (A, Z+1) have higher mass excess and can beta decay into (A, Z), but not vice versa. For

all odd mass numbers A , there is only one known beta-stable isobar. For even A , there are up to three different beta-stable isobars experimentally known; for example, $^{124}_{50}\text{Sn}$, $^{124}_{52}\text{Te}$, and $^{124}_{54}\text{Xe}$ are all beta-stable. There are about 350 known beta-decay stable nuclides.

Competition of Beta Decay Types

Usually unstable nuclides are clearly either “neutron rich” or “proton rich”, with the former undergoing beta decay and the latter undergoing electron capture (or more rarely, due to the higher energy requirements, positron decay). However, in a few cases of odd-proton, odd-neutron radionuclides, it may be energetically favorable for the radionuclide to decay to an even-proton, even-neutron isobar either by undergoing beta-positive or beta-negative decay. An often-cited example is the single isotope $^{64}_{29}\text{Cu}$ (29 protons, 35 neutrons), which illustrates three types of beta decay in competition. Copper-64 has a half-life of about 12.7 hours. This isotope has one unpaired proton and one unpaired neutron, so either the proton or the neutron can decay. This particular nuclide (though not all nuclides in this situation) is almost equally likely to decay through proton decay by positron emission (18%) or electron capture (43%) to $^{64}_{28}\text{Ni}$, as it is through neutron decay by electron emission (39%) to $^{64}_{30}\text{Zn}$.

Stability of Naturally Occurring Nuclides

Most naturally occurring nuclides on earth are beta stable. Those that are not have half-lives ranging from under a second to periods of time significantly greater than the age of the universe. One common example of a long-lived isotope is the odd-proton odd-neutron nuclide $^{40}_{19}\text{K}$, which undergoes all three types of beta decay (β^- , β^+ and electron capture) with a half-life of 1.277×10^9 years.

Conservation Rules for Beta Decay

Baryon Number is Conserved

$$B = \frac{n_q - n_{\bar{q}}}{3}$$

Where,

- n_q is the number of constituent quarks, and
- $n_{\bar{q}}$ is the number of constituent antiquarks.

Beta decay just changes neutron to proton or, in the case of positive beta decay (electron capture) proton to neutron so the number of individual quarks doesn't change. It is only the baryon flavor that changes, here labelled as the isospin.

Up and down quarks have total isospin $I = \frac{1}{2}$ and isospin projections:

$$I_z = \begin{cases} \frac{1}{2} & \text{up quark} \\ -\frac{1}{2} & \text{down quark} \end{cases}$$

All other quarks have $I = 0$.

In general,

$$I_z = \frac{1}{2}(n_u - n_d)$$

Lepton Number is Conserved

$$L \equiv n_l - n_{\bar{l}}$$

So all leptons have assigned a value of +1, antileptons -1, and non-leptonic particles 0.

$$\begin{array}{rccccccc} n & \rightarrow & p & + & e^- & + & \bar{\nu}_e \\ L: & 0 & = & 0 & + & 1 & - & 1 \end{array}$$

Angular Momentum

For allowed decays, the net orbital angular momentum is zero, hence only spin quantum numbers are considered.

The electron and antineutrino are fermions, spin-1/2 objects, therefore they may couple to total $S = 1$ (parallel) or $S = 0$ (anti-parallel).

For forbidden decays, orbital angular momentum must also be taken into consideration.

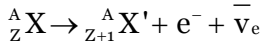
Energy Release

The Q value is defined as the total energy released in a given nuclear decay. In beta decay, Q is therefore also the sum of the kinetic energies of the emitted beta particle, neutrino, and recoiling nucleus. (Because of the large mass of the nucleus compared to that of the beta particle and neutrino, the kinetic energy of the recoiling nucleus can generally be neglected.) Beta particles can therefore be emitted with any kinetic energy ranging from 0 to Q . A typical Q is around 1 MeV, but can range from a few keV to a few tens of MeV.

Since the rest mass of the electron is 511 keV, the most energetic beta particles are ultrarelativistic, with speeds very close to the speed of light.

β^- decay

Consider the generic equation for beta decay:



The Q value for this decay is:

$$Q = \left[m_N({}^A_Z\text{X}) - m_N({}^A_{Z+1}\text{X}') - m_e - m_{\bar{\nu}_e} \right] c^2$$

Where, $m_N({}^A_Z\text{X})$ is the mass of the nucleus of the ${}^A_Z\text{X}$ atom, m_e is the mass of the electron, and $m_{\bar{\nu}_e}$ is the mass of the electron antineutrino. In other words, the total energy released is the mass energy of the initial nucleus, minus the mass energy of the final nucleus, electron, and antineutrino. The mass of the nucleus m_N is related to the standard atomic mass m by:

$$m({}^A_Z\text{X}) c^2 = m_N({}^A_Z\text{X}) c^2 + Zm_e c^2 - \sum_{i=1}^Z B_i$$

That is, the total atomic mass is the mass of the nucleus, plus the mass of the electrons, minus the sum of all electron binding energies B_i for the atom. This equation is rearranged to find $m_N({}^A_Z\text{X})$, and $m_N({}^A_{Z+1}\text{X}')$ is found similarly. Substituting these nuclear masses into the Q-value equation, while neglecting the nearly-zero antineutrino mass and the difference in electron binding energies, which is very small for high-Z atoms, we have:

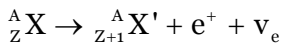
$$Q = \left[m({}^A_Z\text{X}) - m({}^A_{Z+1}\text{X}') \right] c^2$$

This energy is carried away as kinetic energy by the electron and neutrino.

Because the reaction will proceed only when the Q value is positive, β^- decay can occur when the mass of atom ${}^A_Z\text{X}$ is greater than the mass of atom ${}^A_{Z+1}\text{X}'$.

β^+ decay

The equations for β^+ decay are similar, with the generic equation:



Giving,

$$Q = \left[m_N({}^A_Z\text{X}) - m_N({}^A_{Z-1}\text{X}') - m_e - m_{\nu_e} \right] c^2$$

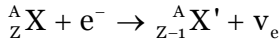
However, in this equation, the electron masses do not cancel, and we are left with:

$$Q = \left[m\left({}_Z^A X\right) - m\left({}_{Z-1}^A X'\right) - 2m_e \right] c^2$$

Because the reaction will proceed only when the Q value is positive, β^+ decay can occur when the mass of atom ${}_Z^A X$ exceeds that of ${}_{Z-1}^A X'$ by at least twice the mass of the electron.

Electron Capture

The analogous calculation for electron capture must take into account the binding energy of the electrons. This is because the atom will be left in an excited state after capturing the electron, and the binding energy of the captured innermost electron is significant. Using the generic equation for electron capture:



We have:

$$Q = \left[m_N\left({}_Z^A X\right) + m_e - m_N\left({}_{Z-1}^A X'\right) - m_{\nu_e} \right] c^2$$

Which simplifies to:

$$Q = \left[m\left({}_Z^A X\right) - m\left({}_{Z-1}^A X'\right) \right] c^2 - B_n$$

Where B_n is the binding energy of the captured electron.

Because the binding energy of the electron is much less than the mass of the electron, nuclei that can undergo β^+ decay can always also undergo electron capture, but the reverse is not true.

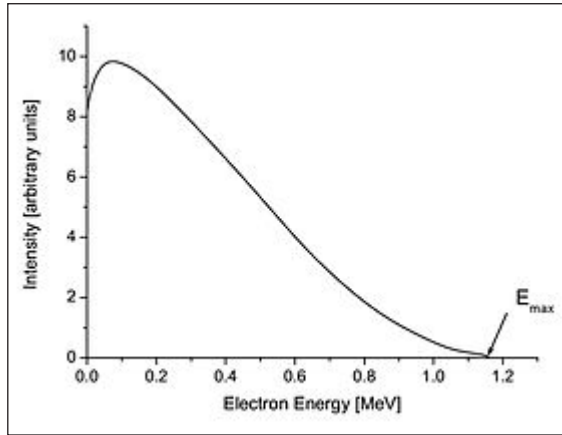
Beta Emission Spectrum

Beta decay can be considered as a perturbation as described in quantum mechanics, and thus Fermi's Golden Rule can be applied. This leads to an expression for the kinetic energy spectrum $N(T)$ of emitted betas as follows:

$$N(T) = C_L(T) F(Z, T) pE(Q - T)^2$$

Where T is the kinetic energy, C_L is a shape function that depends on the forbiddenness of the decay (it is constant for allowed decays), $F(Z, T)$ is the Fermi Function with Z the charge of the final-state nucleus, $E = T + mc^2$ is the total energy, $p = \sqrt{(E/c)^2 - (mc)^2}$ is the momentum, and Q is the Q value of the decay. The kinetic energy of the emitted neutrino is given approximately by Q minus the kinetic energy of the beta.

As an example, the beta decay spectrum of ^{210}Bi (originally called RaE) is shown in figure.



Beta spectrum of ^{210}Bi . $E_{\max} = Q = 1.16$ MeV is the maximum energy.

Fermi Function

The Fermi function that appears in the beta spectrum formula accounts for the Coulomb attraction/repulsion between the emitted beta and the final state nucleus. Approximating the associated wavefunctions to be spherically symmetric, the Fermi function can be analytically calculated to be:

$$F(Z, T) = \frac{2(1+S)}{\Gamma(1+2S)^2} (2p\rho)^{2S-2} e^{\pi\eta} |\Gamma(S+i\eta)|^2$$

Where, p is the final momentum, Γ the Gamma function, and (if α is the fine-structure constant and r_N the radius of the final state nucleus) $S = \sqrt{1 - \alpha^2 Z^2}$, $\eta = \pm Ze^2 c / \hbar p$ (+ for electrons, - for positrons), and $\rho = r_N / \hbar$.

For non-relativistic betas ($Q \ll m_e c^2$), this expression can be approximated by:

$$F(Z, T) \approx \frac{2\pi\eta}{1 - e^{-2\pi\eta}}$$

Kurie Plot

A Kurie plot (also known as a Fermi–Kurie plot) is a graph used in studying beta decay developed by Franz N. D. Kurie, in which the square root of the number of beta particles whose momenta (or energy) lie within a certain narrow range, divided by the Fermi function, is plotted against beta-particle energy. It is a straight line for allowed transitions and some forbidden transitions, in accord with the Fermi beta-decay theory. The energy-axis (x-axis) intercept of a Kurie plot corresponds to the maximum energy imparted to the electron/positron (the decay's Q value). With a Kurie plot one can find the limit on the effective mass of a neutrino.

Helicity (Polarization) of Neutrinos, Electrons and Positrons Emitted in Beta Decay

After the discovery of parity non-conservation, it was found that, in beta decay, electrons are emitted mostly with negative helicity, i.e., they move, naively speaking, like left-handed screws driven into a material (they have negative longitudinal polarization). Conversely, positrons have mostly positive helicity, i.e., they move like right-handed screws. Neutrinos (emitted in positron decay) have negative helicity, while antineutrinos (emitted in electron decay) have positive helicity.

The higher the energy of the particles, the higher their polarization.

Types of Beta Decay Transitions

Beta decays can be classified according to the angular momentum (L value) and total spin (S value) of the emitted radiation. Since total angular momentum must be conserved, including orbital and spin angular momentum, beta decay occurs by a variety of quantum state transitions to various nuclear angular momentum or spin states, known as “Fermi” or “Gamow–Teller” transitions. When beta decay particles carry no angular momentum ($L = 0$), the decay is referred to as “allowed”, otherwise it is “forbidden”.

Other decay modes, which are rare, are known as bound state decay and double beta decay.

Fermi Transitions

A Fermi transition is a beta decay in which the spins of the emitted electron (positron) and anti-neutrino (neutrino) couple to total spin $S = 0$, leading to an angular momentum change $\Delta J = 0$ between the initial and final states of the nucleus (assuming an allowed transition). In the non-relativistic limit, the nuclear part of the operator for a Fermi transition is given by:

$$\mathcal{O}_F = G_V \sum_a \hat{\tau}_{a\pm}$$

With G_V the weak vector coupling constant, τ_{\pm} the isospin raising and lowering operators, and a running over all protons and neutrons in the nucleus.

Gamow – Teller Transitions

A Gamow–Teller transition is a beta decay in which the spins of the emitted electron (positron) and anti-neutrino (neutrino) couple to total spin $S = 1$, leading to an angular momentum change $\Delta J = 0, \pm 1$ between the initial and final states of the nucleus (assuming an allowed transition). In this case, the nuclear part of the operator is given by:

$$\mathcal{O}_{GT} = G_A \sum_a \hat{\sigma}_a \hat{\tau}_{a\pm}$$

With G_A the weak axial-vector coupling constant, and σ the spin Pauli matrices, which can produce a spin-flip in the decaying nucleon.

Forbidden Transitions

When $L > 0$, the decay is referred to as “forbidden”. Nuclear selection rules require high L values to be accompanied by changes in nuclear spin (J) and parity (π). The selection rules for the L th forbidden transitions are:

$$\Delta J = L - 1, L, L + 1; \Delta\pi = (-1)^L$$

Where, $\Delta\pi = 1$ or -1 corresponds to no parity change or parity change, respectively. The special case of a transition between isobaric analogue states, where the structure of the final state is very similar to the structure of the initial state, is referred to as “superallowed” for beta decay, and proceeds very quickly. The following table lists the ΔJ and $\Delta\pi$ values for the first few values of L :

Forbiddenness	ΔJ	$\Delta\pi$
Superallowed	0	no
Allowed	0, 1	no
First forbidden	0, 1, 2	yes
Second forbidden	1, 2, 3	no
Third forbidden	2, 3, 4	yes

Rare Decay Modes

Bound-state β^- Decay

A very small minority of free neutron decays (about four per million) are so-called “two-body decays”, in which the proton, electron and antineutrino are produced, but the electron fails to gain the 13.6 eV energy necessary to escape the proton, and therefore simply remains bound to it, as a neutral hydrogen atom. In this type of beta decay, in essence all of the neutron decay energy is carried off by the antineutrino.

For fully ionized atoms (bare nuclei), it is possible in likewise manner for electrons to fail to escape the atom, and to be emitted from the nucleus into low-lying atomic bound states (orbitals). This cannot occur for neutral atoms with low-lying bound states which are already filled by electrons.

Bound-state β decays were predicted by Daudel, Jean, and Lecoine in 1947, and the phenomenon in fully ionized atoms was first observed for $^{163}\text{Dy}^{66+}$ in 1992 by Jung et al. of the Darmstadt Heavy-Ion Research group. Although neutral ^{163}Dy is a stable isotope, the fully ionized $^{163}\text{Dy}^{66+}$ undergoes β decay into the K and L shells with a half-life of 47 days.

Another possibility is that a fully ionized atom undergoes greatly accelerated β decay, as observed for ^{187}Re by Bosch et al., also at Darmstadt. Neutral ^{187}Re does undergo β decay with a half-life of 42×10^9 years, but for fully ionized $^{187}\text{Re}^{75+}$ this is shortened by a factor of 109 to only 32.9 years. For comparison the variation of decay rates of other nuclear processes due to chemical environment is less than 1%.

DOUBLE BETA DECAY

In nuclear physics, double beta (2β) decay is a type of radioactive decay in which two neutrons are simultaneously transformed into two protons, or vice versa, inside an atomic nucleus. As in single beta decay, this process allows the atom to move closer to the optimal ratio of protons and neutrons. As a result of this transformation, the nucleus emits two detectable beta particles, which are electrons or positrons.

In ordinary double beta decay, which has been observed in several isotopes, two electrons and two electron antineutrinos are emitted from the decaying nucleus. In neutrinoless double beta decay, a hypothesized process that has never been observed, only electrons would be emitted.

Ordinary Double Beta Decay

In a typical double beta decay, two neutrons in the nucleus are converted to protons, and two electrons and two electron antineutrinos are emitted. The process can be thought as two simultaneous beta minus decays. In order for (double) beta decay to be possible, the final nucleus must have a larger binding energy than the original nucleus. For some nuclei, such as germanium-76, the isobar one atomic number higher (arsenic-76) has a smaller binding energy, preventing single beta decay. However, the isobar with atomic number two higher, selenium-76, has a larger binding energy, so double beta decay is allowed.

The emission spectrum of the two electrons can be computed in a similar way to beta emission spectrum using Fermi's Golden Rule. The differential rate is given by:

$$\frac{dN(T_1, T_2, \cos\theta)}{dT_1 dT_2 d\cos\theta} = F(Z, T_1) F(Z, T_2) w_1 p_1 w_2 p_2 (Q - T_1 - T_2)^5 (1 - v_1 v_2 \cos\theta)$$

Where the subscripts refer to each electron, T is kinetic energy, w is total energy, $F(Z, T)$ is the Fermi Function with Z the charge of the final-state nucleus, p is momentum, v is velocity in units of c , $\cos\theta$ is the angle between the electrons, and Q is the Q value of the decay.

For some nuclei, the process occurs as conversion of two protons to neutrons, emitting two electron neutrinos and absorbing two orbital electrons (double electron capture). If

the mass difference between the parent and daughter atoms is more than $1.022 \text{ MeV}/c^2$ (two electron masses), decay is accessible, capture of one orbital electron and emission of one positron. When the mass difference is more than $2.044 \text{ MeV}/c^2$ (four electron masses), emission of two positrons is possible. These theoretical decay branches have not been observed.

Known Double Beta Decay Isotopes

There are 35 naturally occurring isotopes capable of double beta decay. In practice, the decay can be observed when the single beta decay is forbidden by energy conservation. This happens for elements with an even atomic number and even neutron number, which are more stable due to spin-coupling. When single beta decay or alpha decay also occur, the double beta decay rate is generally too low to observe. However, the double beta decay of ^{238}U (also an alpha emitter) has been measured radiochemically. Two other nuclides in which double beta decay has been observed, ^{48}Ca and ^{96}Zr , can also theoretically single beta decay, but this decay is extremely suppressed and has never been observed.

Fourteen isotopes have been experimentally observed undergoing two-neutrino double beta decay ($\beta^-\beta^-$) or double electron capture ($\epsilon\epsilon$). The table below contains nuclides with the latest experimentally measured half-lives, as of December 2016, except for ^{124}Xe (for which double electron capture was first observed in 2019). Where two uncertainties are specified, the first one is statistical uncertainty and the second is systematic.

Nuclide	Half-life, 10^{21} years	Mode	Transition	Method	Experiment
^{48}Ca	$0.064^{+0.007}_{-0.006} \pm^{+0.012}_{-0.009}$	$\beta^-\beta^-$		direct	NEMO-3
^{76}Ge	1.926 ± 0.094	$\beta^-\beta^-$		direct	GERDA
^{78}Kr	$9.2^{+5.5}_{-2.6} \pm 1.3$	$\epsilon\epsilon$		direct	BAKSAN
^{82}Se	$0.096 \pm 0.003 \pm 0.010$	$\beta^-\beta^-$		direct	NEMO-3
^{96}Zr	$0.0235 \pm 0.0014 \pm 0.0016$	$\beta^-\beta^-$		direct	NEMO-3
^{100}Mo	0.00693 ± 0.00004	$\beta^-\beta^-$		direct	NEMO-3
	$0.69^{+0.10}_{-0.08} \pm 0.07$	$\beta^-\beta^-$	$0^+ \rightarrow 0^+_1$		Ge coincidence
^{116}Cd	$0.028 \pm 0.001 \pm 0.0030.026^{+0.009}_{-0.005}$	$\beta^-\beta^-$		direct	NEMO-3 ELEGANT IV
^{128}Te	7200 ± 400	$\beta^-\beta^-$		geo-chemical	
	1800 ± 700				

¹³⁰ Te	$0.82 \pm 0.02 \pm 0.06$	$\beta^-\beta^-$		direct	CUORE-o
¹²⁴ Xe	$18 \pm 5 \pm 1$	$\epsilon\epsilon$		direct	XENON1T
¹³⁶ Xe	$2.165 \pm 0.016 \pm 0.059$	$\beta^-\beta^-$		direct	EXO-200
¹³⁰ Ba	(0.5 – 2.7)	$\epsilon\epsilon$		geo-chemical	
¹⁵⁰ d	$0.00911^{+0.00025}_{-0.00022} \pm 0.00063$	$\beta^-\beta^-$		direct	NEMO-3
	$0.107^{0.046}_{0.026}$	$\beta^-\beta^-$	$0^+ \rightarrow 0^+_1$		Ge coincidence
²³⁸ U	2.0 ± 0.6	$\beta^-\beta^-$		radio-chemical	

Searches for double beta decay in isotopes that present significantly greater experimental challenges are ongoing. One such isotope is ¹³⁴Xe, which is expected to decay in addition to ¹³⁶Xe.

The following known nuclides with $A \leq 260$ are theoretically capable of double beta decay, where red are isotopes that have a double-beta rate measured experimentally and black have yet to be measured experimentally: ⁴⁶Ca, ⁴⁸Ca, ⁷⁰Zn, ⁷⁶Ge, ⁸⁰Se, ⁸²Se, ⁸⁶Kr, ⁹⁴Zr, ⁹⁶Zr, ⁹⁸Mo, ¹⁰⁰Mo, ¹⁰⁴Ru, ¹¹⁰Pd, ¹¹⁴Cd, ¹¹⁶Cd, ¹²²Sn, ¹²⁴Sn, ¹²⁸Te, ¹³⁰Te, ¹³⁴Xe, ¹³⁶Xe, ¹⁴²Ce, ¹⁴⁶Nd, ¹⁴⁸Nd, ¹⁵⁰Nd, ¹⁵⁴Sm, ¹⁶⁰Gd, ¹⁷⁰Er, ¹⁷⁶Yb, ¹⁸⁶W, ¹⁹²Os, ¹⁹⁸Pt, ²⁰⁴Hg, ²¹⁶Po, ²²⁰Rn, ²²²Rn, ²²⁶Ra, ²³²Th, ²³⁸U, ²⁴⁴Pu, ²⁴⁸Cm, ²⁵⁴Cf, ²⁵⁶Cf, and ²⁶⁰Fm.

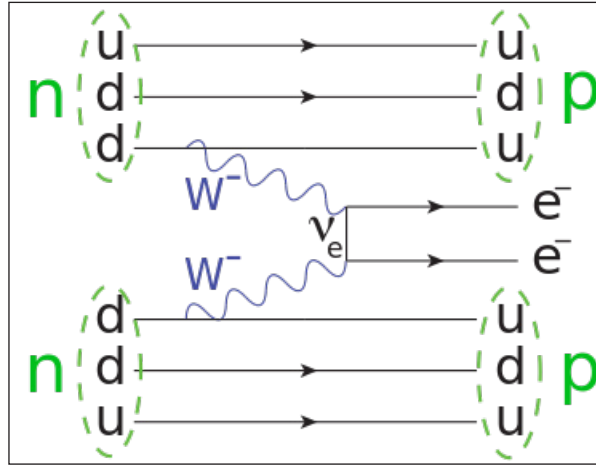
The following known nuclides with $A \leq 260$ are theoretically capable of double electron capture, where red are isotopes that have a double-electron capture rate measured and black have yet to be measured experimentally: ³⁶Ar, ⁴⁰Ca, ⁵⁰Cr, ⁵⁴Fe, ⁵⁸Ni, ⁶⁴Zn, ⁷⁴Se, ⁷⁸Kr, ⁸⁴Sr, ⁹²Mo, ⁹⁶Ru, ¹⁰²Pd, ¹⁰⁶Cd, ¹⁰⁸Cd, ¹¹²Sn, ¹²⁰Te, ¹²⁴Xe, ¹²⁶Xe, ¹³⁰Ba, ¹³²Ba, ¹³⁶Ce, ¹³⁸Ce, ¹⁴⁴Sm, ¹⁴⁸Gd, ¹⁵⁰Gd, ¹⁵²Gd, ¹⁵⁴Dy, ¹⁵⁶Dy, ¹⁵⁸Dy, ¹⁶²Er, ¹⁶⁴Er, ¹⁶⁸Yb, ¹⁷⁴Hf, ¹⁸⁰W, ¹⁸⁴Os, ¹⁹⁰Pt, ¹⁹⁶Hg, ²¹²Rn, ²¹⁴Rn, ²¹⁸Ra, ²²⁴Th, ²³⁰U, ²³⁶Pu, ²⁴²Cm, ²⁵²Fm, and ²⁵⁸No.

Neutrinoless Double Beta Decay

If the neutrino is a Majorana particle (i.e., the antineutrino and the neutrino are actually the same particle), and at least one type of neutrino has non-zero mass (which has been established by the neutrino oscillation experiments), then it is possible for neutrinoless double beta decay to occur. Neutrinoless double beta decay is a lepton number violating process. In the simplest theoretical treatment, known as light neutrino exchange, a nucleon absorbs the neutrino emitted by another nucleon. The exchanged neutrinos are virtual particles.

Figure shows feynman diagram of neutrinoless double beta decay, with two neutrons decaying to two protons. The only emitted products in this process are two electrons,

which can occur if the neutrino and antineutrino are the same particle (i.e. Majorana neutrinos) so the same neutrino can be emitted and absorbed within the nucleus. In conventional double beta decay, two antineutrinos — one arising from each W vertex — are emitted from the nucleus, in addition to the two electrons. The detection of neutrinoless double beta decay is thus a sensitive test of whether neutrinos are Majorana particles.



With only two electrons in the final state, the electrons' total kinetic energy would be approximately the binding energy difference of the initial and final nuclei, with the nuclear recoil accounting for the rest. Because of momentum conservation, electrons are generally emitted back-to-back. The decay rate for this process is given by:

$$\Gamma = G |M|^2 |m_{\beta\beta}|^2$$

Where G is the two-body phase-space factor, M is the nuclear matrix element, and $m_{\beta\beta}$ is the effective Majorana mass of the electron neutrino. In the context of light Majorana neutrino exchange, $m_{\beta\beta}$ is given by:

$$m_{\beta\beta} = \sum_{i=1}^3 m_i U_{ei}^2$$

Where m_i are the neutrino masses and the U_{ei} are elements of the Pontecorvo–Maki–Nakagawa–Sakata (PMNS) matrix. Therefore, observing neutrinoless double beta decay, in addition to confirming the Majorana neutrino nature, can give information on the absolute neutrino mass scale and Majorana phases in the PMNS matrix, subject to interpretation through theoretical models of the nucleus, which determine the nuclear matrix elements, and models of the decay.

The observation of neutrinoless double beta decay would require that at least one neutrino is a Majorana particle, irrespective of whether the process is engendered by neutrino exchange.

Experiments

Numerous experiments have searched for neutrinoless double beta decay. The best-performing experiments have a high mass of the decaying isotope and low backgrounds, with some experiments able to perform particle discrimination and electron tracking. In order to remove backgrounds from cosmic rays, most experiments are located in underground laboratories around the world.

Recent and proposed experiments include:

- Completed experiments:
 - Gotthard TPC,
 - Heidelberg-Moscow, ^{76}Ge detectors,
 - IGEX, ^{76}Ge detectors,
 - NEMO, various isotopes using tracking calorimeters,
 - Cuoricino, ^{130}Te in ultracold TeO_2 crystals.
- Experiments taking data as of November 2017:
 - COBRA, ^{116}Cd in room temperature CdZnTe crystals,
 - CUORE, ^{130}Te in ultracold TeO_2 crystals,
 - EXO, a ^{136}Xe and ^{134}Xe search,
 - GERDA, a ^{76}Ge detector,
 - KamLAND-Zen, a ^{136}Xe search,
 - Majorana, using high purity ^{76}Ge p-type point-contact detectors,
 - XMASS using liquid Xe.
- Proposed/future experiments:
 - CANDLES, ^{48}Ca in CaF_2 , at Kamioka Observatory,
 - MOON, developing 100Mo detectors,
 - AMoRE, ^{100}Mo enriched CaMoO_4 crystals at YangYang underground laboratory,
 - nEXO, using liquid ^{136}Xe in a time projection chamber,
 - LEGEND, Neutrinoless Double-beta Decay of ^{76}Ge ,
 - LUMINEU, exploring ^{100}Mo enriched ZnMoO_4 crystals at LSM, France,
 - NEXT, a Xenon TPC. NEXT-DEMO ran and NEXT-100 will run in 2016,

- SNO+, a liquid scintillator, will study ^{130}Te ,
- SuperNEMO, a NEMO upgrade, will study ^{82}Se ,
- TIN.TIN, a ^{124}Sn detector at INO,
- PandaX-III, an experiment with 200 kg to 1000 kg of 90% enriched ^{136}Xe .

Status

While some experiments have claimed a discovery of neutrinoless double beta decay, modern searches have found no evidence for the decay.

Heidelberg-Moscow Controversy

Some members of the Heidelberg-Moscow collaboration claimed a detection of neutrinoless beta decay in ^{76}Ge in 2001. This claim was criticized by outside physicists as well as other members of the collaboration. In 2006, a refined estimate by the same authors stated the half-life was 2.3×10^{25} years. This half-life has been excluded at high confidence by other experiments, including in ^{76}Ge by GERDA.

Current Results

As of 2017, the strongest limits on neutrinoless double beta decay have come from GERDA in ^{76}Ge , CUORE in ^{130}Te , and EXO-200 and KamLAND-Zen in ^{136}Xe .

Theoretical Higher Simultaneous Beta Decay

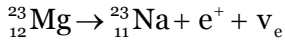
For mass numbers with more than two beta-stable isobars, quadruple beta decay and its inverse, quadruple electron capture, have been proposed as alternatives to double beta decay in the isobars with the greatest energy excess. Such a decay mode has been proposed to be neutrinoless, and energetically possible in eight nuclei, though partial half-lives compared to single or double beta decay are predicted to be very long; hence, quadruple beta decay is unlikely to be observed. The eight candidate nuclei for quadruple beta decay include ^{96}Zr , ^{136}Xe , and ^{150}Nd capable of quadruple beta-minus decay, and ^{124}Xe , ^{130}Ba , ^{148}Gd , and ^{154}Dy capable of quadruple beta-plus decay or electron capture. In theory, quadruple beta decay may be experimentally observable in three of these nuclei, with the most promising candidate being ^{150}Nd .

BETA PLUS DECAY

Positron emission or beta plus decay (β^+ decay) is a subtype of radioactive decay called beta decay, in which a proton inside a radionuclide nucleus is converted into a neutron

while releasing a positron and an electron neutrino (ν_e). Positron emission is mediated by the weak force. The positron is a type of beta particle (β^+), the other beta particle being the electron (β^-) emitted from the β^- decay of a nucleus.

An example of positron emission (β^+ decay) is shown with magnesium-23 decaying into sodium-23:



Because positron emission decreases proton number relative to neutron number, positron decay happens typically in large “proton-rich” radionuclides. Positron decay results in nuclear transmutation, changing an atom of one chemical element into an atom of an element with an atomic number that is less by one unit.

Positron emission occurs only very rarely naturally on earth, when induced by a cosmic ray or from one in a hundred thousand decays of potassium-40, a rare isotope, 0.012% of that element on earth.

Positron emission should not be confused with electron emission or beta minus decay (β^- decay), which occurs when a neutron turns into a proton and the nucleus emits an electron and an antineutrino.

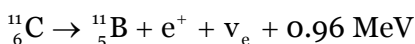
Positron emission is different from proton decay, the hypothetical decay of protons, not necessarily those bound with neutrons, not necessarily through the emission of a positron and not as part of nuclear physics, but rather of particle physics.

Discovery of Positron Emission

In 1934 Frédéric and Irène Joliot-Curie bombarded aluminium with alpha particles to effect the nuclear reaction ${}^4_2\text{He} + {}^{27}_{13}\text{Al} \rightarrow {}^{30}_{15}\text{P} + {}^1_0\text{n}$, and observed that the product isotope ${}^{30}_{15}\text{P}$ emits a positron identical to those found in cosmic rays by Carl David Anderson in 1932. This was the first example of β^+ decay (positron emission). The Curies termed the phenomenon “artificial radioactivity,” since ${}^{30}_{15}\text{P}$ is a short-lived nuclide which does not exist in nature. The discovery of artificial radioactivity would be cited when the husband and wife team won the Nobel Prize.

Positron-emitting Isotopes

Isotopes which undergo this decay and thereby emit positrons include carbon-11, potassium-40, nitrogen-13, oxygen-15, aluminium-26, sodium-22, fluorine-18, strontium-83, and iodine-124. As an example, the following equation describes the beta plus decay of carbon-11 to boron-11, emitting a positron and a neutrino:



Emission Mechanism

Inside protons and neutrons, there are fundamental particles called quarks. The two most common types of quarks are up quarks, which have a charge of $+\frac{2}{3}$, and down quarks, with a $-\frac{1}{3}$ charge. Quarks arrange themselves in sets of three such that they make protons and neutrons. In a proton, whose charge is $+1$, there are two up quarks and one down quark ($\frac{2}{3} + \frac{2}{3} - \frac{1}{3} = 1$). Neutrons, with no charge, have one up quark and two down quarks ($\frac{2}{3} - \frac{1}{3} - \frac{1}{3} = 0$). Via the weak interaction, quarks can change flavor from down to up, resulting in electron emission. Positron emission happens when an up quark changes into a down quark ($\frac{2}{3} - 1 = -\frac{1}{3}$).

Nuclei which decay by positron emission may also decay by electron capture. For low-energy decays, electron capture is energetically favored by $2m_e c^2 = 1.022$ MeV, since the final state has an electron removed rather than a positron added. As the energy of the decay goes up, so does the branching ratio towards positron emission. However, if the energy difference is less than $2m_e c^2$, then positron emission cannot occur and electron capture is the sole decay mode. Certain otherwise electron-capturing isotopes (for instance, ${}^7\text{Be}$) are stable in galactic cosmic rays, because the electrons are stripped away and the decay energy is too small for positron emission.

Energy Conservation

A positron is ejected from the parent nucleus, and the daughter ($Z-1$) atom must shed an orbital electron to balance charge. The overall result is that the mass of two electrons are ejected from the atom (one for the positron and one for the electron), and the β^+ decay is energetically possible only if the mass of the parent atom exceeds the mass of the daughter atom by at least two electron masses (1.02 MeV).

Isotopes which increase in mass under the conversion of a proton to a neutron, or which decrease in mass by less than $2m_e$, cannot spontaneously decay by positron emission.

Application

These isotopes are used in positron emission tomography, a technique used for medical imaging. Note that the energy emitted depends on the isotope that is decaying; the figure of 0.96 MeV applies only to the decay of carbon-11.

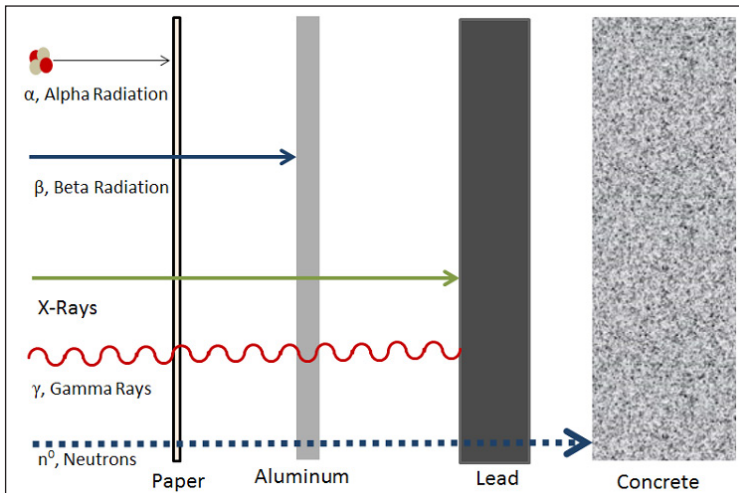
The short-lived positron emitting isotopes ${}^{11}\text{C}$, ${}^{13}\text{N}$, ${}^{15}\text{O}$ and ${}^{18}\text{F}$ used for positron emission tomography are typically produced by proton irradiation of natural or enriched targets.

GAMMA DECAY

Gamma (γ) decay is one type of radioactive decay that a nucleus can undergo. What separates this type of decay process from alpha or beta decay is that no particles are

ejected from the nucleus when it undergoes this type of decay. Instead, a high energy form of electromagnetic radiation - a gamma ray photon - is released. Gamma rays are simply photons that have extremely high energies which are highly ionizing. As well, gamma radiation is unique in the sense that undergoing gamma decay does not change the structure or composition of the atom. Instead, it only changes the energy of the atom since the gamma ray carries no charge nor does it have an associated mass.

In order for a nucleus to undergo gamma decay, it must be in some sort of excited energetic state. Experiments have shown that protons and neutrons are located in discrete energy states within the nucleus, not too different from the excited states that electrons can occupy in atoms. Thus if a proton or a neutron inside of the nucleus jumps up to an excited state - generally following an alpha or beta decay - the new daughter nucleus must somehow release energy to allow the proton or neutron to relax back down to ground state. When the nucleon makes this transition from a high to a low energy state, a gamma photon is emitted.



Different penetration levels of different products of decay, with gamma being one of the most highly penetrating.

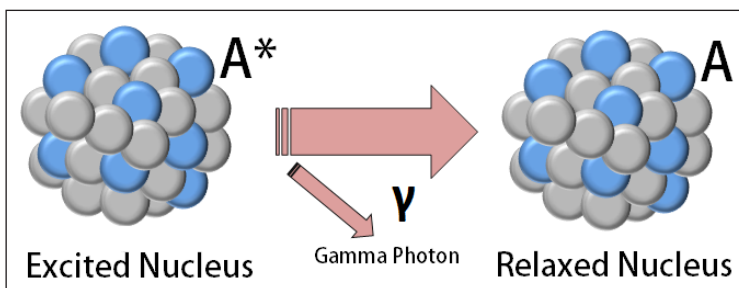


Diagram showing gamma decay of a nucleus.

Knowing that an atom undergoes gamma radiation is important, but it is also possible to determine the frequency of the released gamma radiation if the initial and final states of the nucleon inside the nucleus are known.

In addition to radioactive nuclei, there are many objects in space that emit high levels of gamma radiation.

Applications and Importance

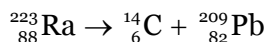
Gamma rays can at times be harmful due to the fact that they are generally very high energy and therefore penetrate matter very easily. Since it penetrates so easily, it is some of the most useful radiation for medical purposes.

Some of the most widely used gamma emitters are cobalt-60, cesium-137, and technetium-99m. Cesium is used widely in radiotherapy - the treatment of cancer using gamma rays - as well as being used to measure soil density at construction sites and to investigate the subterranean layers of the Earth in oil wells. Cobalt is used to sterilize medical equipment and irradiate food, killing bacteria and pasteurizing the food. Technetium-99m (which has a shorter half-life than technetium-99) is the most widely used for diagnostic medical tests to investigate the brain, bone, and internal organs. As well, exposure to gamma radiation can improve the durability of wood and plastics, and is thus used to toughen flooring in high-traffic areas.

In addition, uranium-238 and uranium-235 used in fuel for nuclear power plants - undergo both alpha and gamma decays when used. Immediately following the fission process, gamma rays are released, resulting in high levels of radiation present around the reactor. However, safety precautions are in line to ensure that workers do not get close enough to this radioactive area to be harmed.

CLUSTER DECAY

Cluster decay, also named heavy particle radioactivity or heavy ion radioactivity, is a rare type of nuclear decay in which an atomic nucleus emits a small “cluster” of neutrons and protons, more than in an alpha particle, but less than a typical binary fission fragment. Ternary fission into three fragments also produces products in the cluster size. The loss of protons from the parent nucleus changes it to the nucleus of a different element, the daughter, with a mass number $A_d = A - A_e$ and atomic number $Z_d = Z - Z_e$, where $A_e = N_e + Z_e$. For example:



This type of rare decay mode was observed in radioisotopes that decay predominantly by alpha emission, and it occurs only in a small percentage of the decays for all such isotopes.

The branching ratio with respect to alpha decay is rather small:

$$B = T_a / T_c$$

T_a and T_c are the half-lives of the parent nucleus relative to alpha decay and cluster radioactivity, respectively.

Cluster decay, like alpha decay, is a quantum tunneling process: in order to be emitted, the cluster must penetrate a potential barrier. This is a different process than the more random nuclear disintegration that precedes light fragment emission in ternary fission, which may be a result of a nuclear reaction, but can also be a type of spontaneous radioactive decay in certain nuclides, demonstrating that input energy is not necessarily needed for fission, which remains a fundamentally different process mechanically.

Theoretically, any nucleus with $Z > 40$ for which the released energy (Q value) is a positive quantity, can be a cluster-emitter. In practice, observations are severely restricted to limitations imposed by currently available experimental techniques which require a sufficiently short half-life, $T_c < 10^{32}$ s, and a sufficiently large branching ratio $B > 10^{-17}$.

In the absence of any energy loss for fragment deformation and excitation, as in cold fission phenomena or in alpha decay, the total kinetic energy is equal to the Q -value and is divided between the particles in inverse proportion with their masses, as required by conservation of linear momentum:

$$E_k = QA_d / A$$

Where, A_d is the mass number of the daughter, $A_d = A - A_e$.

Cluster decay exists in an intermediate position between alpha decay (in which a nucleus spits out a ${}^4\text{He}$ nucleus), and spontaneous fission, in which a heavy nucleus splits into two (or more) large fragments and an assorted number of neutrons. Spontaneous fission ends up with a probabilistic distribution of daughter products, which sets it apart from cluster decay. In cluster decay for a given radioisotope, the emitted particle is a light nucleus and the decay method always emits this same particle. For heavier emitted clusters, there is otherwise practically no qualitative difference between cluster decay and spontaneous cold fission.

The quantum tunneling may be calculated either by extending fission theory to a larger mass asymmetry or by heavier emitted particle from alpha decay theory.

Both fission-like and alpha-like approaches are able to express the decay constant $\lambda = \ln 2 / T_c$, as a product of three model-dependent quantities:

$$\lambda = vSP_s$$

Where, v is the frequency of assaults on the barrier per second, S is the preformation probability of the cluster at the nuclear surface, and P_s is the penetrability of the external barrier. In alpha-like theories S is an overlap integral of the wave function of the

three partners (parent, daughter, and emitted cluster). In a fission theory the preformation probability is the penetrability of the internal part of the barrier from the initial turning point R_i to the touching point R_t . Very frequently it is calculated by using the Wentzel-Kramers-Brillouin (WKB) approximation.

A very large number, of the order 10^5 , of parent-emitted cluster combinations were considered in a systematic search for new decay modes. The large amount of computations could be performed in a reasonable time by using the ASAF model developed by Dorin N Poenaru, Walter Greiner, et al. The model was the first to be used to predict measurable quantities in cluster decay. More than 150 cluster decay modes have been predicted before any other kind of half-life calculations have been reported. Comprehensive tables of half-lives, branching ratios, and kinetic energies have been published. Potential barrier shapes similar to that considered within the ASAF model have been calculated by using the macroscopic-microscopic method.

Previously it was shown that even alpha decay may be considered a particular case of cold fission. The ASAF model may be used to describe in a unified manner cold alpha decay, cluster decay, and cold fission.

One can obtain with good approximation one universal curve (UNIV) for any kind of cluster decay mode with a mass number A_s , including alpha decay:

$$\log T = -\log P_s - 22.169 + 0.598(A_s - 1)$$

In a logarithmic scale the equation $\log T = f(\log P_s)$ represents a single straight line which can be conveniently used to estimate the half-life. A single universal curve for alpha decay and cluster decay modes results by expressing $\log T + \log S = f(\log P_s)$. The experimental data on cluster decay in three groups of even-even, even-odd, and odd-even parent nuclei are reproduced with comparable accuracy by both types of universal curves, fission-like UNIV and UDL derived using alpha-like R-matrix theory.

In order to find the released energy:

$$Q = [M - (M_d + M_c)]c^2$$

One can use the compilation of measured masses M , M_d , and M_c of the parent, daughter, and emitted nuclei, c is the light velocity. The mass excess is transformed into energy according to the Einstein's formula $E = mc^2$.

Experiments

The main experimental difficulty in observing cluster decay comes from the need to identify a few rare events among an enormous number of background alpha particle. The quantities experimentally determined are the partial half-life, T_c , and the

kinetic energy of the emitted cluster E_k . There is also a need to identify the emitted particle.

Detection of radiations is based on their interactions with matter, leading mainly to ionizations. Using a semiconductor telescope and conventional electronics to identify the ^{14}C ions, the Rose and Jones's experiment was running for about six months in order to get 11 useful events.

With modern magnetic spectrometers (SOLENO and Enge-split pole), at Orsay and Argonne National Laboratory, a very strong source could be used, so that results were obtained in a run of few hours.

Solid state nuclear track detectors (SSNTD) insensitive to alpha particles and magnetic spectrometers in which alpha particles are deflected by a strong magnetic field have been used to overcome this difficulty. SSNTD are cheap and handy but they need chemical etching and microscope scanning.

A key role in experiments on cluster decay modes performed in Berkeley, Orsay, Dubna, and Milano was played by P. Buford Price, Eid Hourany, Michel Hussonnois, Svetlana Tretyakova, A. A. Ogloblin, Roberto Bonetti, and their coworkers.

The main region of 20 emitters experimentally observed until 2010 is above $Z=86$: ^{221}Fr , $^{221-224,226}\text{Ra}$, $^{223,225}\text{Ac}$, $^{228,230}\text{Th}$, ^{231}Pa , $^{230,232-236}\text{U}$, $^{236,238}\text{Pu}$, and ^{242}Cm . Only upper limits could be detected in the following cases: ^{12}C decay of ^{114}Ba , ^{15}N decay of ^{223}Ac , ^{18}O decay of ^{226}Th , $^{24,26}\text{Ne}$ decays of ^{232}Th and of ^{236}U , ^{28}Mg decays of $^{232,233,235}\text{U}$, ^{30}Mg decay of ^{237}Np , and ^{34}Si decay of ^{240}Pu and of ^{241}Am .

Some of the cluster emitters are members of the three natural radioactive families. Others should be produced by nuclear reactions. Up to now no odd-odd emitter has been observed.

From many decay modes with half-lives and branching ratios relative to alpha decay predicted with the analytical superasymmetric fission (ASAF) model, the following 11 have been experimentally confirmed: ^{14}C , ^{20}O , ^{23}F , $^{22,24-26}\text{Ne}$, $^{28,30}\text{Mg}$, and $^{32,34}\text{Si}$. The experimental data are in good agreement with predicted values. A strong shell effect can be seen: as a rule the shortest value of the half-life is obtained when the daughter nucleus has a magic number of neutrons ($N_d = 126$) and/or protons ($Z_d = 82$).

The known cluster emissions as of 2010 are as follows:

Isotope	Emitted particle	Branching ratio	$\log T(\text{s})$	Q (MeV)
^{114}Ba	^{12}C	$< 3.4 \times 10^{-5}$	> 4.10	18.985
^{221}Fr	^{14}C	8.14×10^{-13}	14.52	31.290
^{221}Ra	^{14}C	1.15×10^{-12}	13.39	32.394

²²² Ra	¹⁴ C	3.7×10^{-10}	11.01	33.049
²²³ Ra	¹⁴ C	8.9×10^{-10}	15.04	31.829
²²⁴ Ra	¹⁴ C	4.3×10^{-11}	15.86	30.535
²²³ Ac	¹⁴ C	3.2×10^{-11}	12.96	33.064
²²⁵ Ac	¹⁴ C	4.5×10^{-12}	17.28	30.476
²²⁶ Ra	¹⁴ C	3.2×10^{-11}	21.19	28.196
²²⁸ Th	²⁰ O	1.13×10^{-13}	20.72	44.723
²³⁰ Th	²⁴ Ne	5.6×10^{-13}	24.61	57.758
²³¹ Pa	²³ F	9.97×10^{-15}	26.02	51.844
	²⁴ Ne	1.34×10^{-11}	22.88	60.408
²³² U	²⁴ Ne	9.16×10^{-12}	20.40	62.309
	²⁸ Mg	$< 1.18 \times 10^{-13}$	> 22.26	74.318
²³³ U	²⁴ Ne	7.2×10^{-13}	24.84	60.484
	²⁵ Ne			60.776
	²⁸ Mg	$< 1.3 \times 10^{-15}$	> 27.59	74.224
²³⁴ U	²⁸ Mg	1.38×10^{-13}	25.14	74.108
	²⁴ Ne	9.9×10^{-14}	25.88	58.825
	²⁶ Ne			59.465
²³⁵ U	²⁴ Ne	8.06×10^{-12}	27.42	57.361
	²⁵ Ne			57.756
	²⁸ Mg	$< 1.8 \times 10^{-12}$	> 28.09	72.162
	²⁹ Mg			72.535
²³⁶ U	²⁴ Ne	$< 9.2 \times 10^{-12}$	> 25.90	55.944
	²⁶ Ne			56.753
	²⁸ Mg	2×10^{-13}	27.58	70.560
	³⁰ Mg			72.299
²³⁶ Pu	²⁸ Mg	2.7×10^{-14}	21.52	79.668
²³⁷ Np	³⁰ Mg	$< 1.8 \times 10^{-14}$	> 27.57	74.814
²³⁸ Pu	³² Si	1.38×10^{-16}	25.27	91.188
	²⁸ Mg	5.62×10^{-17}	25.70	75.910
	³⁰ Mg			76.822
²⁴⁰ Pu	³⁴ Si	$< 6 \times 10^{-15}$	> 25.52	91.026

^{241}Am	^{34}Si	$< 7.4 \times 10^{-16}$	> 25.26	93.923
^{242}Cm	^{34}Si	1×10^{-16}	23.15	96.508

Fine Structure

The fine structure in ^{14}C radioactivity of ^{223}Ra was discussed for the first time by M. Greiner and W. Scheid in 1986. The superconducting spectrometer SOLENO of IPN Orsay has been used since 1984 to identify ^{14}C clusters emitted from $^{222-224,226}\text{Ra}$ nuclei. Moreover, it was used to discover the fine structure observing transitions to excited states of the daughter. A transition with an excited state of ^{14}C was not yet observed.

Surprisingly, the experimentalists had seen a transition to the first excited state of the daughter stronger than that to the ground state. The transition is favoured if the uncoupled nucleon is left in the same state in both parent and daughter nuclei. Otherwise the difference in nuclear structure leads to a large hindrance.

The interpretation was confirmed: the main spherical component of the deformed parent wave function has an $i_{11/2}$ character, i.e. the main component is spherical.

DECAY CHAIN

In nuclear science, the decay chain refers to a series of radioactive decays of different radioactive decay products as a sequential series of transformations. It is also known as a “radioactive cascade”. Most radioisotopes do not decay directly to a stable state, but rather undergo a series of decays until eventually a stable isotope is reached.

Decay stages are referred to by their relationship to previous or subsequent stages. A parent isotope is one that undergoes decay to form a daughter isotope. One example of this is uranium (atomic number 92) decaying into thorium (atomic number 90). The daughter isotope may be stable or it may decay to form a daughter isotope of its own. The daughter of a daughter isotope is sometimes called a granddaughter isotope.

The time it takes for a single parent atom to decay to an atom of its daughter isotope can vary widely, not only between different parent-daughter pairs, but also randomly between identical pairings of parent and daughter isotopes. The decay of each single atom occurs spontaneously, and the decay of an initial population of identical atoms over time t , follows a decaying exponential distribution, $e^{-\lambda t}$, where λ is called a decay constant. One of the properties of an isotope is its half-life, the time by which half of an initial number of identical parent radioisotopes have decayed to their daughters, which is inversely related to λ . Half-lives have been determined in laboratories for many radioisotopes (or radionuclides). These can range from nearly instantaneous (less than 10^{-21} seconds) to more than 10^{19} years.

The intermediate stages each emit the same amount of radioactivity as the original radioisotope (i.e. there is a one-to-one relationship between the numbers of decays in successive stages) but each stage releases a different quantity of energy. If and when equilibrium is achieved, each successive daughter isotope is present in direct proportion to its half-life; but since its activity is inversely proportional to its half-life, each nuclide in the decay chain finally contributes as many individual transformations as the head of the chain, though not the same energy. For example, uranium-238 is weakly radioactive, but pitchblende, a uranium ore, is 13 times more radioactive than the pure uranium metal because of the radium and other daughter isotopes it contains. Not only are unstable radium isotopes significant radioactivity emitters, but as the next stage in the decay chain they also generate radon, a heavy, inert, naturally occurring radioactive gas. Rock containing thorium and/or uranium (such as some granites) emits radon gas that can accumulate in enclosed places such as basements or underground mines.

Actinide Alpha Decay Chains

In the four tables below, the minor branches of decay (with the branching probability of less than 0.0001%) are omitted. The energy release includes the total kinetic energy of all the emitted particles (electrons, alpha particles, gamma quanta, neutrinos, Auger electrons and X-rays) and the recoil nucleus, assuming that the original nucleus was at rest. The letter 'a' represents a year.

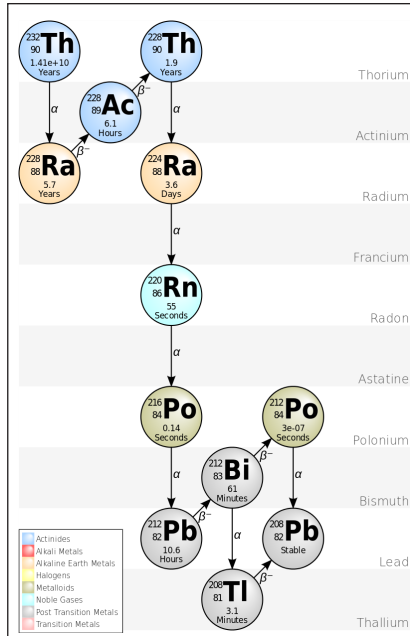
The historic names of the naturally occurring nuclides are also given. These names were used at the time when the decay chains were first discovered and investigated. From these historical names one can locate the particular chain to which the nuclide belongs, and replace it with its modern name.

The three naturally-occurring actinide alpha decay chains given below—thorium, uranium/radium (from U-238), and actinium (from U-235)—each ends with its own specific lead isotope (Pb-208, Pb-206, and Pb-207 respectively). All these isotopes are stable and are also present in nature as primordial nuclides, but their excess amounts in comparison with lead-204 (which has only a primordial origin) can be used in the technique of uranium-lead dating to date rocks.

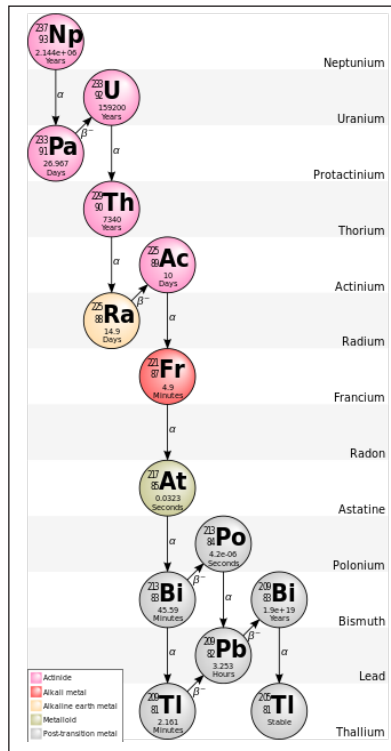
Thorium Series

The total energy released from thorium-232 to lead-208, including the energy lost to neutrinos, is 42.6 MeV.

The $4n$ chain of Th-232 is commonly called the “thorium series” or “thorium cascade”. Beginning with naturally occurring thorium-232, this series includes the following elements: Actinium, bismuth, lead, polonium, radium, radon and thallium. All are present, at least transiently, in any natural thorium-containing sample, whether metal, compound, or mineral. The series terminates with lead-208.



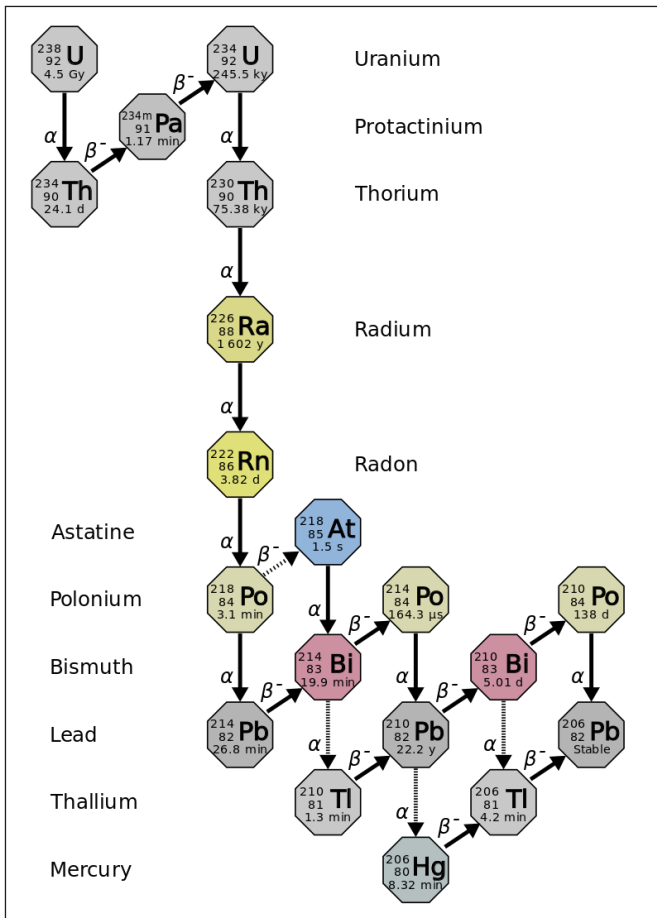
Neptunium Series



The total energy released from californium-249 to thallium-205, including the energy lost to neutrinos, is 66.8 MeV.

The $4n + 1$ chain of ^{237}Np is commonly called the “neptunium series” or “neptunium cascade”. In this series, only two of the isotopes involved are found naturally in significant quantities, namely the final two: bismuth-209 and thallium-205. Some of the other isotopes have been detected in nature, originating from trace quantities of ^{237}Np produced by the $(n,2n)$ knockout reaction in primordial ^{238}U . A smoke detector containing an americium-241 ionization chamber accumulates a significant amount of neptunium-237 as its americium decays; the following elements are also present in it, at least transiently, as decay products of the neptunium: actinium, astatine, bismuth, francium, lead, polonium, protactinium, radium, thallium, thorium, and uranium. Since this series was only discovered and studied in 1947–1948, its nuclides do not have historic names. One unique trait of this decay chain is that the noble gas radon is only produced in a rare branch and not the main decay sequence; thus, it does not migrate through rock nearly as much as the other three decay chains.

Uranium Series



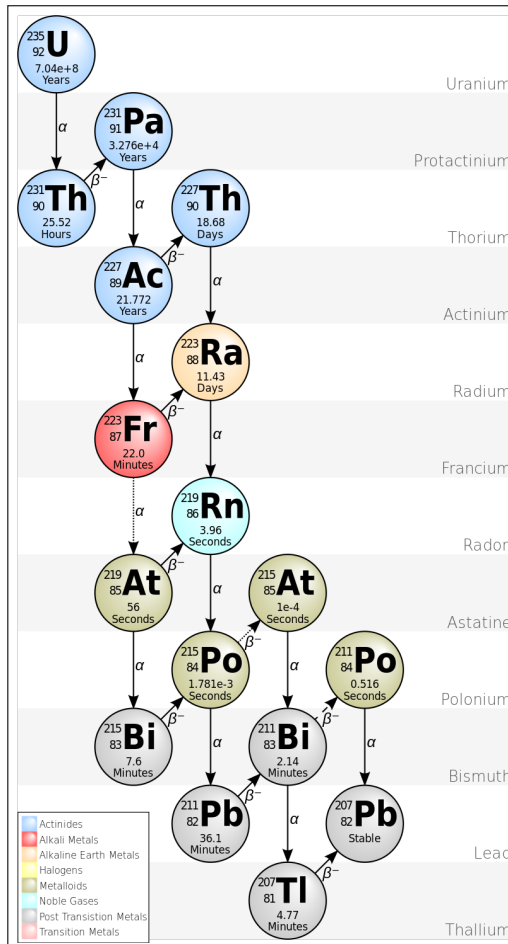
The $4n+2$ chain of U-238 is called the “uranium series” or “radium series”. Beginning with naturally occurring uranium-238, this series includes the following elements: Astatine,

bismuth, lead, polonium, protactinium, radium, radon, thallium, and thorium. All are present, at least transiently, in any natural uranium-containing sample, whether metal, compound, or mineral. The series terminates with lead-206.

The total energy released from uranium-238 to lead-206, including the energy lost to neutrinos, is 51.7 MeV.

Actinium Series

The $4n+3$ chain of uranium-235 is commonly called the “actinium series” or “actinium cascade”. Beginning with the naturally-occurring isotope U-235, this decay series includes the following elements: actinium, astatine, bismuth, francium, lead, polonium, protactinium, radium, radon, thallium, and thorium. All are present, at least transiently, in any sample containing uranium-235, whether metal, compound, ore, or mineral. This series terminates with the stable isotope lead-207.



The total energy released from uranium-235 to lead-207, including the energy lost to neutrinos, is 46.4 MeV.

DECAY ENERGY

The decay energy is the energy released by a radioactive decay. Radioactive decay is the process in which an unstable atomic nucleus loses energy by emitting ionizing particles and radiation. This decay, or loss of energy, results in an atom of one type, called the parent nuclide transforming to an atom of a different type, called the daughter nuclide.

Decay Calculation

The energy difference of the reactants is often written as Q:

$$Q = (\text{Kinetic energy})_{\text{after}} - (\text{Kinetic energy})_{\text{before}},$$

$$Q = ((\text{Rest mass})_{\text{before}} \times c^2) - ((\text{Rest mass})_{\text{after}} \times c^2)$$

Decay energy is usually quoted in terms of the energy units MeV (million electronvolts) or keV (thousand electronvolts).

Types of radioactive decay include:

- Gamma ray,
- Beta decay (decay energy is divided between the emitted electron and the neutrino which is emitted at the same time),
- Alpha decay.

The decay energy is the mass difference dm between the parent and the daughter atom and particles. It is equal to the energy of radiation E . If A is the radioactive activity, i.e. the number of transforming atoms per time, M the molar mass, then the radiation power W is:

$$W = dm \times \left(\frac{A}{M} \right)$$

Or,


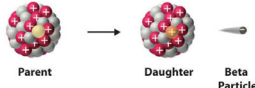
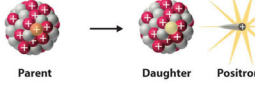
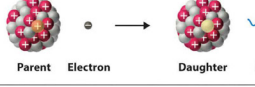
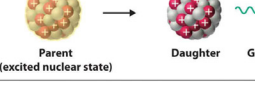
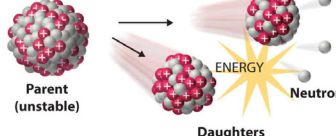
$$W = E \times \left(\frac{A}{M} \right)$$

Example: ^{60}Co decays into ^{60}Ni . The mass difference dm is 0.003u. The radiated energy is approximately 2.8 MeV. The molar weight is 59.93. The half-life T of 5.27 year corresponds to the activity $A = (N^* (-\ln(2))) / T$, where N is the number of atoms per mol. Taking care of the units the radiation power for ^{60}Co is 17.9 W/g.

Radiation power in W/g for several isotopes:

- ^{60}Co : 17.9
- ^{238}Pu : 0.57
- ^{137}Cs : 0.6
- ^{241}Am : 0.1
- ^{210}Po : 140 (T=136 d)
- ^{90}Sr : 0.9
- ^{226}Ra : 0.02

PROTON DECAY

Decay Type	Radiation Emitted	Generic Equation	Model
Alpha decay	$^4_2\alpha$	$^A_ZX \longrightarrow ^{A-4}_{Z-2}X' + ^4_2\alpha$	 <p>Parent → Daughter + Alpha Particle</p>
Beta decay	$^0_{-1}\beta$	$^A_ZX \longrightarrow ^A_{Z+1}X' + ^0_{-1}\beta$	 <p>Parent → Daughter + Beta Particle</p>
Positron emission	$^0_{+1}\beta$	$^A_ZX \longrightarrow ^A_{Z-1}X' + ^0_{+1}\beta$	 <p>Parent → Daughter + Positron</p>
Electron capture	X rays	$^A_ZX + ^0_{-1}e \longrightarrow ^A_{Z-1}X' + \text{X ray}$	 <p>Parent + Electron → Daughter + X ray</p>
Gamma emission	$^0_0\gamma$	$^A_ZX^* \xrightarrow{\text{Relaxation}} ^A_ZX + ^0_0\gamma$	 <p>Parent (excited nuclear state) → Daughter + Gamma ray</p>
Spontaneous fission	Neutrons	$^A_{Z+Y}X \longrightarrow ^A_ZX' + ^B_YX' + C^1_0n$	 <p>Parent (unstable) → Daughters + Neutrons + ENERGY</p>

Example: Proton and Neutron Decay.

Proton decay is a rare type of radioactive decay of nuclei containing excess protons, in which a proton is simply ejected from the nucleus. Note that, a free proton (a proton

not bound to nucleons or electrons) is a stable particle that has not been observed to break down spontaneously to other particles.

Proton emission occurs in the most proton-rich/neutron-deficient nuclides (prompt proton emission), and also from high-lying excited states in a nucleus following a positive beta decay. Similarly as for neutron emission, the rate of emission of these neutrons following a positive beta decay is governed primarily by beta decay, therefore this emission is known as beta-delayed proton emission.

The mechanism of the decay process is very similar to alpha decay. Proton decay is also a quantum tunneling process. In order to be emitted, the proton must penetrate a potential barrier. For a proton to escape a nucleus, the proton separation energy must be negative – the proton is therefore unbound, and tunnels out of the nucleus in a finite time. Some nuclei decay via double proton emission, such as ^{45}Fe .

If a nucleus decays via proton emission, atomic and mass numbers change by one and a daughter nucleus becomes a different element. Nuclei which can decay by this mode are described as lying highly above the neutron drip line. Proton emission is not seen in naturally occurring isotopes. Proton radioactive isotopes can be produced via nuclear reactions, usually using particle accelerators.

References

- Radioactivity, science: britannica.com, Retrieved 10 June, 2020
- Radioactive-decay, radiation: epa.gov, Retrieved 16 January, 2020
- Giuliani, A.; Poves, A. (2012). “Neutrinoless Double-Beta Decay” (PDF). *Advances in High Energy Physics*. 2012: 1–38. doi:10.1155/2012/857016
- Alpha-decay, science: britannica.com, Retrieved 18 February, 2020
- Gamma-decay, encyclopedia: energyeducation.ca, Retrieved 16 June, 2020
- Proton-decay-proton-emission, nuclear-power-reactor-physics-atomic-nuclear-physics-radioactive-decay: nuclear-power.net, Retrieved 14 July, 2020
- Dorin N Poenaru, Walter Greiner (2011). *Cluster Radioactivity*, Ch. 1 of *Clusters in Nuclei I*. Lecture Notes in Physics 818. Springer, Berlin. pp. 1–56. ISBN 978-3-642-13898-0

Applications of Nuclear Technology

5

CHAPTER

There are a wide range of applications of nuclear technology in the fields of medicine and defense. It is used in gamma camera, fast neutron therapy, radiation therapy, nuclear weapon design and delivery, underground nuclear weapon testing, etc. This chapter discusses the applications of nuclear technology in detail.

MEDICAL APPLICATIONS

Nuclear medicine and radiology are the whole of medical techniques that involve radiation or radioactivity to diagnose, treat and prevent disease. While radiology has been used for close to a century, “nuclear medicine” began approximately 50 years ago. Today, about one-third of all procedures used in modern hospitals involve radiation or radioactivity. These procedures are among the best and most effective life-saving tools available, they are safe and painless and don’t require anesthesia, and they are helpful to a broad span of medical specialties, from pediatrics to cardiology to psychiatry.

While both nuclear medicine and radiology is used in diagnostic procedures (to determine a patient’s health, monitor the course of an illness or follow the progress of treatment) and therapeutic procedures (to treat illnesses), they are implemented differently. In nuclear medicine, radioisotopes are introduced into the body internally, whereas in radiology X-rays penetrate the body from outside the body.

Major Advances in Nuclear Medicine Diagnosis and Treatment

Exploratory surgery used to be the way doctors investigated health problems. Doctors would cut, poke, and prod. But since the 1940’s, nuclear technologies have offered an increasing array of diagnostic techniques that help patients avoid the pain of surgery while their physicians gain knowledge of the body’s inner workings.

X-rays, MRI scanners, CAT scans, and ultrasound each use nuclear science and technology to troubleshoot different parts of the body and diagnose conditions. Each of these are non-invasive procedures, meaning patients do not need to undergo surgery. More advanced nuclear medicine uses computers, detectors, and radioisotopes to give doctors even more information about a patient’s internal workings. Known as nuclear imaging, these procedures include bone scanning, Positron Emission Tomography

(PET), Single Photon Emission Computed Tomography (SPECT) and Cardiovascular Imaging. The use of these procedures depends on the patient's symptoms.

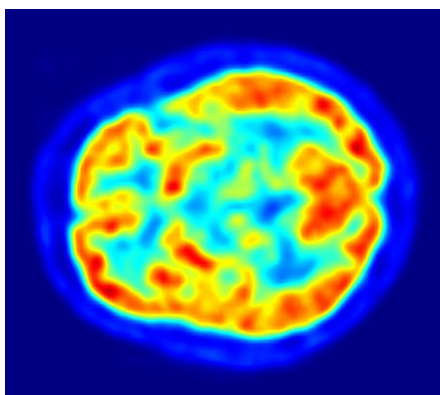
Radioisotopes are useful because the radiation they emit can be located in the body. The isotopes can be administered by injection, inhalation, or orally. A gamma camera captures images from isotopes in the body that emit radiation. Then, computers enhance the image, allowing physicians to detect tumors and fractures, measure blood flow, or determine thyroid and pulmonary functions.

The first radiopharmaceutical to be widely used was the fission product, iodine-131, in the form of the simple salt, sodium iodide. Its use was established in the late forties as a diagnostic test for certain thyroid disorders. Since the drug could be administered orally, in solution, it was referred to in the press as the "Atomic Cocktail".

Scintigraphy

Scintigraphy also known as a gamma scan, is a diagnostic test in nuclear medicine, where radioisotopes attached to drugs that travel to a specific organ or tissue (radiopharmaceuticals) are taken internally and the emitted gamma radiation is captured by external detectors (gamma cameras) to form two-dimensional images in a similar process to the capture of x-ray images. In contrast, SPECT and positron emission tomography (PET) form 3-dimensional images, and are therefore classified as separate techniques to scintigraphy, although they also use gamma cameras to detect internal radiation. Scintigraphy is unlike a diagnostic X-ray where external radiation is passed through the body to form an image.

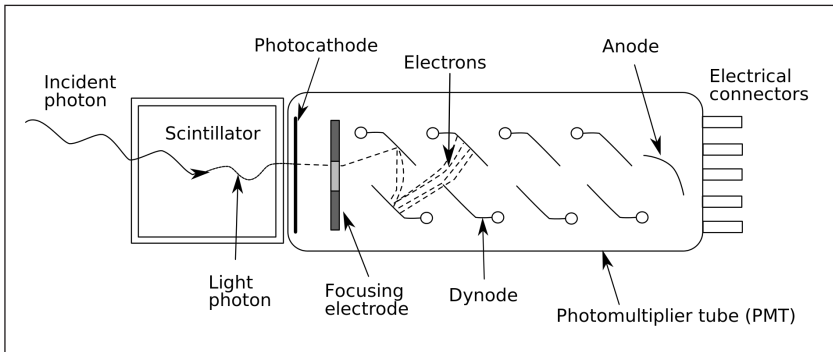
Process



Computer representation of false-color image of a cross section of human brain, based on scintigraphy in Positron-Emission Tomography.

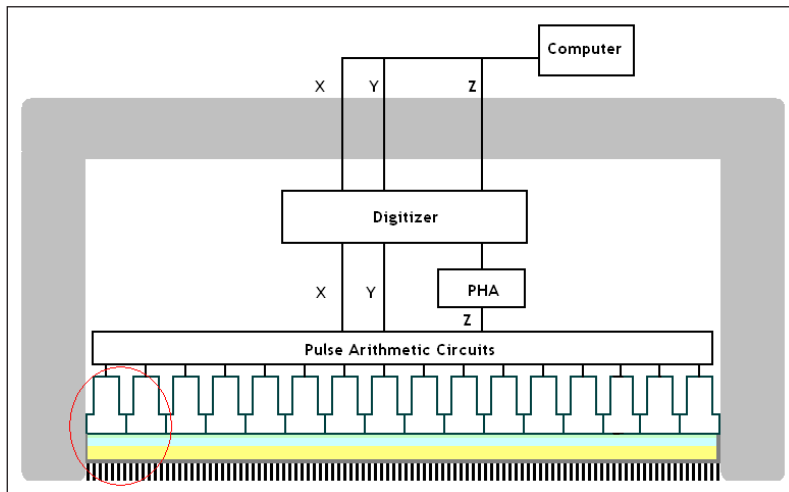
Scintigraphy is an imaging method of nuclear events provoked by collisions or charged current interactions among nuclear particles or ionizing radiation and atoms which result in a brief, localised pulse of electromagnetic radiation, usually in the visible light range (Cherenkov radiation). This pulse (scintillation) is usually detected and

amplified by a photomultiplier or charged coupled device elements, and its resulting electrical waveform is processed by computers to provide two- and three-dimensional images of a subject or region of interest.



Schematic of a photomultiplier tube coupled to a scintillator.

Scintillography is mainly used in scintillation cameras in experimental physics. For example, huge neutrino detection underground tanks filled with tetrachloroethylene are surrounded by arrays of photo detectors in order to capture the extremely rare event of a collision between the fluid's atoms and a neutrino.



Cross section of a gamma camera.

Another extensive use of scintillography is in medical imaging techniques which use gamma ray detectors called gamma cameras. Detectors coated with materials which scintillate when subjected to gamma rays are scanned with optical photon detectors and scintillation counters. The subjects are injected with special radionuclides which irradiate in the gamma range inside the region of interest, such as the heart or the brain. A special type of gamma camera is the SPECT (Single Photon Emission Computed Tomography). Another medical scintillography technique, the Positron-emission tomography (PET), which uses the scintillations provoked by electron-positron annihilation phenomena.

By Organ or Organ System

Biliary System (Cholescintigraphy)

Scintigraphy of the biliary system is called cholescintigraphy and is done to diagnose obstruction of the bile ducts by a gallstone (cholelithiasis), a tumor, or another cause. It can also diagnose gallbladder diseases, e.g. bile leaks or biliary fistulas. In cholescintigraphy, the injected radioactive chemical is taken up by the liver and secreted into the bile. The radiopharmaceutical then goes into the bile ducts, the gallbladder, and the intestines. The gamma camera is placed on the abdomen to picture these perfused organs. Other scintigraphic tests are done similarly.

Lung Scintigraphy



Lung scintigraphy evaluating lung cancer.

The most common indication for lung scintigraphy is to diagnose pulmonary embolism, e.g. with a ventilation/perfusion scan and may be appropriate for excluding PE in pregnancy. Less common indications include evaluation of lung transplantation, pre-operative evaluation, and evaluation of right-to-left shunts.

In the ventilation phase of a ventilation/perfusion scan, a gaseous radionuclide xenon or technetium DTPA in an aerosol form (or ideally using Technegas, a radioaerosol invented in Australia by Dr Bill Burch and Dr Richard Fawdry) is inhaled by the patient through a mouthpiece or mask that covers the nose and mouth. The perfusion phase of the test involves the intravenous injection of radioactive technetium macro aggregated albumin (Tc99m-MAA). A gamma camera acquires the images for both phases of the study.

Bone

For example, the ligand methylene-diphosphonate (MDP) can be preferentially taken up by bone. By chemically attaching technetium-99m to MDP, radioactivity can be transported and attached to bone via the hydroxyapatite for imaging. Any increased physiological function, such as a fracture in the bone, will usually mean increased concentration of the tracer.

Heart

A thallium stress test is a form of scintigraphy, where the amount of thallium-201 detected in cardiac tissues correlates with tissue blood supply. Viable cardiac cells have normal Na^+/K^+ ion exchange pumps. Thallium binds the K^+ pumps and is transported into the cells. Exercise or dipyridamole induces widening (vasodilation) of normal coronary arteries. This produces coronary steal from areas of ischemia where arteries are already maximally dilated. Areas of infarct or ischemic tissue will remain “cold”. Pre- and post-stress thallium may indicate areas that will benefit from myocardial revascularization. Redistribution indicates the existence of coronary steal and the presence of ischemic coronary artery disease.

Parathyroid

Tc99m-sestamibi is used to detect parathyroid adenomas.

Thyroid

To detect metastases/function of thyroid, the isotopes technetium-99m or iodine-123 are generally used, and for this purpose the iodide isotope does not need to be attached to another protein or molecule, because thyroid tissue takes up free iodide actively.

Full Body

Examples are gallium scans, indium white blood cell scans, iobenguane scan (MIBG) and octreotide scans. The MIBG scan detects adrenergic tissue and thus can be used to identify the location of tumors such as pheochromocytomas and neuroblastomas.

Function Tests

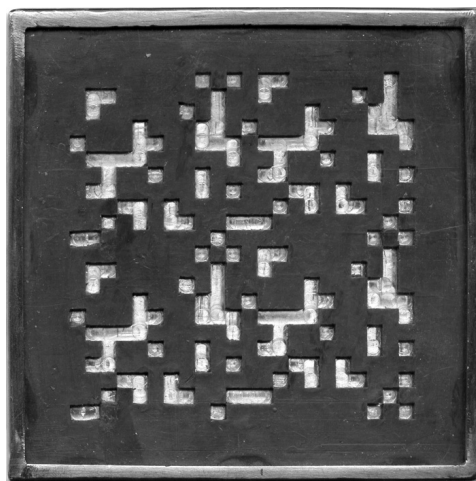
Certain tests, such as the Schilling test and urea breath test, use radioisotopes but are not used to produce a specific image.

Gamma Camera

A gamma camera (γ -camera), also called a scintillation camera or Anger camera, is a device used to image gamma radiation emitting radioisotopes, a technique known

as scintigraphy. The applications of scintigraphy include early drug development and nuclear medical imaging to view and analyse images of the human body or the distribution of medically injected, inhaled, or ingested radionuclides emitting gamma rays.

Imaging Techniques



Coded aperture mask for gamma camera (for SPECT).

Scintigraphy (“scint”) is the use of gamma cameras to capture emitted radiation from internal radioisotopes to create two-dimensional images.

SPECT (single photon emission computed tomography) imaging, as used in nuclear cardiac stress testing, is performed using gamma cameras. Usually one, two or three detectors or heads, are slowly rotated around the patient’s torso.

Multi-headed gamma cameras can also be used for positron emission tomography (PET) scanning, provided that their hardware and software can be configured to detect “coincidences” (near simultaneous events on 2 different heads). Gamma camera PET is markedly inferior to PET imaging with a purpose designed PET scanner, as the scintillator crystal has poor sensitivity for the high-energy annihilation photons, and the detector area is significantly smaller. However, given the low cost of a gamma camera and its additional flexibility compared to a dedicated PET scanner, this technique is useful where the expense and resource implications of a PET scanner cannot be justified.

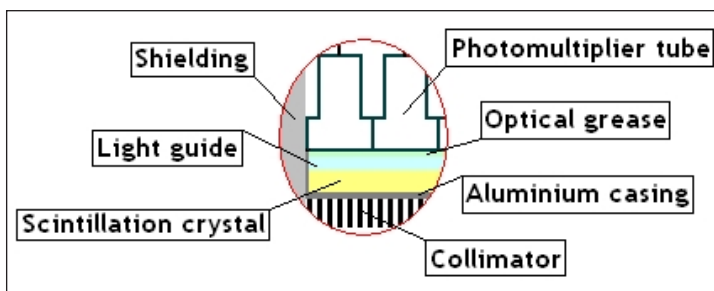
Construction

A gamma camera consists of one or more flat crystal planes (or detectors) optically coupled to an array of photomultiplier tubes in an assembly known as a “head”, mounted on a gantry. The gantry is connected to a computer system that both controls the operation of the camera and acquires and stores images. The construction of a gamma camera is sometimes known as a compartmental radiation construction.



Gamma camera.

The system accumulates events, or counts, of gamma photons that are absorbed by the crystal in the camera. Usually a large flat crystal of sodium iodide with thallium doping in a light-sealed housing is used. The highly efficient capture method of this combination for detecting gamma rays was discovered in 1944 by Sir Samuel Curran whilst he was working on the Manhattan Project at the University of California at Berkeley. Nobel prize-winning physicist Robert Hofstadter also worked on the technique in 1948.



Details of the cross section of a gamma camera.

The crystal scintillates in response to incident gamma radiation. When a gamma photon leaves the patient (who has been injected with a radioactive pharmaceutical), it knocks an electron loose from an iodine atom in the crystal, and a faint flash of light is produced when the dislocated electron again finds a minimal energy state. The initial phenomenon of the excited electron is similar to the photoelectric effect and (particularly with gamma rays) the Compton effect. After the flash of light is produced, it is detected. Photomultiplier tubes (PMTs) behind the crystal detect the fluorescent flashes (events) and a computer sums the counts. The computer reconstructs and displays a two dimensional image of the relative spatial count density on a monitor. This reconstructed image reflects the distribution and relative concentration of radioactive tracer elements present in the organs and tissues imaged.

Signal Processing

Hal Anger developed the first gamma camera in 1957. His original design, frequently called the Anger camera, is still widely used today. The Anger camera uses sets of

vacuum tube photomultipliers (PMT). Generally each tube has an exposed face of about 7.6 cm in diameter and the tubes are arranged in hexagon configurations, behind the absorbing crystal. The electronic circuit connecting the photodetectors is wired so as to reflect the relative coincidence of light fluorescence as sensed by the members of the hexagon detector array. All the PMTs simultaneously detect the (presumed) same flash of light to varying degrees, depending on their position from the actual individual event. Thus the spatial location of each single flash of fluorescence is reflected as a pattern of voltages within the interconnecting circuit array.

The location of the interaction between the gamma ray and the crystal can be determined by processing the voltage signals from the photomultipliers; in simple terms, the location can be found by weighting the position of each photomultiplier tube by the strength of its signal, and then calculating a mean position from the weighted positions. The total sum of the voltages from each photomultiplier, measured by a pulse height analyzer is proportional to the energy of the gamma ray interaction, thus allowing discrimination between different isotopes or between scattered and direct photons.

Spatial Resolution

In order to obtain spatial information about the gamma-ray emissions from an imaging subject (e.g. a person's heart muscle cells which have absorbed an intravenous injected radioactive, usually thallium-201 or technetium-99m, medicinal imaging agent) a method of correlating the detected photons with their point of origin is required.

The conventional method is to place a collimator over the detection crystal/PMT array. The collimator consists of a thick sheet of lead, typically 25 to 75 millimetres (1 to 3 in) thick, with thousands of adjacent holes through it. The individual holes limit photons which can be detected by the crystal to a cone; the point of the cone is at the midline center of any given hole and extends from the collimator surface outward. However, the collimator is also one of the sources of blurring within the image; lead does not totally attenuate incident gamma photons, there can be some crosstalk between holes.

Unlike a lens, as used in visible light cameras, the collimator attenuates most (>99%) of incident photons and thus greatly limits the sensitivity of the camera system. Large amounts of radiation must be present so as to provide enough exposure for the camera system to detect sufficient scintillation dots to form a picture.

Other methods of image localization (pinhole, rotating slat collimator with CZT) have been proposed and tested; however, none have entered widespread routine clinical use.

The best current camera system designs can differentiate two separate point sources of gamma photons located at 6 to 12 mm depending on distance from the collimator, the type of collimator and radio-nuclide. Spatial resolution decreases rapidly at increasing distances from the camera face. This limits the spatial accuracy of the computer image: it is a fuzzy image made up of many dots of detected but not precisely located

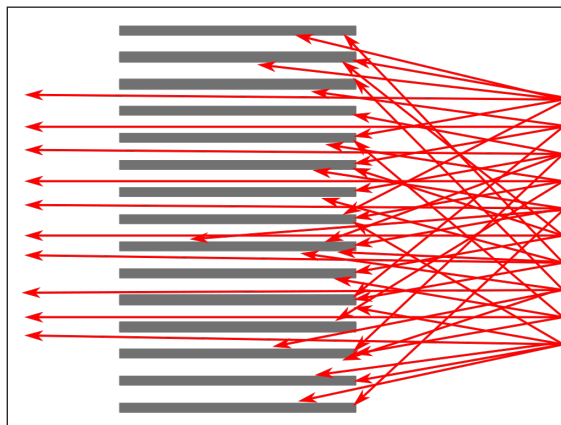
scintillation. This is a major limitation for heart muscle imaging systems; the thickest normal heart muscle in the left ventricle is about 1.2 cm and most of the left ventricle muscle is about 0.8 cm, always moving and much of it beyond 5 cm from the collimator face. To help compensate, better imaging systems limit scintillation counting to a portion of the heart contraction cycle, called gating, however this further limits system sensitivity.

Single-photon Emission (SPECT)

Single-photon emission computed tomography (SPECT, or less commonly, SPET) is a nuclear medicine tomographic imaging technique using gamma rays. It is very similar to conventional nuclear medicine planar imaging using a gamma camera (that is, scintigraphy), but is able to provide true 3D information. This information is typically presented as cross-sectional slices through the patient, but can be freely reformatted or manipulated as required.

The technique needs delivery of a gamma-emitting radioisotope (a radionuclide) into the patient, normally through injection into the bloodstream. On occasion, the radioisotope is a simple soluble dissolved ion, such as an isotope of gallium (III). Most of the time, though, a marker radioisotope is attached to a specific ligand to create a radioligand, whose properties bind it to certain types of tissues. This marriage allows the combination of ligand and radiopharmaceutical to be carried and bound to a place of interest in the body, where the ligand concentration is seen by a gamma camera.

Principles



Collimator used to collimate gamma rays (red arrows) in a gamma camera.

Instead of just “taking a picture of anatomical structures”, a SPECT scan monitors level of biological activity at each place in the 3-D region analyzed. Emissions from the radionuclide indicate amounts of blood flow in the capillaries of the imaged regions. In the same way that a plain X-ray is a 2-dimensional (2-D) view of a 3-dimensional structure, the image obtained by a gamma camera is a 2-D view of 3-D distribution of a radionuclide.



SPECT scanner, consisting of two gamma cameras.

SPECT imaging is performed by using a gamma camera to acquire multiple 2-D images (also called projections), from multiple angles. A computer is then used to apply a tomographic reconstruction algorithm to the multiple projections, yielding a 3-D data set. This data set may then be manipulated to show thin slices along any chosen axis of the body, similar to those obtained from other tomographic techniques, such as magnetic resonance imaging (MRI), X-ray computed tomography (X-ray CT), and positron emission tomography (PET).

SPECT is similar to PET in its use of radioactive tracer material and detection of gamma rays. In contrast with PET, the tracers used in SPECT emit gamma radiation that is measured directly, whereas PET tracers emit positrons that annihilate with electrons up to a few millimeters away, causing two gamma photons to be emitted in opposite directions. A PET scanner detects these emissions “coincident” in time, which provides more radiation event localization information and, thus, higher spatial resolution images than SPECT (which has about 1 cm resolution). SPECT scans are significantly less expensive than PET scans, in part because they are able to use longer-lived and more easily obtained radioisotopes than PET.



SPECT machine performing a total body bone scan. The patient lies on a table that slides through the machine, while a pair of gamma cameras rotates around her.

Because SPECT acquisition is very similar to planar gamma camera imaging, the same radiopharmaceuticals may be used. If a patient is examined in another type of nuclear

medicine scan, but the images are non-diagnostic, it may be possible to proceed straight to SPECT by moving the patient to a SPECT instrument, or even by simply reconfiguring the camera for SPECT image acquisition while the patient remains on the table.

To acquire SPECT images, the gamma camera is rotated around the patient. Projections are acquired at defined points during the rotation, typically every 3–6 degrees. In most cases, a full 360-degree rotation is used to obtain an optimal reconstruction. The time taken to obtain each projection is also variable, but 15–20 seconds is typical. This gives a total scan time of 15–20 minutes.

Multi-headed gamma cameras can accelerate acquisition. For example, a dual-headed camera can be used with heads spaced 180 degrees apart, allowing two projections to be acquired simultaneously, with each head requiring 180 degrees of rotation. Triple-head cameras with 120-degree spacing are also used.

Cardiac gated acquisitions are possible with SPECT, just as with planar imaging techniques such as multi gated acquisition scan (MUGA). Triggered by electrocardiogram (EKG) to obtain differential information about the heart in various parts of its cycle, gated myocardial SPECT can be used to obtain quantitative information about myocardial perfusion, thickness, and contractility of the myocardium during various parts of the cardiac cycle, and also to allow calculation of left ventricular ejection fraction, stroke volume, and cardiac output.

Application

SPECT can be used to complement any gamma imaging study, where a true 3D representation can be helpful, such as tumor imaging, infection (leukocyte) imaging, thyroid imaging or bone scintigraphy.

Because SPECT permits accurate localisation in 3D space, it can be used to provide information about localised function in internal organs, such as functional cardiac or brain imaging.

Myocardial Perfusion Imaging

Myocardial perfusion imaging (MPI) is a form of functional cardiac imaging, used for the diagnosis of ischemic heart disease. The underlying principle is that under conditions of stress, diseased myocardium receives less blood flow than normal myocardium. MPI is one of several types of cardiac stress test.

A cardiac specific radiopharmaceutical is administered, e.g., ^{99m}Tc -tetrofosmin (Myoview, GE healthcare), ^{99m}Tc -sestamibi (Cardiolite, Bristol-Myers Squibb) or Thallium-201 chloride. Following this, the heart rate is raised to induce myocardial stress, either by exercise on a treadmill or pharmacologically with adenosine, dobutamine, or dipyridamole (aminophylline can be used to reverse the effects of dipyridamole).

SPECT imaging performed after stress reveals the distribution of the radiopharmaceutical, and therefore the relative blood flow to the different regions of the myocardium. Diagnosis is made by comparing stress images to a further set of images obtained at rest which are normally acquired prior to the stress images.

MPI has been demonstrated to have an overall accuracy of about 83% (sensitivity: 85%; specificity: 72%), and is comparable with (or better than) other non-invasive tests for ischemic heart disease.

Functional Brain Imaging

Usually, the gamma-emitting tracer used in functional brain imaging is ^{99m}Tc -HMPAO (hexamethylpropylene amine oxime). ^{99m}Tc is a metastable nuclear isomer that emits gamma rays that can be detected by a gamma camera. Attaching it to HMPAO allows ^{99m}Tc to be taken up by brain tissue in a manner proportional to brain blood flow, in turn allowing cerebral blood flow to be assessed with the nuclear gamma camera.

Because blood flow in the brain is tightly coupled to local brain metabolism and energy use, the ^{99m}Tc -HMPAO tracer (as well as the similar ^{99m}Tc -EC tracer) is used to assess brain metabolism regionally, in an attempt to diagnose and differentiate the different causal pathologies of dementia. Meta-analysis of many reported studies suggests that SPECT with this tracer is about 74% sensitive at diagnosing Alzheimer's disease vs. 81% sensitivity for clinical exam (cognitive testing, etc). More recent studies have shown the accuracy of SPECT in Alzheimer's diagnosis may be as high as 88%. In meta-analysis, SPECT was superior to clinical exam and clinical criteria (91% vs. 70%) in being able to differentiate Alzheimer's disease from vascular dementias. This latter ability relates to SPECT's imaging of local metabolism of the brain, in which the patchy loss of cortical metabolism seen in multiple strokes differs clearly from the more even or "smooth" loss of non-occipital cortical brain function typical of Alzheimer's disease.

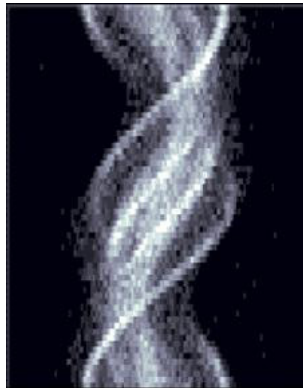
^{99m}Tc -HMPAO SPECT scanning competes with fludeoxyglucose (FDG) PET scanning of the brain, which works to assess regional brain glucose metabolism, to provide very similar information about local brain damage from many processes. SPECT is more widely available, because the radioisotope used is longer-lasting and far less expensive in SPECT, and the gamma scanning equipment is less expensive as well. While ^{99m}Tc is extracted from relatively simple technetium-99m generators, which are delivered to hospitals and scanning centers weekly to supply fresh radioisotope, FDG PET relies on FDG, which is made in an expensive medical cyclotron and "hot-lab" (automated chemistry lab for radiopharmaceutical manufacture), and then delivered immediately to scanning sites because of the natural short 110-minute half-life of Fluorine-18.

Applications in Nuclear Technology

In the nuclear power sector, the SPECT technique can be applied to image radioisotope distributions in irradiated nuclear fuels. Due to the irradiation of nuclear fuel

(e.g. uranium) with neutrons in a nuclear reactor, a wide array of gamma-emitting radionuclides are naturally produced in the fuel, such as fission products (cesium-137, barium-140 and europium-154) and activation products (chromium-51 and cobalt-58). These may be imaged using SPECT in order to verify the presence of fuel rods in a stored fuel assembly for IAEA safeguards purposes, to validate predictions of core simulation codes or to study the behavior of the nuclear fuel in normal operation or in accident scenarios.

Reconstruction



SPECT Sinogram.

Reconstructed images typically have resolutions of 64×64 or 128×128 pixels, with the pixel sizes ranging from 3–6 mm. The number of projections acquired is chosen to be approximately equal to the width of the resulting images. In general, the resulting reconstructed images will be of lower resolution, have increased noise than planar images, and be susceptible to artifacts.

Scanning is time consuming, and it is essential that there is no patient movement during the scan time. Movement can cause significant degradation of the reconstructed images, although movement compensation reconstruction techniques can help with this. A highly uneven distribution of radiopharmaceutical also has the potential to cause artifacts. A very intense area of activity (e.g., the bladder) can cause extensive streaking of the images and obscure neighboring areas of activity. This is a limitation of the filtered back projection reconstruction algorithm. Iterative reconstruction is an alternative algorithm that is growing in importance, as it is less sensitive to artifacts and can also correct for attenuation and depth dependent blurring. Furthermore, iterative algorithms can be made more efficacious using the Superiorization methodology.

Attenuation of the gamma rays within the patient can lead to significant underestimation of activity in deep tissues, compared to superficial tissues. Approximate correction is possible, based on relative position of the activity, and optimal correction is obtained with measured attenuation values. Modern SPECT equipment is available with an integrated X-ray CT scanner. As X-ray CT images are an attenuation map of the tissues, this

data can be incorporated into the SPECT reconstruction to correct for attenuation. It also provides a precisely registered CT image, which can provide additional anatomical information.

Scatter of the gamma rays as well as the random nature of gamma rays can also lead to the degradation of quality of SPECT images and cause loss of resolution. Scatter correction and resolution recovery are also applied to improve resolution of SPECT images.

SPECT/CT

In some cases a SPECT gamma scanner may be built to operate with a conventional CT scanner, with coregistration of images. As in PET/CT, this allows location of tumors or tissues which may be seen on SPECT scintigraphy, but are difficult to locate precisely with regard to other anatomical structures. Such scans are most useful for tissues outside the brain, where location of tissues may be far more variable. For example, SPECT/CT may be used in sestamibi parathyroid scan applications, where the technique is useful in locating ectopic parathyroid adenomas which may not be in their usual locations in the thyroid gland.

Quality Control

The overall performance of SPECT systems can be performed by quality control tools such as the Jaszczak phantom.

Positron-emission Tomography (PET)

Positron-emission tomography (PET) is a nuclear medicine functional imaging technique that is used to observe metabolic processes in the body as an aid to the diagnosis of disease. The system detects pairs of gamma rays emitted indirectly by a positron-emitting radioligand, most commonly fluorine-18, which is introduced into the body on a biologically active molecule called a radioactive tracer. Different ligands are used for different imaging purposes, depending on what the radiologist/researcher wants to detect. Three-dimensional images of tracer concentration within the body are then constructed by computer analysis. In modern PET computed tomography scanners, three-dimensional imaging is often accomplished with the aid of a computed tomography X-ray scan performed on the patient during the same session, in the same machine.

If the biologically active tracer molecule chosen for PET is fluorodeoxyglucose (FDG), an analogue of glucose, the concentrations of tracer imaged will indicate tissue metabolic activity as it corresponds to the regional glucose uptake. Use of this tracer to explore the possibility of cancer metastasis (i.e., spreading to other sites) is the most common type of PET scan in standard medical care (representing 90% of current scans). Metabolic trapping of the radioactive glucose molecule allows the PET scan to be utilized. The

same tracer may also be used for PET investigation and diagnosis of types of dementia. Less often, other radioactive tracers, usually but not always labeled with fluorine-18, are used to image the tissue concentration of other types of molecules of interest.

One of the disadvantages of PET scanners is their operating cost. A similar imaging process to PET is single-photon emission computed tomography (SPECT), which also uses radioligands to detect molecules in the brain, and is less expensive.

PET is both a medical and research tool. It is used heavily in clinical oncology (medical imaging of tumours and the search for metastases), and for clinical diagnosis of certain diffuse brain diseases such as those causing various types of dementias. PET is also an important research tool to map normal human brain and heart function, and support drug development.

PET is also used in pre-clinical studies using animals, where it allows repeated investigations into the same subjects. This is particularly valuable in cancer research, as it results in an increase in the statistical quality of the data (subjects can act as their own control) and substantially reduces the numbers of animals required for a given study.



PET/CT-System with 16-slice CT; the ceiling mounted device is an injection pump for CT contrast agent.

Alternative methods of scanning include x-ray computed tomography (CT), magnetic resonance imaging (MRI) and functional magnetic resonance imaging (fMRI), ultrasound and single-photon emission computed tomography (SPECT).

While some imaging scans such as CT and MRI isolate organic anatomic changes in the body, PET and SPECT are capable of detecting areas of molecular biology detail (even prior to anatomic change). PET scanning does these using radiolabelled molecular probes that have different rates of uptake depending on the type and function of tissue involved. Changing of regional blood flow in various anatomic structures (as a measure of the injected positron emitter) can be visualized and relatively quantified with a PET scan.

PET imaging is best performed using a dedicated PET scanner. It is also possible to acquire PET images using a conventional dual-head gamma camera fitted with a coincidence detector. Although the quality of gamma-camera PET is considerably lower and acquisition is slower, this method allows institutions with low demand for PET to provide on-site imaging, instead of referring patients to another centre or relying on a visit by a mobile scanner.

Oncology

PET scanning with the tracer fluorine-18 (^{18}F) fluorodeoxyglucose (FDG), called FDG-PET, is widely used in clinical oncology. This tracer is a glucose analog that is taken up by glucose-using cells and phosphorylated by hexokinase (whose mitochondrial form is greatly elevated in rapidly growing malignant tumors). A typical dose of FDG used in an oncological scan has an effective radiation dose of 7.6 mSv. Because the hydroxyl group that is replaced by fluorine-18 to generate FDG is required for the next step in glucose metabolism in all cells, no further reactions occur in FDG. Furthermore, most tissues (with the notable exception of liver and kidneys) cannot remove the phosphate added by hexokinase. This means that FDG is trapped in any cell that takes it up until it decays, since phosphorylated sugars, due to their ionic charge, cannot exit from the cell. This results in intense radiolabeling of tissues with high glucose uptake, such as the normal brain, liver, kidneys, and most cancers. As a result, FDG-PET can be used for diagnosis, staging, and monitoring treatment of cancers, particularly in Hodgkin's lymphoma, non-Hodgkin lymphoma, and lung cancer.

A few other isotopes and radiotracers are slowly being introduced into oncology for specific purposes. For example, ^{11}C -labelled metomidate (^{11}C -metomidate), has been used to detect tumors of adrenocortical origin. Also, FDOPA PET/CT (or F-18-DOPA PET/CT), in centers which offer it, has proven to be a more sensitive alternative to finding, and also localizing, pheochromocytoma than the MIBG scan.

Neuroimaging

1. Neurology: PET neuroimaging is based on an assumption that areas of high radioactivity are associated with brain activity. What is actually measured indirectly is the flow of blood to different parts of the brain, which is, in general, believed to be correlated, and has been measured using the tracer oxygen-15. Because of its 2-minute half-life, O-15 must be piped directly from a medical cyclotron for such uses, which is difficult.

Examples:

- In practice, since the brain is normally a rapid user of glucose, and since brain pathologies such as Alzheimer's disease greatly decrease brain metabolism of both glucose and oxygen in tandem, standard FDG-PET of the brain, which measures regional glucose use, may also be successfully used to differentiate Alzheimer's disease from other dementing processes, and also to make early

diagnoses of Alzheimer's disease. The advantage of FDG-PET for these uses is its much wider availability. Some radioactive tracers used for Alzheimer's are florbetapir F18, flutemetamol F18, and florbetabenF18, which are all used to detect amyloid-beta plaques (a potential biomarker for Alzheimer's) in the brain.

- PET imaging with FDG can also be used for localization of seizure focus: A seizure focus will appear as hypometabolic during an interictal scan. Several radiotracers (i.e. radioligands) have been developed for PET that are ligands for specific neuroreceptor subtypes such as [¹¹C] raclopride, [¹⁸F] fallypride and [¹⁸F] desmethoxyfallypride for dopamine D2/D3 receptors, [¹¹C] McN 5652 and [¹¹C] DASB for serotonin transporters, [¹⁸F] Mefway for serotonin 5HT1A receptors, [¹⁸F] Nifene for nicotinic acetylcholine receptors or enzyme substrates (e.g. 6-FDOPA for the AADC enzyme). These agents permit the visualization of neuroreceptor pools in the context of a plurality of neuropsychiatric and neurologic illnesses.

The development of a number of novel probes for noninvasive, in vivo PET imaging of neuroaggregate in human brain has brought amyloid imaging to the doorstep of clinical use. The earliest amyloid imaging probes included 2-(1-{6-[(2-[¹⁸F] fluoroethyl)(methyl)amino]-2-naphthyl}ethylidene)malononitrile ([¹⁸F]FDDNP) developed at the University of California, Los Angeles and N-methyl-[¹¹C]2-(4'-methylaminophenyl)-6-hydroxybenzothiazole (termed Pittsburgh compound B) developed at the University of Pittsburgh. These amyloid imaging probes permit the visualization of amyloid plaques in the brains of Alzheimer's patients and could assist clinicians in making a positive clinical diagnosis of AD pre-mortem and aid in the development of novel anti-amyloid therapies. [¹¹C]PMP (N-[¹¹C] methylpiperidin-4-yl propionate) is a novel radiopharmaceutical used in PET imaging to determine the activity of the acetylcholinergic neurotransmitter system by acting as a substrate for acetylcholinesterase. Post-mortem examinations of AD patients have shown decreased levels of acetylcholinesterase. [¹¹C] PMP is used to map the acetylcholinesterase activity in the brain, which could allow for pre-mortem diagnoses of AD and help to monitor AD treatments. Avid Radiopharmaceuticals has developed and commercialized a compound called florbetapir that uses the longer-lasting radionuclide fluorine-18 to detect amyloid plaques using PET scans.

2. Neuropsychology/Cognitive neuroscience: To examine links between specific psychological processes or disorders and brain activity.

3. Psychiatry: Numerous compounds that bind selectively to neuroreceptors of interest in biological psychiatry have been radiolabeled with C-11 or F-18. Radioligands that bind to dopamine receptors (D1, D2 receptor, and reuptake transporter), serotonin receptors (5HT1A, 5HT2A, reuptake transporter) opioid receptors (mu) and other sites have been used successfully in studies with human subjects. Studies have been performed examining the state of these receptors in patients compared to healthy controls in schizophrenia, substance abuse, mood disorders and other psychiatric conditions.

4. Stereotactic surgery and radiosurgery: PET-image guided surgery facilitates treatment of intracranial tumors, arteriovenous malformations and other surgically treatable conditions.

Cardiology

Cardiology, atherosclerosis and vascular disease study: In clinical cardiology, FDG-PET can identify so-called “hibernating myocardium”, but its cost-effectiveness in this role versus SPECT is unclear. FDG-PET imaging of atherosclerosis to detect patients at risk of stroke is also feasible and can help test the efficacy of novel anti-atherosclerosis therapies.

Infectious Diseases

Imaging infections with molecular imaging technologies can improve diagnosis and treatment follow-up. PET has been widely used to image bacterial infections clinically by using fluorodeoxyglucose (FDG) to identify the infection-associated inflammatory response.

Three different PET contrast agents have been developed to image bacterial infections *in vivo*: [^{18}F] maltose, [^{18}F]maltohexaose and [^{18}F]2-fluorodeoxysorbitol (FDS). FDS has also the added benefit of being able to target only Enterobacteriaceae.

Pharmacokinetics

Pharmacokinetics: In pre-clinical trials, it is possible to radiolabel a new drug and inject it into animals. Such scans are referred to as biodistribution studies. The uptake of the drug, the tissues in which it concentrates, and its eventual elimination, can be monitored far more quickly and cost effectively than the older technique of killing and dissecting the animals to discover the same information. Much more commonly, drug occupancy at a purported site of action can be inferred indirectly by competition studies between unlabeled drug and radiolabeled compounds known *a priori* to bind with specificity to the site. A single radioligand can be used this way to test many potential drug candidates for the same target. A related technique involves scanning with radioligands that compete with an endogenous (naturally occurring) substance at a given receptor to demonstrate that a drug causes the release of the natural substance.

Small Animal Imaging

PET technology for small animal imaging: A miniature PE tomograph has been constructed that is small enough for a fully conscious and mobile rat to wear on its head while walking around. This RatCAP (Rat Conscious Animal PET) allows animals to be scanned without the confounding effects of anesthesia. PET scanners designed specifically for imaging rodents, often referred to as microPET, as well as scanners for small

primates, are marketed for academic and pharmaceutical research. The scanners are apparently based on microminiature scintillators and amplified avalanche photodiodes (APDs) through a new system recently invented uses single chip silicon photomultipliers.

In 2018 the UC Davis School of Veterinary Medicine became the first veterinary center to employ a small clinical PET-scanner as a pet-PET scan, for clinical (rather than research) animal diagnosis. Because of cost as well as the marginal utility of detecting cancer metastases in companion animals (the primary use of this modality), veterinary PET scanning is expected to be rarely available in the immediate future.

Musculo-skeletal Imaging

Musculoskeletal imaging: PET has been shown to be a feasible technique for studying skeletal muscles during exercises like walking. One of the main advantages of using PET is that it can also provide muscle activation data about deeper lying muscles such as the vastus intermedialis and the gluteus minimus, as compared to other muscle studying techniques like electromyography, which can be used only on superficial muscles (i.e., directly under the skin). A clear disadvantage is that PET provides no timing information about muscle activation because it has to be measured after the exercise is completed. This is due to the time it takes for FDG to accumulate in the activated muscles.

Safety

PET scanning is non-invasive, but it does involve exposure to ionizing radiation.

^{18}F -FDG, which is now the standard radiotracer used for PET neuroimaging and cancer patient management, has an effective radiation dose of 14 mSv.

The amount of radiation in ^{18}F -FDG is similar to the effective dose of spending one year in the American city of Denver, Colorado (12.4 mSv/year). For comparison, radiation dosage for other medical procedures range from 0.02 mSv for a chest x-ray and 6.5–8 mSv for a CT scan of the chest. Average civil aircrews are exposed to 3 mSv/year, and the whole body occupational dose limit for nuclear energy workers in the USA is 50mSv/year.

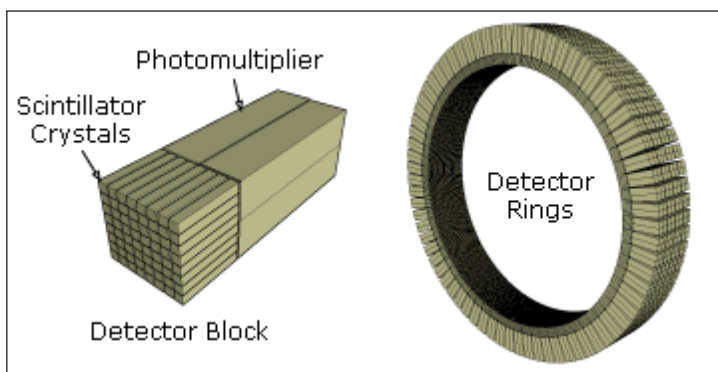
For PET-CT scanning, the radiation exposure may be substantial—around 23–26 mSv (for a 70 kg person—dose is likely to be higher for higher body weights).

Operation

Radionuclides and Radiotracers

Radionuclides used in PET scanning are typically isotopes with short half-lives such as carbon-11 (~20 min), nitrogen-13 (~10 min), oxygen-15 (~2 min), fluorine-18 (~110

min), gallium-68 (~67 min), zirconium-89 (~78.41 hours), or rubidium-82 (~1.27 min). These radionuclides are incorporated either into compounds normally used by the body such as glucose (or glucose analogues), water, or ammonia, or into molecules that bind to receptors or other sites of drug action. Such labelled compounds are known as radiotracers. PET technology can be used to trace the biologic pathway of any compound in living humans (and many other species as well), provided it can be radiolabeled with a PET isotope. Thus, the specific processes that can be probed with PET are virtually limitless, and radiotracers for new target molecules and processes are continuing to be synthesized; as of this writing there are already dozens in clinical use and hundreds applied in research. At present, by far the most commonly used radiotracer in clinical PET scanning is fluorodeoxyglucose (also called FDG or fludeoxyglucose), an analogue of glucose that is labeled with fluorine-18. This radiotracer is used in essentially all scans for oncology and most scans in neurology, and thus makes up the large majority of all of the radiotracer (> 95%) used in PET and PET-CT scanning.

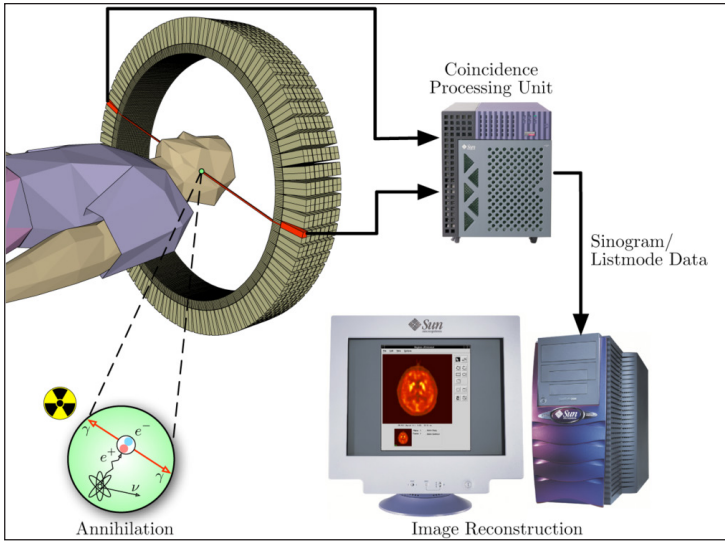


Schematic view of a detector block and ring of a PET scanner.

Due to the short half-lives of most positron-emitting radioisotopes, the radiotracers have traditionally been produced using a cyclotron in close proximity to the PET imaging facility. The half-life of fluorine-18 is long enough that radiotracers labeled with fluorine-18 can be manufactured commercially at offsite locations and shipped to imaging centers. Recently rubidium-82 generators have become commercially available. These contain strontium-82, which decays by electron capture to produce positron-emitting rubidium-82.

Emission

To conduct the scan, a short-lived radioactive tracer isotope is injected into the living subject (usually into blood circulation). Each tracer atom has been chemically incorporated into a biologically active molecule. There is a waiting period while the active molecule becomes concentrated in tissues of interest; then the subject is placed in the imaging scanner. The molecule most commonly used for this purpose is F-18 labeled fluorodeoxyglucose (FDG), a sugar, for which the waiting period is typically an hour. During the scan, a record of tissue concentration is made as the tracer decays.



Schema of a PET acquisition process.

As the radioisotope undergoes positron emission decay (also known as positive beta decay), it emits a positron, an antiparticle of the electron with opposite charge. The emitted positron travels in tissue for a short distance (typically less than 1 mm, but dependent on the isotope), during which time it loses kinetic energy, until it decelerates to a point where it can interact with an electron. The encounter annihilates both electron and positron, producing a pair of annihilation (gamma) photons moving in approximately opposite directions. These are detected when they reach a scintillator in the scanning device, creating a burst of light which is detected by photomultiplier tubes or silicon avalanche photodiodes (Si APD). The technique depends on simultaneous or coincident detection of the pair of photons moving in approximately opposite directions (they would be exactly opposite in their center of mass frame, but the scanner has no way to know this, and so has a built-in slight direction-error tolerance). Photons that do not arrive in temporal “pairs” (i.e. within a timing-window of a few nanoseconds) are ignored.

Localization of the Positron Annihilation Event

The most significant fraction of electron–positron annihilations results in two 511 keV gamma photons being emitted at almost 180 degrees to each other; hence, it is possible to localize their source along a straight line of coincidence (also called the line of response, or LOR). In practice, the LOR has a non-zero width as the emitted photons are not exactly 180 degrees apart. If the resolving time of the detectors is less than 500 picoseconds rather than about 10 nanoseconds, it is possible to localize the event to a segment of a chord, whose length is determined by the detector timing resolution. As the timing resolution improves, the signal-to-noise ratio (SNR) of the image will improve, requiring fewer events to achieve the same image quality. This technology is not yet common, but it is available on some new systems.

Image Reconstruction

The raw data collected by a PET scanner are a list of ‘coincidence events’ representing near-simultaneous detection (typically, within a window of 6 to 12 nanoseconds of each other) of annihilation photons by a pair of detectors. Each coincidence event represents a line in space connecting the two detectors along which the positron emission occurred (i.e., the line of response (LOR)).

Analytical techniques, much like the reconstruction of computed tomography (CT) and single-photon emission computed tomography (SPECT) data, are commonly used, although the data set collected in PET is much poorer than CT, so reconstruction techniques are more difficult. Coincidence events can be grouped into projection images, called sinograms. The sinograms are sorted by the angle of each view and tilt (for 3D images). The sinogram images are analogous to the projections captured by computed tomography (CT) scanners, and can be reconstructed in a similar way. The statistics of data thereby obtained are much worse than those obtained through transmission tomography. A normal PET data set has millions of counts for the whole acquisition, while the CT can reach a few billion counts. This contributes to PET images appearing “noisier” than CT. Two major sources of noise in PET are scatter (a detected pair of photons, at least one of which was deflected from its original path by interaction with matter in the field of view, leading to the pair being assigned to an incorrect LOR) and random events (photons originating from two different annihilation events but incorrectly recorded as a coincidence pair because their arrival at their respective detectors occurred within a coincidence timing window).

In practice, considerable pre-processing of the data is required—correction for random coincidences, estimation and subtraction of scattered photons, detector dead-time correction (after the detection of a photon, the detector must “cool down” again) and detector-sensitivity correction (for both inherent detector sensitivity and changes in sensitivity due to angle of incidence).

Filtered back projection (FBP) has been frequently used to reconstruct images from the projections. This algorithm has the advantage of being simple while having a low requirement for computing resources. Disadvantages are that shot noise in the raw data is prominent in the reconstructed images, and areas of high tracer uptake tend to form streaks across the image. Also, FBP treats the data deterministically—it does not account for the inherent randomness associated with PET data, thus requiring all the pre-reconstruction corrections.

1. Statistical, likelihood-based approaches: Statistical, likelihood-based iterative expectation-maximization algorithms such as the Shepp-Vardi algorithm are now the preferred method of reconstruction. These algorithms compute an estimate of the likely distribution of annihilation events that led to the measured data, based on statistical principles. The advantage is a better noise profile and resistance to the streak artifacts common with FBP, but the disadvantage is higher computer resource requirements.

A further advantage of statistical image reconstruction techniques is that the physical effects that would need to be pre-corrected for when using an analytical reconstruction algorithm, such as scattered photons, random coincidences, attenuation and detector dead-time, can be incorporated into the likelihood model being used in the reconstruction, allowing for additional noise reduction. Iterative reconstruction has also been shown to result in improvements in the resolution of the reconstructed images, since more sophisticated models of the scanner Physics can be incorporated into the likelihood model than those used by analytical reconstruction methods, allowing for improved quantification of the radioactivity distribution.

Research has shown that Bayesian methods that involve a Poisson likelihood function and an appropriate prior probability (e.g., a smoothing prior leading to total variation regularization or a Laplacian distribution leading to ℓ_1 -based regularization in a wavelet or other domain), such as via Ulf Grenander's Sieve estimator or via Bayes penalty methods or via I.J. Good's roughness method may yield superior performance to expectation-maximization-based methods which involve a Poisson likelihood function but do not involve such a prior.

2. Attenuation correction: Quantitative PET Imaging requires attenuation correction. In these systems attenuation correction is based on a transmission scan using ^{68}Ge rotating rod source.

Transmission scans directly measure attenuation values at 511keV. Attenuation occurs when photons emitted by the radiotracer inside the body are absorbed by intervening tissue between the detector and the emission of the photon. As different LORs must traverse different thicknesses of tissue, the photons are attenuated differentially. The result is that structures deep in the body are reconstructed as having falsely low tracer uptake. Contemporary scanners can estimate attenuation using integrated x-ray CT equipment, in place of earlier equipment that offered a crude form of CT using a gamma ray (positron emitting) source and the PET detectors.

While attenuation-corrected images are generally more faithful representations, the correction process is itself susceptible to significant artifacts. As a result, both corrected and uncorrected images are always reconstructed and read together.

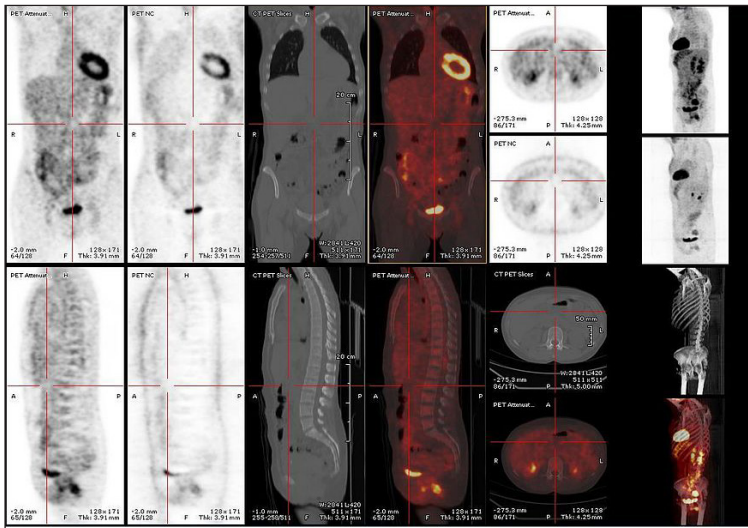
3. 2D/3D reconstruction: Early PET scanners had only a single ring of detectors; hence the acquisition of data and subsequent reconstruction was restricted to a single transverse plane. More modern scanners now include multiple rings, essentially forming a cylinder of detectors.

There are two approaches to reconstructing data from such a scanner: 1) treat each ring as a separate entity, so that only coincidences within a ring are detected, the image from each ring can then be reconstructed individually (2D reconstruction), or 2) allow coincidences to be detected between rings as well as within rings, then reconstruct the entire volume together (3D).

3D techniques have better sensitivity (because more coincidences are detected and used) and therefore less noise, but are more sensitive to the effects of scatter and random coincidences, as well as requiring correspondingly greater computer resources. The advent of sub-nanosecond timing resolution detectors affords better random coincidence rejection, thus favoring 3D image reconstruction.

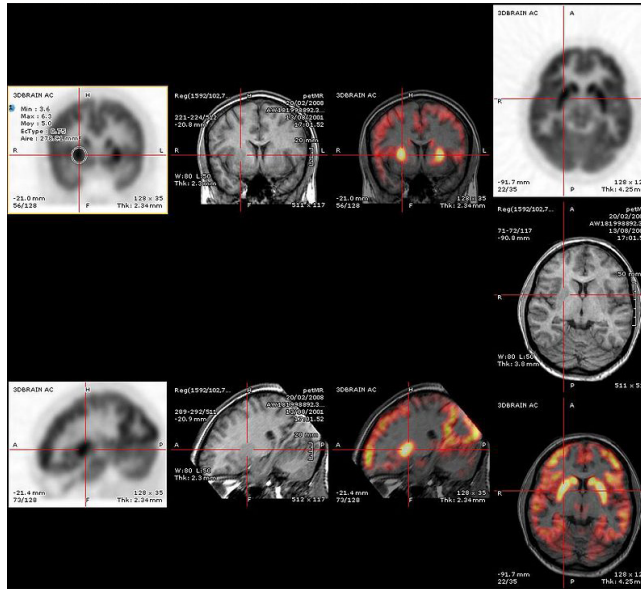
4. Time-of-flight (TOF) PET: For modern systems with a higher time resolution (roughly 3 nanoseconds) a technique called “Time-of-flight” is used to improve the overall performance. Time-of-flight PET makes use of very fast gamma-ray detectors and data processing system which can more precisely decide the difference in time between the detection of the two photons. Although it is technically impossible to localize the point of origin of the annihilation event exactly (currently within 10 cm) thus image reconstruction is still needed, TOF technique gives a remarkable improvement in image quality, especially signal-to-noise ratio.

Combination of PET with CT or MRI



Complete body PET-CT fusion image.

PET scans are increasingly read alongside CT or magnetic resonance imaging (MRI) scans, with the combination (called “co-registration”) giving both anatomic and metabolic information (i.e., what the structure is, and what it is doing biochemically). Because PET imaging is most useful in combination with anatomical imaging, such as CT, modern PET scanners are now available with integrated high-end multi-detector-row CT scanners (so-called “PET-CT”). Because the two scans can be performed in immediate sequence during the same session, with the patient not changing position between the two types of scans, the two sets of images are more precisely registered, so that areas of abnormality on the PET imaging can be more perfectly correlated with anatomy on the CT images. This is very useful in showing detailed views of moving organs or structures with higher anatomical variation, which is more common outside the brain.



Brain PET-MRI fusion image.

At the Jülich Institute of Neurosciences and Biophysics, the world's largest PET-MRI device began operation in April 2009: a 9.4-tesla magnetic resonance tomograph (MRT) combined with a positron emission tomograph (PET). Presently, only the head and brain can be imaged at these high magnetic field strengths.

For brain imaging, registration of CT, MRI and PET scans may be accomplished without the need for an integrated PET-CT or PET-MRI scanner by using a device known as the N-localizer.

Limitations

The minimization of radiation dose to the subject is an attractive feature of the use of short-lived radionuclides. Besides its established role as a diagnostic technique, PET has an expanding role as a method to assess the response to therapy, in particular, cancer therapy, where the risk to the patient from lack of knowledge about disease progress is much greater than the risk from the test radiation. Since the tracers are radioactive, the elderly and pregnant are unable to use it due to risks posed by radiation.

Limitations to the widespread use of PET arise from the high costs of cyclotrons needed to produce the short-lived radionuclides for PET scanning and the need for specially adapted on-site chemical synthesis apparatus to produce the radiopharmaceuticals after radioisotope preparation. Organic radiotracer molecules that will contain a positron-emitting radioisotope cannot be synthesized first and then the radioisotope prepared within them, because bombardment with a cyclotron to prepare the radioisotope destroys any organic carrier for it. Instead, the isotope must be prepared first, then afterward, the chemistry to prepare any organic radiotracer (such as FDG) accomplished

very quickly, in the short time before the isotope decays. Few hospitals and universities are capable of maintaining such systems, and most clinical PET is supported by third-party suppliers of radiotracers that can supply many sites simultaneously. This limitation restricts clinical PET primarily to the use of tracers labelled with fluorine-18, which has a half-life of 110 minutes and can be transported a reasonable distance before use, or to rubidium-82 (used as rubidium-82 chloride) with a half-life of 1.27 minutes, which is created in a portable generator and is used for myocardial perfusion studies. Nevertheless, in recent years a few on-site cyclotrons with integrated shielding and “hot labs” (automated chemistry labs that are able to work with radioisotopes) have begun to accompany PET units to remote hospitals. The presence of the small on-site cyclotron promises to expand in the future as the cyclotrons shrink in response to the high cost of isotope transportation to remote PET machines. In recent years the shortage of PET scans has been alleviated in the US, as rollout of radiopharmacies to supply radioisotopes has grown 30%/year.

Because the half-life of fluorine-18 is about two hours, the prepared dose of a radiopharmaceutical bearing this radionuclide will undergo multiple half-lives of decay during the working day. This necessitates frequent recalibration of the remaining dose (determination of activity per unit volume) and careful planning with respect to patient scheduling.

Cost

As of August 2008, Cancer Care Ontario reports that the current average incremental cost to perform a PET scan in the province is Can\$1,000–1,200 per scan. This includes the cost of the radiopharmaceutical and a stipend for the physician reading the scan.

In the United States, a PET scan is estimated to be ~\$5,000, and most insurance companies don't pay for routine PET scans after cancer treatment due to the fact that these scans are often unnecessary and present potentially more risks than benefits.

In England, the NHS reference cost (2015–2016) for an adult outpatient PET scan is £798, and £242 for direct access services.

In Australia, as of July 2018, the Medicare Benefits Schedule Fee for whole body FDG PET ranges from A\$953 to A\$999, depending on the indication for the scan.

Quality Control

The overall performance of PET systems can be evaluated by quality control tools such as the Jaszczak phantom.

Fast Neutron Therapy

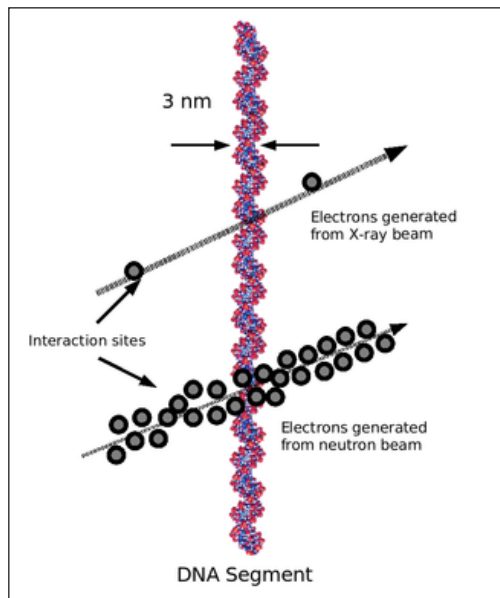
Fast neutron therapy utilizes high energy neutrons typically between 50 and 70 MeV

to treat cancer. Most fast neutron therapy beams are produced by reactors, cyclotrons ($d+Be$) and linear accelerators. Neutron therapy is currently available in Germany, Russia, South Africa and the United States. In the United States, three treatment centers are operational in Seattle, Washington, Detroit, Michigan and Batavia, Illinois. The Detroit and Seattle centers use a cyclotron which produces a proton beam impinging upon a beryllium target; the Batavia center at Fermilab uses a proton linear accelerator.

Advantages

Radiation therapy kills cancer cells in two ways depending on the effective energy of the radiative source. The amount of energy deposited as the particles traverse a section of tissue is referred to as the linear energy transfer (LET). X-rays produce low LET radiation, and protons and neutrons produce high LET radiation. Low LET radiation damages cells predominantly through the generation of reactive oxygen species. The neutron is uncharged and damages cells by direct effect on nuclear structures. Malignant tumors tend to have low oxygen levels and thus can be resistant to low LET radiation. This gives an advantage to neutrons in certain situations. One advantage is a generally shorter treatment cycle. To kill the same number of cancerous cells, neutrons require one third the effective dose as protons. Another advantage is the established ability of neutrons to better treat some cancers, such as salivary gland, adenoid cystic carcinomas and certain types of brain tumors, especially high-grade gliomas.

LET



Comparison of Low LET electrons and High LET electrons.

When therapeutic energy X-rays (1 to 25 MeV) interact with cells in human tissue, they do so mainly by Compton interactions, and produce relatively high energy

secondary electrons. These high energy electrons deposit their energy at about 1 keV/ μm . By comparison, the charged particles produced at a site of a neutron interaction may deliver their energy at a rate of 30–80 keV/ μm . The amount of energy deposited as the particles traverse a section of tissue is referred to as the linear energy transfer (LET). X-rays produce low LET radiation, and neutrons produce high LET radiation.

Because the electrons produced from X-rays have high energy and low LET, when they interact with a cell typically only a few ionizations will occur. It is likely then that the low LET radiation will cause only single strand breaks of the DNA helix. Single strand breaks of DNA molecules can be readily repaired, and so the effect on the target cell is not necessarily lethal. By contrast, the high LET charged particles produced from neutron irradiation cause many ionizations as they traverse a cell, and so double-strand breaks of the DNA molecule are possible. DNA repair of double-strand breaks are much more difficult for a cell to repair, and more likely to lead to cell death.

DNA repair mechanisms are quite efficient, and during a cell's lifetime many thousands of single strand DNA breaks will be repaired. A sufficient dose of ionizing radiation, however, delivers so many DNA breaks that it overwhelms the capability of the cellular mechanisms to cope.

Heavy ion therapy (e.g. carbon ions) makes use of the similarly high LET of $^{12}\text{C}^{6+}$ ions.

Because of the high LET, the relative radiation damage (relative biological effect or RBE) of fast neutrons is 4 times that of X-rays, meaning 1 rad of fast neutrons is equal to 4 rads of X-rays. The RBE of neutrons is also energy dependent, so neutron beams produced with different energy spectra at different facilities will have different RBE values.

Oxygen Effect

The presence of oxygen in a cell acts as a radiosensitizer, making the effects of the radiation more damaging. Tumor cells typically have a lower oxygen content than normal tissue. This medical condition is known as tumor hypoxia and therefore the oxygen effect acts to decrease the sensitivity of tumor tissue. The oxygen effect may be quantitatively described by the Oxygen Enhancement Ratio (OER). Generally it is believed that neutron irradiation overcomes the effect of tumor hypoxia, although there are counterarguments

Clinical Uses

The efficacy of neutron beams for use on prostate cancer has been shown through randomized trials. Fast neutron therapy has been applied successfully against salivary gland tumors. Adenoid cystic carcinomas have also been treated. Various other head and neck tumors have been examined.

Side Effects

No cancer therapy is without the risk of side effects. Neutron therapy is a very powerful nuclear scalpel that has to be utilized with exquisite care. For instance, some of the most remarkable cures it has been able to achieve are with cancers of the head and neck. Many of these cancers cannot effectively be treated with other therapies. However, neutron damage to nearby vulnerable areas such as the brain and sensory neurons can produce irreversible brain atrophy, blindness, etc. The risk of these side effects can be greatly mitigated by several techniques, but they cannot be totally eliminated. Moreover, some patients are more susceptible to such side effects than others and this cannot be predicted in advance. The patient ultimately must decide whether the advantages of a possibly lasting cure outweigh the risks of this treatment when faced with an otherwise incurable cancer.

Fast Neutron Centers

Several centers around the world have used fast neutrons for treating cancer. Due to lack of funding and support, at present only three are active in the USA. The University of Washington and the Gershenson Radiation Oncology Center operate fast neutron therapy beams and both are equipped with a Multi-Leaf Collimator (MLC) to shape the neutron beam.

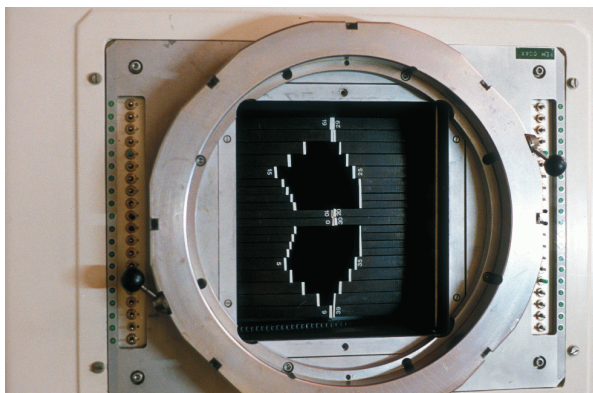
University of Washington

The Radiation Oncology Department operates a proton cyclotron that produces fast neutrons from directing 50.5 MeV protons onto a beryllium target. The UW Cyclotron is equipped with a gantry mounted delivery system and an MLC to produce shaped fields. The UW Neutron system is referred to as the Clinical Neutron Therapy System (CNTS). The CNTS is typical of most neutron therapy systems. A large, well shielded building is required to cut down on radiation exposure to the general public and to house the necessary equipment.

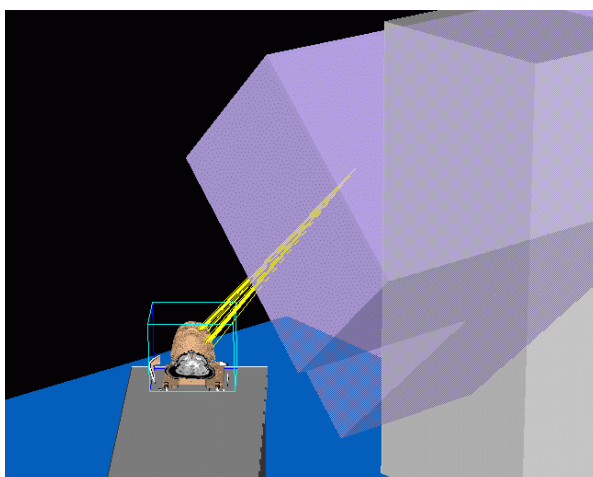
University of Washington CNTS



UW Cyclotron.



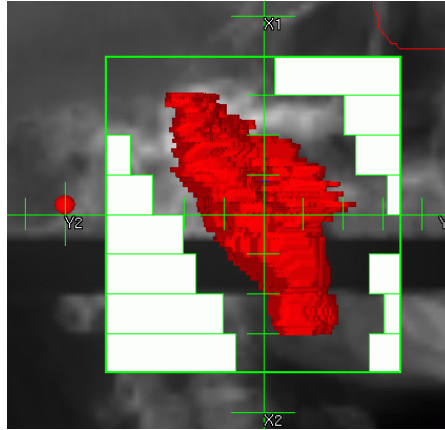
Multi-Leaf Collimator (MLC) used to shape the neutron beam.



Schematic of a treatment field delivery. The patient couch has been rotated, along with the gantry so the neutron beam will enter obliquely, to give maximum sparing of normal tissue.

A beamline transports the proton beam from the cyclotron to a gantry system. The gantry system contains magnets for deflecting and focusing the proton beam onto the beryllium target. The end of the gantry system is referred to as the head, and contains dosimetry systems to measure the dose, along with the MLC and other beam shaping devices. The advantage of having a beam transport and gantry are that the cyclotron can remain stationary, and the radiation source can be rotated around the patient. Along with varying the orientation of the treatment couch which the patient is positioned on, variation of the gantry position allows radiation to be directed from virtually any angle, allowing sparing of normal tissue and maximum radiation dose to the tumor.

During treatment, only the patient remains inside the treatment room (called a vault) and the therapists will remotely control the treatment, viewing the patient via video cameras. Each delivery of a set neutron beam geometry is referred to as a treatment field or beam. The treatment delivery is planned to deliver the radiation as effectively as possible, and usually results in fields that conform to the shape of the gross target, with any extension to cover microscopic disease.

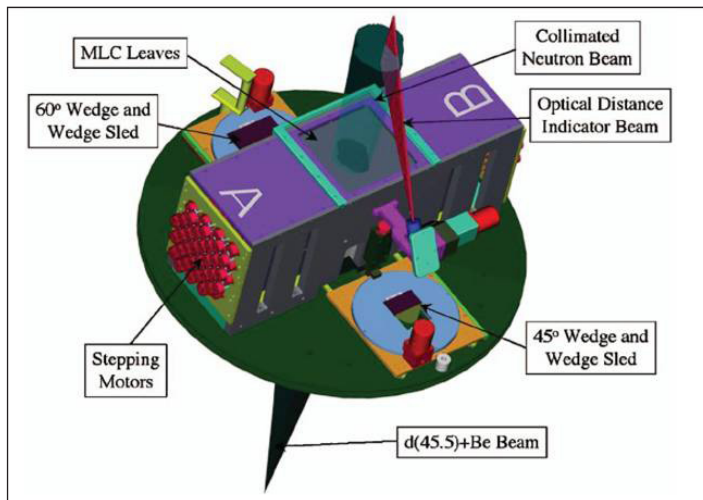


Example of a treatment neutron field collimated using a neutron MLC.

Karmanos Cancer Center/Wayne State University

The neutron therapy facility at the Gershenson Radiation Oncology Center at Karmanos Cancer Center/Wayne State University (KCC/WSU) in Detroit bears some similarities to the CNTS at the University of Washington, but also has many unique characteristics. This unit was decommissioned in 2011.

MLC on KCC/WSU Cyclotron



Schematic of MLC.

While the CNTS accelerates protons, the KCC facility produces its neutron beam by accelerating 48.5 MeV deuterons onto a beryllium target. This method produces a neutron beam with depth dose characteristics roughly similar to those of a 4 MV photon beam. The deuterons are accelerated using a gantry mounted superconducting cyclotron (GMSCC), eliminating the need for extra beam steering magnets and allowing the neutron source to rotate a full 360° around the patient couch.

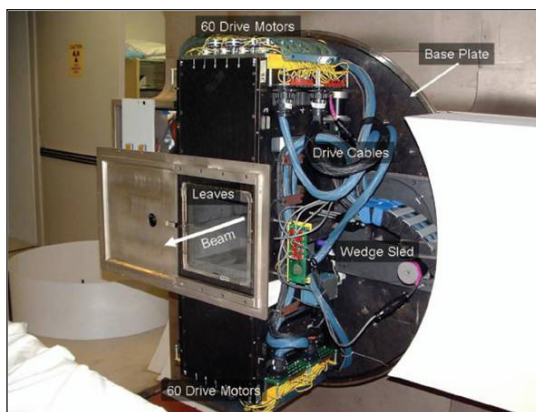
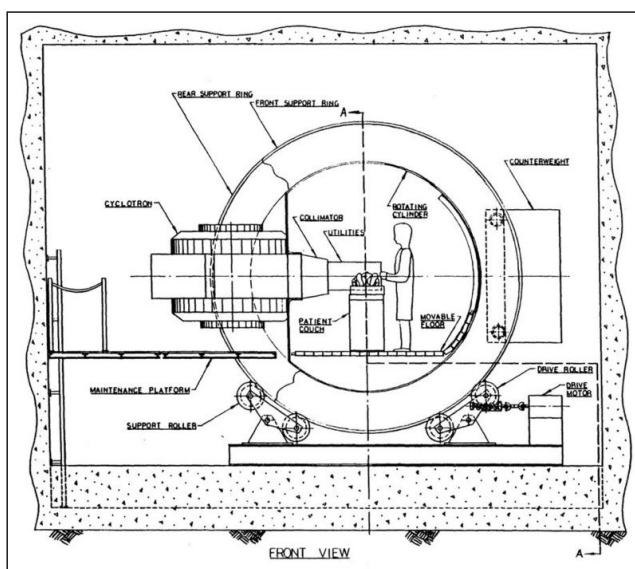


Photo of the MLC.



Schematic of the KCC/WSU gantry mounted superconducting cyclotron.

The KCC facility is also equipped with an MLC beam shaping device, the only other neutron therapy center in the USA besides the CNTS. The MLC at the KCC facility has been supplemented with treatment planning software that allows for the implementation of Intensity Modulated Neutron Radiotherapy (IMNRT), a recent advance in neutron beam therapy which allows for more radiation dose to the targeted tumor site than 3-D neutron therapy.

KCC/WSU has more experience than anyone in the world using neutron therapy for prostate cancer, having treated nearly 1,000 patients during the past 10 years.

Fermilab/Northern Illinois University

The Fermilab neutron therapy center first treated patients in 1976, and since that time has treated over 3,000 patients. In 2004, the Northern Illinois University began

managing the center. The neutrons produced by the linear accelerator at Fermilab have the highest energies available in the US and among the highest in the world.

Radiation Therapy

Radiation therapy or radiotherapy, often abbreviated RT, RTx, or XRT, is a therapy using ionizing radiation, generally as part of cancer treatment to control or kill malignant cells and normally delivered by a linear accelerator. Radiation therapy may be curative in a number of types of cancer if they are localized to one area of the body. It may also be used as part of adjuvant therapy, to prevent tumor recurrence after surgery to remove a primary malignant tumor (for example, early stages of breast cancer). Radiation therapy is synergistic with chemotherapy, and has been used before, during, and after chemotherapy in susceptible cancers. The subspecialty of oncology concerned with radiotherapy is called radiation oncology.

Radiation therapy is commonly applied to the cancerous tumor because of its ability to control cell growth. Ionizing radiation works by damaging the DNA of cancerous tissue leading to cellular death. To spare normal tissues (such as skin or organs which radiation must pass through to treat the tumor), shaped radiation beams are aimed from several angles of exposure to intersect at the tumor, providing a much larger absorbed dose there than in the surrounding, healthy tissue. Besides the tumour itself, the radiation fields may also include the draining lymph nodes if they are clinically or radiologically involved with tumor, or if there is thought to be a risk of subclinical malignant spread. It is necessary to include a margin of normal tissue around the tumor to allow for uncertainties in daily set-up and internal tumor motion. These uncertainties can be caused by internal movement (for example, respiration and bladder filling) and movement of external skin marks relative to the tumor position.

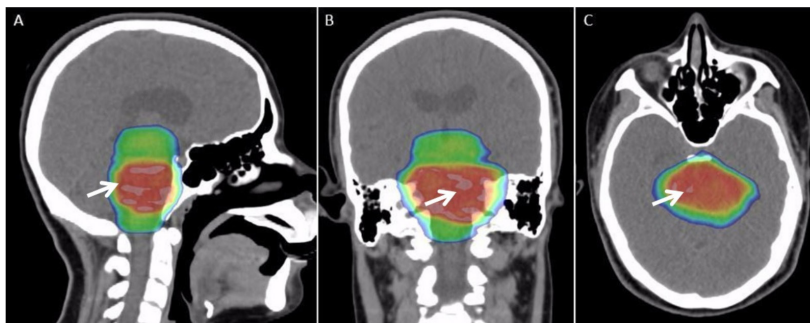
Radiation oncology is the medical specialty concerned with prescribing radiation, and is distinct from radiology, the use of radiation in medical imaging and diagnosis. Radiation may be prescribed by a radiation oncologist with intent to cure (“curative”) or for adjuvant therapy. It may also be used as palliative treatment (where cure is not possible and the aim is for local disease control or symptomatic relief) or as therapeutic treatment (where the therapy has survival benefit and it can be curative). It is also common to combine radiation therapy with surgery, chemotherapy, hormone therapy, immunotherapy or some mixture of the four. Most common cancer types can be treated with radiation therapy in some way.

The precise treatment intent (curative, adjuvant, neoadjuvant therapeutic or palliative) will depend on the tumor type, location, and stage, as well as the general health of the patient. Total body irradiation (TBI) is a radiation therapy technique used to prepare the body to receive a bone marrow transplant. Brachytherapy, in which a radioactive source is placed inside or next to the area requiring treatment, is another form of radiation therapy that minimizes exposure to healthy tissue during procedures

to treat cancers of the breast, prostate and other organs. Radiation therapy has several applications in non-malignant conditions, such as the treatment of trigeminal neuralgia, acoustic neuromas, severe thyroid eye disease, pterygium, pigmented villonodular synovitis, and prevention of keloid scar growth, vascular restenosis, and heterotopic ossification. The use of radiation therapy in non-malignant conditions is limited partly by worries about the risk of radiation-induced cancers.

Medical Uses

Different cancers respond to radiation therapy in different ways.



Radiation therapy for a patient with a diffuse intrinsic pontine glioma, with radiation dose color-coded.

The response of a cancer to radiation is described by its radiosensitivity. Highly radiosensitive cancer cells are rapidly killed by modest doses of radiation. These include leukemias, most lymphomas and germ cell tumors. The majority of epithelial cancers are only moderately radiosensitive, and require a significantly higher dose of radiation (60-70 Gy) to achieve a radical cure. Some types of cancer are notably radioresistant, that is, much higher doses are required to produce a radical cure than may be safe in clinical practice. Renal cell cancer and melanoma are generally considered to be radioresistant but radiation therapy is still a palliative option for many patients with metastatic melanoma. Combining radiation therapy with immunotherapy is an active area of investigation and has shown some promise for melanoma and other cancers.

It is important to distinguish the radiosensitivity of a particular tumor, which to some extent is a laboratory measure, from the radiation “curability” of a cancer in actual clinical practice. For example, leukemias are not generally curable with radiation therapy, because they are disseminated through the body. Lymphoma may be radically curable if it is localised to one area of the body. Similarly, many of the common, moderately radioresponsive tumors are routinely treated with curative doses of radiation therapy if they are at an early stage. For example: non-melanoma skin cancer, head and neck cancer, breast cancer, non-small cell lung cancer, cervical cancer, anal cancer, and prostate cancer. Metastatic cancers are generally incurable with radiation therapy because it is not possible to treat the whole body.

Before treatment, a CT scan is often performed to identify the tumor and surrounding

normal structures. The patient receives small skin marks to guide the placement of treatment fields. Patient positioning is crucial at this stage as the patient will have to be set-up in the identical position during treatment. Many patient positioning devices have been developed for this purpose, including masks and cushions which can be molded to the patient.

The response of a tumor to radiation therapy is also related to its size. Due to complex radiobiology, very large tumors respond less well to radiation than smaller tumors or microscopic disease. Various strategies are used to overcome this effect. The most common technique is surgical resection prior to radiation therapy. This is most commonly seen in the treatment of breast cancer with wide local excision or mastectomy followed by adjuvant radiation therapy. Another method is to shrink the tumor with neoadjuvant chemotherapy prior to radical radiation therapy. A third technique is to enhance the radiosensitivity of the cancer by giving certain drugs during a course of radiation therapy. Examples of radiosensitizing drugs include: Cisplatin, Nimorazole, and Cetuximab.

The impact of radiotherapy varies between different types of cancer and different groups. For example, for breast cancer after breast-conserving surgery, radiotherapy has been found to halve the rate at which the disease recurs.

Side Effects

Radiation therapy is in itself painless. Many low-dose palliative treatments (for example, radiation therapy to bony metastases) cause minimal or no side effects, although short-term pain flare-up can be experienced in the days following treatment due to oedema compressing nerves in the treated area. Higher doses can cause varying side effects during treatment (acute side effects), in the months or years following treatment (long-term side effects), or after re-treatment (cumulative side effects). The nature, severity, and longevity of side effects depends on the organs that receive the radiation, the treatment itself (type of radiation, dose, fractionation, concurrent chemotherapy), and the patient.

Most side effects are predictable and expected. Side effects from radiation are usually limited to the area of the patient's body that is under treatment. Side effects are dose-dependent; for example higher doses of head and neck radiation can be associated with cardiovascular complications, thyroid dysfunction, and pituitary axis dysfunction. Modern radiation therapy aims to reduce side effects to a minimum and to help the patient understand and deal with side effects that are unavoidable.

The main side effects reported are fatigue and skin irritation, like a mild to moderate sun burn. The fatigue often sets in during the middle of a course of treatment and can last for weeks after treatment ends. The irritated skin will heal, but may not be as elastic as it was before.

Acute Side Effects

Nausea and Vomiting

This is not a general side effect of radiation therapy, and mechanistically is associated only with treatment of the stomach or abdomen (which commonly react a few hours after treatment), or with radiation therapy to certain nausea-producing structures in the head during treatment of certain head and neck tumors, most commonly the vestibules of the inner ears. As with any distressing treatment, some patients vomit immediately during radiotherapy, or even in anticipation of it, but this is considered a psychological response. Nausea for any reason can be treated with antiemetics.

Damage to the Epithelial Surfaces

Epithelial surfaces may sustain damage from radiation therapy. Depending on the area being treated, this may include the skin, oral mucosa, pharyngeal, bowel mucosa and ureter. The rates of onset of damage and recovery from it depend upon the turnover rate of epithelial cells. Typically the skin starts to become pink and sore several weeks into treatment. The reaction may become more severe during the treatment and for up to about one week following the end of radiation therapy, and the skin may break down. Although this moist desquamation is uncomfortable, recovery is usually quick. Skin reactions tend to be worse in areas where there are natural folds in the skin, such as underneath the female breast, behind the ear, and in the groin.

Mouth, Throat and Stomach Sores

If the head and neck area is treated, temporary soreness and ulceration commonly occur in the mouth and throat. If severe, this can affect swallowing, and the patient may need painkillers and nutritional support/food supplements. The esophagus can also become sore if it is treated directly, or if, as commonly occurs; it receives a dose of collateral radiation during treatment of lung cancer. When treating liver malignancies and metastases, it is possible for collateral radiation to cause gastric, stomach or duodenal ulcers. This collateral radiation is commonly caused by non-targeted delivery (reflux) of the radioactive agents being infused. Methods, techniques and devices are available to lower the occurrence of this type of adverse side effect.

Intestinal Discomfort

The lower bowel may be treated directly with radiation (treatment of rectal or anal cancer) or be exposed by radiation therapy to other pelvic structures (prostate, bladder, female genital tract). Typical symptoms are soreness, diarrhoea, and nausea.

Swelling

As part of the general inflammation that occurs, swelling of soft tissues may cause

problems during radiation therapy. This is a concern during treatment of brain tumors and brain metastases, especially where there is pre-existing raised intracranial pressure or where the tumor is causing near-total obstruction of a lumen (e.g., trachea or main bronchus). Surgical intervention may be considered prior to treatment with radiation. If surgery is deemed unnecessary or inappropriate, the patient may receive steroids during radiation therapy to reduce swelling.

Infertility

The gonads (ovaries and testicles) are very sensitive to radiation. They may be unable to produce gametes following direct exposure to most normal treatment doses of radiation. Treatment planning for all body sites is designed to minimize, if not completely exclude dose to the gonads if they are not the primary area of treatment.

Late Side Effects

Late side effects occur months to years after treatment and are generally limited to the area that has been treated. They are often due to damage of blood vessels and connective tissue cells. Many late effects are reduced by fractionating treatment into smaller parts.

Fibrosis

Tissues which have been irradiated tend to become less elastic over time due to a diffuse scarring process.

Epilation

Epilation (hair loss) may occur on any hair bearing skin with doses above 1 Gy. It only occurs within the radiation field/s. Hair loss may be permanent with a single dose of 10 Gy, but if the dose is fractionated permanent hair loss may not occur until dose exceeds 45 Gy.

Dryness

The salivary glands and tear glands have a radiation tolerance of about 30 Gy in 2 Gy fractions, a dose which is exceeded by most radical head and neck cancer treatments. Dry mouth (xerostomia) and dry eyes (xerophthalmia) can become irritating long-term problems and severely reduce the patient's quality of life. Similarly, sweat glands in treated skin (such as the armpit) tend to stop working, and the naturally moist vaginal mucosa is often dry following pelvic irradiation.

Lymphedema

Lymphedema, a condition of localized fluid retention and tissue swelling, can result

from damage to the lymphatic system sustained during radiation therapy. It is the most commonly reported complication in breast radiation therapy patients who receive adjuvant axillary radiotherapy following surgery to clear the axillary lymph nodes.

Cancer

Radiation is a potential cause of cancer, and secondary malignancies are seen in some patients. Cancer survivors are already more likely than the general population to develop malignancies due to a number of factors including lifestyle choices, genetics, and previous radiation treatment. It is difficult to directly quantify the rates of these secondary cancers from any single cause. Studies have found radiation therapy as the cause of secondary malignancies for only a small minority of patients. New techniques such as proton beam therapy and carbon ion radiotherapy which aims to reduce dose to healthy tissues will lower these risks. It starts to occur 4 - 6 years following treatment, although some haematological malignancies may develop within 3 years. In the vast majority of cases, this risk is greatly outweighed by the reduction in risk conferred by treating the primary cancer even in pediatric malignancies which carry a higher burden of secondary malignancies.

Cardiovascular Disease

Radiation can increase the risk of heart disease and death as observed in previous breast cancer RT regimens. Therapeutic radiation increases the risk of a subsequent cardiovascular event (i.e., heart attack or stroke) by 1.5 to 4 times a person's normal rate, aggravating factors included. The increase is dose dependent, related to the RT's dose strength, volume and location.

Cardiovascular late side effects have been termed radiation-induced heart disease (RIHD) and radiation-induced vascular disease (RIVD). Symptoms are dose dependent and include cardiomyopathy, myocardial fibrosis, valvular heart disease, coronary artery disease, heart arrhythmia and peripheral artery disease. Radiation-induced fibrosis, vascular cell damage and oxidative stress can lead to these and other late side effect symptoms. Most radiation-induced cardiovascular diseases occur 10 or more years post treatment, making causality determinations more difficult.

Cognitive Decline

In cases of radiation applied to the head radiation therapy may cause cognitive decline. Cognitive decline was especially apparent in young children, between the ages of 5 to 11. Studies found, for example, that the IQ of 5-year-old children declined each year after treatment by several IQ points.

Radiation Enteropathy

The gastrointestinal tract can be damaged following abdominal and pelvic radiotherapy.

Atrophy, fibrosis and vascular changes produce malabsorption, diarrhea, steatorrhea and bleeding with bile acid diarrhea and vitamin B12 malabsorption commonly found due to ileal involvement. Pelvic radiation disease includes radiation proctitis, producing bleeding, diarrhoea and urgency, and can also cause radiation cystitis when the bladder is affected.

Radiation-induced Polyneuropathy

Radiation treatments are vitally necessary but may damage nerves near the target area or within the delivery path as nerve tissue is also radiosensitive. Nerve damage from ionizing radiation occurs in phases, the initial phase from microvascular injury, capillary damage and nerve demyelination. Subsequent damage occurs from vascular constriction and nerve compression due to uncontrolled fibrous tissue growth caused by radiation. Radiation-induced polyneuropathy, ICD-10-CM Code G62.82, occurs in approximately 1-5% of those receiving radiation therapies.

Depending upon the irradiated zone, late effect neuropathy may occur in either the central nervous system (CNS) or the peripheral nervous system (PNS). In the CNS for example, cranial nerve injury typically presents as a visual acuity loss 1-14 years post treatment. In the PNS, injury to the plexus nerves presents as radiation-induced brachial plexopathy or radiation-induced lumbosacral plexopathy appearing up to 3 decades post treatment.

Cumulative Side Effects

Cumulative effects from this process should not be confused with long-term effects—when short-term effects have disappeared and long-term effects are subclinical, reirradiation can still be problematic. These doses are calculated by the radiation oncologist and many factors are taken into account before the subsequent radiation takes place.

Effects on Reproduction

During the first two weeks after fertilization, radiation therapy is lethal but not teratogenic. High doses of radiation during pregnancy induce anomalies, impaired growth and intellectual disability, and there may be an increased risk of childhood leukemia and other tumours in the offspring.

In males previously having undergone radiotherapy, there appears to be no increase in genetic defects or congenital malformations in their children conceived after therapy. However, the use of assisted reproductive technologies and micromanipulation techniques might increase this risk.

Effects on Pituitary System

Hypopituitarism commonly develops after radiation therapy for sellar and parasellar

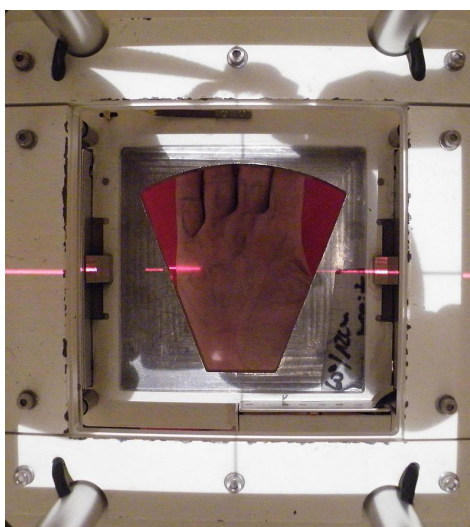
neoplasms, extrasellar brain tumours, head and neck tumours, and following whole body irradiation for systemic malignancies. Radiation-induced hypopituitarism mainly affects growth hormone and gonadal hormones. In contrast, adrenocorticotrophic hormone (ACTH) and thyroid stimulating hormone (TSH) deficiencies are the least common among people with radiation-induced hypopituitarism. Changes in prolactin-secretion is usually mild, and vasopressin deficiency appears to be very rare as a consequence of radiation.

Radiation Therapy Accidents

There are rigorous procedures in place to minimise the risk of accidental overexposure of radiation therapy to patients. However, mistakes do occasionally occur; for example, the radiation therapy machine Therac-25 was responsible for at least six accidents between 1985 and 1987, where patients were given up to one hundred times the intended dose; two people were killed directly by the radiation overdoses. From 2005 to 2010, a hospital in Missouri overexposed 76 patients (most with brain cancer) during a five-year period because new radiation equipment had been set up incorrectly.

Although medical errors are exceptionally rare, radiation oncologists, medical physicists and other members of the radiation therapy treatment team are working to eliminate them. ASTRO has launched a safety initiative called Target Safely that, among other things, aims to record errors nationwide so that doctors can learn from each and every mistake and prevent them from happening. ASTRO also publishes a list of questions for patients to ask their doctors about radiation safety to ensure every treatment is as safe as possible.

Use in Non-cancerous Diseases



The beam's eye view of the radiotherapy portal on the hand's surface with the lead shield cut-out placed in the machine's gantry.

Radiation therapy is used to treat early stage Dupuytren's disease and Ledderhose disease. When Dupuytren's disease is at the nodules and cords stage or fingers are at a minimal deformation stage of less than 10 degrees, then radiation therapy is used to prevent further progress of the disease. Radiation therapy is also used post-surgery in some cases to prevent the disease continuing to progress. Low doses of radiation are used typically three gray of radiation for five days, with a break of three months followed by another phase of three gray of radiation for five days.

Technique

Mechanism of Action

Radiation therapy works by damaging the DNA of cancerous cells. This DNA damage is caused by one of two types of energy, photon or charged particle. This damage is either direct or indirect ionization of the atoms which make up the DNA chain. Indirect ionization happens as a result of the ionization of water, forming free radicals, notably hydroxyl radicals, which then damage the DNA.

In photon therapy, most of the radiation effect is through free radicals. Cells have mechanisms for repairing single-strand DNA damage and double-stranded DNA damage. However, double-stranded DNA breaks are much more difficult to repair, and can lead to dramatic chromosomal abnormalities and genetic deletions. Targeting double-stranded breaks increases the probability that cells will undergo cell death. Cancer cells are generally less differentiated and more stem cell-like; they reproduce more than most healthy differentiated cells, and have a diminished ability to repair sub-lethal damage. Single-strand DNA damage is then passed on through cell division; damage to the cancer cells' DNA accumulates, causing them to die or reproduce more slowly.

One of the major limitations of photon radiation therapy is that the cells of solid tumors become deficient in oxygen. Solid tumors can outgrow their blood supply, causing a low-oxygen state known as hypoxia. Oxygen is a potent radiosensitizer, increasing the effectiveness of a given dose of radiation by forming DNA-damaging free radicals. Tumor cells in a hypoxic environment may be as much as 2 to 3 times more resistant to radiation damage than those in a normal oxygen environment. Much research has been devoted to overcoming hypoxia including the use of high pressure oxygen tanks, hyperthermia therapy (heat therapy which dilates blood vessels to the tumor site), blood substitutes that carry increased oxygen, hypoxic cell radiosensitizer drugs such as misonidazole and metronidazole, and hypoxic cytotoxins (tissue poisons), such as tirapazamine. Newer research approaches are currently being studied, including preclinical and clinical investigations into the use of an oxygen diffusion-enhancing compound such as trans sodium crocetin (TSC) as a radiosensitizer.

Charged particles such as protons and boron, carbon, and neon ions can cause direct damage to cancer cell DNA through high-LET (linear energy transfer) and have an

antitumor effect independent of tumor oxygen supply because these particles act mostly via direct energy transfer usually causing double-stranded DNA breaks. Due to their relatively large mass, protons and other charged particles have little lateral side scatter in the tissue—the beam does not broaden much, stays focused on the tumor shape, and delivers small dose side-effects to surrounding tissue. They also more precisely target the tumor using the Bragg peak effect. This procedure reduces damage to healthy tissue between the charged particle radiation source and the tumor and sets a finite range for tissue damage after the tumor has been reached. In contrast, IMRT's use of uncharged particles causes its energy to damage healthy cells when it exits the body. This exiting damage is not therapeutic, can increase treatment side effects, and increases the probability of secondary cancer induction. This difference is very important in cases where the close proximity of other organs makes any stray ionization very damaging (example: head and neck cancers). This x-ray exposure is especially bad for children, due to their growing bodies, and they have a 30% chance of a second malignancy after 5 years post initial RT.

Dose

The amount of radiation used in photon radiation therapy is measured in grays (Gy), and varies depending on the type and stage of cancer being treated. For curative cases, the typical dose for a solid epithelial tumor ranges from 60 to 80 Gy, while lymphomas are treated with 20 to 40 Gy.

Preventive (adjuvant) doses are typically around 45–60 Gy in 1.8–2 Gy fractions (for breast, head, and neck cancers.) Many other factors are considered by radiation oncologists when selecting a dose, including whether the patient is receiving chemotherapy, patient comorbidities, whether radiation therapy is being administered before or after surgery, and the degree of success of surgery.

Delivery parameters of a prescribed dose are determined during treatment planning (part of dosimetry). Treatment planning is generally performed on dedicated computers using specialized treatment planning software. Depending on the radiation delivery method, several angles or sources may be used to sum to the total necessary dose. The planner will try to design a plan that delivers a uniform prescription dose to the tumor and minimizes dose to surrounding healthy tissues.

In radiation therapy, three-dimensional dose distributions may be evaluated using the dosimetry technique known as gel dosimetry.

Fractionation

The total dose is fractionated (spread out over time) for several important reasons. Fractionation allows normal cells time to recover, while tumor cells are generally less efficient in repair between fractions. Fractionation also allows tumor cells that were in a relatively radio-resistant phase of the cell cycle during one treatment to cycle into a

sensitive phase of the cycle before the next fraction is given. Similarly, tumor cells that were chronically or acutely hypoxic (and therefore more radioresistant) may reoxygenate between fractions, improving the tumor cell kill.

Fractionation regimens are individualised between different radiation therapy centers and even between individual doctors. In North America, Australia, and Europe, the typical fractionation schedule for adults is 1.8 to 2 Gy per day, five days a week. In some cancer types, prolongation of the fraction schedule over too long can allow for the tumor to begin repopulating, and for these tumor types, including head-and-neck and cervical squamous cell cancers, radiation treatment is preferably completed within a certain amount of time. For children, a typical fraction size may be 1.5 to 1.8 Gy per day, as smaller fraction sizes are associated with reduced incidence and severity of late-onset side effects in normal tissues.

In some cases, two fractions per day are used near the end of a course of treatment. This schedule, known as a concomitant boost regimen or hyperfractionation, is used on tumors that regenerate more quickly when they are smaller. In particular, tumors in the head-and-neck demonstrate this behavior.

Patients receiving palliative radiation to treat uncomplicated painful bone metastasis should not receive more than a single fraction of radiation. A single treatment gives comparable pain relief and morbidity outcomes to multiple-fraction treatments, and for patients with limited life expectancy, a single treatment is best to improve patient comfort.

Schedules for Fractionation

One fractionation schedule that is increasingly being used and continues to be studied is hypofractionation. This is a radiation treatment in which the total dose of radiation is divided into large doses. Typical doses vary significantly by cancer type, from 2.2 Gy/fraction to 20 Gy/fraction, the latter being typical of stereotactic treatments (stereotactic ablative body radiotherapy, or SABR – also known as SBRT, or stereotactic body radiotherapy) for subcranial lesions, or SRS (stereotactic radiosurgery) for intracranial lesions. The rationale of hypofractionation is to reduce the probability of local recurrence by denying clonogenic cells the time they require to reproduce and also to exploit the radiosensitivity of some tumors. In particular, stereotactic treatments are intended to destroy clonogenic cells by a process of ablation – i.e. the delivery of a dose intended to destroy clonogenic cells directly, rather than to interrupt the process of clonogenic cell division repeatedly (apoptosis), as in routine radiotherapy.

Estimation of Dose based on Target Sensitivity

Different cancer types have different radiation sensitivity. However, predicting the sensitivity based on genomic or proteomic analyses of biopsy samples has proved difficult.

An alternative approach to genomics and proteomics was offered by the discovery that radiation protection in microbes is offered by non-enzymatic complexes of manganese and small organic metabolites. The content and variation of manganese (measurable by electron paramagnetic resonance) were found to be good predictors of radiosensitivity, and this finding extends also to human cells. An association was confirmed between total cellular manganese contents and their variation, and clinically-inferred radiore-sponsiveness in different tumor cells, a finding that may be useful for more precise radiodosages and improved treatment of cancer patients.

Types

Historically, the three main divisions of radiation therapy are:

- External beam radiation therapy (EBRT or XRT) or teletherapy.
- Brachytherapy or sealed source radiation therapy.
- Systemic radioisotope therapy or unsealed source radiotherapy.

The differences relate to the position of the radiation source; external is outside the body, brachytherapy uses sealed radioactive sources placed precisely in the area under treatment, and systemic radioisotopes are given by infusion or oral ingestion. Brachytherapy can use temporary or permanent placement of radioactive sources. The temporary sources are usually placed by a technique called afterloading. In afterloading a hollow tube or applicator is placed surgically in the organ to be treated, and the sources are loaded into the applicator after the applicator is implanted. This minimizes radiation exposure to health care personnel.

Particle therapy is a special case of external beam radiation therapy where the particles are protons or heavier ions.

External Beam Radiation Therapy

The following three sections refer to treatment using x-rays:

Conventional External Beam Radiation Therapy

Historically conventional external beam radiation therapy (2DXRT) was delivered via two-dimensional beams using kilovoltage therapy x-ray units or medical linear accelerators which generate high energy x-rays. 2DXRT mainly consists of a single beam of radiation delivered to the patient from several directions: often front or back, and both sides.

Conventional refers to the way the treatment is planned or simulated on a specially calibrated diagnostic x-ray machine known as a simulator because it recreates the linear accelerator actions (or sometimes by eye), and to the usually well-established

arrangements of the radiation beams to achieve a desired plan. The aim of simulation is to accurately target or localize the volume which is to be treated. This technique is well established and is generally quick and reliable. The worry is that some high-dose treatments may be limited by the radiation toxicity capacity of healthy tissues which lie close to the target tumor volume.

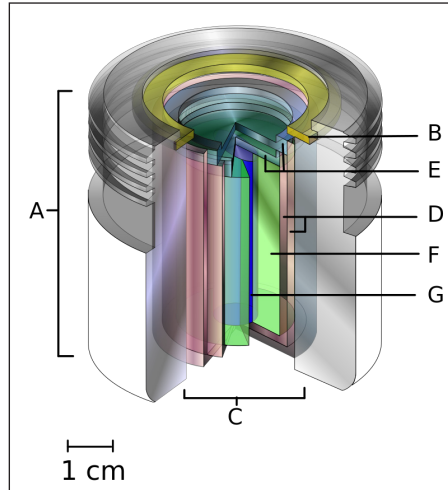


Figure indicates a teletherapy radiation capsule composed of the following: A. an international standard source holder (usually lead), B. a retaining ring, C. a teletherapy “source” composed of, E. two nested stainless steel canisters welded to, E. two stainless steel lids surrounding, F. a protective internal shield (usually uranium metal or a tungsten alloy) and G. a cylinder of radioactive source material, often but not always cobalt-60. The diameter of the “source” is 30 mm.

An example of this problem is seen in radiation of the prostate gland, where the sensitivity of the adjacent rectum limited the dose which could be safely prescribed using 2DXRT planning to such an extent that tumor control may not be easily achievable. Prior to the invention of the CT, physicians and physicists had limited knowledge about the true radiation dosage delivered to both cancerous and healthy tissue. For this reason, 3-dimensional conformal radiation therapy has become the standard treatment for almost all tumor sites. More recently other forms of imaging are used including MRI, PET, SPECT and Ultrasound.

Stereotactic Radiation

Stereotactic radiation is a specialized type of external beam radiation therapy. It uses focused radiation beams targeting a well-defined tumor using extremely detailed imaging scans. Radiation oncologists perform stereotactic treatments, often with the help of a neurosurgeon for tumors in the brain or spine.

There are two types of stereotactic radiation. Stereotactic radiosurgery (SRS) is when

doctors use a single or several stereotactic radiation treatments of the brain or spine. Stereotactic body radiation therapy (SBRT) refers to one or several stereotactic radiation treatments with the body, such as the lungs.

Some doctors say an advantage to stereotactic treatments is that they deliver the right amount of radiation to the cancer in a shorter amount of time than traditional treatments, which can often take 6 to 11 weeks. Plus treatments are given with extreme accuracy, which should limit the effect of the radiation on healthy tissues. One problem with stereotactic treatments is that they are only suitable for certain small tumors.

Stereotactic treatments can be confusing because many hospitals call the treatments by the name of the manufacturer rather than calling it SRS or SBRT. Brand names for these treatments include Axesse, Cyberknife, Gamma Knife, Novalis, Primatom, Synergy, X-Knife, TomoTherapy, Trilogy and Truebeam. This list changes as equipment manufacturers continue to develop new, specialized technologies to treat cancers.

Virtual Simulation and 3-dimensional Conformal Radiation Therapy

The planning of radiation therapy treatment has been revolutionized by the ability to delineate tumors and adjacent normal structures in three dimensions using specialized CT and/or MRI scanners and planning software.

Virtual simulation, the most basic form of planning, allows more accurate placement of radiation beams than is possible using conventional X-rays, where soft-tissue structures are often difficult to assess and normal tissues difficult to protect.

An enhancement of virtual simulation is 3-dimensional conformal radiation therapy (3DCRT), in which the profile of each radiation beam is shaped to fit the profile of the target from a beam's eye view (BEV) using a multileaf collimator (MLC) and a variable number of beams. When the treatment volume conforms to the shape of the tumor, the relative toxicity of radiation to the surrounding normal tissues is reduced, allowing a higher dose of radiation to be delivered to the tumor than conventional techniques would allow.

Intensity-modulated Radiation Therapy (IMRT)

Intensity-modulated radiation therapy (IMRT) is an advanced type of high-precision radiation that is the next generation of 3DCRT. IMRT also improves the ability to conform the treatment volume to concave tumor shapes, for example when the tumor is wrapped around a vulnerable structure such as the spinal cord or a major organ or blood vessel. Computer-controlled x-ray accelerators distribute precise radiation doses to malignant tumors or specific areas within the tumor. The pattern of radiation delivery is determined using highly tailored computing applications to perform optimization

and treatment simulation (Treatment Planning). The radiation dose is consistent with the 3-D shape of the tumor by controlling, or modulating, the radiation beam's intensity. The radiation dose intensity is elevated near the gross tumor volume while radiation among the neighboring normal tissues is decreased or avoided completely. This results in better tumor targeting, lessened side effects, and improved treatment outcomes than even 3DCRT.



Varian TruBeam Linear Accelerator, used for delivering IMRT.

3DCRT is still used extensively for many body sites but the use of IMRT is growing in more complicated body sites such as CNS, head and neck, prostate, breast, and lung. Unfortunately, IMRT is limited by its need for additional time from experienced medical personnel. This is because physicians must manually delineate the tumors one CT image at a time through the entire disease site which can take much longer than 3DCRT preparation. Then, medical physicists and dosimetrists must be engaged to create a viable treatment plan. Also, the IMRT technology has only been used commercially since the late 1990s even at the most advanced cancer centers, so radiation oncologists who did not learn it as part of their residency programs must find additional sources of education before implementing IMRT.

Proof of improved survival benefit from either of these two techniques over conventional radiation therapy (2DXRT) is growing for many tumor sites, but the ability to reduce toxicity is generally accepted. This is particularly the case for head and neck cancers in a series of pivotal trials performed by Professor Christopher Nutting of the Royal Marsden Hospital. Both techniques enable dose escalation, potentially increasing usefulness. There has been some concern, particularly with IMRT, about increased exposure of normal tissue to radiation and the consequent potential for secondary malignancy. Overconfidence in the accuracy of imaging may increase the chance of missing lesions that are invisible on the planning scans (and therefore not included in the treatment plan) or that move between or during a treatment (for example, due to respiration or inadequate patient immobilization). New techniques are being developed to better control this uncertainty—for example, real-time imaging combined

with real-time adjustment of the therapeutic beams. This new technology is called image-guided radiation therapy (IGRT) or four-dimensional radiation therapy.

Another technique is the real-time tracking and localization of one or more small implantable electric devices implanted inside or close to the tumor. There are various types of medical implantable devices that are used for this purpose. It can be a magnetic transponder which senses the magnetic field generated by several transmitting coils, and then transmits the measurements back to the positioning system to determine the location. The implantable device can also be a small wireless transmitter sending out an RF signal which then will be received by a sensor array and used for localization and real-time tracking of the tumor position.

A well-studied issue with IRMT is the “tongue and groove effect” which results in unwanted underdosing, due to irradiating through extended tongues and grooves of overlapping MLC (multileaf collimator) leaves. While solutions to this issue have been developed, which either reduce the TG effect to negligible amounts or remove it completely, they depend upon the method of IMRT being used and some of them carry costs of their own. Some texts distinguish “tongue and groove error” from “tongue or groove error”, according as both or one side of the aperture is occluded.

Volumetric Modulated Arc Therapy (VMAT)

Volumetric modulated arc therapy (VMAT) is a radiation technique introduced in 2007 which can achieve highly conformal dose distributions on target volume coverage and sparing of normal tissues. The specificity of this technique is to modify three parameters during the treatment. VMAT delivers radiation by rotating gantry (usually 360° rotating fields with one or more arcs), changing speed and shape of the beam with a multileaf collimator (MLC) (“sliding window” system of moving) and fluence output rate (dose rate) of the medical linear accelerator. VMAT has an advantage in patient treatment, compared with conventional static field intensity modulated radiotherapy (IMRT), of reduced radiation delivery times. Comparisons between VMAT and conventional IMRT for their sparing of healthy tissues and Organs at Risk (OAR) depend upon the cancer type. In the treatment of nasopharyngeal, oropharyngeal and hypopharyngeal carcinomas VMAT provides equivalent or better OAR protection. In the treatment of prostate cancer the OAR protection result is mixed with some studies favoring VMAT, others favoring IMRT.

Automated Planning

Automated treatment planning has become an integrated part of radiotherapy treatment planning. There are in general two approaches of automated planning. 1) Knowledge based planning where the treatment planning system has a library of high quality plans, from which it can predict the target and OAR DVH. 2) The other approach is commonly called protocol based planning, where the treatment planning system tried

to mimic an experienced treatment planner and through an iterative process evaluates the plan quality from on the basis of the protocol.

Particle Therapy

In particle therapy (proton therapy being one example), energetic ionizing particles (protons or carbon ions) are directed at the target tumor. The dose increases while the particle penetrates the tissue, up to a maximum (the Bragg peak) that occurs near the end of the particle's range, and it then drops to (almost) zero. The advantage of this energy deposition profile is that less energy is deposited into the healthy tissue surrounding the target tissue.

Auger Therapy

Auger therapy (AT) makes use of a very high dose of ionizing radiation in situ that provides molecular modifications at an atomic scale. AT differs from conventional radiation therapy in several aspects; it neither relies upon radioactive nuclei to cause cellular radiation damage at a cellular dimension, nor engages multiple external pencil-beams from different directions to zero-in to deliver a dose to the targeted area with reduced dose outside the targeted tissue/organ locations. Instead, the in situ delivery of a very high dose at the molecular level using AT aims for in situ molecular modifications involving molecular breakages and molecular re-arrangements such as a change of stacking structures as well as cellular metabolic functions related to the said molecule structures.

Contact X-ray Brachytherapy

Contact x-ray brachytherapy (also called "CXB", "electronic brachytherapy" or the "Papillon Technique") is a type of radiation therapy using kilovoltage X-rays applied close to the tumour to treat rectal cancer. The process involves inserting the x-ray tube through the anus into the rectum and placing it against the cancerous tissue, and then high doses of X-rays are emitted directly into the tumor at two weekly intervals. It is typically used for treating early rectal cancer in patients who may not be candidates for surgery. A 2015 NICE review found the main side effect to be bleeding that occurred in about 38% of cases, and radiation-induced ulcer which occurred in 27% of cases.

Brachytherapy (Sealed Source Radiotherapy)

Brachytherapy is delivered by placing radiation source(s) inside or next to the area requiring treatment. Brachytherapy is commonly used as an effective treatment for cervical, prostate, breast, and skin cancer and can also be used to treat tumours in many other body sites.



A SAVI brachytherapy device.

In brachytherapy, radiation sources are precisely placed directly at the site of the cancerous tumour. This means that the irradiation only affects a very localized area – exposure to radiation of healthy tissues further away from the sources is reduced. These characteristics of brachytherapy provide advantages over external beam radiation therapy – the tumour can be treated with very high doses of localized radiation, whilst reducing the probability of unnecessary damage to surrounding healthy tissues. A course of brachytherapy can often be completed in less time than other radiation therapy techniques. This can help reduce the chance of surviving cancer cells dividing and growing in the intervals between each radiation therapy dose.

As one example of the localized nature of breast brachytherapy, the SAVI device delivers the radiation dose through multiple catheters, each of which can be individually controlled. This approach decreases the exposure of healthy tissue and resulting side effects, compared both to external beam radiation therapy and older methods of breast brachytherapy.

Unsealed Source Radiotherapy (Systemic Radioisotope Therapy)

Systemic radioisotope therapy (RIT) is a form of targeted therapy. Targeting can be due to the chemical properties of the isotope such as radioiodine which is specifically absorbed by the thyroid gland a thousandfold better than other bodily organs. Targeting can also be achieved by attaching the radioisotope to another molecule or antibody to guide it to the target tissue. The radioisotopes are delivered through infusion (into the bloodstream) or ingestion. Examples are the infusion of metaiodobenzylguanidine (MIBG) to treat neuroblastoma, of oral iodine-131 to treat thyroid cancer or thyrotoxicosis, and of hormone-bound lutetium-177 and yttrium-90 to treat neuroendocrine tumors (peptide receptor radionuclide therapy).

Another example is the injection of radioactive yttrium-90 or holmium-166 microspheres into the hepatic artery to radioembolize liver tumors or liver metastases. These microspheres are used for the treatment approach known as selective internal radiation therapy. The microspheres are approximately 30 μm in diameter (about one-third of a

human hair) and are delivered directly into the artery supplying blood to the tumors. These treatments begin by guiding a catheter up through the femoral artery in the leg, navigating to the desired target site and administering treatment. The blood feeding the tumor will carry the microspheres directly to the tumor enabling a more selective approach than traditional systemic chemotherapy. There are currently three different kinds of microspheres: SIR-Spheres, TheraSphere and QuiremSpheres.

A major use of systemic radioisotope therapy is in the treatment of bone metastasis from cancer. The radioisotopes travel selectively to areas of damaged bone, and spare normal undamaged bone. Isotopes commonly used in the treatment of bone metastasis are radium-223, strontium-89 and samarium (^{153}Sm) lexidronam.

In 2002, the United States Food and Drug Administration (FDA) approved ibritumomab tiuxetan (Zevalin), which is an anti-CD20 monoclonal antibody conjugated to yttrium-90. In 2003, the FDA approved the tositumomab/iodine (^{131}I) tositumomab regimen (Bexxar), which is a combination of an iodine-131 labelled and an unlabelled anti-CD20 monoclonal antibody. These medications were the first agents of what is known as radioimmunotherapy, and they were approved for the treatment of refractory non-Hodgkin's lymphoma.

Intraoperative Radiotherapy

Intraoperative radiation therapy (IORT) is applying therapeutic levels of radiation to a target area, such as a cancer tumor, while the area is exposed during surgery.

Rationale

The rationale for IORT is to deliver a high dose of radiation precisely to the targeted area with minimal exposure of surrounding tissues which are displaced or shielded during the IORT. Conventional radiation techniques such as external beam radiotherapy (EBRT) following surgical removal of the tumor have several drawbacks: The tumor bed where the highest dose should be applied is frequently missed due to the complex localization of the wound cavity even when modern radiotherapy planning is used. Additionally, the usual delay between the surgical removal of the tumor and EBRT may allow a repopulation of the tumor cells. These potentially harmful effects can be avoided by delivering the radiation more precisely to the targeted tissues leading to immediate sterilization of residual tumor cells. Another aspect is that wound fluid has a stimulating effect on tumor cells. IORT was found to inhibit the stimulating effects of wound fluid.

Deep Inspiration Breath-hold

Deep inspiration breath-hold (DIBH) is a method of delivering radiotherapy while limiting radiation exposure to the heart and lungs. It is used primarily for treating left-sided breast cancer. The technique involves a patient holding their breath during

treatment. There are two basic methods of performing DIBH: free-breathing breath-hold and spirometry-monitored deep inspiration breath hold.

Radioactive Iodine Uptake Test

The radioactive iodine uptake test is a type of scan used in the diagnosis of thyroid problems, particularly hyperthyroidism. It is entirely different from radioactive iodine therapy (RAI therapy), which uses much higher doses to destroy cancerous cells. The RAIU test is also used as a follow up to RAI therapy to verify that no thyroid cells survived, which could still be cancerous.

The patient swallows a radioisotope of iodine in the form of capsule or fluid, and the absorption (uptake) of this radiotracer by the thyroid is studied after 4–6 hours and after 24 hours with the aid of a scintillation counter. The dose is typically 0.15–0.37 MBq (4–10 μ Ci) of ^{131}I iodide, or 3.7–7.4 MBq (100–200 μ Ci) of ^{123}I iodide. The RAIU test is a reliable measurement when using a dedicated probe with a reproducibility of 1 percent and a 95%-least-significant-change of 3 percent.

The normal uptake is between 15 and 25 percent, but this may be forced down if, in the meantime, the patient has eaten foods high in iodine, such as dairy products and seafood. Low uptake suggests thyroiditis, high uptake suggests Graves' disease, and unevenness in uptake suggests the presence of a nodule.

^{123}I has a shorter half-life than ^{131}I (a half day vs. 8.1 days), so use of ^{123}I exposes the body to less radiation, at the expense of less time to evaluate delayed scan images. Furthermore, ^{123}I emits gamma radiation, while ^{131}I emits gamma and beta radiation.

MILITARY APPLICATIONS

Nuclear Weapons Delivery

Nuclear weapons delivery is the technology and systems used to place a nuclear weapon at the position of detonation, on or near its target. Several methods have been developed to carry out this task.

Strategic nuclear weapons are used primarily as part of a doctrine of deterrence by threatening large targets, such as cities. Weapons meant for use in limited military maneuvers, such as destroying specific military, communications, or infrastructure targets, are known as tactical nuclear weapons. In terms of explosive yields, nowadays the former have much larger yield than the latter, even though it is not a rule. The bombs that destroyed Hiroshima and Nagasaki in 1945 (with TNT equivalents between 15 and 22 kilotons) were weaker than many of today's tactical weapons, yet they achieved the desired effect when used strategically.

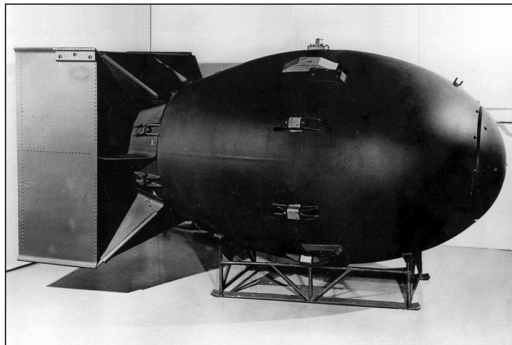
Nuclear Triad

A nuclear triad refers to a strategic nuclear arsenal which consists of three components, traditionally strategic bombers, intercontinental ballistic missiles (ICBMs), and submarine-launched ballistic missiles (SLBMs). The purpose of having a three-branched nuclear capability is to significantly reduce the possibility that an enemy could destroy all of a nation's nuclear forces in a first-strike attack; this, in turn, ensures a credible threat of a second strike, and thus increases a nation's nuclear deterrence.

Main Delivery Mechanisms

Gravity Bomb

Historically, the first method of delivery, and the method used in the only two nuclear weapons actually used in warfare, was a gravity bomb dropped by a plane. In the years leading up to the development and deployment of nuclear-armed missiles, nuclear bombs represented the most practical means of nuclear weapons delivery; even today, and especially with the decommissioning of nuclear missiles, aerial bombing remains the primary means of offensive nuclear weapons delivery, and the majority of US nuclear warheads are represented in bombs, although some are in the form of missiles.



The “Little Boy” and the “Fat Man” devices were large and cumbersome gravity bombs.

Gravity bombs are designed to be dropped from a plane, which requires that the weapon be able to withstand vibrations and changes in air temperature and pressure during the course of a flight. Early weapons often had a removable core for safety, known as in flight insertion (IFI) cores, being inserted or assembled by the air crew during flight. They had to meet safety conditions, to prevent accidental detonation or dropping. A variety of types also had to have a fuse to initiate detonation. US nuclear weapons that met these criteria are designated by the letter “B” followed, without a hyphen, by the sequential number of the “physics package” it contains. The “B61”, for example, was the primary bomb in the US arsenal for decades.

Various air-dropping techniques exist, including toss bombing, parachute-retarded delivery, and laydown modes, intended to give the dropping aircraft time to escape the ensuing blast.

The earliest gravity nuclear bombs (Little Boy and Fat Man) of the United States could only be carried, during the era of their creation, by the special Silverplate limited production (65 airframes by 1947) version of the B-29 Superfortress. The next generation of weapons were still so big and heavy that they could only be carried by bombers such as the six/ten-engined, seventy-meter wingspan B-36 Peacemaker, the eight jet-engined B-52 Stratofortress, and jet-powered British RAF V bombers, but by the mid-1950s smaller weapons had been developed that could be carried and deployed by fighter-bombers.

Ballistic Missile

Missiles using a ballistic trajectory usually deliver a warhead over the horizon, at distances of thousands of kilometers, as in the case of intercontinental ballistic missiles (ICBMs) and submarine-launched ballistic missiles (SLBMs). Most ballistic missiles exit the Earth's atmosphere and re-enter it in their sub-orbital spaceflight.



Trident II SLBM launched by Royal Navy Vanguard-class submarine.

Placement of nuclear missiles on the low Earth orbit has been banned by the Outer Space Treaty as early as 1967. Also, the eventual Soviet Fractional Orbital Bombardment System (FOBS) that served a similar purpose—it was just deliberately designed to deorbit before completing a full circle—was phased out in January 1983 in compliance with the SALT II treaty.

An ICBM is more than 20 times as fast as a bomber and more than 10 times as fast as a fighter plane, and also flying at a much higher altitude, and therefore more difficult to defend against. ICBMs can also be fired quickly in the event of a surprise attack.

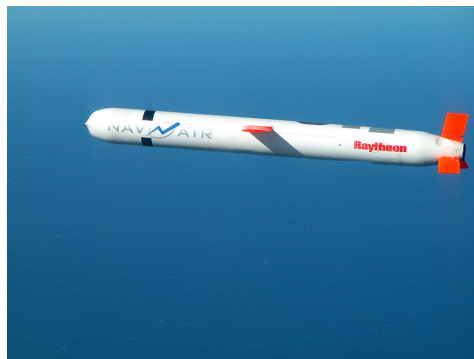
Early ballistic missiles carried a single warhead, often of megaton-range yield. Because of the limited accuracy of the missiles, this kind of high yield was considered necessary in order to ensure a particular target's destruction. Since the 1970s modern

ballistic weapons have seen the development of far more accurate targeting technologies, particularly due to improvements in inertial guidance systems. This set the stage for smaller warheads in the hundreds-of-kilotons-range yield, and consequently for ICBMs having multiple independently targetable reentry vehicles (MIRV). Advances in technology have enabled a single missile to launch a payload containing several warheads. The number of independent warheads capable of deployment from ballistic missiles depends on the weapons platform the missile is launched from. For example, one D5 Trident missile carried by an Ohio-class submarine is capable of launching eight independent warheads, while a Typhoon has missiles capable of deploying 10 warheads at a time. MIRV has a number of advantages over a missile with a single warhead. With small additional costs, it allows a single missile to strike multiple targets, or to inflict maximum damage on a single target by attacking it with multiple warheads. It makes anti-ballistic missile defense even more difficult, and even less economically viable, than before.

Missile warheads in the American arsenal are indicated by the letter “W”; for example, the W61 missile warhead would have the same physics package as the B61 gravity bomb described above, but it would have different environmental requirements, and different safety requirements since it would not be crew-tended after launch and remain atop a missile for a great length of time.

Cruise Missile

A cruise missile is a jet engine or rocket-propelled missile that flies at low altitude using an automated guidance system (usually inertial navigation, sometimes supplemented by either GPS or mid-course updates from friendly forces) to make them harder to detect or intercept. Cruise missiles can carry a nuclear warhead. They have a shorter range and smaller payloads than ballistic missiles, so their warheads are smaller and less powerful.



Cruise missiles have a shorter range than ICBMs. U/RGM-109E Tomahawk pictured (not nuclear capable anymore).

The AGM-86 ALCM is the US Air Force’s current nuclear-armed air-launched cruise missile. The ALCM is only carried on the B-52 Stratofortress which can carry 20 missiles.

Thus the cruise missiles themselves can be compared with MIRV warheads. The BGM/UGM-109 Tomahawk submarine-launched cruise missile is capable of carrying nuclear warheads, but all nuclear warheads were removed.

Cruise missiles may also be launched from mobile launchers on the ground, and from naval ships.

There is no letter change in the US arsenal to distinguish the warheads of cruise missiles from those for ballistic missiles.

Cruise missiles, even with their lower payload, have a number of advantages over ballistic missiles for the purposes of delivering nuclear strikes:

- Launch of a cruise missile is difficult to detect early from satellites and other long-range means, contributing to a surprise factor of attack.
- That, coupled with the ability to actively maneuver in flight, allows for penetration of strategic anti-missile systems aimed at intercepting ballistic missiles on calculated trajectory of flight.

U.S. and Soviet intermediate-range, ground-launched cruise missiles were eliminated under the Intermediate-range Nuclear Forces Treaty from 1987 to 2019, following U.S. withdrawal.

Other Delivery Systems

Other delivery methods included artillery shells, mines such as the Medium Atomic Demolition Munition and the novel Blue Peacock, nuclear depth charges, and nuclear torpedoes. An 'Atomic Bazooka' was also fielded, designed to be used against large formations of tanks.



The Mk-17 was an early US thermonuclear weapon and weighed around 21 short tons (19,000 kg).

In the 1950s the US developed small nuclear warheads for air defense use, such as the Nike Hercules. From the 1950s to the 1980s, the United States and Canada fielded a

low-yield nuclear-tipped air-to-air rocket, the AIR-2 Genie. Further developments of this concept, some with much larger warheads, led to the early anti-ballistic missiles. The United States have largely taken nuclear air-defense weapons out of service with the fall of the Soviet Union in the early 1990s. Russia updated its nuclear tipped Soviet era anti-ballistic missile (ABM) system, known as the A-135 anti-ballistic missile system in 1995. It is believed that the, in development successor to the nuclear A-135, the A-235 Samolet-M will dispense with nuclear interception warheads and instead rely on a conventional hit-to-kill capability to destroy its target.



The Davy Crockett artillery shell is the smallest known nuclear weapon developed by the US.

Small, two-man portable tactical weapons (erroneously referred to as suitcase bombs), such as the Special Atomic Demolition Munition, have been developed, although the difficulty to combine sufficient yield with portability limits their military utility.

Hypersonic Glide Vehicles are a new potential method of nuclear delivery. They can be potentially combined with ICBM MIRVs such as RS-28 Sarmat.

Costs

According to an audit by the Brookings Institution, between 1940 and 1996, the US spent \$9.49 trillion in present-day terms on nuclear weapons programs. 57 percent of which was spent on building delivery mechanisms for nuclear weapons. 6.3 percent of the total, \$595 billion in present-day terms, was spent on weapon nuclear waste management, for example, cleaning up the Hanford site with environmental remediation, and 7 percent of the total, \$667 billion was spent on the manufacturing of nuclear weapons themselves.

Technology Spin-offs

Strictly speaking however not all this 57 percent was spent solely on “weapons programs” delivery systems.



Edward White during the first US “Spacewalk” Extravehicular activity (EVA), Project Gemini.

Launch Vehicles

For example, two such delivery mechanisms, the Atlas ICBM and Titan II, were re-purposed as human launch vehicles for human spaceflight, both were used in the civilian Project Mercury and Project Gemini programs respectively, which are regarded as stepping stones in the evolution of US human spaceflight. The Atlas vehicle sent John Glenn, the first American into orbit. Similarly in the Soviet Union it was the R-7 ICBM/launch vehicle that placed the first artificial satellite in space, Sputnik, on 4 October 1957, and the first human spaceflight in history was accomplished on a derivative of the R-7, the Vostok, on 12 April 1961, by cosmonaut Yuri Gagarin. A modernized version of the R-7 is still in use as the launch vehicle for the Russian Federation, in the form of the Soyuz spacecraft.

Weather Satellites

The first true weather satellite, the TIROS-1 was launched on the Thor-Able launch vehicle in April 1960. The PGM-17 Thor was the first operational IRBM (intermediate ballistic missile) deployed by the US Air Force (USAF). The Soviet Union’s first fully operational weather satellite, the Meteor 1 was launched on 26 March 1969 on the Vostok rocket, a derivative of the R-7 ICBM.

Lubricants

WD-40 was first used by Convair to protect the outer skin, and more importantly, the paper thin “balloon tanks” of the Atlas missile from rust and corrosion. These stainless steel fuel tanks were so thin that, when empty, they had to be kept inflated with nitrogen gas to prevent their collapse.

Thermal Isolation

In 1953, Dr. S. Donald Stookey of the Corning Research and Development Division invented Pyroceram, a white glass-ceramic material capable of withstanding a thermal shock (sudden temperature change) of up to 450 °C (840 °F). It evolved from materials originally developed for a US ballistic missile program, and Stookey's research involved heat-resistant material for nose cones.

Satellite Assisted Positioning

Precise navigation would enable United States submarines to get an accurate fix of their positions before they launched their SLBMs, this spurred development of triangulation methods that ultimately culminated in GPS. The motivation for having accurate launch position fixes, and missile velocities, is twofold. It results in a tighter target impact circular error probable and therefore by extension, reduces the need for the earlier generation of heavy multi-megaton nuclear warheads, such as the W53 to ensure the target is destroyed. With increased target accuracy, a greater number of lighter, multi-kiloton range warheads can be packed on a given missile, giving a higher number of separate targets that can be hit per missile.

Global Positioning System

During a Labor Day weekend in 1973, a meeting of about twelve military officers at the Pentagon discussed the creation of a Defense Navigation Satellite System (DNSS). It was at this meeting that “the real synthesis that became GPS was created.” Later that year, the DNSS program was named Navstar, or Navigation System Using Timing and Ranging.

During the development of the submarine-launched Polaris missile, a requirement to accurately know the submarine's location was needed to ensure high circular error probable warhead target accuracy. This led the US to develop the Transit system. In 1959, ARPA (renamed DARPA in 1972) also played a role in Transit.

The first satellite navigation system, Transit, used by the United States Navy, was first successfully tested in 1960. It used a constellation of five satellites and could provide a navigational fix approximately once per hour. In 1967, the US Navy developed the Timation satellite that proved the ability to place accurate clocks in space, a technology required by the latter Global Positioning System. In the 1970s, the ground-based Omega Navigation System, based on phase comparison of signal transmission from pairs of stations, became the first worldwide radio navigation system. Limitations of these systems drove the need for a more universal navigation solution with greater accuracy.

While there were wide needs for accurate navigation in military and civilian sectors, almost none of those was seen as justification for the billions of dollars it would cost in research, development, deployment, and operation for a constellation of navigation satellites. During the Cold War arms race, the nuclear threat to the existence of the

United States was the one need that did justify this cost in the view of the United States Congress. This deterrent effect is why GPS was funded. The nuclear triad consisted of the United States Navy's submarine-launched ballistic missiles (SLBMs) along with United States Air Force (USAF) strategic bombers and intercontinental ballistic missiles (ICBMs). Considered vital to the nuclear-deterrence posture, accurate determination of the SLBM launch position was a force multiplier.

Precise navigation would enable United States submarines to get an accurate fix of their positions before they launched their SLBMs. The USAF, with two-thirds of the nuclear triad, also had requirements for a more accurate and reliable navigation system. The Navy and Air Force were developing their own technologies in parallel to solve what was essentially the same problem. To increase the survivability of ICBMs, there was a proposal to use mobile launch platforms (such as Russian SS-24 and SS-25) and so the need to fix the launch position had similarity to the SLBM situation.

In 1960, the Air Force proposed a radio-navigation system called MOSAIC (MOBILE System for Accurate ICBM Control) that was essentially a 3-D LORAN. A follow-on study, Project 57, was worked in 1963 and it was "in this study that the GPS concept was born". That same year, the concept was pursued as Project 621B, which had "many of the attributes that you now see in GPS" and promised increased accuracy for Air Force bombers as well as ICBMs. Updates from the Navy Transit system were too slow for the high speeds of Air Force operation. The Navy Research Laboratory continued advancements with their Timation (Time Navigation) satellites, first launched in 1967, and with the third one in 1974 carrying the first atomic clock into orbit.

Another important predecessor to GPS came from a different branch of the United States military. In 1964, the United States Army orbited its first Sequential Collation of Range (SECOR) satellite used for geodetic surveying. The SECOR system included three ground-based transmitters from known locations that would send signals to the satellite transponder in orbit. A fourth ground-based station, at an undetermined position, could then use those signals to fix its location precisely. The last SECOR satellite was launched in 1969. Decades later, during the early years of GPS, civilian surveying became one of the first fields to make use of the new technology, because surveyors could reap benefits of signals from the less-than-complete GPS constellation years before it was declared operational. GPS can be thought of as an evolution of the SECOR system where the ground-based transmitters have been migrated into orbit.

Nuclear Weapon Design

Nuclear weapon designs are physical, chemical, and engineering arrangements that cause the physics package of a nuclear weapon to detonate. There are three existing basic design types:

- Pure fission weapons, the simplest and least technically demanding, were the

first nuclear weapons built and have so far been the only type ever used in an act of war (over wartime Japan).

- Boosted fission weapons improve on the implosion design using small quantities of fusion fuel to enhance the fission chain reaction. Boosting can more than double the weapon's fission energy yield.
- Staged thermonuclear weapons are essentially arrangements of two or more "stages", most usually two. The first stage is always a boosted fission weapon as above. Its detonation causes it to shine intensely with x-radiation, which illuminates and implodes the second stage filled with a large quantity of fusion fuel. This sets in motion a sequence of events which results in a thermonuclear, or fusion, burn. This process affords potential yields up to hundreds of times those of fission weapons.

A fourth type, pure fusion weapons, is a purely theoretical possibility. Such weapons would produce far fewer radioactive byproducts than current designs, although they would release huge numbers of neutrons.

Pure fission weapons historically have been the first type to be built by new nuclear powers. Large industrial states with well-developed nuclear arsenals have two-stage thermonuclear weapons, which are the most compact, scalable, and cost effective option once the necessary technical base and industrial infrastructure are built.

Most known innovations in nuclear weapon design originated in the United States, although some were later developed independently by other states.

In early news accounts, pure fission weapons were called atomic bombs or A-bombs and weapons involving fusion were called hydrogen bombs or H-bombs. Practitioners, however, favor the terms nuclear and thermonuclear, respectively.

Nuclear Reactions

Nuclear fission separates or splits heavier atoms to form lighter atoms. Nuclear fusion combines lighter atoms to form heavier atoms. Both reactions generate roughly a million times more energy than comparable chemical reactions, making nuclear bombs a million times more powerful than non-nuclear bombs, which a French patent claimed in May 1939.

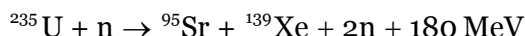
In some ways, fission and fusion are opposite and complementary reactions, but the particulars are unique for each. To understand how nuclear weapons are designed, it is useful to know the important similarities and differences between fission and fusion. The following explanation uses rounded numbers and approximations.

Fission

When a free neutron hits the nucleus of a fissile atom like uranium-235 (^{235}U), the

uranium nucleus splits into two smaller nuclei called fission fragments, plus more neutrons. Fission can be self-sustaining because it produces more neutrons of the speed required to cause new fissions.

The U-235 nucleus can split in many ways, provided the atomic numbers add up to 92 and the atomic masses add to 236 (uranium plus the extra neutron). The following equation shows one possible split, namely into strontium-95 (^{95}Sr), xenon-139 (^{139}Xe), and two neutrons (n), plus energy:



The immediate energy release per atom is about 180 million electron volts (MeV); i.e., 74 TJ/kg. Only 7% of this is gamma radiation and kinetic energy of fission neutrons. The remaining 93% is kinetic energy (or energy of motion) of the charged fission fragments, flying away from each other mutually repelled by the positive charge of their protons (38 for strontium, 54 for xenon). This initial kinetic energy is 67 TJ/kg, imparting an initial speed of about 12,000 kilometers per second. The charged fragments' high electric charge causes many inelastic collisions with nearby atoms, and these fragments remain trapped inside the bomb's uranium pit and tamper until their motion is converted into heat. This takes about a millionth of a second (a microsecond), by which time the core and tamper of the bomb have expanded to plasma several meters in diameter with a temperature of tens of millions of degrees Celsius.

This is hot enough to emit black-body radiation in the X-ray spectrum. These X-rays are absorbed by the surrounding air, producing the fireball and blast of a nuclear explosion.

Most fission products have too many neutrons to be stable so they are radioactive by beta decay, converting neutrons into protons by throwing off beta particles (electrons) and gamma rays. Their half-lives range from milliseconds to about 200,000 years. Many decay into isotopes that are themselves radioactive, so from 1 to 6 (average 3) decays may be required to reach stability. In reactors, the radioactive products are the nuclear waste in spent fuel. In bombs, they become radioactive fallout, both local and global.

Meanwhile, inside the exploding bomb, the free neutrons released by fission carry away about 3% of the initial fission energy. Neutron kinetic energy adds to the blast energy of a bomb, but not as effectively as the energy from charged fragments, since neutrons are not slowed as quickly. The main contribution of fission neutrons to the bomb's power is the initiation of other fissions. Over half of the neutrons escape the bomb core, but the rest strike U-235 nuclei causing them to fission in an exponentially growing chain reaction (1, 2, 4, 8, 16, etc). Starting from one atom, the number of fissions can theoretically double a hundred times in a microsecond, which could consume all uranium or plutonium up to hundreds of tons by the hundredth link in the chain. In practice, bombs do not contain hundreds of tons of uranium or plutonium. Instead, typically (in

a modern weapon) the core of a weapon contains only about 5 kilograms of plutonium, of which only 2 to 2.5 kilograms, representing 40 to 50 kilotons of energy, undergoes fission before the core blows itself apart.

Holding an exploding bomb together is the greatest challenge of fission weapon design. The heat of fission rapidly expands the fission core, spreading apart the target nuclei and making space for the neutrons to escape without being captured. The chain reaction stops.

Materials which can sustain a chain reaction are called fissile. The two fissile materials used in nuclear weapons are: U-235, also known as highly enriched uranium (HEU), or alloy (Oy) meaning Oak Ridge Alloy, or 25 (the last digits of the atomic number, which is 92 for uranium, and the atomic weight, here 235, respectively); and Pu-239, also known as plutonium, or 49 (from 94 and 239).

Uranium's most common isotope, U-238, is fissionable but not fissile (meaning that it cannot sustain a chain reaction by itself but can be made to fission with fast neutrons). Its aliases include natural or unenriched uranium, depleted uranium (DU), tubealloy (Tu), and 28. It cannot sustain a chain reaction, because its own fission neutrons are not powerful enough to cause more U-238 fission. The neutrons released by fusion will fission U-238. This U-238 fission reaction produces most of the energy in a typical two-stage thermonuclear weapon.

Fusion

Fusion produces neutrons which dissipate energy from the reaction. In weapons, the most important fusion reaction is called the D-T reaction. Using the heat and pressure of fission, hydrogen-2, or deuterium (^2D), fuses with hydrogen-3, or tritium (^3T), to form helium-4 (^4He) plus one neutron (n) and energy:



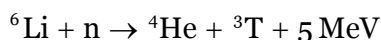
The total energy output, 17.6 MeV, is one tenth of that with fission, but the ingredients are only one-fiftieth as massive, so the energy output per unit mass is approximately five times as great. In this fusion reaction, 14 of the 17.6 MeV (80% of the energy released in the reaction) shows up as the kinetic energy of the neutron, which, having no electric charge and being almost as massive as the hydrogen nuclei that created it, can escape the scene without leaving its energy behind to help sustain the reaction – or to generate x-rays for blast and fire.

The only practical way to capture most of the fusion energy is to trap the neutrons inside a massive bottle of heavy material such as lead, uranium, or plutonium. If the 14 MeV neutron is captured by uranium (of either isotope; 14 MeV is high enough to fission both ^{235}U and ^{238}U) or plutonium, the result is fission and the release of 180 MeV of fission energy, multiplying the energy output tenfold.

For weapon use, fission is necessary to start fusion, helps to sustain fusion, and captures and multiplies the energy carried by the fusion neutrons. In the case of a neutron bomb, the last-mentioned factor does not apply, since the objective is to facilitate the escape of neutrons, rather than to use them to increase the weapon's raw power.

Tritium Production

A third important nuclear reaction is the one that creates tritium, essential to the type of fusion used in weapons. Tritium, or hydrogen-3, is made by bombarding lithium-6 (${}^6\text{Li}$) with a neutron (n). This neutron bombardment will cause the lithium-6 nucleus to split, producing helium-4 (${}^4\text{He}$) plus tritium (${}^3\text{T}$) and energy:



A nuclear reactor is necessary to provide the neutrons if the tritium is to be provided before the weapon is used. The industrial-scale conversion of lithium-6 to tritium is very similar to the conversion of uranium-238 into plutonium-239. In both cases the feed material is placed inside a nuclear reactor and removed for processing after a period of time.

Alternatively, neutrons from earlier stage fusion reactions can be used to fission lithium-6 (in the form of lithium deuteride for example) and form tritium during detonation. This approach reduces the amount of tritium-based fuel in a weapon.

The fission of one plutonium atom releases ten times more total energy than the fusion of one tritium atom. For this reason, tritium is included in nuclear weapon components only when it causes more fission than its production sacrifices, namely in the case of fusion-boosted fission.

Of the four basic types of nuclear weapon, the first, pure fission uses the first of the three nuclear reactions above. The second, fusion-boosted fission uses the first two. The third, two-stage thermonuclear, uses all three.

Pure Fission Weapons

The first task of a nuclear weapon design is to rapidly assemble a supercritical mass of fissile uranium or plutonium. A supercritical mass is one in which the percentage of fission-produced neutrons captured by another fissile nucleus is large enough that each fission event, on average, causes more than one additional fission event.

Once the critical mass is assembled, at maximum density, a burst of neutrons is supplied to start as many chain reactions as possible. Early weapons used a modulated neutron generator codenamed "Urchin" inside the pit containing polonium-210 and beryllium separated by a thin barrier. Implosion of the pit crushed the neutron generator, mixing

the two metals, thereby allowing alpha particles from the polonium to interact with beryllium to produce free neutrons. In modern weapons, the neutron generator is a high-voltage vacuum tube containing a particle accelerator which bombards a deuterium/tritium-metal hydride target with deuterium and tritium ions. The resulting small-scale fusion produces neutrons at a protected location outside the physics package, from which they penetrate the pit. This method allows better control of the timing of chain reaction initiation.

The critical mass of an uncompressed sphere of bare metal is 50 kg (110 lb) for uranium-235 and 16 kg (35 lb) for delta-phase plutonium-239. In practical applications, the amount of material required for criticality is modified by shape, purity, density, and the proximity to neutron-reflecting material, all of which affect the escape or capture of neutrons.

To avoid a chain reaction during handling, the fissile material in the weapon must be sub-critical before detonation. It may consist of one or more components containing less than one uncompressed critical mass each. A thin hollow shell can have more than the bare-sphere critical mass, as can a cylinder, which can be arbitrarily long without ever reaching criticality.

A tamper is an optional layer of dense material surrounding the fissile material. Due to its inertia it delays the expansion of the reacting material, increasing the efficiency of the weapon. Often the same layer serves both as tamper and as neutron reflector.

Gun-type Assembly Weapon

Little Boy, the Hiroshima bomb, used 64 kg (141 lb) of uranium with an average enrichment of around 80%, or 51 kg (112 lb) of U-235, just about the bare-metal critical mass. When assembled inside its tamper/reflector of tungsten carbide, the 64 kg (141 lb) was more than twice critical mass. Before the detonation, the uranium-235 was formed into two sub-critical pieces, one of which was later fired down a gun barrel to join the other, starting the nuclear explosion. Analysis shows that less than 2% of the uranium mass underwent fission; the remainder, representing most of the entire wartime output of the giant Y-12 factories at Oak Ridge, scattered uselessly.

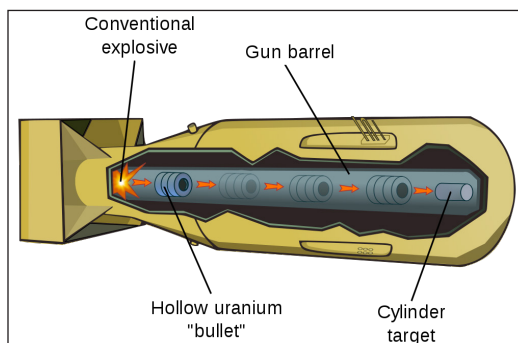
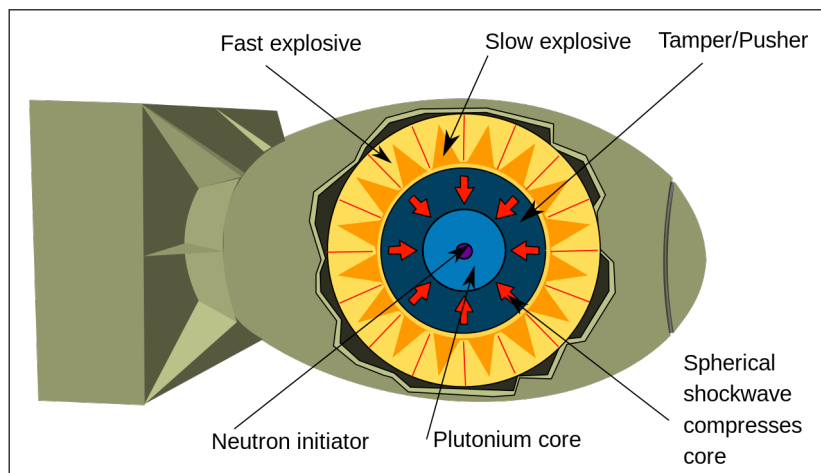


Diagram of a gun-type fission weapon.

The inefficiency was caused by the speed with which the uncompressed fissioning uranium expanded and became sub-critical by virtue of decreased density. Despite its inefficiency, this design, because of its shape, was adapted for use in small-diameter, cylindrical artillery shells (a gun-type warhead fired from the barrel of a much larger gun). Such warheads were deployed by the United States until 1992, accounting for a significant fraction of the U-235 in the arsenal, and were some of the first weapons dismantled to comply with treaties limiting warhead numbers. The rationale for this decision was undoubtedly a combination of the lower yield and grave safety issues associated with the gun-type design.

Implosion-type Weapon

For both the Trinity device and the Fat Man, the Nagasaki bomb, nearly identical plutonium fission through implosion designs was used. The Fat Man device specifically used 6.2 kg (14 lb), about 350 ml or 12 US fl oz in volume, of Pu-239, which is only 41% of bare-sphere critical mass. Surrounded by a U-238 reflector/tamper, the Fat Man's pit was brought close to critical mass by the neutron-reflecting properties of the U-238. During detonation, criticality was achieved by implosion. The plutonium pit was squeezed to increase its density by simultaneous detonation, as with the "Trinity" test detonation three weeks earlier, of the conventional explosives placed uniformly around the pit. The explosives were detonated by multiple exploding-bridgewire detonators. It is estimated that only about 20% of the plutonium underwent fission; the rest, about 5 kg (11 lb), was scattered.



An implosion shock wave might be of such short duration that only part of the pit is compressed at any instant as the wave passes through it. To prevent this, a pusher shell may be needed. The pusher is located between the explosive lens and the tamper. It works by reflecting some of the shock wave backwards, thereby having the effect of lengthening its duration. It is made out of a low density metal—such as aluminium, beryllium, or an alloy of the two metals (aluminium is easier and safer to shape, and

is two orders of magnitude cheaper; beryllium has high-neutron-reflective capability). Fat Man used an aluminium pusher.

The series of RaLa Experiment tests of implosion-type fission weapon design concepts, carried out from July 1944 through February 1945 at the Los Alamos Laboratory and a remote site 14.3 km (9 miles) east of it in Bayo Canyon, proved the practicality of the implosion design for a fission device, with the February 1945 tests positively determining its usability for the final Trinity/Fat Man plutonium implosion design.

The key to Fat Man's greater efficiency was the inward momentum of the massive U-238 tamper. (The natural uranium tamper did not undergo fission from thermal neutrons, but did contribute perhaps 20% of the total yield from fission by fast neutrons). Once the chain reaction started in the plutonium, the momentum of the implosion had to be reversed before expansion could stop the fission. By holding everything together for a few hundred nanoseconds more, the efficiency was increased.

Plutonium Pit

The core of an implosion weapon – the fissile material and any reflector or tamper bonded to it – is known as the pit. Some weapons tested during the 1950s used pits made with U-235 alone, or in composite with plutonium, but all-plutonium pits are the smallest in diameter and have been the standard since the early 1960s.

Casting and then machining plutonium is difficult not only because of its toxicity, but also because plutonium has many different metallic phases. As plutonium cools, changes in phase result in distortion and cracking. This distortion is normally overcome by alloying it with 30–35 mMol (0.9–1.0% by weight) galliums, forming a plutonium-gallium alloy, which causes it to take up its delta phase over a wide temperature range. When cooling from molten it then has only a single phase change, from epsilon to delta, instead of the four changes it would otherwise pass through. Other trivalent metals would also work, but gallium has a small neutron absorption cross section and helps protect the plutonium against corrosion. A drawback is that gallium compounds are corrosive and so if the plutonium is recovered from dismantled weapons for conversion to plutonium dioxide for power reactors, there is the difficulty of removing the gallium.

Because plutonium is chemically reactive it is common to plate the completed pit with a thin layer of inert metal, which also reduces the toxic hazard. The gadget used galvanic silver plating; afterwards, nickel deposited from nickel tetracarbonyl vapors was used, gold was preferred for many years. Recent designs improve safety by plating pits with vanadium to make the pits more fire-resistant.

Levitated-pit Implosion

The first improvement on the Fat Man design was to put an air space between the tamper and the pit to create a hammer-on-nail impact. The pit, supported on a hollow

cone inside the tamper cavity, was said to be levitated. The three tests of Operation Sandstone, in 1948, used Fat Man designs with levitated pits. The largest yield was 49 kilotons, more than twice the yield of the unlevitated Fat Man.

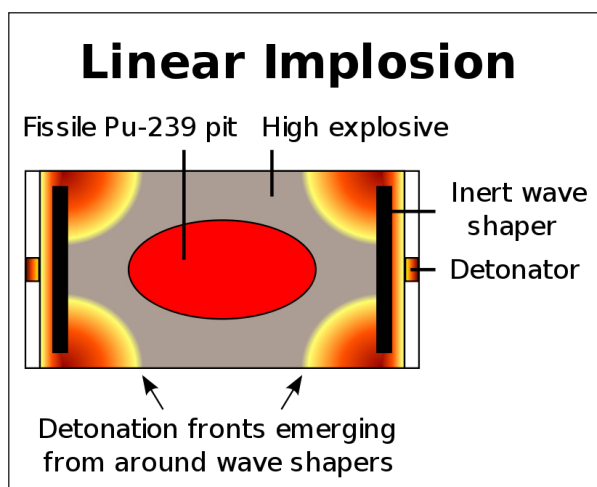
It was immediately clear that implosion was the best design for a fission weapon. Its only drawback seemed to be its diameter. Fat Man was 1.5 metres (5 ft) wide vs 61 centimetres (2 ft) for Little Boy.

Eleven years later, implosion designs had advanced sufficiently that the 1.5-metre (5 ft)-diameter sphere of Fat Man had been reduced to a 0.3-metre (1 ft)-diameter cylinder 0.61 metres (2 ft) long, the Swan device.

The Pu-239 pit of Fat Man was only 9.1 centimetres (3.6 in) in diameter, the size of a softball. The bulk of Fat Man's girth was the implosion mechanism, namely concentric layers of U-238, aluminium, and high explosives. The key to reducing that girth was the two-point implosion design.

Two-point Linear Implosion

In the two-point linear implosion, the nuclear fuel is cast into a solid shape and placed within the center of a cylinder of high explosive. Detonators are placed at either end of the explosive cylinder, and a plate-like insert, or shaper, is placed in the explosive just inside the detonators. When the detonators are fired, the initial detonation is trapped between the shaper and the end of the cylinder, causing it to travel out to the edges of the shaper where it is diffracted around the edges into the main mass of explosive. This causes the detonation to form into a ring that proceeds inwards from the shaper.



Due to the lack of a tamper or lenses to shape the progression, the detonation does not reach the pit in a spherical shape. To produce the desired spherical implosion, the fissile material itself is shaped to produce the same effect. Due to the physics of the shock wave propagation within the explosive mass, this requires the pit to be an oblong

shape, roughly egg shaped. The shock wave first reaches the pit at its tips, driving them inward and causing the mass to become spherical. The shock may also change plutonium from delta to alpha phase, increasing its density by 23%, but without the inward momentum of a true implosion.

The lack of compression makes such designs inefficient, but the simplicity and small diameter make it suitable for use in artillery shells and atomic demolition munitions – ADMs – also known as backpack or suitcase nukes; an example is the W48 artillery shell, the smallest nuclear weapon ever built or deployed. All such low-yield battlefield weapons, whether gun-type U-235 designs or linear implosion Pu-239 designs, pay a high price in fissile material in order to achieve diameters between six and ten inches (15 and 25 cm).

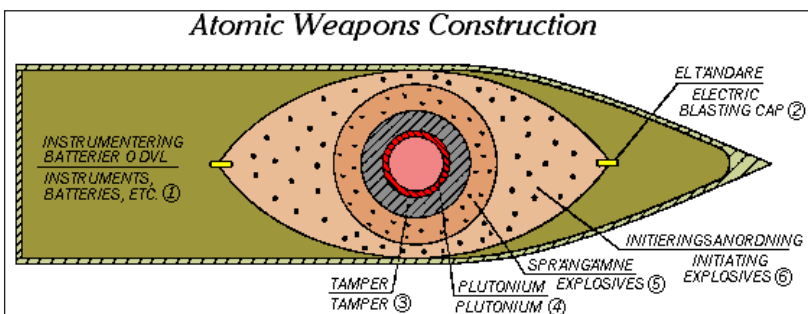
Two-point Hollow-pit Implosion

A more efficient two-point implosion system uses two high explosive lenses and a hollow pit.

A hollow plutonium pit was the original plan for the 1945 Fat Man bomb, but there was not enough time to develop and test the implosion system for it. A simpler solid-pit design was considered more reliable, given the time constraints, but it required a heavy U-238 tamper, a thick aluminium pusher, and three tons of high explosives.

After the war, interest in the hollow pit design was revived. Its obvious advantage is that a hollow shell of plutonium, shock-deformed and driven inward toward its empty center, would carry momentum into its violent assembly as a solid sphere. It would be self-tamping, requiring a smaller U-238 tamper, no aluminium pusher and less high explosive.

The Fat Man bomb had two concentric, spherical shells of high explosives, each about 25 cm (10 in) thick. The inner shell drove the implosion. The outer shell consisted of a soccer-ball pattern of 32 high explosive lenses, each of which converted the convex wave from its detonator into a concave wave matching the contour of the outer surface of the inner shell. If these 32 lenses could be replaced with only two, the high explosive sphere could become an ellipsoid (prolate spheroid) with a much smaller diameter.



A good illustration of these two features is a 1956 drawing from the Swedish nuclear weapons program (which was terminated before it produced a test explosion). The drawing shows the essential elements of the two-point hollow-pit design.

The mechanism of the high explosive lens is not shown in the Swedish drawing, but a standard lens made of fast and slow high explosives, as in Fat Man, would be much longer than the shape depicted. For a single high explosive lens to generate a concave wave that envelops an entire hemisphere, it must either be very long or the part of the wave on a direct line from the detonator to the pit must be slowed dramatically.

A slow high explosive is too fast, but the flying plate of an “air lens” is not. A metal plate, shock-deformed and pushed across an empty space, can be designed to move slowly enough. A two-point implosion system using air lens technology can have a length no more than twice its diameter, as in the Swedish diagram.

Fusion-boosted Fission Weapons

The next step in miniaturization was to speed up the fissioning of the pit to reduce the minimum inertial confinement time. This would allow the efficient fission of the fuel with less mass in the form of tamper or the fuel itself. The key to achieving faster fission would be to introduce more neutrons, and among the many ways to do this, adding a fusion reaction was relatively easy in the case of a hollow pit.

The easiest fusion reaction to achieve is found in a 50–50 mixture of tritium and deuterium. For fusion power experiments this mixture must be held at high temperatures for relatively lengthy times in order to have an efficient reaction. For explosive use, however, the goal is not to produce efficient fusion, but simply provide extra neutrons early in the process. Since a nuclear explosion is supercritical, any extra neutrons will be multiplied by the chain reaction, so even tiny quantities introduced early can have a large effect on the final outcome. For this reason, even the relatively low compression pressures and times (in fusion terms) found in the center of a hollow pit warhead are enough to create the desired effect.

In the boosted design, the fusion fuel in gas form is pumped into the pit during arming. This will fuse into helium and release free neutrons soon after fission begins. The neutrons will start a large number of new chain reactions while the pit is still critical or nearly critical. Once the hollow pit is perfected, there is little reason not to boost; deuterium and tritium are easily produced in the small quantities needed, and the technical aspects are trivial.

The concept of fusion-boosted fission was first tested on May 25, 1951, in the Item shot of Operation Greenhouse, Eniwetok, yield 45.5 kilotons.

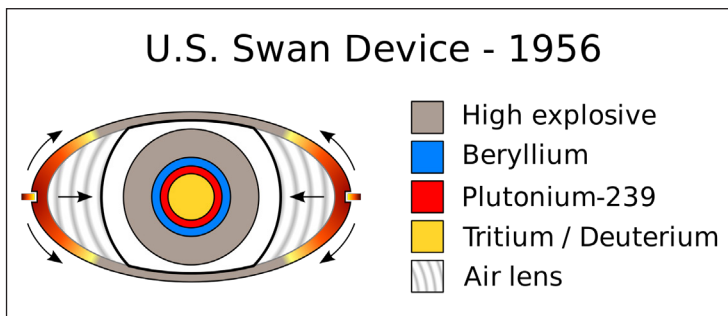
Boosting reduces diameter in three ways, all the result of faster fission:

- Since the compressed pit does not need to be held together as long, the massive

U-238 tamper can be replaced by a light-weight beryllium shell (to reflect escaping neutrons back into the pit). The diameter is reduced.

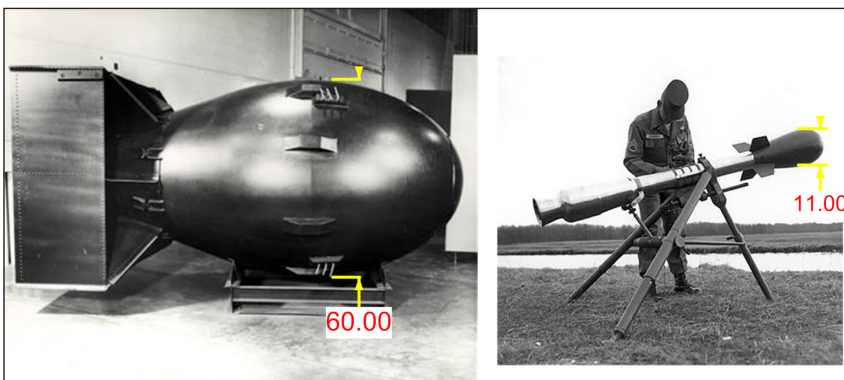
- The mass of the pit can be reduced by half, without reducing yield. Diameter is reduced again.
- Since the mass of the metal being imploded (tamper plus pit) is reduced, a smaller charge of high explosive is needed, reducing diameter even further.

Since boosting is required to attain full design yield, any reduction in boosting reduces yield. Boosted weapons are thus variable-yield weapons (also known as dial-a-yield); yield can be reduced any time before detonation simply by reducing the amount of deuterium/tritium inserted into the pit during the arming procedure.



The first device whose dimensions suggest employment of all these features (two-point, hollow-pit, fusion-boosted implosion) was the Swan device. It had a cylindrical shape with a diameter of 11.6 in (29 cm) and a length of 22.8 in (58 cm).

It was first tested standalone and then as the primary of a two-stage thermonuclear device during Operation Redwing. It was weaponized as the Robin primary and became the first off-the-shelf, multi-use primary, and the prototype for all that followed.



After the success of Swan, 11 or 12 inches (28 or 30 cm) seemed to become the standard diameter of boosted single-stage devices tested during the 1950s. Length was usually twice the diameter, but one such device, which became the W54 warhead, was closer

to a sphere, only 15 inches (38 cm) long. It was tested two dozen times in the 1957–62 period before being deployed. No other design had such a long string of test failures.

One of the applications of the W54 was the Davy Crockett XM-388 recoilless rifle projectile. It had a dimension of just 11 inches (28 cm), and is shown here in comparison to its Fat Man predecessor (60 inches (150 cm)).

Another benefit of boosting, in addition to making weapons smaller, lighter, and with less fissile material for a given yield, is that it renders weapons immune to radiation interference (RI). It was discovered in the mid-1950s that plutonium pits would be particularly susceptible to partial predetonation if exposed to the intense radiation of a nearby nuclear explosion (electronics might also be damaged, but this was a separate problem). RI was a particular problem before effective early warning radar systems because a first strike attack might make retaliatory weapons useless. Boosting reduces the amount of plutonium needed in a weapon to below the quantity which would be vulnerable to this effect.

Two-stage Thermonuclear Weapons

Pure fission or fusion-boosted fission weapons can be made to yield hundreds of kilotons, at great expense in fissile material and tritium, but by far the most efficient way to increase nuclear weapon yield beyond ten or so kilotons is to add a second independent stage, called a secondary.



Ivy Mike, the first two-stage thermonuclear detonation, 10.4 megatons.

In the 1940s, bomb designers at Los Alamos thought the secondary would be a canister of deuterium in liquefied or hydride form. The fusion reaction would be D-D, harder to achieve than D-T, but more affordable. A fission bomb at one end would shock-compress and heats the near end, and fusion would propagate through the canister to the far end. Mathematical simulations showed it would not work, even with large amounts of expensive tritium added.

The entire fusion fuel canister would need to be enveloped by fission energy, to both compress and heat it, as with the booster charge in a boosted primary. The design

breakthrough came in January 1951, when Edward Teller and Stanislaw Ulam invented radiation implosion—for nearly three decades known publicly only as the Teller-Ulam H-bomb secret.

The concept of radiation implosion was first tested on May 9, 1951, in the George shot of Operation Greenhouse, Eniwetok, yield 225 kilotons. The first full test was on November 1, 1952, the Mike shot of Operation Ivy, Eniwetok, yield 10.4 megatons.

In radiation implosion, the burst of X-ray energy coming from an exploding primary is captured and contained within an opaque-walled radiation channel which surrounds the nuclear energy components of the secondary. The radiation quickly turns the plastic foam that had been filling the channel into a plasma which is mostly transparent to X-rays, and the radiation is absorbed in the outermost layers of the pusher/tamper surrounding the secondary, which ablates and applies a massive force (much like an inside out rocket engine) causing the fusion fuel capsule to implode much like the pit of the primary. As the secondary implodes a fissile “spark plug” at its center ignites and provides neutrons and heat which enable the lithium deuteride fusion fuel to produce tritium and ignite as well. The fission and fusion chain reactions exchange neutrons with each other and boost the efficiency of both reactions. The greater implosive force, enhanced efficiency of the fissile “spark plug” due to boosting via fusion neutrons, and the fusion explosion itself provide significantly greater explosive yield from the secondary despite often not being much larger than the primary.

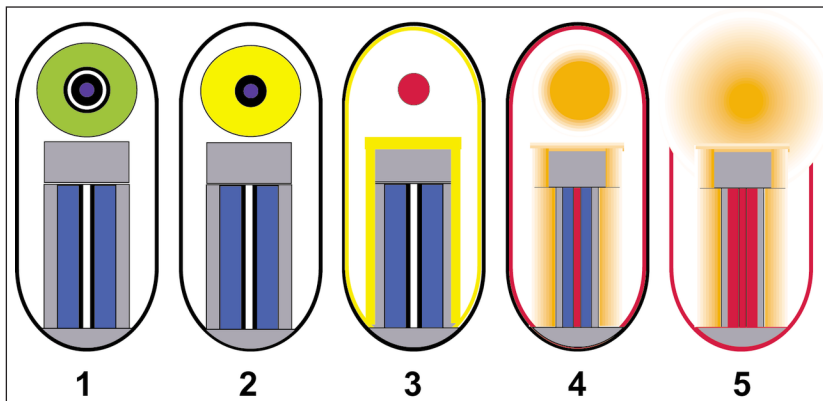


Figure shows ablation mechanism firing sequence:

- Warhead before firing: The nested spheres at the top are the fission primary; the cylinders below are the fusion secondary device.
- Fission primary’s explosives have detonated and collapsed the primary’s fissile pit.
- The primary’s fission reaction has run to completion, and the primary is now at several million degrees and radiating gamma and hard X-rays, heating up the inside of the hohlraum, the shield, and the secondary’s tamper.

- The primary's reaction is over and it has expanded. The surface of the pusher for the secondary is now so hot that it is also ablating or expanding away, pushing the rest of the secondary (tamper, fusion fuel, and fissile spark plug) inwards. The spark plug starts to fission. Not depicted: the radiation case is also ablating and expanding outwards (omitted for clarity of diagram).
- The secondary's fuel has started the fusion reaction and shortly will burn up. A fireball starts to form.

For example, for the Redwing Mohawk test on July 3, 1956, a secondary called the Flute was attached to the Swan primary. The Flute was 15 inches (38 cm) in diameter and 23.4 inches (59 cm) long, about the size of the Swan. But it weighed ten times as much and yielded 24 times as much energy (355 kilotons, vs 15 kilotons).

Equally important, the active ingredients in the Flute probably cost no more than those in the Swan. Most of the fission came from cheap U-238, and the tritium was manufactured in place during the explosion. Only the spark plug at the axis of the secondary needed to be fissile.

A spherical secondary can achieve higher implosion densities than a cylindrical secondary, because spherical implosion pushes in from all directions toward the same spot. However, in warheads yielding more than one megaton, the diameter of a spherical secondary would be too large for most applications. A cylindrical secondary is necessary in such cases. The small, cone-shaped re-entry vehicles in multiple-warhead ballistic missiles after 1970 tended to have warheads with spherical secondaries, and yields of a few hundred kilotons.

As with boosting, the advantages of the two-stage thermonuclear design are so great that there is little incentive not to use it, once a nation has mastered the technology.

In engineering terms, radiation implosion allows for the exploitation of several known features of nuclear bomb materials which heretofore had eluded practical application. For example:

- The optimal way to store deuterium in a reasonably dense state is to chemically bond it with lithium, as lithium deuteride. But the lithium-6 isotope is also the raw material for tritium production, and an exploding bomb is a nuclear reactor. Radiation implosion will hold everything together long enough to permit the complete conversion of lithium-6 into tritium, while the bomb explodes. So the bonding agent for deuterium permits use of the D-T fusion reaction without any pre-manufactured tritium being stored in the secondary. The tritium production constraint disappears.
- For the secondary to be imploded by the hot, radiation-induced plasma surrounding it, it must remain cool for the first microsecond, i.e., it must be encased

in a massive radiation (heat) shield. The shield's massiveness allows it to double as a tamper, adding momentum and duration to the implosion. No material is better suited for both of these jobs than ordinary, cheap uranium-238, which also happens to undergo fission when struck by the neutrons produced by D-T fusion. This casing, called the pusher, thus has three jobs: to keep the secondary cool; to hold it, inertially, in a highly compressed state; and, finally, to serve as the chief energy source for the entire bomb. The consumable pusher makes the bomb more a uranium fission bomb than a hydrogen fusion bomb. Insiders never used the term "hydrogen bomb".

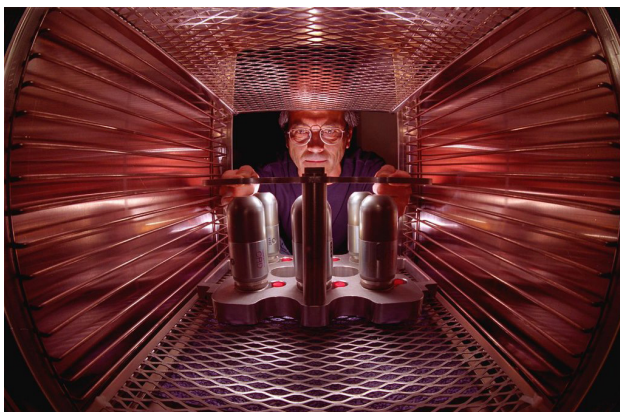
- Finally, the heat for fusion ignition comes not from the primary but from a second fission bomb called the spark plug, embedded in the heart of the secondary. The implosion of the secondary implodes this spark plug, detonating it and igniting fusion in the material around it, but the spark plug then continues to fission in the neutron-rich environment until it is fully consumed, adding significantly to the yield.

The initial impetus behind the two-stage weapon was President Truman's 1950 promise to build a 10-megaton hydrogen superbomb as the U.S. response to the 1949 test of the first Soviet fission bomb. But the resulting invention turned out to be the cheapest and most compact way to build small nuclear bombs as well as large ones, erasing any meaningful distinction between A-bombs and H-bombs, and between boosters and supers. All preferred techniques for fission and fusion explosions are incorporated into one all-encompassing, fully scalable design principle. Even 6-inch (150 mm) diameter nuclear artillery shells can be two-stage thermonuclears.

In the ensuing fifty years, nobody has come up with a more efficient way to build a nuclear bomb. It is the design of choice for the United States, Russia, the United Kingdom, China, and France, the five thermonuclear powers. On 3 September 2017 North Korea carried out what it reported as its first "two-stage thermo-nuclear weapon" test. According to Dr. Theodore Taylor, after reviewing leaked photographs of disassembled weapons components taken before 1986, Israel possessed boosted weapons and would require supercomputers of that era to advance further toward full two-stage weapons in the megaton range without nuclear test detonations. The other nuclear-armed nations, India and Pakistan, probably have single-stage weapons, possibly boosted.

Interstage

In a two-stage thermonuclear weapon the energy from the primary impacts the secondary. An essential energy transfer modulator called the interstage, between the primary and the secondary, protects the secondary's fusion fuel from heating too quickly, which could cause it to explode in a conventional (and small) heat explosion before the fusion and fission reactions get a chance to start.



W76 Neutron Tubes in a Gun Carriage Style Fixture.

There is very little information in the open literature about the mechanism of the interstage. Its first mention in a U.S. government document formally released to the public appears to be a caption in a graphic promoting the Reliable Replacement Warhead Program in 2007. If built, this new design would replace “toxic, brittle material” and “expensive ‘special’ material” in the interstage. This statement suggests the interstage may contain beryllium to moderate the flux of neutrons from the primary, and perhaps something to absorb and re-radiate the x-rays in a particular manner. There is also some speculation that this interstage material, which may be code-named FOGBANK, might be an aerogel, possibly doped with beryllium and/or other substances.

The interstage and the secondary are encased together inside a stainless steel membrane to form the canned subassembly (CSA), an arrangement which has never been depicted in any open-source drawing. The most detailed illustration of an interstage shows a British thermonuclear weapon with a cluster of items between its primary and a cylindrical secondary. They are labeled “end-cap and neutron focus lens”, “reflector/neutron gun carriage”, and “reflector wrap”. The origin of the drawing, posted on the internet by Greenpeace, is uncertain, and there is no accompanying explanation.

Specific Designs

While every nuclear weapon design falls into one of the above categories, specific designs have occasionally become the subject of news accounts and public discussion, often with incorrect descriptions about how they work and what they do. Examples:

Hydrogen Bombs

While all modern nuclear weapons (fission and fusion alike) make some use of D-T fusion, in the public perception hydrogen bombs are multi-megaton devices a thousand times more powerful than Hiroshima’s Little Boy. Such high-yield bombs are actually two-stage thermonuclears, scaled up to the desired yield, with uranium fission, as usual, providing most of their energy.

The idea of the hydrogen bomb first came to public attention in 1949, when prominent scientists openly recommended against building nuclear bombs more powerful than the standard pure-fission model, on both moral and practical grounds. Their assumption was that critical mass considerations would limit the potential size of fission explosions, but that a fusion explosion could be as large as its supply of fuel, which has no critical mass limit. In 1949, the Soviets exploded their first fission bomb, and in 1950 U.S. President Harry S. Truman ended the H-bomb debate by ordering the Los Alamos designers to build one.

In 1952, the 10.4-megaton Ivy Mike explosion was announced as the first hydrogen bomb test, reinforcing the idea that hydrogen bombs are a thousand times more powerful than fission bombs.

In 1954, J. Robert Oppenheimer was labeled a hydrogen bomb opponent. The public did not know there were two kinds of hydrogen bomb (neither of which is accurately described as a hydrogen bomb). On May 23, when his security clearance was revoked, item three of the four public findings against him was “his conduct in the hydrogen bomb program.” In 1949, Oppenheimer had supported single-stage fusion-boosted fission bombs, to maximize the explosive power of the arsenal given the trade-off between plutonium and tritium production. He opposed two-stage thermonuclear bombs until 1951, when radiation implosion, which he called “technically sweet”, first made them practical. The complexity of his position was not revealed to the public until 1976, nine years after his death.

When ballistic missiles replaced bombers in the 1960s, most multi-megaton bombs were replaced by missile warheads (also two-stage thermonuclears) scaled down to one megaton or less.

Alarm Clock/Sloika

The first effort to exploit the symbiotic relationship between fission and fusion was a 1940s design that mixed fission and fusion fuel in alternating thin layers. As a single-stage device, it would have been a cumbersome application of boosted fission. It first became practical when incorporated into the secondary of a two-stage thermonuclear weapon.

The U.S. name, Alarm Clock, came from Teller: he called it that because it might “wake up the world” to the possibility of the potential of the Super. The Russian name for the same design was more descriptive: Sloika, a layered pastry cake. A single-stage Soviet Sloika was tested on August 12, 1953. No single-stage U.S. version was tested, but the Union shot of Operation Castle, April 26, 1954, was a two-stage thermonuclear device code-named Alarm Clock. Its yield, at Bikini, was 6.9 megatons.

Because the Soviet Sloika test used dry lithium-6 deuteride eight months before the first U.S. test to use it, it was sometimes claimed that the USSR won the H-bomb

race, even though the United States tested and developed the first hydrogen bomb: the Ivy Mike H-bomb test. The 1952 U.S. Ivy Mike test used cryogenically cooled liquid deuterium as the fusion fuel in the secondary, and employed the D-D fusion reaction. However, the first Soviet test to use a radiation-imploded secondary, the essential feature of a true H-bomb, was on November 23, 1955, three years after Ivy Mike. In fact, real work on the implosion scheme in the Soviet Union only commenced in the very early part of 1953, several months after the successful testing of Sloika.

Clean Bombs

On March 1, 1954, the largest-ever U.S. nuclear test explosion, the 15-megaton Bravo shot of Operation Castle at Bikini Atoll, delivered a promptly lethal dose of fission-product fallout to more than 6,000 square miles (16,000 km²) of Pacific Ocean surface. Radiation injuries to Marshall Islanders and Japanese fishermen made that fact public and revealed the role of fission in hydrogen bombs.



Bassoon, the prototype for a 9.3-megaton clean bomb or a 25-megaton dirty bomb. Dirty version shown here, before its 1956 test. The two attachments on the left are light pipes.

In response to the public alarm over fallout, an effort was made to design a clean multi-megaton weapon, relying almost entirely on fusion. The energy produced by the fissioning of unenriched natural uranium, when used as the tamper material in the secondary and subsequent stages in the Teller-Ulam design, can far exceed the energy released by fusion, as was the case in the Castle Bravo test; realizing that a non-fissionable tamper material is an essential requirement in a 'clean' bomb, it is clear that in such a bomb there will be a relatively massive amount of material that does not contribute energy by either fission or fusion. So for a given weight, 'dirty' weapons with fissionable tampers are much more powerful than a 'clean' weapon (or, for an equal yield, they are much lighter). The earliest known incidence of a three-stage device being tested, with the third stage, called the tertiary, being ignited by the secondary, was May 27, 1956 in the Bassoon device. This device was tested in the Zuni shot of Operation

Redwing. This shot used non-fissionable tampers; an inert substitute material such as tungsten or lead was used. Its yield was 3.5 megatons, 85% fusion and only 15% fission.

The public records for devices that produced the highest proportion of their yield via fusion reactions are the peaceful nuclear explosions of the 1970s, with the 3 detonations that excavated part of Pechora–Kama Canal being cited as 98% fusion each in the Taiga test's 15 kiloton explosive yield devices; that is, a total fission fraction of 0.3 kilotons in a 15 kt device. Others include the 50 megaton Tsar Bomba at 97% fusion, the 9.3 megaton Hardtack Poplar test at 95.2%, and the 4.5 megaton Redwing Navajo test at 95% fusion.

On July 19, 1956, AEC Chairman Lewis Strauss said that the Redwing Zuni shot clean bomb test “produced much of importance from a humanitarian aspect.” However, less than two days after this announcement, the dirty version of Bassoon, called Bassoon Prime, with a uranium-238 tamper in place, was tested on a barge off the coast of Bikini Atoll as the Redwing Tewa shot. The Bassoon Prime produced a 5-megaton yield, of which 87% came from fission. Data obtained from this test, and others, culminated in the eventual deployment of the highest yielding US nuclear weapon known, and the highest yield-to-weight weapon ever made, a three-stage thermonuclear weapon with a maximum “dirty” yield of 25 megatons, designated as the B41 nuclear bomb, which was to be carried by U.S. Air Force bombers until it was decommissioned; this weapon was never fully tested.

As such, high-yield clean bombs appear to have been of little value from a military standpoint. The actual deployed weapons were the dirty versions, which maximized yield for the same size device. The need for low fission fraction nuclear devices was driven only by the likes of Project Orion and peaceful nuclear explosions - for earth excavation with little contamination of the resulting excavated area.

Third Generation Nuclear Weapons

First and second generation nuclear weapons release energy as omnidirectional blasts. Third generation nuclear weapons are experimental special effect warheads and devices that can release energy in a directed manner, some of which were tested during the Cold War but were never deployed. These include:

- Project Prometheus, also known as “Nuclear Shotgun”, which would have used a nuclear explosion to accelerate kinetic penetrators against ICBMs.
- Project Excalibur, a nuclear-pumped X-ray laser.

Fourth Generation Nuclear Weapons

Newer 4th-generation nuclear weapons designs including pure fusion weapons and antimatter-catalyzed nuclear pulse propulsion-like devices are being studied by the five largest nuclear weapon states.

Nanotechnology can theoretically produce miniaturised laser-triggered pure fusion weapons that will be easier to produce than conventional nuclear weapons.

Cobalt Bombs

A doomsday bomb, made popular by Nevil Shute's 1957 novel, and subsequent 1959 movie, *On the Beach*, the cobalt bomb is a hydrogen bomb with a jacket of cobalt. The neutron-activated cobalt would have maximized the environmental damage from radioactive fallout. These bombs were popularized in the 1964 film *Dr. Strangelove or: How I Learned to Stop Worrying and Love the Bomb*; the material added to the bombs is referred to in the film as 'cobalt-thorium G'.

Such "salted" weapons were requested by the U.S. Air Force and seriously investigated, possibly built and tested, but not deployed. In the 1964 edition of the DOD/AEC book *The Effects of Nuclear Weapons*, a new section titled *Radiological Warfare* clarified the issue. Fission products are as deadly as neutron-activated cobalt. The standard high-fission thermonuclear weapon is automatically a weapon of radiological warfare, as dirty as a cobalt bomb.

Initially, gamma radiation from the fission products of an equivalent size fission-fusion-fission bomb are much more intense than Co-60: 15,000 times more intense at 1 hour; 35 times more intense at 1 week; 5 times more intense at 1 month; and about equal at 6 months. Thereafter fission drops off rapidly so that Co-60 fallout is 8 times more intense than fission at 1 year and 150 times more intense at 5 years. The very long-lived isotopes produced by fission would overtake the ^{60}Co again after about 75 years.

The triple "taiga" nuclear salvo test, as part of the preliminary March 1971 Pechora-Kama Canal project, produced a small amount of fission products and therefore a comparatively large amount of case material activated products are responsible for most of the residual activity at the site today, namely Co-60. With this fusion generated neutron activation product being responsible for about half of the gamma dose now at the test site, albeit with that dose being too small to cause deleterious effects, normal green vegetation exists all around the lake that was formed.

Fission-fusion-fission Bombs vs. Three-stage (Tertiary) Bombs

In 1954, to explain the surprising amount of fission-product fallout produced by hydrogen bombs, Ralph Lapp coined the term fission-fusion-fission to describe a process inside what he called a three-stage thermonuclear weapon. His process explanation was correct, but his choice of terms caused confusion in the open literature. The stages of a nuclear weapon are not fission, fusion, and fission. They are the primary, the secondary, and, in a very few exceptional and powerful weapons no longer in service, the tertiary. Tertiary (three-stage) designs, such as the U.S. B41 nuclear bomb and the Soviet Tsar Bomba, were developed in the late 1950s and early 1960s; all have since been

retired, as the typical multi-megaton yields of tertiary bombs do not destroy targets efficiently, since they waste energy in a sphere above and below an area of land. For this reason, all tertiary bombs have given way in modern nuclear arsenals to multiple smaller two-stage bomb tactics. Such two-stage bombs, even though less efficient in yield, are nevertheless more destructive for their total bomb weight, because they can be distributed over a roughly two-dimensional area of land at the target.

All so-called “fission-fusion-fission” weapons (i.e., all conventional modern thermonuclear warheads) employ the additional step of “jacket fissioning”, using fusion neutrons. This works as follows: the high-energy or “fast” neutrons generated by fusion are used to fission a fissionable jacket located around the fusion stage. In the past this jacket was often made of natural or depleted uranium; but today’s weapons in which there is a premium on weight and size (i.e., virtually all modern strategic weapons) use moderately-to-highly enriched uranium as the jacketing material. The fast fission of the secondary jacket in fission-fusion-fission bombs is sometimes referred to as a “third stage” in the bomb, but it should not be confused with the obsolete true three-stage thermonuclear design, in which there existed another complete tertiary fusion stage.

In the era of open-air atomic testing, the fission jacket was sometimes omitted, in order to create so-called “clean bombs”, or to reduce the amount of radioactive fallout from fission products in very large multi-megaton blasts. This was done most often in the testing of very large tertiary bomb designs, such as the Tsar Bomba and the Zuni test shot of Operation Redwing. In the testing of such weapons, it was assumed (and sometimes shown operationally) that a jacket of natural uranium or enriched uranium could always be added to a given unjacketed bomb, if desired, to increase the yield from two to five times.

Arbitrarily Large Multi-staged Devices

The idea of a device which has an arbitrarily large number of Teller-Ulam stages, with each driving a larger radiation-driven implosion than the preceding stage, is frequently suggested, but technically disputed. There are “well-known sketches and some reasonable-looking calculations in the open literature about two-stage weapons, but no similarly accurate descriptions of true three stage concepts.”

According to George Lemmer’s 1967 Air Force and Strategic Deterrence 1951–1960 paper, in 1957, LANL stated that a 1,000-megaton warhead could be built. Apparently there were three of these US designs analyzed in the gigaton (1,000-megaton) range; LLNL’s GNOMON and SUNDIAL – objects that cast shadows – and LANL’s “TAV”. SUNDIAL attempting to have a 10 Gt yield, while the Gnomon and TAV designs attempted to produce a yield of 1 Gt. A freedom of information request was filed (FOIA 13-00049-K) for information on the three above US designs. The request was denied under statutory exemptions relating to classified material; the denial was appealed, but the request was finally denied again in April 2016.

Following the concern caused by the estimated gigaton scale of the 1994 Comet Shoemaker-Levy 9 impacts on the planet Jupiter, in a 1995 meeting at Lawrence Livermore National Laboratory (LLNL), Edward Teller proposed to a collective of U.S. and Russian ex-Cold War weapons designers that they collaborate on designing a 1000-megaton nuclear explosive device for diverting extinction-class asteroids (10+ km in diameter), which would be employed in the event that one of these asteroids were on an impact trajectory with Earth.

There have also been some calculations made in 1979 by Lowell Wood, Teller's protégé, that Teller's initially-unworkable "classical Super" design, analogous to igniting a candlestick of deuterium fuel, could potentially achieve ignition reliably were it touched off by a sufficiently-large Teller-Ulam device, rather than the gun-type fission weapon used in the original design.

Neutron Bombs

A neutron bomb, technically referred to as an enhanced radiation weapon (ERW), is a type of tactical nuclear weapon designed specifically to release a large portion of its energy as energetic neutron radiation. This contrasts with standard thermonuclear weapons, which are designed to capture this intense neutron radiation to increase its overall explosive yield. In terms of yield, ERWs typically produce about one-tenth that of a fission-type atomic weapon. Even with their significantly lower explosive power, ERWs are still capable of much greater destruction than any conventional bomb. Meanwhile, relative to other nuclear weapons, damage is more focused on biological material than on material infrastructure (though extreme blast and heat effects are not eliminated).

ERWs are more accurately described as suppressed yield weapons. When the yield of a nuclear weapon is less than one kiloton, its lethal radius from blast, 700 m (2,300 ft), is less than that from its neutron radiation. However, the blast is more than potent enough to destroy most structures, which are less resistant to blast effects than even unprotected human beings. Blast pressures of upwards of 20 PSI are survivable, whereas most buildings will collapse with a pressure of only 5 PSI.

Commonly misconceived as a weapon designed to kill populations and leave infrastructure intact, these bombs are still very capable of leveling buildings over a large radius. The intent of their design was to kill tank crews – tanks giving excellent protection against blast and heat, surviving (relatively) very close to a detonation. And with the Soviets' vast tank battalions during the Cold War, this was the perfect weapon to counter them. The neutron radiation could instantly incapacitate a tank crew out to roughly the same distance that the heat and blast would incapacitate an unprotected human (depending on design). The tank chassis would also be rendered highly radioactive, temporarily preventing its re-use by a fresh crew.

Neutron weapons were also intended for use in other applications, however. For

example, they are effective in anti-nuclear defenses – the neutron flux being capable of neutralising an incoming warhead at a greater range than heat or blast. Nuclear warheads are very resistant to physical damage, but are very difficult to harden against extreme neutron flux.

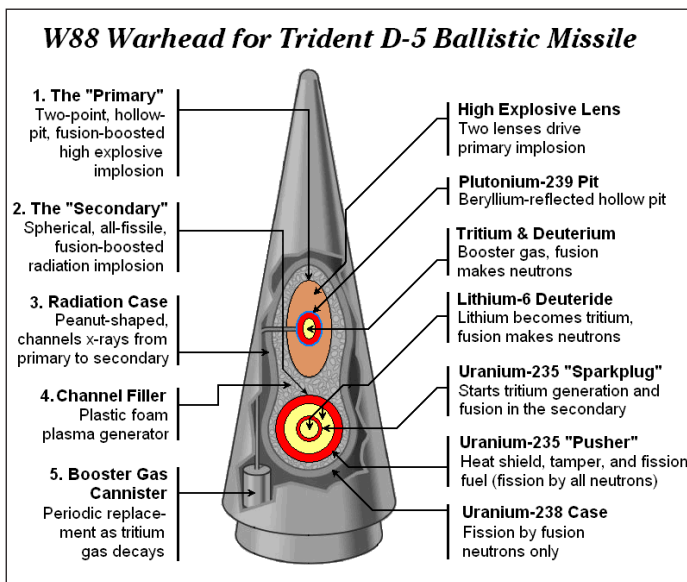
Table: Energy distribution of weapon.

	Standard	Enhanced
Blast	50%	40%
Thermal energy	35%	25%
Instant radiation	5%	30%
Residual radiation	10%	5%

ERWs were two-stage thermonuclears with all non-essential uranium removed to minimize fission yield. Fusion provided the neutrons. Developed in the 1950s, they were first deployed in the 1970s, by U.S. forces in Europe. The last ones were retired in the 1990s.

A neutron bomb is only feasible if the yield is sufficiently high that efficient fusion stage ignition is possible, and if the yield is low enough that the case thickness will not absorb too many neutrons. This means that neutron bombs have a yield range of 1–10 kilotons, with fission proportion varying from 50% at 1-kiloton to 25% at 10-kilotons (all of which comes from the primary stage). The neutron output per kiloton is then 10–15 times greater than for a pure fission implosion weapon or for a strategic warhead like a W87 or W88.

Oralloy Thermonuclear Warheads



Drawing of W-88.

In 1999, nuclear weapon design was in the news again, for the first time in decades. In January, the U.S. House of Representatives released the Cox Report (Christopher Cox R-CA) which alleged that China had somehow acquired classified information about the U.S. W88 warhead. Nine months later, Wen Ho Lee, a Taiwanese immigrant working at Los Alamos, was publicly accused of spying, arrested, and served nine months in pre-trial detention, before the case against him was dismissed. It is not clear that there was, in fact, any espionage.

In the course of eighteen months of news coverage, the W88 warhead was described in unusual detail. The New York Times printed a schematic diagram on its front page. The most detailed drawing appeared in *A Convenient Spy*, the 2001 book on the Wen Ho Lee case by Dan Stober and Ian Hoffman, adapted and shown here with permission.

Designed for use on Trident II (D-5) submarine-launched ballistic missiles, the W88 entered service in 1990 and was the last warhead designed for the U.S. arsenal. It has been described as the most advanced, although open literature accounts do not indicate any major design features that were not available to U.S. designers in 1958.

The above diagram shows all the standard features of ballistic missile warheads since the 1960s, with two exceptions that give it a higher yield for its size.

- The outer layer of the secondary, called the “pusher”, which serves three functions: heat shield, tamper, and fission fuel, is made of U-235 instead of U-238, hence the name Oralloid (U-235) Thermonuclear. Being fissile, rather than merely fissionable, allows the pusher to fission faster and more completely, increasing yield. This feature is available only to nations with a great wealth of fissile uranium. The United States is estimated to have 500 tons.
- The secondary is located in the wide end of the re-entry cone, where it can be larger, and thus more powerful. The usual arrangement is to put the heavier, denser secondary in the narrow end for greater aerodynamic stability during re-entry from outer space, and to allow more room for a bulky primary in the wider part of the cone. (The W87 warhead drawing in the W87 article shows the usual arrangement.) Because of this new geometry, the W88 primary uses compact conventional high explosives (CHE) to save space, rather than the more usual, and bulky but safer, insensitive high explosives (IHE). The re-entry cone probably has ballast in the nose for aerodynamic stability.

The alternating layers of fission and fusion material in the secondary are an application of the Alarm Clock/Sloika principle.

Reliable Replacement Warhead

The United States has not produced any nuclear warheads since 1989, when the Rocky Flats pit production plant, near Boulder, Colorado, was shut down for environmental

reasons. With the end of the Cold War two years later, the production line was idled except for inspection and maintenance functions.

The National Nuclear Security Administration, the latest successor for nuclear weapons to the Atomic Energy Commission and the Department of Energy, has proposed building a new pit facility and starting the production line for a new warhead called the Reliable Replacement Warhead (RRW). Two advertised safety improvements of the RRW would be a return to the use of “insensitive high explosives which are far less susceptible to accidental detonation”, and the elimination of “certain hazardous materials, such as beryllium, that are harmful to people and the environment.” Because of the U.S. moratorium on nuclear explosive testing, any new design would rely on previously tested concepts.

Underground Nuclear Weapons Testing

Underground nuclear testing is the test detonation of nuclear weapons that is performed underground. When the device being tested is buried at sufficient depth, the explosion may be contained, with no release of radioactive materials to the atmosphere.

The extreme heat and pressure of an underground nuclear explosion causes changes in the surrounding rock. The rock closest to the location of the test is vaporised, forming a cavity. Farther away, there are zones of crushed, cracked, and irreversibly strained rock. Following the explosion, the rock above the cavity may collapse, forming a rubble chimney. If this chimney reaches the surface, a bowl-shaped subsidence crater may form.



Preparation for an underground nuclear test at the Nevada Test Site in the 1990s.

The first underground test took place in 1951; further tests provided information that eventually led to the signing of the Limited Test Ban Treaty in 1963, which banned all nuclear tests except for those performed underground. From then until the signing of the Comprehensive Test Ban Treaty in 1996, most nuclear tests were performed underground, in order to prevent nuclear fallout from entering into the atmosphere.

Although public concern about fallout from nuclear testing grew in the early 1950s, fallout was discovered after the Trinity test in 1945. Photographic film manufacturers would later report ‘fogged’ films; this was traced to packaging materials sourced from Indiana crops, contaminated by the Trinity and later tests at the Nevada Test Site, over 1,000 miles away. Intense fallout from the 1953 Simon test was documented as far as Albany, New York.

The fallout from the March 1954 Bravo test in the Pacific would have “scientific, political and social implications that have continued for more than 40 years”. The multi-megaton test caused fallout to occur on the islands of the Rongerik and Rongelap atolls, and a Japanese fishing boat known as the Daigo Fukuryū Maru (Lucky Dragon). Prior to this test, there was “insufficient” appreciation of the dangers of fallout.

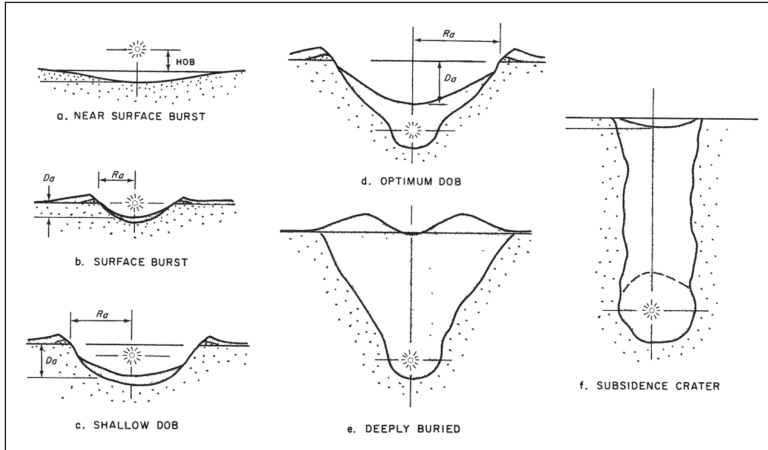
The test became an international incident. In a PBS interview, the historian Martha Smith argued: “In Japan, it becomes a huge issue in terms of not just the government and its protest against the United States, but all different groups and all different peoples in Japan start to protest. It becomes a big issue in the media. There are all kinds of letters and protests that come from, not surprisingly, Japanese fishermen, the fishermen’s wives; there are student groups, all different types of people; that protest against the Americans’ use of the Pacific for nuclear testing. They’re very concerned about, first of all, why the United States even has the right to be carrying out those kinds of tests in the Pacific. They’re also concerned about the health and environmental impact.” The Prime Minister of India “voiced the heightened international concern” when he called for the elimination of all nuclear testing worldwide.

Knowledge about fallout and its effects grew, and with it concern about the global environment and long-term genetic damage. Talks between the United States, the United Kingdom, Canada, France, and the Soviet Union began in May 1955 on the subject of an international agreement to end nuclear tests. On August 5, 1963, representatives of the United States, the Soviet Union, and the United Kingdom signed the Limited Test Ban Treaty, forbidding testing of nuclear weapons in the atmosphere, in space, and underwater. Agreement was facilitated by the decision to allow underground testing, eliminating the need for on-site inspections that concerned the Soviets. Underground testing was allowed, provided that it does not cause “radioactive debris to be present outside the territorial limits of the State under whose jurisdiction or control such explosion is conducted”.

Effects

The effects of an underground nuclear test may vary according to factors including the depth and yield of the explosion, as well as the nature of the surrounding rock. If the test is conducted at sufficient depth, the test is said to be contained, with no venting of gases or other contaminants to the environment. In contrast, if the device is buried at insufficient depth (“underburied”), then rock may be expelled by the explosion, forming

a crater surrounded by ejecta, and releasing high-pressure gases to the atmosphere (the resulting crater is usually conical in profile, circular, and may range between tens to hundreds of metres in diameter and depth). One figure used in determining how deeply the device should be buried is the scaled depth of burial, or -burst. This figure is calculated as the burial depth in metres divided by the cube root of the yield in kilotons. It is estimated that, in order to ensure containment, this figure should be greater than 100.



Relative crater sizes and shapes resulting from various burst depths.

The energy of the nuclear explosion is released in one microsecond. In the following few microseconds, the test hardware and surrounding rock are vaporised, with temperatures of several million degrees and pressures of several million atmospheres. Within milliseconds, a bubble of high-pressure gas and steam is formed. The heat and expanding shock wave cause the surrounding rock to vaporise, or be melted further away, creating a melt cavity. The shock-induced motion and high internal pressure cause this cavity to expand outwards, which continues over several tenths of a second until the pressure has fallen sufficiently, to a level roughly comparable with the weight of the rock above, and can no longer grow. Although not observed in every explosion, four distinct zones (including the melt cavity) have been described in the surrounding rock. The crushed zone, about two times the radius of the cavity, consists of rock that has lost all of its former integrity. The cracked zone, about three times the cavity radius, consists of rock with radial and concentric fissures. Finally, the zone of irreversible strain consists of rock deformed by the pressure. The following layer undergoes only an elastic deformation; the strain and subsequent release then forms a seismic wave. A few seconds later the molten rock starts collecting on the bottom of the cavity and the cavity content begins cooling. The rebound after the shock wave causes compressive forces to build up around the cavity, called a stress containment cage, sealing the cracks.

Table: Zones in surrounding rock.

Name	Radius
Melt cavity	$4-12 \text{ m}/kt^{1/3}$

Crushed zone	30–40 m/kt ^{1/3}
Cracked zone	80–120 m/kt ^{1/3}
Zone of irreversible strain	800–1100 m/kt ^{1/3}

Several minutes to days later, once the heat dissipates enough, the steam condenses, and the pressure in the cavity falls below the level needed to support the overburden, the rock above the void falls into the cavity. Depending on various factors, including the yield and characteristics of the burial, this collapse may extend to the surface. If it does, a subsidence crater is created. Such a crater is usually bowl-shaped, and ranges in size from a few tens of metres to over a kilometre in diameter. At the Nevada Test Site, 95 percent of tests conducted at a scaled depth of burial (SDOB) of less than 150 caused surface collapses, compared with about half of tests conducted at a SDOB of less than 180. The radius r (in feet) of the cavity is proportional to the cube root of the yield y (in kilotons), $r = 55 * \sqrt[3]{y}$; an 8 kiloton explosion will create a cavity with radius of 110 feet.



Rubble mound formed.

Other surface features may include disturbed ground, pressure ridges, faults, water movement (including changes to the water table level), rockfalls, and ground slump. Most of the gas in the cavity is composed of steam; its volume decreases dramatically as the temperature falls and the steam condenses. There are however other gases, mostly carbon dioxide and hydrogen, which do not condense and remain gaseous. The carbon dioxide is produced by thermal decomposition of carbonates; hydrogen is created by reaction of iron and other metals from the nuclear device and surrounding equipment. The amounts of carbonates and water in the soil and the available iron have to be considered in evaluating the test site containment; water-saturated clay soils may cause structural collapse and venting. Hard basement rock may reflect shock waves of the explosion, also possibly causing structural weakening and venting. The non-condensable gases may stay absorbed in the pores in the soil. Large amount of such gases can however maintain enough pressure to drive the fission products to the ground.



Radioactivity release during Baneberry.

Escape of radioactivity from the cavity is known as containment failure. Massive, prompt, uncontrolled releases of fission products, driven by the pressure of steam or gas, are known as venting; an example of such failure is the Baneberry test. Slow, low-pressure uncontrolled releases of radioactivity are known as seeps; these have little to no energy, are not visible and have to be detected by instruments. Late-time seeps are releases of noncondensable gases days or weeks after the blast, by diffusion through pores and crack, probably assisted by a decrease of atmospheric pressure (so called atmospheric pumping). When the test tunnel has to be accessed, controlled tunnel purging is performed; the gases are filtered, diluted by air and released to atmosphere when the winds will disperse them over sparsely populated areas. Small activity leaks resulting from operational aspects of tests are called operational releases; they may occur e.g. during drilling into the explosion location during core sampling, or during the sampling of explosion gases. The radionuclide composition differs by the type of releases; large prompt venting releases significant fraction (up to 10%) of fission products, while late-time seeps contain only the most volatile gases. Soil absorbs the reactive chemical compounds, so the only nuclides filtered through soil into the atmosphere are the noble gases, primarily krypton-85 and xenon-133.

The released nuclides can undergo bioaccumulation. Iodine-131, strontium-90 and caesium-137 are concentrated in milk of grazing cows; cow milk is therefore a convenient, sensitive fallout indicator. Soft tissues of animals can be analyzed for gamma emitters, bones and liver for strontium and plutonium, and blood, urine and soft tissues are analyzed for tritium.

Although there were early concerns about earthquakes arising as a result of underground tests, there is no evidence that this has occurred. However, fault movements and ground fractures have been reported, and explosions often precede a series of aftershocks,

thought to be a result of cavity collapse and chimney formation. In a few cases, seismic energy released by fault movements has exceeded that of the explosion itself.

International Treaties

Signed in Moscow on August 5, 1963 by representatives of the United States, the Soviet Union, and the United Kingdom, the Limited Test Ban Treaty agreed to ban nuclear testing in the atmosphere, in space, and underwater. Due to the Soviet government's concern about the need for the on-site inspections, underground tests were excluded from the ban. 108 countries would eventually sign the treaty, with the significant exception of China.

In 1974, the United States and the Soviet Union signed the Threshold Test Ban Treaty, which banned underground tests with yields greater than 150 kilotons. By the 1990s, technologies to monitor and detect underground tests had matured to the point that tests of one kiloton or over could be detected with high probability, and in 1996 negotiations began under the auspices of the United Nations to develop a comprehensive test ban. The resulting Comprehensive Nuclear-Test-Ban Treaty was signed in 1996 by the United States, Russia, United Kingdom, France, and China. However, following the United States Senate decision not to ratify the treaty in 1999, it is still yet to be ratified by 8 of the required 44 'Annex 2' states and so has not entered into force as United Nations law.

Monitoring

In the late 1940s, the United States began to develop the capability to detect atmospheric testing using air sampling; this system was able to detect the first Soviet test in 1949. Over the next decade, this system was improved, and a network of seismic monitoring stations was established to detect underground tests. Development of the Threshold Test Ban Treaty in the mid-1970s led to an improved understanding of the relationship between test yield and resulting seismic magnitude.

When negotiations began in the mid-1990s to develop a comprehensive test ban, the international community was reluctant to rely upon the detection capabilities of individual nuclear weapons states (especially the United States), and instead wanted an international detection system. The resulting International Monitoring System consists of a network of a total of 321 monitoring stations and 16 radionuclide laboratories. Fifty "primary" seismic stations send data continuously to the International Data Center, along with 120 "auxiliary" stations which send data on request. The resulting data is used to locate the epicentre, and distinguish between the seismic signatures of an underground nuclear explosion and an earthquake. Additionally, eighty radionuclide stations detect radioactive particles vented by underground explosions. Certain radionuclides constitute clear evidence of nuclear tests; the presence of noble gases can indicate whether an underground explosion has taken place. Finally, eleven hydroacoustic stations and sixty infrasound stations monitor underwater and atmospheric tests.

FUSION REACTOR

Fusion reactor, also called fusion power plant or thermonuclear reactor is a device to produce electrical power from the energy released in a nuclear fusion reaction. The use of nuclear fusion reactions for electricity generation remains theoretical.

Since the 1930s, scientists have known that the Sun and other stars generate their energy by nuclear fusion. They realized that if fusion energy generation could be replicated in a controlled manner on Earth, it might very well provide a safe, clean, and inexhaustible source of energy. The 1950s saw the beginning of a worldwide research effort to develop a fusion reactor.

General Characteristics

The energy-producing mechanism in a fusion reactor is the joining together of two light atomic nuclei. When two nuclei fuse, a small amount of mass is converted into a large amount of energy. Energy (E) and mass (m) are related through Einstein's relation, $E = mc^2$, by the large conversion factor c^2 , where c is the speed of light (about 3×10^8 metres per second, or 186,000 miles per second). Mass can be converted to energy also by nuclear fission, the splitting of a heavy nucleus. This splitting process is utilized in nuclear reactors.

Fusion reactions are inhibited by the electrical repulsive force, called the Coulomb force that acts between two positively charged nuclei. For fusion to occur, the two nuclei must approach each other at high speed in order to overcome their electrical repulsion and attain a sufficiently small separation (less than one-trillionth of a centimetre) so that the short-range strong force dominates. For the production of useful amounts of energy, a large number of nuclei must undergo fusion; that is to say, a gas of fusing nuclei must be produced. In a gas at extremely high temperatures, the average nucleus contains sufficient kinetic energy to undergo fusion. Such a medium can be produced by heating an ordinary gas beyond the temperature at which electrons are knocked out of their atoms. The result is an ionized gas consisting of free negative electrons and positive nuclei. This ionized gas is in a plasma state, the fourth state of matter. Most of the matter in the universe is in the plasma state.

At the core of experimental fusion reactors is a high-temperature plasma. Fusion occurs between the nuclei, with the electrons present only to maintain macroscopic charge neutrality. The temperature of the plasma is about 100,000,000 kelvins (K; about 100,000,000 °C, or 180,000,000 °F), which is more than six times the temperature at the centre of the Sun. (Higher temperatures are required for the lower pressures and densities encountered in fusion reactors.) Plasma loses energy through processes such as radiation, conduction, and convection, so sustaining hot plasma requires that fusion reactions add enough energy to balance the energy losses. In order to achieve this balance, the product of the plasma's density and its energy confinement time (the time it takes the plasma to lose its energy if unreplaced) must exceed a critical value.

Stars, including the Sun, consist of plasmas that generate energy by fusion reactions. In these natural fusion reactors, plasma is confined at high pressures by the immense gravitational field. It is not possible to assemble on Earth plasma sufficiently massive to be gravitationally confined. For terrestrial applications, there are two main approaches to controlled fusion—namely, magnetic confinement and inertial confinement.

In magnetic confinement low-density plasma is confined for a long period of time by a magnetic field. The plasma density is roughly 10^{21} particles per cubic metre, which is many thousands of times less than the density of air at room temperature. The energy confinement time must then be at least one second—i.e., the energy in the plasma must be replaced every second.

In inertial confinement no attempt is made to confine the plasma beyond the time it takes the plasma to disassemble. The energy confinement time is simply the time it takes the fusing plasma to expand. Confined only by its own inertia, the plasma survives for only about one-billionth of a second (one nanosecond). Hence, breakeven in this scheme requires a very large particle density, typically about 10^{30} particles per cubic metre, which is about 100 times the density of a liquid. A thermonuclear bomb is an example of inertially confined plasma. In an inertial confinement power plant, the extreme density is achieved by compressing a millimetre-scale solid pellet of fuel with lasers or particle beams. These approaches are sometimes referred to as laser fusion or particle-beam fusion.

The fusion reaction least difficult to achieve combines a deuteron (the nucleus of a deuterium atom) with a triton (the nucleus of a tritium atom). Both nuclei are isotopes of the hydrogen nucleus and contain a single unit of positive electric charge. Deuterium-tritium (D-T) fusion thus requires the nuclei to have lower kinetic energy than is needed for the fusion of more highly charged, heavier nuclei. The two products of the reaction are an alpha particle (the nucleus of a helium atom) at an energy of 3.5 million electron volts (MeV) and a neutron at an energy of 14.1 MeV (1 MeV is the energy equivalent of a temperature of about 10,000,000,000 K). The neutron, lacking electric charge, is not affected by electric or magnetic fields and can escape the plasma to deposit its energy in a surrounding material, such as lithium. The heat generated in the lithium “blanket” can then be converted to electrical energy by conventional means, such as steam-driven turbines. The electrically charged alpha particles, meanwhile, collide with the deuterons and tritons (by their electrical interaction) and can be magnetically confined within the plasma, thereby transferring their energy to the reacting nuclei. When this redeposition of the fusion energy into the plasma exceeds the power lost from the plasma, the plasma will be self-sustaining, or “ignited.”

Although tritium does not occur naturally, tritons and alpha particles are produced when neutrons from the D-T fusion reactions are captured in the surrounding lithium blanket. The tritons are then fed back into the plasma. In this respect, D-T fusion reactors are unique as they use their waste (neutrons) to generate more fuel. Overall,

a D-T fusion reactor uses deuterium and lithium as fuel and generates helium as a reaction by-product. Deuterium can be readily obtained from seawater—about one in every 3,000 water molecules contains a deuterium atom. Lithium is also abundant and inexpensive. In fact, there is enough deuterium and lithium in the oceans to provide for the world's energy needs for billions of years. With deuterium and lithium as the fuel, a D-T fusion reactor would be an effectively inexhaustible source of energy.

A practical fusion reactor would also have several attractive safety and environmental features. First, a fusion reactor would not release the pollutants that accompany the combustion of fossil fuels—in particular, the gases that contribute to global warming. Second, because the fusion reaction is not a chain reaction, a fusion reactor cannot undergo a runaway chain reaction, or “meltdown,” as can happen in a fission reactor. The fusion reaction requires confined hot plasma, and any interruption of a plasma control system would extinguish the plasma and terminate fusion. Third, the main products of a fusion reaction (helium atoms) are not radioactive. Although some radioactive by-products are produced by the absorption of neutrons in the surrounding material, low-activation materials exist such that these by-products have much shorter half-lives and are less toxic than the waste products of a nuclear reactor. Examples of such low-activation materials include special steels or ceramic composites (e.g., silicon carbide).

Principles of Magnetic Confinement

Confinement Physics

Magnetic confinement of plasmas is the most highly developed approach to controlled fusion. A large part of the problem of fusion has been the attainment of magnetic field configurations that effectively confine the plasma. A successful configuration must meet three criteria: (1) the plasma must be in a time-independent equilibrium state, (2) the equilibrium must be macroscopically stable, and (3) the leakage of plasma energy to the bounding wall must be small.

Charged particles tend to spiral about a magnetic line of force. It is necessary that these particle trajectories do not intersect the bounding wall. Simultaneously, the thermal energy of all the particles exerts an expansive pressure force on the plasma. For the plasma to be in equilibrium, the magnetic force acting on the electric current within the plasma must balance the pressure force at every point in the plasma.

This equilibrium must be stable, which is to say that the plasma will return to its original state following any small perturbation, such as continual random thermal “noise” fluctuations. In contrast, unstable plasma would likely depart from its equilibrium state and rapidly (perhaps in less than one-thousandth of a second) escape the confining magnetic field following any small perturbation.

Plasma in stable equilibrium can be maintained indefinitely if the leakage of energy

from the plasma is balanced by energy input. If the plasma energy loss is too large, then ignition cannot be achieved. An unavoidable diffusion of energy across the magnetic field lines will occur from the collisions between the particles. The net effect is to transport energy from the hot core to the wall. In theory, this transport process, known as classical diffusion, is not strong in hot fusion plasmas and can be compensated by heat from the alpha particle fusion products. In experiments, however, energy is lost from the plasma at 10 to 100 times that expected from classical diffusion theory. Solution of the anomalous transport problem involves research into fundamental topics in plasma physics, such as plasma turbulence.

Many different types of magnetic configurations for plasma confinement have been devised and tested over the years. These may be grouped into two classes: closed, toroidal configurations and open, linear configurations. Toroidal devices are the most highly developed. In a simple straight magnetic field, the plasma would be free to stream out the ends. End loss can be eliminated by forming the plasma and field in the closed shape of a doughnut, or torus, or, in an approach called mirror confinement, by “plugging” the ends of such a device magnetically and electrostatically.

Toroidal Confinement

The most extensively investigated toroidal confinement concept is the tokamak. The tokamak (an acronym derived from the Russian words for “toroidal magnetic confinement”) was introduced in the mid-1960s by Soviet plasma physicists. The magnetic lines of force are helices that spiral around the torus. The helical magnetic field has two components: (1) a toroidal component, which points the long way around the torus, and (2) a poloidal component directed the short way around the machine. Both components are necessary for the plasma to be in stable equilibrium. If the poloidal field were zero, so that the field lines were simply circles wrapped about the torus, then the plasma would not be in equilibrium. The particles would not strictly follow the field lines but would drift to the walls. The addition of the poloidal field provides particle orbits that are contained within the device. If the toroidal field were zero, so that the magnetic field lines were directed only the short way around the torus, the plasma would be in equilibrium, but it would be unstable. The plasma column would develop growing distortions, or kinks, which would carry the plasma into the wall.

The toroidal field is produced by coils that surround the toroidal vacuum chamber containing the plasma. (The plasma must be situated within an evacuated chamber to prevent it from being cooled by interactions with air molecules.) In order to minimize power losses in the coils, designs involving superconducting coils have begun to replace copper coils. The plasma in a tokamak fusion reactor would have a major diameter in the range of 10 metres (33 feet) and a minor diameter of roughly 2 to 3 metres. The plasma current would likely be on the order of tens of millions of amperes, and the flux density of the toroidal magnetic field would measure several teslas. In order to help guide research and development, scientists frequently perform conceptual designs of

fusion reactors. One such concept is shown in the figure. This device in theory would generate 1 gigawatt (1 billion watts) of electric power—sufficient to meet the electricity needs of a large city.

The poloidal field is generated by a toroidal electric current that is forced to flow within the conducting plasma. Faraday's law of induction can be used to initiate and build up the current. A solenoid located in the hole of the torus can be used to generate magnetic flux that increases over time. The time-varying flux induces a toroidal electric field that drives the plasma current. This technique efficiently drives pulsed plasma current. However, it cannot be used for a steady-state current, which would require a magnetic flux increasing indefinitely over time. Unfortunately, a pulsed reactor would suffer from many engineering problems, such as materials fatigue, and thus other methods have been developed to drive a steady-state current to produce the poloidal magnetic field.

A technique known as radio-frequency (RF) current drive employs electromagnetic radiation to generate a steady-state current. Electromagnetic waves are injected into the plasma so that they propagate within the plasma in one direction around the torus. The speed of the waves is chosen to equal roughly the average speed of the electrons in the plasma. The wave electric field (which in plasma has a component along its direction of travel) can then continuously accelerate the electrons as the wave and particles move together around the torus. The electrons develop a net motion, or current, in one direction.

Another established current-drive technique is neutral-beam current drive. A beam of high-energy neutral atoms is injected into the plasma along the toroidal direction. The neutral beam will freely enter the plasma since it is unaffected by the magnetic field. The neutral atoms become ionized by collisions with the electrons. The beam then consists of energetic positively charged nuclei that are confined within the plasma by the magnetic field. The high-speed ions travel toroidally along the magnetic field and collide with the electrons, pushing them in one direction and thereby producing a current.

Both RF and neutral-beam current-drive techniques have a low efficiency (i.e., they require a large amount of power to drive the plasma current). Fortunately, a remarkable effect occurs in tokamak plasmas that reduces the need for external current drive. If the plasma pressure is greater in the core than at the edge, this pressure differential spontaneously drives a toroidal current in the plasma. This current is called the bootstrap current. It can be considered a type of thermoelectric effect, but its origin is in the complex particle dynamics that arise in a toroidal plasma. It has been observed in experiments and is now included routinely in advanced experiments and in tokamak reactor designs.

Other toroidal confinement concepts that offer potential advantages over the tokamak are being developed. Three such alternatives are the stellarator, reversed-field pinch (RFP), and compact torus concepts. The stellarator and RFP are much like the

tokamak. In the stellarator the magnetic field is produced by external coils only. Thus, the plasma current is essentially zero, and the problems inherent in sustaining large plasma current are absent. The RFP differs from the tokamak in that it operates with a weak toroidal magnetic field. This results in a compact, high-power-density reactor with copper (instead of superconducting) coils. Compact tori are toroidal plasmas with no hole in the centre of the torus. Reactors based on compact tori are small and avoid the engineering complications of coils linking the plasma torus.

Mirror Confinement

An alternative approach to magnetic confinement is to employ a straight configuration in which the end loss is reduced by a combination of magnetic and electric plugging. In such a linear fusion reactor the magnetic field strength is increased at the ends. Charged particles that approach the end slow down, and many are reflected from this “magnetic mirror.” (The same magnetic reflection mechanism traps particles in the Earth’s magnetosphere, specifically in the Van Allen radiation belts). Unfortunately, particles with extremely high speed along the field are not stopped by the mirror. To inhibit this leakage, electrostatic plugging is provided. An additional section of plasma is added at each end beyond the magnetic mirror. The plasma in these “end plugs” produces an electrostatic potential barrier to nuclei. The overall configuration is called a tandem mirror.

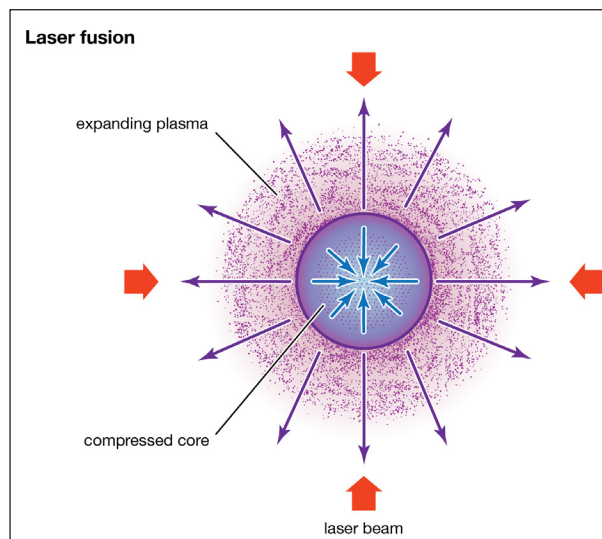
Plasma Heating

Plasma needs to be heated to about 100,000,000 K for fusion reactions to take place. Two plasma-heating methods have been highly developed: electromagnetic wave heating and neutral-beam injection heating. In the former, electromagnetic waves are directed by antennas at the surface of the plasma. The waves penetrate the plasma and transfer their energy to the constituent particles. Ionized gases can support the propagation of a remarkably large variety of waves not found in other forms of matter. Effective wave-heating techniques employ frequencies from the radio-frequency range to the microwave range. Power absorption often relies upon a resonant interaction between the wave and plasma. For example, if the frequency of the electromagnetic wave is equal to the frequency at which a nucleus gyrates about a magnetic field line, this resonant nucleus absorbs energy from the wave. This technique is called ion cyclotron resonance heating. Similarly, electron cyclotron resonance heating may be used to heat electrons. Such electron heating requires very high frequencies (tens to hundreds of gigahertz), such as produced by free-electron lasers and gyrotron tubes.

In the second method, beams of neutral atoms at high energy (up to about one million electron volts) are injected into the plasma, rather as in the neutral-beam current drive described above. When used for heating, however, the beams are injected in both directions around the torus, so that no net momentum is imparted to the plasma. The slowing down, or transfer of beam energy to the plasma, constitutes the heating mechanism.

Principles of Inertial Confinement

In an inertial confinement fusion (ICF) reactor, a tiny solid pellet of fuel—such as deuterium-tritium (D-T)—would be compressed to tremendous density and temperature so that fusion power is produced in the few nanoseconds before the pellet blows apart. The compression is accomplished by focusing an intense laser beam or a charged particle beam, referred to as the driver, upon the small pellet (typically 1 to 10 mm in diameter). For efficient thermonuclear burn, the time allotted for the pellet to burn must be less than the disassembly time. This means that, in the compressed state, the product of the pellet mass density and the pellet radius must exceed about 3 grams per square centimetre. A high mass density will hasten the burn, and a large radius will slow the disassembly time. The ratio of fusion energy produced in the pellet explosion to the driver energy is called the pellet gain. High pellet gains of 100 or more are required for an ICF reactor.



Laser fusion.

Pellets are multilayered, consisting of several concentric spheres. The surface of the pellet is ionized by the driver beam, and ablation of the ionized material generates a large inward force on the pellet. Recoil from the ablation implodes the inner layer, producing a shock wave that compresses the inner layers of the D-T fuel. The implosion speed is several hundred kilometres per second, produced by a force equivalent to some 10 billion atmospheres. The target layers are designed such that the laser or particle-beam energy provides compression, not heat (entropy), during this stage. At the final stage of compression, the pellet is compressed to 1,000 to 10,000 times the density of typical solids.

In conventional ICF (usually referred to as shock-heated ICF), the laser or particle-beam energy pulses are accurately set such that the shocks produced during the implosion phase converge in the centre of the pellet, heating it to fusion temperatures. The burn

initiates in the central D-T layer and spreads outward as the alpha particles collide with and heat the rest of the pellet to a value sufficient to produce fusion reactions. Ignition occurs, and the pellet, now dense plasma, is burned up in a small microexplosion. An alternative method for ICF, known as fast ignition, has emerged in recent years because of rapid progress in generating intense picosecond (10–12 second) laser systems. Fast ignition can reduce the driver energy considerably. In this scheme, the main laser or particle beam is used to compress the fuel similar to shock heating. Then a short, intense laser pulse heats a small portion of the compressed fuel to fusion temperature, initiating the fusion burn. This approach may lead to target gains that are 3 to 10 times larger than in shock heating.

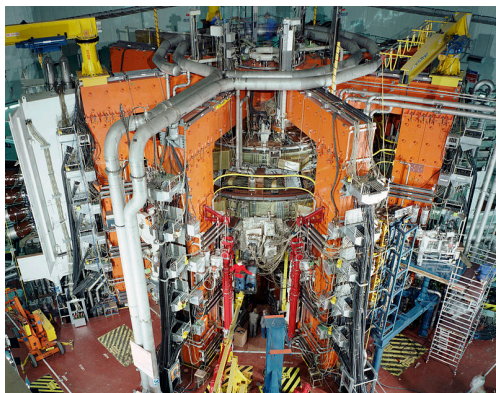
It is essential that the implosion of the outer layer of the target be symmetric and uniform to a high degree of accuracy. Any asymmetry can grow during compression, and, more important, the shocks may not precisely converge on the centre, which would prevent ignition of the fuel. Thus, the pellet must be manufactured with a high degree of smoothness, with tolerances of less than a thousandth of a millimetre. The driver should also deposit its energy on the pellet uniformly, with a variation of less than 1 percent. There are two methods to achieve this uniformity. In the first method, known as indirect drive, the pellet is located inside a hollow cylindrical shell known as a hohlraum, and the driver is aimed at the walls of the hohlraum. The hohlraum absorbs the driver's energy and then radiates the target with intense X-rays, which cause the pellet to heat and implode. Because a hohlraum is effectively a resonant cavity, the X-ray intensity on the target will be quite uniform even if few driver beams are used. The drawback of this technique is that the target gain is reduced because of inefficiency in converting the driver energy to X-rays. A higher gain is seen in the second method, known as direct drive, but here the driver system is much more complex, as many driver beams and special optical elements are needed to achieve the necessary uniform delivery of energy to the target.

FUSION POWER

Fusion power is a proposed form of power generation that would generate electricity by using heat from nuclear fusion reactions. In a fusion process, two lighter atomic nuclei combine to form a heavier nucleus, while releasing energy. Devices designed to harness this energy are known as fusion reactors.

Fusion processes require fuel and a confined environment with sufficient temperature, pressure and confinement time to create plasma in which fusion can occur. The combination of these figures that results in a power-producing system is known as the Lawson criterion. In stars, the most common fuel is hydrogen, and gravity provides extremely long confinement times that reach the conditions needed for fusion energy production. Proposed fusion reactors generally use hydrogen isotopes such as deuterium

and tritium, which react more easily than hydrogen to allow them to reach the Lawson criterion requirements with less extreme conditions. Most designs aim to heat their fuel to tens of millions of degrees, which presents a major challenge in producing a successful design.



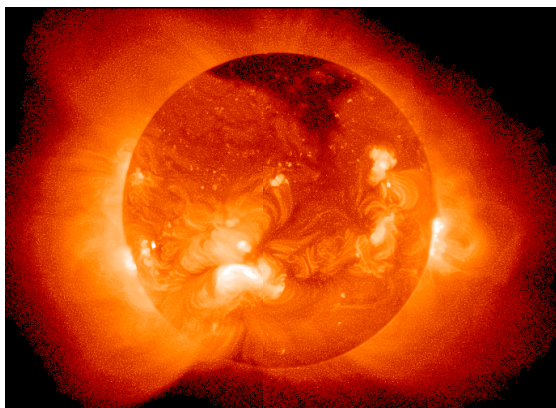
The Joint European Torus (JET) magnetic fusion experiment.

As a source of power, nuclear fusion is expected to have several advantages over fission. These include reduced radioactivity in operation and little high-level nuclear waste, ample fuel supplies, and increased safety. However, achieving the necessary combination of temperature, pressure, and duration has proven to be difficult to produce in a practical and economical manner. Research into fusion reactors began in the 1940s, but to date, no design has produced more fusion power output than the electrical power input, defeating the purpose. A second issue that affects common reactions, is managing neutrons that are released during the reaction, which over time degrade many common materials used within the reaction chamber.

Fusion researchers have investigated various confinement concepts. The early emphasis was on three main systems: z-pinch, stellarator and magnetic mirror. The current leading designs are the tokamak and inertial confinement (ICF) by laser. Both designs are under research at very large scales, most notably the ITER tokamak in France, and the National Ignition Facility laser in the United States. Researchers are also studying other designs that may offer cheaper approaches. Among these alternatives there is increasing interest in magnetized target fusion and inertial electrostatic confinement, and new variations of the stellarator.

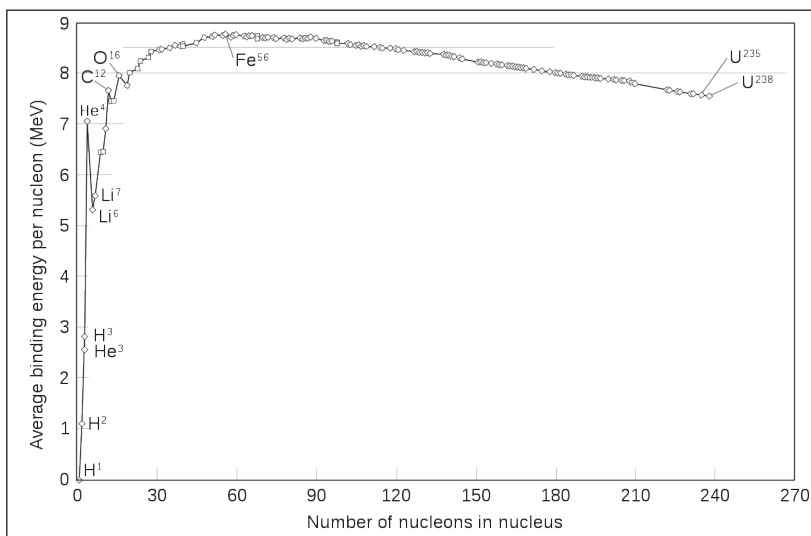
Mechanism

Fusion reactions occur when two or more atomic nuclei come close enough for long enough that the nuclear force pulling them together exceeds the electrostatic force pushing them apart, fusing them into heavier nuclei. For nuclei lighter than iron-56, the reaction is exothermic, releasing energy. For nuclei heavier than iron-56, the reaction is endothermic, requiring an external source of energy. Hence, nuclei smaller than iron-56 are more likely to fuse while those heavier than iron-56 are more likely to break apart.



The Sun, like other stars, is a natural fusion reactor, where stellar nucleosynthesis transforms lighter elements into heavier elements with the release of energy.

The strong force acts only over short distances, while the repulsive electrostatic force acts over longer distances. In order to undergo fusion, the fuel atoms need to be given enough energy to approach each other close enough for the strong force to become active. The amount of kinetic energy needed to bring the fuel atoms close enough is known as the “Coulomb barrier”. Ways of providing this energy include speeding up atoms in a particle accelerator, or heating them to high temperatures.

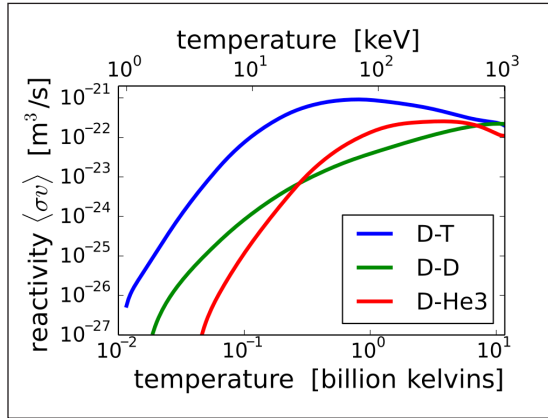


Binding energy for different atomic nuclei. Iron-56 has the highest, making it the most stable. Nuclei to the left are likely to fuse; those to the right are likely to split.

Once an atom is heated above its ionization energy, its electrons are stripped away (it is ionized), leaving just the bare nucleus (the ion). The result is a hot cloud of ions and the electrons formerly attached to them. This cloud is known as plasma. Because the charges are separated, plasmas are electrically conductive and magnetically controllable. Many fusion devices take advantage of this to control the particles as they are heated.

Cross Section

A reaction's cross section, denoted σ , is the measure of the probability that a fusion reaction will happen. This depends on the relative velocity of the two nuclei. Higher relative velocities generally increase the probability, but the probability begins to decrease again at very high energies. Cross sections for many fusion reactions were measured (mainly in the 1970s) using particle beams.



The fusion reaction rate increases rapidly with temperature until it maximizes and then gradually drops off. The deuterium-tritium fusion rate peaks at a lower temperature (about 70 keV, or 800 million kelvins) and at a higher value than other reactions commonly considered for fusion energy.

In plasma, particle velocity can be characterized using a probability distribution. If the plasma is thermalized, the distribution looks like a bell curve, or maxwellian distribution. In this case, it is useful to use the average particle cross section over the velocity distribution. This is entered into the volumetric fusion rate:

$$P_{\text{fusion}} = n_A n_B \langle \sigma v_{A,B} \rangle E_{\text{fusion}}$$

Where,

- P_{fusion} is the energy made by fusion, per time and volume.
- n is the number density of species A or B, of the particles in the volume.
- $\langle \sigma v_{A,B} \rangle$ is the cross section of that reaction, average over all the velocities of the two species v .
- E_{fusion} is the energy released by that fusion reaction.

Lawson Criterion

The Lawson Criterion shows how energy output varies with temperature, density,

speed of collision, and fuel. This equation was central to John Lawson’s analysis of fusion working with a hot plasma. Lawson assumed an energy balance.

$$P_{\text{out}} = \eta_{\text{capture}} (P_{\text{fusion}} - P_{\text{conduction}} - P_{\text{radiation}})$$

where,

- η , efficiency.
- $P_{\text{conduction}}$, conduction losses as energy laden mass leaves.
- $P_{\text{radiation}}$, radiation losses as energy leaves as light.
- P_{out} , net power from fusion.
- P_{fusion} , is rate of energy generated by the fusion reactions.

Plasma clouds lose energy through conduction and radiation. Conduction occurs when ions, electrons or neutrals impact other substances, typically a surface of the device, and transfer a portion of their kinetic energy to the other atoms. Radiation is energy that leaves the cloud as light in the visible, UV, IR, or X-ray spectra. Radiation increases with temperature. Fusion power technologies must overcome these losses.

Triple Product: Density, Temperature and Time

The Lawson criterion argues that a machine holding thermalized and quasi-neutral plasma has to meet basic criteria to overcome radiation losses, conduction losses and reach efficiency of 30 percent. This became known as the “triple product”: the plasma density, temperature and confinement time.

In magnetic confinement designs, the density is very low, on the order of a “good vacuum”. This means that useful reaction rates require the temperature and confinement time to be increased to offset the low density. Fusion-relevant temperatures have been achieved using a variety of heating methods that were developed in the early 1970s, and in modern machines, as of 2019, the major remaining issue is the confinement time. Plasmas in strong magnetic fields are subject to a number of inherent instabilities, which must be suppressed to reach useful times. One way to do this is to simply make the reactor volume larger, which reduces the rate of leakage due to classical diffusion. This is why modern designs like ITER are so large.

In contrast, inertial confinement systems approach useful triple product values via higher density, and have vanishingly small confinement times. In modern machines like NIF, the initial frozen hydrogen fuel load has a density less than water which is increased to about 100 times the density of lead. In these conditions, the rate of fusion is so high that the entire fuel load undergoes fusion in the microseconds it takes for the heat generated by the reactions to blow the fuel apart. Although modern ICF machines

like NIF are also extremely large, this is a function of their “driver” design, not an inherent design criterion of the fusion process itself.

Energy Capture

Multiple approaches have been proposed for energy capture. The simplest is to heat a fluid. Most designs concentrate on the D-T reaction, which releases much of its energy in a neutron. Electrically neutral, the neutron escapes the confinement. In most such designs, it is ultimately captured in a thick “blanket” of lithium surrounding the reactor core. When struck by a high-energy neutron, the lithium can produce tritium, which is then fed back into the reactor. The energy of this reaction also heats the blanket, which is then actively cooled with a working fluid and then that fluid is used to drive conventional turbomachinery.

It has also been proposed to use the neutrons to breed additional fission fuel in a blanket of nuclear waste, a concept known as a fission-fusion hybrid. In these systems, the power output is enhanced by the fission events, and power is extracted using systems like those in conventional fission reactors.

Designs that use other fuels, notably the p-B reaction, release much more of their energy in the form of charged particles. In these cases, alternate power extraction systems based on the movement of these charges are possible. Direct energy conversion was developed at LLNL in the 1980s as a method to maintain a voltage using the fusion reaction products. This has demonstrated energy capture efficiency of 48 percent.

Methods

Plasma Behavior

Plasma is an ionized gas that conducts electricity. In bulk, it is modeled using magnetohydrodynamics, which is a combination of the Navier–Stokes equations governing fluids and Maxwell’s equations governing how magnetic and electric fields behave. Fusion exploits several plasma properties, including:

- Self-organizing plasma conducts electric and magnetic fields. Its motions can generate fields that can in turn contain it.
- Diamagnetic plasma can generate its own internal magnetic field. This can reject an externally applied magnetic field, making it diamagnetic.
- Magnetic mirrors can reflect plasma when it moves from a low to high density field.

Magnetic Confinement

- Tokamak: The most well-developed and well-funded approach to fusion energy. This method races hot plasma around in a magnetically confined torus, with an

internal current. When completed, ITER will be the world's largest tokamak. As of April 2012 an estimated 215 experimental tokamaks were either planned, decommissioned or currently operating worldwide.

- Spherical tokamak: Also known as spherical torus. A variation on the tokamak with a spherical shape.
- Stellarator: Twisted rings of hot plasma. The stellarator attempts to create a natural twisted plasma path, using external magnets, while tokamaks create those magnetic fields using an internal current. Stellarators were developed by Lyman Spitzer in 1950 and have four designs: Torsatron, Heliotron, Heliac and Helias. One example is Wendelstein 7-X, a German fusion device that produced its first plasma on December 10, 2015. It is the world's largest stellarator, designed to investigate the suitability of this type of device for a power station.
- Internal rings: Stellarators create twisted plasma using external magnets, while tokamaks do so using a current induced in the plasma. Several classes of designs provide this twist using conductors inside the plasma. Early calculations showed that collisions between the plasma and the supports for the conductors would remove energy faster than the fusion reactions could replace. Modern variations, including the Levitated Dipole Experiment (LDX), use a solid superconducting torus that is magnetically levitated inside the reactor chamber.
- Magnetic mirror: Developed by Richard F. Post and teams at LLNL in the 1960s. Magnetic mirrors reflected hot plasma back and forth in a line. Variations included the Tandem Mirror, magnetic bottle and the biconic cusp. A series of well-funded, large, mirror machines were built by the US government in the 1970s and 1980s, principally at Lawrence Livermore National Laboratory. However, calculations in the 1970s demonstrated it was unlikely these would ever be commercially useful.
- Bumpy torus: A number of magnetic mirrors are arranged end-to-end in a toroidal ring. Any fuel ions that leak out of one are confined in a neighboring mirror, permitting the plasma pressure to be raised arbitrarily high without loss. An experimental facility, the ELMO Bumpy Torus or EBT was built and tested at Oak Ridge National Laboratory in the 1970s.
- Field-reversed configuration: This device traps plasma in a self-organized quasi-stable structure; where the particle motion makes an internal magnetic field which then traps itself.
- Spheromak: Very similar to a field-reversed configuration, a semi-stable plasma structure made by using the plasmas' own self-generated magnetic field. A spheromak has both toroidal and poloidal fields, while a field-reversed configuration has no toroidal field.

- Reversed field pinch: Here the plasma moves inside a ring. It has an internal magnetic field. Moving out from the center of this ring, the magnetic field reverses direction.

Inertial Confinement

- Indirect drive: In this technique, lasers heat a structure known as a Hohlraum that becomes so hot it begins to radiate huge amounts of x-ray light. These x-rays heat a small pellet of fuel, causing it to collapse inward to compress the fuel. The largest system using this method is the National Ignition Facility, followed closely by Laser Mégajoule.
- Direct drive: A variation of the ICF technique in which the lasers directly on the fuel pellet. Notable direct drive experiments have been conducted at the Laboratory for Laser Energetics and the GEKKO XII facilities. Good implosions require fuel pellets with close to a perfect shape in order to generate a symmetrical inward shock wave that produces the high-density plasma.
- Fast ignition: This method uses two laser blasts. The first blast compresses the fusion fuel, while the second high energy pulse ignites it. As of 2019 this technique is no longer favored for energy production due to a number of unexpected problems.
- Magneto-inertial fusion or Magnetized Liner Inertial Fusion: This combines a laser pulse with a magnetic pinch. The pinch community refers to it as magnetized liner inertial fusion while the ICF community refers to it as magneto-inertial fusion.
- Heavy Ion Beams There is also proposals to do inertial confinement fusion with ion beams instead of laser beams. The main difference is that the beam has momentum due to mass, whereas lasers do not. However, given what has been learned using laser devices, it appears unlikely that ion beams can be focussed both spatially and in time to the exacting needs of ICF.
- Z-machine a unique approach to ICF is the z-machine, which sends a huge electrical current through thin tungsten wires, heating them to x-ray temperatures. Like the indirect drive approach, these x-rays then compress a fuel capsule.

Magnetic or Electric Pinches

- Z-Pinch: This method sends a strong current (in the z-direction) through the plasma. The current generates a magnetic field that squeezes the plasma to fusion conditions. Pinches were the first method for man-made controlled fusion. However, it was later discovered that the z-pinch has inherent instabilities that limit its compression and heating to values far too low for practical fusion, and

the largest such machine, the UK's ZETA, was the last major experiment of the sort. Exploration of the problems in z-pinch led to the tokamak design. Later variation on the design includes dense plasma focus (DPF).

- **Theta-Pinch:** This method sends a current around the outside of a plasma column, in the theta direction. This induces a magnetic field running down the center of the plasma, as opposed to around it. The early theta-pinch device Scylla was the first to conclusively demonstrate fusion, but later work demonstrated it had inherent limits that made it uninteresting for power production.
- **Screw Pinch:** This method combines a theta and z-pinch for improved stabilization.

Inertial Electrostatic Confinement

- **Fusor:** This method uses an electric field to heat ions to fusion conditions. The machine typically uses two spherical cages, a cathode inside the anode, inside a vacuum. These machines are not considered a viable approach to net power because of their high conduction and radiation losses. They are simple enough to build that amateurs have fused atoms using them.
- **Polywell:** This design attempts to combine magnetic confinement with electrostatic fields, to avoid the conduction losses generated by the cage.

Other Methods

- **Magnetized target fusion:** This method confines hot plasma using a magnetic field and squeezes it using inertia. Examples include LANL FRX-L machine, General Fusion and the plasma liner experiment.
- **Cluster Impact Fusion** Microscopic droplets of heavy water are accelerated at great velocity into a target or into one another. Researchers at Brookhaven reported positive results which were later refuted by further experimentation. Fusion effects were actually produced because of contamination of the droplets.
- **Uncontrolled:** Fusion has been initiated by man, using uncontrolled fission explosions to ignite so-called Hydrogen Bombs. Early proposals for fusion power included using bombs to initiate reactions.
- **Beam fusion:** A beam of high energy particles can be fired at another beam or target and fusion will occur. This was used in the 1970s and 1980s to study the cross sections of high energy fusion reactions.
- **Bubble fusion:** This was a fusion reaction that was supposed to occur inside extraordinarily large collapsing gas bubbles, created during acoustic liquid cavitation. This approach was discredited.

- **Cold fusion:** This is a hypothetical type of nuclear reaction that would occur at, or near, room temperature. Cold fusion is discredited and gained a reputation as pathological science.
- **Muon-catalyzed fusion:** This approach replaces electrons in diatomic molecules of isotopes of hydrogen with muons - far more massive particles with the same electric charge. Their greater mass results in the nuclei getting close enough such that the strong interaction can cause fusion to occur. Currently, muons require more energy to produce than can be obtained from muon-catalyzed fusion. Unless this is solved, muon-catalyzed fusion is impractical for power generation.

Common Tools

Heating

Gas is heated to form plasma hot enough to start fusion reactions. A number of heating schemes have been explored: Radiofrequency Heating a radio wave is applied to the plasma, causing it to oscillate. This is basically the same concept as a microwave oven. This is also known as electron cyclotron resonance heating or Dielectric heating.

- **Electrostatic Heating:** An electric field can do work on charged ions or electrons, heating them.
- **Neutral Beam Injection:** An external source of hydrogen is ionized and accelerated by an electric field to form a charged beam which is shone through a source of neutral hydrogen gas towards the plasma which itself is ionized and contained in the reactor by a magnetic field. Some of the intermediate hydrogen gas is accelerated towards the plasma by collisions with the charged beam while remaining neutral: this neutral beam is thus unaffected by the magnetic field and so shines through it into the plasma. Once inside the plasma the neutral beam transmits energy to the plasma by collisions as a result of which it becomes ionized and thus contained by the magnetic field thereby both heating and refuelling the reactor in one operation. The remainder of the charged beam is diverted by magnetic fields onto cooled beam dumps.
- **Antiproton annihilation:** Theoretically a quantity of antiprotons injected into a mass of fusion fuel can induce thermonuclear reactions. This possibility as a method of spacecraft propulsion, known as Antimatter-catalyzed nuclear pulse propulsion, was investigated at Pennsylvania State University in connection with the proposed AIMStar project.
- **Magnetic Oscillations.**

Measurement

- Thomson Scattering: Light scatters from plasma. This light can be detected and used to reconstruct the plasmas' behavior. This technique can be used to find its density and temperature. It is common in inertial confinement fusion, Tokamaks and fusors. In ICF systems, this can be done by firing a second beam into a gold foil adjacent to the target. This makes x-rays that scatter or traverse the plasma. In Tokamaks, this can be done using mirrors and detectors to reflect light across a plane (two dimensions) or in a line (one dimension).
- Langmuir probe: This is a metal object placed in plasma. A potential is applied to it, giving it a positive or negative voltage against the surrounding plasma. The metal collects charged particles, drawing a current. As the voltage changes, the current changes. This makes a IV Curve. The IV-curve can be used to determine the local plasma density, potential and temperature.
- Neutron detectors: Deuterium or tritium fusion produces neutrons. Neutrons interact with surrounding matter in ways that can be detected. Several types of neutron detectors exist which can record the rate at which neutrons are produced during fusion reactions. They are an essential tool for demonstrating success.
- Flux loop: A loop of wire is inserted into the magnetic field. As the field passes through the loop, a current is made. The current is measured and used to find the total magnetic flux through that loop. This has been used on the National Compact Stellarator Experiment, the polywell and the LDX machines.
- X-ray detector: All plasma loses energy by emitting light. This covers the whole spectrum: visible, IR, UV, and X-rays. This occurs anytime a particle changes velocity, for any reason. If the reason is deflection by a magnetic field, the radiation is Cyclotron radiation at low speeds and Synchrotron radiation at high speeds. If the reason is deflection by another particle, plasma radiates X-rays, known as Bremsstrahlung radiation. X-rays are termed in both hard and soft, based on their energy.

Power Production

It has been proposed that steam turbines be used to convert the heat from the fusion chamber into electricity. The heat is transferred into a working fluid that turns into steam, driving electric generators.

Neutron blankets Deuterium and tritium fusion generates neutrons. This varies by technique (NIF has a record of $3E14$ neutrons per second while a typical fusor produces $1E5-1E9$ neutrons per second). It has been proposed to use these neutrons as a way to regenerate spent fission fuel or as a way to breed tritium using a

breeder blanket consisting of liquid lithium or, as in more recent reactor designs, a helium cooled pebble bed consisting of lithium bearing ceramic pebbles fabricated from materials such as Lithium titanate, lithium orthosilicate or mixtures of these phases.

Direct conversion This is a method where the kinetic energy of a particle is converted into voltage. It was first suggested by Richard F. Post in conjunction with magnetic mirrors, in the late sixties. It has also been suggested for Field-Reversed Configurations. The process takes the plasma, expands it, and converts a large fraction of the random energy of the fusion products into directed motion. The particles are then collected on electrodes at various large electrical potentials. This method has demonstrated an experimental efficiency of 48 percent.

Records

Fusion records have been set by a number of devices. Here are some:

Q

The ratio of energy extracted against the amount of energy supplied. This record is considered to be set by the Joint European Torus (JET) in 1997 when the device extracted 16 MW of power. However, this ratio can be seen three different ways:

- 0.69 is the actual point in time ratio between “fusion power” and actual input power in the plasma (23 MW).
- 0.069 is the ratio between the “fusion” power and the power required to produce the 23MW input power (essentially it takes into account the efficiency of the NB system).
- 0.0069 is the ratio between the “fusion” power and the total peak power required for a JET pulse. This takes into account all the power from the grid plus the one from the two large JET flywheel generators.

Runtime

In Field Reversed Configurations, the longest run time is 300 ms, set by the Princeton Field Reversed Configuration in August 2016. However this involved no fusion.

Beta

The fusion power trends as the plasma confinement rose to the fourth power. Hence, getting a strong plasma trap is of real value to a fusion power plant. Plasma has a very good electrical conductivity. This opens the possibility of confining the plasma with magnetic field, generally known as magnetic confinement. The field puts a magnetic

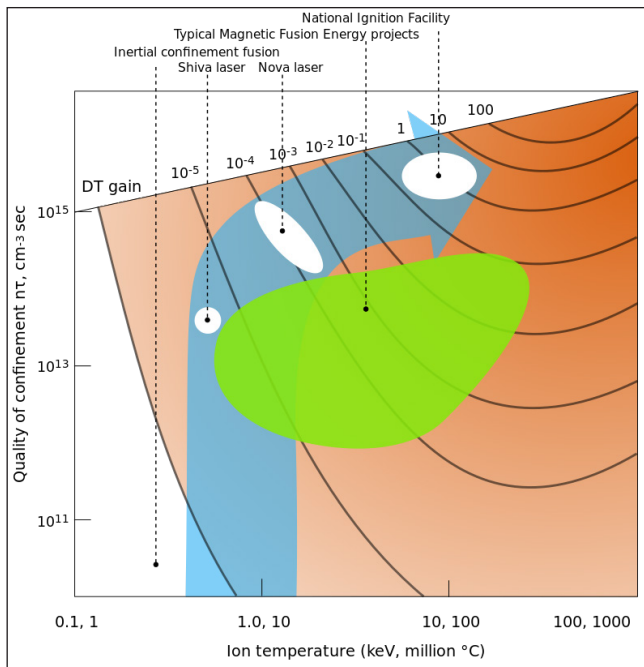
pressure on the plasma, which holds it in. A widely used measure of magnetic trapping in fusion is the beta ratio:

$$\beta = \frac{p}{p_{\text{mag}}} = \frac{nk_B T}{(B^2 / 2\mu_0)}$$

This is the ratio of the externally applied field to the internal pressure of the plasma. A value of 1 is ideal trapping. Some examples of beta values include:

- The START machine: 0.32,
- The Levitated dipole experiment: 0.26,
- Spheromaks: ≈ 0.1 , Maximum 0.2 based on Mercier limit,
- The DIII-D machine: 0.126,
- The Gas Dynamic Trap a magnetic mirror: 0.6 for $5E-3$ seconds,
- The Sustained Spheromak Plasma Experiment at Los Alamos National labs < 0.05 for $4E-6$ seconds.

Confinement



Parameter space occupied by inertial fusion energy and magnetic fusion energy devices as of the mid-1990s. The regime allowing thermonuclear ignition with high gain lies near the upper right corner of the plot.

Confinement refers to all the conditions necessary to keep plasma dense and hot long enough to undergo fusion. Here are some general principles:

- **Equilibrium:** The forces acting on the plasma must be balanced for containment. One exception is inertial confinement, where the relevant physics must occur faster than the disassembly time.
- **Stability:** The plasma must be so constructed so that disturbances will not lead to the plasma disassembling.
- **Transport or conduction:** The loss of material must be sufficiently slow. The plasma carries off energy with it, so rapid loss of material will disrupt any machines power balance. Material can be lost by transport into different regions or conduction through a solid or liquid.

To produce self-sustaining fusion, the energy released by the reaction (or at least a fraction of it) must be used to heat new reactant nuclei and keep them hot long enough that they also undergo fusion reactions.

Unconfined

The first human-made, large-scale fusion reaction was the test of the hydrogen bomb, Ivy Mike, in 1952. As part of the PACER project, it was once proposed to use hydrogen bombs as a source of power by detonating them in caverns and then generating electricity from the heat produced, but such a power station is unlikely ever to be constructed.

Magnetic Confinement

- **Magnetic Mirror:** One example of magnetic confinement is with the magnetic mirror effect. If a particle follows the field line and enters a region of higher field strength, the particles can be reflected. There are several devices that try to use this effect. The most famous was the magnetic mirror machines, which was a series of large, expensive devices built at the Lawrence Livermore National Laboratory from the 1960s to mid-1980s. Some other examples include the magnetic bottles and Biconic cusp. Because the mirror machines were straight, they had some advantages over a ring shape. First, mirrors were easier to construct and maintain and second direct conversion energy capture, was easier to implement. As the confinement achieved in experiments was poor, this approach was abandoned.
- **Magnetic Loops:** Another example of magnetic confinement is to bend the field lines back on themselves, either in circles or more commonly in nested toroidal surfaces. The most highly developed system of this type is the tokamak, with the stellarator being next most advanced, followed by the Reversed field

pinch. Compact toroids, especially the Field-Reversed Configuration and the spheromak, attempt to combine the advantages of toroidal magnetic surfaces with those of a simply connected (non-toroidal) machine, resulting in a mechanically simpler and smaller confinement area.

Inertial Confinement

Inertial confinement is the use of rapidly imploding shell to heat and confine plasma. The shell is imploded using a direct laser blast (direct drive) or a secondary x-ray blast (indirect drive) or heavy ion beams. Theoretically, fusion using lasers would be done using tiny pellets of fuel that explode several times a second. To induce the explosion, the pellet must be compressed to about 30 times solid density with energetic beams. If direct drive is used—the beams are focused directly on the pellet—it can in principle be very efficient, but in practice is difficult to obtain the needed uniformity. The alternative approach, indirect drive, uses beams to heat a shell, and then the shell radiates x-rays, which then implode the pellet. The beams are commonly laser beams, but heavy and light ion beams and electron beams have all been investigated.

Electrostatic Confinement

There are also electrostatic confinement fusion devices. These devices confine ions using electrostatic fields. The best known is the Fusor. This device has a cathode inside an anode wire cage. Positive ions fly towards the negative inner cage, and are heated by the electric field in the process. If they miss the inner cage they can collide and fuse. Ions typically hit the cathode, however, creating prohibitory high conduction losses. Also, fusion rates in fusors are very low because of competing physical effects, such as energy loss in the form of light radiation. Designs have been proposed to avoid the problems associated with the cage, by generating the field using a non-neutral cloud. These include a plasma oscillating device, a magnetically-shielded-grid, a penning trap, the polywell and the F1 cathode driver concept. The technology is relatively immature, however, and many scientific and engineering questions remain.

Fuels

By firing particle beams at targets, many fusion reactions have been tested, while the fuels considered for power have all been light elements like the isotopes of hydrogen—protium, deuterium, and tritium. The deuterium and helium-3 reaction requires helium-3, an isotope of helium so scarce on Earth that it would have to be mined extraterrestrially or produced by other nuclear reactions. Finally, researchers hope to perform the protium and boron-11 reaction, because it does not directly produce neutrons, though side reactions can.

Deuterium and Tritium

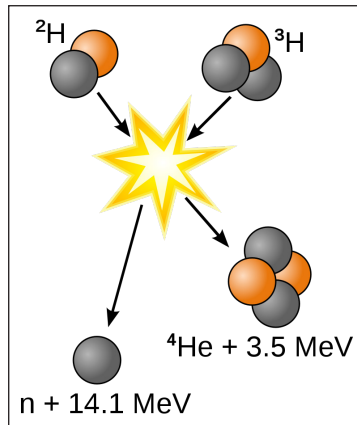
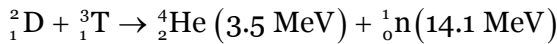
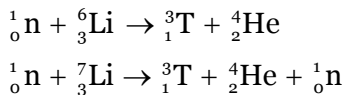


Diagram of the D-T reaction.

The easiest nuclear reaction, at the lowest energy, is:



This reaction is common in research, industrial and military applications, usually as a convenient source of neutrons. Deuterium is a naturally occurring isotope of hydrogen and is commonly available. The large mass ratio of the hydrogen isotopes makes their separation easy compared to the difficult uranium enrichment process. Tritium is a natural isotope of hydrogen, but because it has a short half-life of 12.32 years, it is hard to find, store, produce, and is expensive. Consequently, the deuterium-tritium fuel cycle requires the breeding of tritium from lithium using one of the following reactions:



The reactant neutron is supplied by the D-T fusion reaction shown above, and the one that has the greatest yield of energy. The reaction with ${}^6\text{Li}$ is exothermic, providing a small energy gain for the reactor. The reaction with ${}^7\text{Li}$ is endothermic but does not consume the neutron. At least some neutron multiplication reactions are required to replace the neutrons lost to absorption by other elements. Leading candidate neutron multiplication materials are beryllium and lead however the ${}^7\text{Li}$ reaction above also helps to keep the neutron population high. Natural lithium is mainly ${}^7\text{Li}$ however this has a low tritium production cross section compared to ${}^6\text{Li}$ so most reactor designs use breeder blankets with enriched ${}^6\text{Li}$.

Several drawbacks are commonly attributed to D-T fusion power:

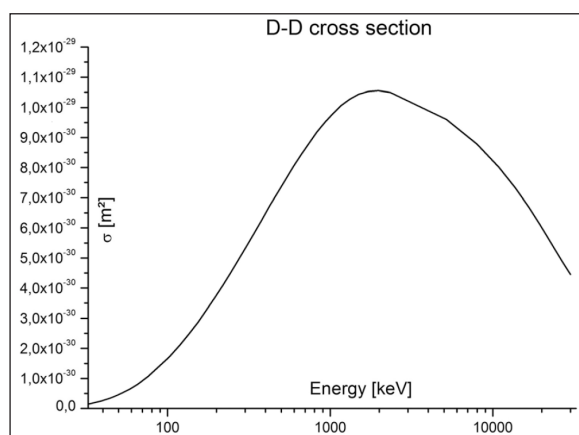
- It produces substantial amounts of neutrons that result in the neutron activation of the reactor materials.

- Only about 20% of the fusion energy yield appears in the form of charged particles with the remainder carried off by neutrons, which limits the extent to which direct energy conversion techniques might be applied.
- It requires the handling of the radioisotope tritium. Similar to hydrogen, tritium is difficult to contain and may leak from reactors in some quantity. Some estimates suggest that this would represent a fairly large environmental release of radioactivity.

The neutron flux expected in a commercial D-T fusion reactor is about 100 times that of current fission power reactors, posing problems for material design. After a series of D-T tests at JET, the vacuum vessel was sufficiently radioactive that remote handling was required for the year following the tests.

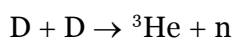
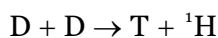
In a production setting, the neutrons would be used to react with lithium in the context of a breeder blanket comprising lithium ceramic pebbles or liquid lithium, in order to create more tritium. This also deposits the energy of the neutrons in the lithium, which would then be transferred to drive electrical production. The lithium neutron absorption reaction protects the outer portions of the reactor from the neutron flux. Newer designs, the advanced tokamak in particular, also use lithium inside the reactor core as a key element of the design. The plasma interacts directly with the lithium, preventing a problem known as “recycling”. The advantage of this design was demonstrated in the Lithium Tokamak Experiment.

Deuterium



Deuterium fusion cross section (in square meters) at different ion collision energies.

This is the second easiest fusion reaction, fusing two deuterium nuclei. The reaction has two branches that occur with nearly equal probability:



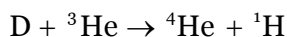
This reaction is also common in research. The optimum energy to initiate this reaction is 15 keV, only slightly higher than the optimum for the D-T reaction. The first branch does not produce neutrons, but it does produce tritium, so that a D-D reactor will not be completely tritium-free, even though it does not require an input of tritium or lithium. Unless the tritons can be quickly removed, most of the tritium produced would be burned before leaving the reactor, which would reduce the handling of tritium, but would produce more neutrons, some of which are very energetic. The neutron from the second branch has an energy of only 2.45 MeV (0.393 pJ), whereas the neutron from the D-T reaction has an energy of 14.1 MeV (2.26 pJ), resulting in a wider range of isotope production and material damage. When the tritons are removed quickly while allowing the ^3He to react, the fuel cycle is called “tritium suppressed fusion” The removed tritium decays to ^3He with a 12.5 year half-life. By recycling the ^3He produced from the decay of tritium back into the fusion reactor, the fusion reactor does not require materials resistant to fast 14.1 MeV (2.26 pJ) neutrons.

Assuming complete tritium burn-up, the reduction in the fraction of fusion energy carried by neutrons would be only about 18%, so that the primary advantage of the D-D fuel cycle is that tritium breeding would not be required. Other advantages are independence from scarce lithium resources and a somewhat softer neutron spectrum. The disadvantage of D-D compared to D-T is that the energy confinement time (at a given pressure) must be 30 times longer and the power produced (at a given pressure and volume) would be 68 times less.

Assuming complete removal of tritium and recycling of ^3He , only 6% of the fusion energy is carried by neutrons. The tritium-suppressed D-D fusion requires an energy confinement that is 10 times longer compared to D-T and a plasma temperature that is twice as high.

Deuterium and Helium-3

A second-generation approach to controlled fusion power involves combining helium-3 (^3He) and deuterium (^2H):

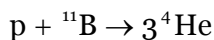


This reaction produces a helium-4 nucleus (^4He) and a high-energy proton. As with the p-11B aneutronic fusion fuel cycle, most of the reaction energy is released as charged particles, reducing activation of the reactor housing and potentially allowing more efficient energy harvesting (via any of several speculative technologies). In practice, D-D side reactions produce a significant number of neutrons, resulting in p- ^{11}B being the preferred cycle for aneutronic fusion.

Proton, Boron-11

Both material science problems and non-proliferation concerns are greatly

diminished if aneutronic fusion can be achieved. Theoretically, the most reactive a-neutronic fusion fuel is ${}^3\text{He}$. However, obtaining reasonable quantities of ${}^3\text{He}$ would require large scale mining operations on the moon or in the atmosphere of Uranus or Saturn, which raise other, quite considerable technical difficulties. Therefore, the most promising candidate fuel for such fusion is fusing the readily available hydrogen-1 (i.e. a proton) and boron. Their fusion releases no neutrons, but produces energetic charged alpha (helium) particles whose energy can directly be converted to electric power:



Under reasonable assumptions, side reactions will result in only about 0.1% of the fusion power being carried by neutrons, which means that neutron scattering is not used for energy transfer and material activation is reduced several thousand times. Unfortunately, the optimum temperature for this reaction of 123 keV is nearly ten times higher than that for pure hydrogen reactions, and the energy confinement must be 500 times better than that required for the D-T reaction. In addition the power density is 2500 times lower than for D-T, although per unit mass of fuel, this is still considerably higher than for fission reactors.

Because the confinement properties of conventional approaches to fusion such as the tokamak and laser pellet fusion are marginal, most proposals for aneutronic fusion are based on radically different confinement concepts, such as the Polywell and the Dense Plasma Focus. In 2013 a research team led by Christine Labaune at École Polytechnique in Palaiseau, France, reported a new fusion rate record for proton-boron fusion, with an estimated 80 million fusion reactions during 1.5 nanoseconds laser fire, over 100 times more than previous proton-boron experiments.

Material Selection

Considerations

Even on smaller plasma production scales, the material of the containment apparatus will be intensely blasted with matter and energy. Designs for plasma containment must consider:

- A heating and cooling cycle, up to a 10 MW/m² thermal load.
- Neutron radiation, which over time leads to neutron activation and embrittlement.
- High energy ions leaving at tens to hundreds of electronvolts.
- Alpha particles leaving at millions of electronvolts.

- Electrons leaving at high energy.
- Light radiation (IR, visible, UV, X-ray).

Depending on the approach, these effects may be higher or lower than typical fission reactors like the pressurized water reactor (PWR). One estimate put the radiation at 100 times that of a typical PWR. Materials need to be selected or developed that can withstand these basic conditions. Depending on the approach, however, there may be other considerations such as electrical conductivity, magnetic permeability and mechanical strength. There is also a need for materials whose primary components and impurities do not result in long-lived radioactive wastes.

Durability

For long term use, each atom in the wall is expected to be hit by a neutron and displaced about a hundred times before the material is replaced. High-energy neutrons will produce hydrogen and helium by way of various nuclear reactions that tends to form bubbles at grain boundaries and result in swelling, blistering or embrittlement.

Selection

One can choose either a low-Z material, such as graphite or beryllium, or a high-Z material, usually tungsten with molybdenum as a second choice. Use of liquid metals (lithium, gallium, tin) has also been proposed, e.g., by injection of 1–5 mm thick streams flowing at 10 m/s on solid substrates.

If graphite is used, the gross erosion rates due to physical and chemical sputtering would be many meters per year, so one must rely on redeposition of the sputtered material. The location of the redeposition will not exactly coincide with the location of the sputtering, so one is still left with erosion rates that may be prohibitive. An even larger problem is the tritium co-deposited with the redeposited graphite. The tritium inventory in graphite layers and dust in a reactor could quickly build up to many kilograms, representing a waste of resources and a serious radiological hazard in case of an accident. The consensus of the fusion community seems to be that graphite, although a very attractive material for fusion experiments cannot be the primary plasma-facing material (PFM) in a commercial reactor.

The sputtering rate of tungsten by the plasma fuel ions is orders of magnitude smaller than that of carbon, and tritium is much less incorporated into redeposited tungsten, making this a more attractive choice. On the other hand, tungsten impurities in plasma are much more damaging than carbon impurities, and self-sputtering of tungsten can be high, so it will be necessary to ensure that the plasma in contact with the tungsten is not too hot (a few tens of eV rather than hundreds of eV). Tungsten also has disadvantages in terms of eddy currents and melting in off-normal events, as well as some radiological issues.

Safety and the Environment

Accident Potential

Unlike nuclear fission, fusion requires extremely precise and controlled temperature, pressure and magnetic field parameters for any net energy to be produced. If a reactor suffers damage or loses even a small degree of required control, fusion reactions and heat generation would rapidly cease. Additionally, fusion reactors contain only small amounts of fuel, enough to “burn” for minutes, or in some cases, microseconds. Unless they are actively refueled, the reactions will quickly end. Therefore, fusion reactors are considered immune from catastrophic meltdown.

For similar reasons, runaway reactions cannot occur in a fusion reactor. The plasma is burnt at optimal conditions, and any significant change will simply quench the reactions. The reaction process is so delicate that this level of safety is inherent. Although the plasma in a fusion power station is expected to have a volume of 1,000 cubic metres (35,000 cu ft.) or more, the plasma density is low and typically contains only a few grams of fuel in use. If the fuel supply is closed, the reaction stops within seconds. In comparison, a fission reactor is typically loaded with enough fuel for several months or years, and no additional fuel is necessary to continue the reaction. It is this large amount of fuel that gives rise to the possibility of a meltdown; nothing like this exists in a fusion reactor.

In the magnetic approach, strong fields are developed in coils that are held in place mechanically by the reactor structure. Failure of this structure could release this tension and allow the magnet to “explode” outward. The severity of this event would be similar to any other industrial accident or an MRI machine quench/explosion, and could be effectively stopped with a containment building similar to those used in existing (fission) nuclear generators. The laser-driven inertial approach is generally lower-stress because of the increased size of the reaction chamber. Although failure of the reaction chamber is possible, simply stopping fuel delivery would prevent any sort of catastrophic failure.

Most reactor designs rely on liquid hydrogen as both a coolant and a method for converting stray neutrons from the reaction into tritium, which is fed back into the reactor as fuel. Hydrogen is highly flammable, and in the case of a fire it is possible that the hydrogen stored on-site could be burned up and escapes. In this case, the tritium contents of the hydrogen would be released into the atmosphere, posing a radiation risk. Calculations suggest that at about 1 kilogram (2.2 lb), the total amount of tritium and other radioactive gases in a typical power station would be so small that they would have diluted to legally acceptable limits by the time they blew as far as the station’s perimeter fence.

The likelihood of small industrial accidents, including the local release of radioactivity and injury to staff, cannot be estimated yet. These would include accidental releases of lithium or tritium or mishandling of decommissioned radioactive components of the reactor itself.

Magnet Quench

A quench is an abnormal termination of magnet operation that occurs when part of the superconducting coil enters the normal (resistive) state. This can occur because the field inside the magnet is too large, the rate of change of field is too large (causing eddy currents and resultant heating in the copper support matrix), or a combination of the two.

More rarely a defect in the magnet can cause a quench. When this happens, that particular spot is subject to rapid Joule heating from the enormous current, which raises the temperature of the surrounding regions. This pushes those regions into the normal state as well, which leads to more heating in a chain reaction. The entire magnet rapidly becomes normal (this can take several seconds, depending on the size of the superconducting coil). This is accompanied by a loud bang as the energy in the magnetic field is converted to heat, and rapid boil-off of the cryogenic fluid. The abrupt decrease of current can result in kilovolt inductive voltage spikes and arcing. Permanent damage to the magnet is rare, but components can be damaged by localized heating, high voltages, or large mechanical forces.

In practice, magnets usually have safety devices to stop or limit the current when the beginning of a quench is detected. If a large magnet undergoes a quench, the inert vapor formed by the evaporating cryogenic fluid can present a significant asphyxiation hazard to operators by displacing breathable air.

A large section of the superconducting magnets in CERN's Large Hadron Collider unexpectedly quenched during start-up operations in 2008, necessitating the replacement of a number of magnets. In order to mitigate against potentially destructive quenches, the superconducting magnets that form the LHC are equipped with fast-ramping heaters which are activated once a quench event is detected by the complex quench protection system. As the dipole bending magnets are connected in series, each power circuit includes 154 individual magnets, and should a quench event occur, the entire combined stored energy of these magnets must be dumped at once. This energy is transferred into dumps that are massive blocks of metal which heat up to several hundreds of degrees Celsius—because of resistive heating—in a matter of seconds. Although undesirable, a magnet quench is a “fairly routine event” during the operation of a particle accelerator.

Effluents

The natural product of the fusion reaction is a small amount of helium, which is completely harmless to life. Of more concern is tritium, which, like other isotopes of hydrogen, is difficult to retain completely. During normal operation, some amount of tritium will be continually released.

Although tritium is volatile and biologically active, the health risk posed by a release is much lower than that of most radioactive contaminants, because of tritium's short

half-life (12.32 years) and very low decay energy (~ 14.95 keV), and because it does not bioaccumulate (instead being cycled out of the body as water, with a biological half-life of 7 to 14 days). Current ITER designs are investigating total containment facilities for any tritium.

Waste Management

The large flux of high-energy neutrons in a reactor will make the structural materials radioactive. The radioactive inventory at shut-down may be comparable to that of a fission reactor, but there are important differences.

The half-life of the radioisotopes produced by fusion tends to be less than those from fission, so that the inventory decreases more rapidly. Unlike fission reactors, whose waste remains radioactive for thousands of years, most of the radioactive material in a fusion reactor would be the reactor core itself, which would be dangerous for about 50 years, and low-level waste for another 100. Although this waste will be considerably more radioactive during those 50 years than fission waste, the very short half-life makes the process very attractive, as the waste management is fairly straightforward. By 500 years the material would have the same radiotoxicity as coal ash.

Additionally, the choice of materials used in a fusion reactor is less constrained than in a fission design, where many materials are required for their specific neutron cross-sections. This allows a fusion reactor to be designed using materials that are selected specifically to be “low activation”, materials that do not easily become radioactive. Vanadium, for example, would become much less radioactive than stainless steel. Carbon fiber materials are also low-activation, as well as being strong and light, and are a promising area of study for laser-inertial reactors where a magnetic field is not required.

In general terms, fusion reactors would create far less radioactive material than a fission reactor, the material it would create is less damaging biologically, and the radioactivity “burns off” within a time period that is well within existing engineering capabilities for safe long-term waste storage.

Nuclear Proliferation

Although fusion power uses nuclear technology, the overlap with nuclear weapons would be limited. A huge amount of tritium could be produced by a fusion power station; tritium is used in the trigger of hydrogen bombs and in a modern boosted fission weapon, but it can also be produced by nuclear fission. The energetic neutrons from a fusion reactor could be used to breed weapons-grade plutonium or uranium for an atomic bomb (for example by transmutation of U^{238} to Pu^{239} , or Th^{232} to U^{233}).

A study conducted 2011 assessed the risk of three scenarios:

- Use in small-scale fusion station: As a result of much higher power consumption,

heat dissipation and a more recognizable design compared to enrichment gas centrifuges this choice would be much easier to detect and therefore implausible.

- Modifications to produce weapon-usable material in a commercial facility: The production potential is significant. But no fertile or fissile substances necessary for the production of weapon-usable materials needs to be present at a civil fusion system at all. If not shielded, a detection of these materials can be done by their characteristic gamma radiation. The underlying redesign could be detected by regular design information verifications. In the (technically more feasible) case of solid breeder blanket modules, it would be necessary for incoming components to be inspected for the presence of fertile material, otherwise plutonium for several weapons could be produced each year.
- Prioritizing a fast production of weapon-grade material regardless of secrecy: The fastest way to produce weapon usable material was seen in modifying a prior civil fusion power station. Unlike in some nuclear power stations, there is no weapon compatible material during civil use. Even without the need for covert action this modification would still take about 2 months to start the production and at least an additional week to generate a significant amount for weapon production. This was seen as enough time to detect a military use and to react with diplomatic or military means. To stop the production, a military destruction of inevitable parts of the facility leaving out the reactor itself would be sufficient. This, together with the intrinsic safety of fusion power would only bear a low risk of radioactive contamination.

Another study concludes that “large fusion reactors – even if not designed for fissile material breeding – could easily produce several hundred kg Pu per year with high weapon quality and very low source material requirements.” It was emphasized that the implementation of features for intrinsic proliferation resistance might only be possible at this phase of research and development. The theoretical and computational tools needed for hydrogen bomb design are closely related to those needed for inertial confinement fusion, but have very little in common with the more scientifically developed magnetic confinement fusion.

Energy Source

Large-scale reactors using neutronic fuels (e.g. ITER) and thermal power production (turbine based) are most comparable to fission power from an engineering and economics viewpoint. Both fission and fusion power stations involve a relatively compact heat source powering a conventional steam turbine-based power station, while producing enough neutron radiation to make activation of the station materials problematic. The main distinction is that fusion power produces no high-level radioactive waste (though activated station materials still need to be disposed of). There are some power

station ideas that may significantly lower the cost or size of such stations; however, research in these areas is nowhere near as advanced as in tokamaks.

Fusion power commonly proposes the use of deuterium, an isotope of hydrogen, as fuel and in many current designs also use lithium. Assuming a fusion energy output equal to the 1995 global power output of about 100 EJ/yr ($= 1 \times 10^{20}$ J/yr) and that this does not increase in the future, which is unlikely, then the known current lithium reserves would last 3000 years. Lithium from sea water would last 60 million years, however, and a more complicated fusion process using only deuterium would have fuel for 150 billion years. To put this in context, 150 billion years is close to 30 times the remaining lifespan of the sun, and more than 10 times the estimated age of the universe.

Economics

While fusion power is still in early stages of development, substantial sums have been and continue to be invested in research. In the EU almost €10 billion was spent on fusion research up to the end of the 1990s, and the new ITER reactor alone is budgeted at €6.6 billion total for the timeframe between 2008 and 2020.

It is estimated that up to the point of possible implementation of electricity generation by nuclear fusion, R&D will need further promotion totalling around €60–80 billion over a period of 50 years or so (of which €20–30 billion within the EU) based on a report from 2002. Nuclear fusion research receives €750 million (excluding ITER funding) from the European Union, compared with €810 million for sustainable energy research, putting research into fusion power well ahead of that of any single rivaling technology. Indeed, the size of the investments and time frame of the expected results mean that fusion research is almost exclusively publicly funded, while research in other forms of energy can be done by the private sector. In spite of that, a number of start-up companies active in the field of fusion power have managed to attract private money.

Advantages

Fusion power would provide more energy for a given weight of fuel than any fuel-consuming energy source currently in use, and the fuel itself (primarily deuterium) exists abundantly in the Earth's ocean: about 1 in 6500 hydrogen atoms in seawater is deuterium. Although this may seem a low proportion (about 0.015%), because nuclear fusion reactions are so much more energetic than chemical combustion and seawater is easier to access and more plentiful than fossil fuels, fusion could potentially supply the world's energy needs for millions of years.

A scenario has been presented of the effect of the commercialization of fusion power on the future of human civilization. ITER and later DEMO are envisioned to bring online the first commercial nuclear fusion energy reactor by 2050. Using this as the starting

point and the history of the uptake of nuclear fission reactors as a guide, the scenario depicts a rapid take up of nuclear fusion energy starting after the middle of this century.

Fusion power could be used in interstellar space where solar energy is not available.

NEUTRON GENERATOR

Neutron generators are the source of neutrons for various applications. The different methods offer advantages and disadvantages in volume and energy of neutrons, portability, service life, and other factors.

Neutron Generation from Radioisotopes

Many radioisotopes continuously emit neutrons. This can be advantageous, when neutrons are desired, or a problem if one isotope of an element emits neutrons that are not needed in an application. A transuranic element, Californium's ^{252}Cf isotope is widely used as a portable source for analysis.

Plutonium has isotopes that both capture and emit neutrons. ^{239}Pu is the neutron acceptor in nuclear weapons, but ^{240}Pu , a neutron emitter, can cause predetonation; bomb-grade plutonium is not only 239-rich but 240-low. ^{240}Pu , however, is beneficial in power reactors.

In the first nuclear weapons, an initiator, at the center of the fissionable material, emitted neutrons. Codenamed the "Urchin", it was a sphere of mixed polonium (^{210}Po) and beryllium. Without going through its complex mechanical design, the basic material was a hollow beryllium sphere, grooved on the inside, and with a solid beryllium pellet at the center. As the urchin was explosively compressed and vaporized, alpha particles emitted by the Po-210 then struck beryllium atoms, which released neutrons. The bomb also depended on a number of other mechanical aids to generate enough neutrons for the critical mass, such as neutron-reflecting outer shells that redirected neutrons into the core.

Neutron Generation from Particle Accelerators

Later neutron sources based on linear particle accelerators, which is a cylinder with an ion source at one end and an ion target at the other end. The space between them contains deuterium, tritium, or some mixture depending on the specific generator design. Electrical current supplied to the source causes an electrical arc and generates hydrogen ions, which are then accelerate using electromagnetic force from another, accelerating electrode, which sends the accelerated cloud into the target. Individual neutrons (i.e., not a beam) are generated by the ions hitting the target, which has one or more hydrogen isotopes on its surface.

The most obvious difference between the unclassified generators used in industry, and the classified detectors used in weapons, is size and ruggedness. Both types do have a superficial resemblance to a household hair dryer, with the ion source at the motor/heater end. The first tube used titanium hydride targets, but the standard in the industry uses scandium hydride.

One unclassified design described by Sublette is the Milli-Second Pulse (MSP) tube developed at Sandia. "It has a scandium tritide target, containing 7 curies of tritium as 5.85 mg of ScT₂ deposited on a 9.9 cm² molybdenum backing. A 0.19-0.25 amp deuteron beam current produces about 4-5 x 10⁷ neutrons/amp-microsecond in a 1.2 millisecond pulse with accelerator voltages of 130-150 KeV for a total of 1.2 x 10¹⁰ neutrons per pulse. For comparison the classified Sandia model TC-655, which was developed for nuclear weapons, produced a nominal 3 x 10⁹ neutron pulse." The neutrons are not produced as a burst, as a stream that triggers successive neutron multiplication cycles in the ultimate target. In the design of an ENI, the critical parameters are the beam intensity, and the speed and shape of the initial ionization pulse.

In a weapon, the ENI can be placed wherever mechanically convenient, as long as it is within 1-2 meters of the core and not separated by a neutron absorber. Since the neutron generator usually contains tritium, radioactive decay of the tritium means that the generators are components that need periodic replacement.

New, more compact and long-lived ENIs are available. Obviously, an ENI for a bomb does not need a long service life once active, but industrial generators have tended to exhaust their ions. New generator designs, however, provide the target with a source of fresh ions. The lifetime of these new devices may be in the thousands of hours.

Neutron Generation from Nuclear Reactors

While nuclear reactors are the least portable source of neutrons, they also can be the most powerful, and offer a range of neutron characteristics that are especially useful in analysis. By using different reactors, different placement of targets with respect to the reactor, and the moderators used in the reactor, the widest possible range of neutron fluxes can be obtained. The flux distributions contain thermal, epithermal, and fast neutrons.

References

- Medical-uses, know-nuclear-applications: nuclearconnect.org, Retrieved 23 July, 2020
- Fusion-reactor, science: britannica.com, Retrieved 16 May, 2020
- Neutron-generator: m.tau.ac.il, Retrieved 19 June, 2020
- Saha, Gopal B. (2006). *Physics and radiobiology of nuclear medicine* (3rd ed.). New York: Springer. doi:10.1007/978-0-387-36281-6. ISBN 978-0-387-30754-1

- Bailey, D.L; D.W. Townsend; P.E. Valk; M.N. Maisey (2005). Positron-Emission Tomography: Basic Sciences. Secaucus, NJ: Springer-Verlag. ISBN 978-1-85233-798-8
- Seidlitz A, Combs SE, Debus J, Baumann M (2016). “Practice points for radiation oncology”. In Kerr DJ, Haller DG, van de Velde CJ, Baumann M (eds.). Oxford Textbook of Oncology. Oxford University Press. p. 173. ISBN 9780191065101

PERMISSIONS

All chapters in this book are published with permission under the Creative Commons Attribution Share Alike License or equivalent. Every chapter published in this book has been scrutinized by our experts. Their significance has been extensively debated. The topics covered herein carry significant information for a comprehensive understanding. They may even be implemented as practical applications or may be referred to as a beginning point for further studies.

We would like to thank the editorial team for lending their expertise to make the book truly unique. They have played a crucial role in the development of this book. Without their invaluable contributions this book wouldn't have been possible. They have made vital efforts to compile up to date information on the varied aspects of this subject to make this book a valuable addition to the collection of many professionals and students.

This book was conceptualized with the vision of imparting up-to-date and integrated information in this field. To ensure the same, a matchless editorial board was set up. Every individual on the board went through rigorous rounds of assessment to prove their worth. After which they invested a large part of their time researching and compiling the most relevant data for our readers.

The editorial board has been involved in producing this book since its inception. They have spent rigorous hours researching and exploring the diverse topics which have resulted in the successful publishing of this book. They have passed on their knowledge of decades through this book. To expedite this challenging task, the publisher supported the team at every step. A small team of assistant editors was also appointed to further simplify the editing procedure and attain best results for the readers.

Apart from the editorial board, the designing team has also invested a significant amount of their time in understanding the subject and creating the most relevant covers. They scrutinized every image to scout for the most suitable representation of the subject and create an appropriate cover for the book.

The publishing team has been an ardent support to the editorial, designing and production team. Their endless efforts to recruit the best for this project, has resulted in the accomplishment of this book. They are a veteran in the field of academics and their pool of knowledge is as vast as their experience in printing. Their expertise and guidance has proved useful at every step. Their uncompromising quality standards have made this book an exceptional effort. Their encouragement from time to time has been an inspiration for everyone.

The publisher and the editorial board hope that this book will prove to be a valuable piece of knowledge for students, practitioners and scholars across the globe.

INDEX

A

Actinium, 131, 133-134
Alpha Decay, 7, 50, 60, 86, 88-91, 94-97, 103-104, 117, 125-128, 131, 135, 137
Alpha Radiation, 10, 50
Angular Momentum, 21, 26-27, 29-30, 43, 100-101, 110, 114
Atomic Mass, 2-5, 49, 59, 64, 87, 90-91, 111
Atomic Nucleus, 1-2, 4, 6-10, 15-17, 19-20, 32, 49, 62, 86, 104-106, 108, 116, 125, 135

B

Beta Decay, 7, 31, 40, 49-50, 53, 60, 86, 89, 97-100, 104-105, 108-121, 123-124, 135, 137, 158, 199
Beta Emission Spectrum, 112, 116
Beta Particle, 38, 104, 110, 122
Binding Energy, 4, 8, 10, 20, 22, 33, 35, 39-40, 44, 59, 63-65, 88, 91, 104, 112, 116, 119, 237
Bubble Fusion, 73, 243

C

Cluster Decay, 59, 125-128
Cold Fission, 126-127
Controlled Fusion, 78, 81-83, 85, 91, 230, 242, 252
Cosmic Rays, 59, 120, 122-123
Coulomb Repulsion, 34, 36, 42, 78

D

Daughter Isotope, 92, 130-131
Decay Chain, 38-39, 102, 130-131, 133
Decay Constant, 92, 94-95, 98, 100, 126, 130

E

Electric Dipole, 27-28, 100
Electromagnetic Radiations, 86
Electron Capture, 90, 92, 97, 99, 105, 107-109, 112, 116-118, 121, 123, 157
Electron Cloud, 1-3, 86
Excitation Energy, 5, 36-37, 41, 43-44, 46

F

Fermi Decay, 98
Fermi Function, 112-113, 116

Fermi Theory, 97
Fissile Nucleus, 47, 201
Fission Decay Chains, 38

G

Gamma Rays, 7, 32, 36, 40, 49, 62, 68, 86, 102, 124-125, 140, 143-144, 146-147, 149-151, 199
Gamma Transitions, 100-101

H

Harmonic Oscillator, 21-22, 24-25, 27, 29
Helium, 2, 17, 37, 49, 63-64, 68-69, 74, 77-78, 82, 86, 90-91, 94, 105, 200-201, 207, 229-230, 246, 249, 252-254, 256
Hydrogen Nuclei, 4, 17, 63-64, 68, 78, 200

I

Inertial Confinement, 69, 71, 77, 207, 229, 234, 236, 239, 242, 245, 248-249, 258
Inertial Confinement Fusion, 71, 234, 242, 245, 258
Ionizing Radiation, 8, 102, 139, 156, 165, 170, 176, 186
Isotopic Mass, 4

K

Kinetic Energy, 35-36, 40-41, 44, 47-50, 76, 78, 95, 110-112, 116, 119, 126, 128, 131, 135, 158, 199-200, 228-229, 237, 239, 246

L

Lanthanide, 42
Lepton Number, 105, 110, 118
Liquid Drop, 19-20, 33, 42, 60
Lithium, 7, 17, 68-69, 77, 79, 88, 201, 210-211, 214, 229-230, 240, 246, 250-252, 254-255, 259

M

Majorana Particle, 118-119
Mesons, 2, 17, 29
Molar Mass, 135

N

Neutrino Exchange, 118-119
Neutron Capture, 16, 93

Neutron Generator, 201-202, 260-261
Neutron Number, 3, 12, 65, 88, 96, 117, 122
Nuclear Force, 2, 8-9, 13-15, 17, 19, 27, 33-34, 42, 236
Nuclear Fusion, 11, 32, 62, 65-72, 74-75, 77, 79, 198, 228, 235-236, 259-260
Nuclear Radius, 6, 95-96, 101

O

Orbital Electron, 86, 97, 117, 123

P

Packing Fraction, 12
Pascal Triangle, 22, 26
Pauli Exclusion Principle, 3, 20, 30
Perchlorate Ion, 57-58
Photofission, 35, 62, 85
Plasma State, 66-67, 71, 228
Plutonium, 32, 35, 37, 46, 48, 61-62, 66, 90, 96, 199-204, 206, 209, 214, 226, 257-258, 260
Positron Emission, 90, 99, 104-107, 109, 121-123, 138-139, 143, 147, 158-159, 162
Potassium Iodide, 56, 58
Potential Energy, 34, 41, 43-44, 46-47, 77, 95
Proton Decay, 109, 122, 136-137

Q

Quantum Energy, 100
Quantum Numbers, 23, 110

R

Radioactive Decay, 7, 10, 15, 32, 38, 40, 48, 52, 59-61, 86, 88, 90-91, 93, 102, 104, 116, 121, 123, 126, 130, 135-136, 261
Radioactive Transitions, 88, 91
Radium Isotopes, 38, 131

S

Scission Point, 34, 41, 43-44, 46-47
Selenium, 116
Shell Model, 7, 19-21, 24-25, 27-31, 42-43
Spontaneous Fission, 37-39, 45, 52, 61, 88, 91, 126

T

Thermonuclear Fusion, 75-76, 88
Thermonuclear Reactor, 84, 228
Tritium, 8, 49, 62-65, 67, 69, 71-76, 78-80, 83, 87, 105, 200-202, 207-211, 214, 226, 229, 234, 236, 238, 240, 245, 249-252, 254-257, 260-261

U

Uranium, 5, 10, 32, 35, 37-40, 44, 46, 48-52, 55, 59-62, 66, 87-90, 96, 102-103, 125, 133-134, 150, 182, 198-204, 212-213, 218, 220-221, 250, 257

V

Valence Space, 28

W

Weisskopf Formula, 101